

Tailored Heterogeneity Indices in Anionic Polymerization

A. EISENBERG, *Department of Chemistry, University of California, Los Angeles, California*, and D. A. McQUARRIE, *North American Aviation Science Center, Thousand Oaks, California*

Synopsis

Equations are derived for the differential molecular weight distribution curve and for the heterogeneity index for several types of delayed initiator addition in anionic polymerization. All the results are in closed and easily used form, and depend only upon the product of the rate constant of the propagation reaction, the total initiator concentration, and a parameter representative of the rate of initiator addition. The results are plotted versus the above-mentioned product, so that one can determine the heterogeneity index to be expected under a wide range of the variables involved.

I. INTRODUCTION

While it has been known for a long time that the rate of initiator addition strongly influences the molecular weight distribution of polymer in anionic polymerization,¹ no quantitative estimates of this effect over wide ranges of the variables involved have been published. Here an attempt is made not only to solve that problem, but also to suggest how, by varying rates of initiator addition, a wide range of heterogeneity indices and molecular weight distributions can be achieved in anionic polymerization.

Anionic polymerization is more ideally suited for the formation of essentially monodisperse polymers than any other synthetic method. When using this technique, an initiator such as sodium naphthalene in tetrahydrofuran (THF) is mixed very rapidly with a solution (usually also in THF) of a vinyl monomer, such as styrene, possessing a low lying unoccupied molecular orbital. Initiation is accomplished by the transfer of the extra electron from the naphthalene to the styrene, which is transformed into a free-radical anion, which then dimerizes and polymerizes to yield a polymeric dianion. Since in the absence of impurities no termination takes place, polymerization proceeds until either all of the available monomer has been consumed or until equilibrium has been achieved.²⁻⁴ Throughout the polymerization process, all the chains remain "alive," i.e., the total number of active sites remains unchanged, and all of them have an equal chance of growth, in direct contrast to polymerization by free-radical initiators⁵ in which initiation, termination, and chain transfer take place continuously. The last of these is absent in the anionic polymeriza-

tion of most monomers, exceptions being only materials like 9-vinyl-anthracene,⁶ acenaphthylene,⁷ and acrylonitrile.⁸ Several discussions of molecular heterogeneity in polymerization of this type can be found in the literature. In treating the molecular weight distribution in a polymerization process in which the number of growing chains remains constant (ethylene oxide polymerization by ethylene glycol), Flory⁹ has shown that the molecular weight distribution is given by a narrow Poisson distribution, i.e., essentially a monodisperse distribution. Brown and Szwarc¹⁰ pointed out that this also applies to the polymerization of "living" polymers when the rate constant of the polymerization reaction is very much faster than that of the depolymerization reaction. If this is not the case, i.e., if the equilibrium monomer concentration is appreciable, the "most probable" distribution¹¹ results.

Among the other treatments of molecular weight distributions in anionic polymerization may be mentioned the study by Gold,¹² who considered the effect on the heterogeneity index of a variation in the rate constant for initiation (the rate constant of the propagation reaction remaining constant) and showed that ratios of these two rate constants varying by as much as 10^{-2} to 10^{+6} yielded polymer of a maximum heterogeneity index of ca. 1.4. Nanda and Jain¹³ subsequently simplified Gold's mathematical approach. Finally, a series of theoretical studies has been undertaken to elucidate the effect of impurities in the monomer and of chain transfer on the heterogeneity, as well as of differences in the rate constants for the first few steps^{17b} of the reaction.¹⁴⁻¹⁷

II. THE PRESENT PROBLEM

The narrowest molecular weight distribution that has been achieved in the anionic polymerization of vinyl monomers is of the order of 1.05.¹⁸ This was achieved by a careful exclusion of impurities and usually by very rapid mixing of monomer and initiator. Under no circumstances, however, can mixing be truly instantaneous, which implies that even narrower distributions could be achieved if more rapid mixing were possible. On the other hand, in many anionic polymerization runs, heterogeneities of the order of 1.5 are encountered, even in the absence of impurities, which implies that the rate of addition is all-important in determining the final distribution. This, in turn shows that by a proper choice of the rate of addition of initiator, a wide range of distributions can be achieved. This is highly desirable, because among other reasons, many physical properties of a polymer depend not only on the average molecular weight, but also on the molecular weight distribution. Studies of the effect of the latter on many physical properties have to be made on mixtures of polymers, which, while they may have the desired number-average molecular weight and the desired heterogeneity index (weight average divided by number average) may show several peaks in the differential distribution curve, the effect of which cannot be properly evaluated.

In the subsequent section the effect of the rate of addition of initiator on the heterogeneity index will be derived for three different types of addition histories. Examples of differential distribution curves will be shown, and the results presented in such a way as to allow, from the final heterogeneity index, to judge the "effective" or the desired rate of initiator addition. Furthermore, if the rate of addition is known, it will be possible to calculate, approximately at least, the rate constant of the propagation reaction.

The following assumptions are made:

(1) No impurities are present in the monomer which could terminate the chains. While this is difficult to achieve perfectly, in practice one can come very close to it, for instance by distilling the monomer into the reaction flask from a "living" polymer solution, particularly if the system has a high equilibrium monomer concentration at the distillation temperature, as is the case in α -methylstyrene.

(2) The initiation is instantaneous, or its rate constant is not slower than that of the polymerization reaction. This can be achieved easily by making the initiator itself a very short dianion of the material to be polymerized.

(3) No equilibrium polymerization effects are encountered, i.e., the polymerization proceeds essentially to completion. Even in the case of α -methylstyrene this can be achieved by carrying out the polymerization at a low enough temperature.

(4) All polymer chains initiated at the same instant grow to identical lengths. This is only an approximation, but the results to be presented here will be affected only within a small range of values by this assumption.

(5) The concentration of monomer is low enough and that of the initiator high enough so that the effective total monomer concentration (bound and unbound) does not change in the course of the addition of initiator (volume effects are absent).

(6) The rate constant of the propagation reaction does not change with initiator concentration. While in most cases this is only an approximation,¹⁹ it was shown²⁰ that this is the case if a high enough concentration of counterions is present initially.

In the next sections we shall derive equations for the heterogeneity index and molecular weight distributions for several forms of the rate of addition of the initiator.

III. DERIVATIONS

Let $M(t)$ be the concentration of monomer and let $x(t)$ be the rate of addition of initiator. Then if $\chi(t)$ is the cumulative concentration of initiator, i.e.,

$$\chi(t) = \int_0^t x(u) du \quad (1)$$

then since the rate of polymerization has been shown to be first order in both monomer and initiator

$$dM/dt = -k\chi(t)M(t) \quad (2)$$

where k is the rate constant for the polymerization step. Since we assume that each of the active chains or "living" polymers in solution grows at the same rate, then we may write

$$dP/dt = - [1/\chi(t)](dM/dt) \quad (3)$$

where dP/dt is the rate of growth of the polymer chains. Substitution of eq. (2) into eq. (3) gives

$$dP/dt = kM(t) \quad (4)$$

as expected. Substituting the solution of eq. (2) into eq. (4) gives

$$P(t) = kM_0 \int_0^t \exp \left\{ -k \int_0^y \chi(u) du \right\} dy \quad (5)$$

where y is an integration variable having the dimension of time, and M_0 is the initial concentration of monomer. Note that $P(t) - P(u)$ is the degree of polymerization at time t for chains initiated at time u . For future use we define

$$\langle a \rangle = \int_0^\infty x(t) [P(\infty) - P(t)] dt \quad (6)$$

$$\langle a^2 \rangle = \int_0^\infty x(t) [P(\infty) - P(t)]^2 dt \quad (7)$$

which in Flory's¹¹ notation are $\sum n_i P_i$ and $\sum n_i P_i^2$, respectively, and

$$\chi_0 = \int_0^\infty x(t) dt \quad (8)$$

We note that

$$\langle a \rangle / \chi_0 = P_n = \text{final number-average molecular weight}$$

$$\langle a^2 \rangle / \langle a \rangle = P_w = \text{final weight-average molecular weight}$$

$$(\langle a^2 \rangle / \langle a \rangle^2) \chi_0 = \text{h.i.} = \text{heterogeneity index}$$

We shall now consider three different addition histories: (I) instantaneous addition; (II) constant rate of addition; (III) exponentially decreasing rate of addition.

Case I. Instantaneous Addition

In the ideal case of instantaneous addition, we write

$$x(t) = \chi_0 \delta(t)$$

where $\delta(t)$ is a delta function. Equations (2) and (5) give

$$M(t) = M_0 \exp \{ -\chi_0 kt \} \tag{9}$$

$$P(t) = (M_0/\chi_0)(1 - \exp \{ -k\chi_0 t \}) \tag{10}$$

and so

$$\langle a \rangle = M_0 \tag{11}$$

$$\langle a^2 \rangle = \langle a \rangle^2$$

and the heterogeneity index is unity, indicative of the monodispersity expected under these ideal conditions.

Case II. Constant Rate of Addition

Although it may be impossible to add all of the initiator at one instant as in case I, it is possible to add it at a constant rate. Let

$$\begin{aligned} x(t) &= \beta & 0 < t < \alpha \\ x(t) &= 0 & t > \alpha \end{aligned} \tag{12}$$

On noting that $\alpha\beta = \chi_0$ and letting $\eta = k\chi_0\alpha$, eq. (5) becomes

$$\begin{aligned} P(t) &= (M_0/\chi_0)(\eta\pi/2)^{1/2}\Phi[(k\beta/2)^{1/2}t] & 0 < t < \alpha \\ P(t) &= (M_0/\chi_0)(\eta\pi/2)^{1/2}\Phi[(\eta/2)^{1/2}] & t > \alpha \\ &+ (M_0/\chi_0) \exp \{ \eta/2 \} (\exp \{ -\eta \} - \exp \{ -k\chi_0 t \}) \end{aligned} \tag{13}$$

where $\Phi(x)$ is the error function:²¹

$$\Phi(x) = \frac{2}{\sqrt{\pi}} \int_0^x \exp \{ -u^2 \} du$$

If $\alpha \rightarrow 0$, with $\beta\alpha = \chi_0$, eq. (13) reduces to eq. (10).

Using eq. (13), we obtain

$$\begin{aligned} \langle a \rangle &= \chi_0 P(\infty) - \beta \int_0^\alpha P(u) du \\ &= \chi_0 P(\infty) - M_0(k\beta\pi/2)^{1/2} \int_0^\alpha \Phi[(k\beta/2)^{1/2}u] du \\ &= M_0 \end{aligned} \tag{14}$$

$$\begin{aligned} \langle a^2 \rangle &= (2M_0^2/\chi_0) \exp \{ -\eta/2 \} - (M_0^2/\chi_0) \exp \{ -\eta \} \\ &+ (2M_0^2/\chi_0)(\pi\eta/2)^{1/2}\Phi[(\eta/2)^{1/2}] - (M_0^2/\chi_0)(\pi\eta)^{1/2}\Phi[\eta^{1/2}] \end{aligned} \tag{15}$$

To arrive at eqs. (14) and (15) we have used the relations (easily proven by integration by parts),

$$\int_0^x \Phi(t) dt = x\Phi(x) + (1/\sqrt{\pi})(\exp\{-x^2\} - 1)$$

$$\int_0^x \Phi^2(t) dt = x\Phi^2(x) + (2/\sqrt{\pi}) \exp\{-x^2\}\Phi(x) - (2/\pi)^{1/2}\Phi(\sqrt{2}x)$$

Equations (14) and (15) give a heterogeneity index

$$\text{h.i.} = 2 \exp\{-\eta/2\} - \exp\{-\eta\} + 2(\pi\eta/2)^{1/2}\Phi[(\eta/2)^{1/2}] - (\pi\eta)^{1/2}\Phi[(\eta^{1/2})] \quad (16)$$

which for small values of η becomes

$$\text{h.i.} = 1 + (\eta^2/12) - (\eta^3/30) + (\eta^4/192) + \dots \quad (17)$$

The result for large values of η is $(\sqrt{2} - 1)\sqrt{\pi\eta} = 0.734\eta^{1/2}$. One can then determine the heterogeneity index from the experimental values of k , χ_0 , and α . These equations will be discussed numerically in section IV.

Case III. Exponentially Decreasing Rate of Addition

Under certain conditions of discharge of the initiator through a capillary, it is possible to introduce the initiator at an exponentially decreasing rate,* and so $x(t) = \beta\chi_0 e^{-\beta t}$, where β is a function of the geometry of the capillary and the physical properties of the liquid. This constant is probably best determined empirically. $P(t)$ is

$$P(t) = kM_0 \exp\{\xi\} \int_0^t \exp\{-k\chi_0 u\} \exp\{-\xi e^{-\beta u}\} du$$

where $\xi = k\chi_0/\beta$. If the compound exponential is expanded and then integrated term by term, one gets

$$P(t) = \frac{M_0\xi \exp\{\xi\}}{\chi_0} \sum_{j=0}^{\infty} \frac{(-\xi)^j}{j!(\xi+j)} [1 - \exp\{-\beta(\xi+j)t\}] \quad (18)$$

For

$$P(\infty) - P(u) = \frac{M_0\xi \exp\{\xi\}}{\chi_0} \sum_{j=0}^{\infty} \frac{(-\xi)^j}{j!(\xi+j)} \exp\{-\beta(\xi+j)u\}$$

then

$$\langle a \rangle = M_0\xi e^{\xi} \sum_{j=0}^{\infty} \frac{(-\xi)^j}{j!(\xi+j)(\xi+j+1)} = M_0\xi e^{\xi} g(\xi) \quad (19)$$

It will be shown later that $g(\xi) = e^{-\xi}/\xi$, and so $\langle a \rangle = M_0$ as it must.

* This equation may be derived from Poiseuille's Law by setting the pressure proportional to the height of a reservoir above the capillary.

Similarly

$$\begin{aligned} \langle a^2 \rangle &= \frac{M_0^2 \xi^2 e^{2\xi}}{\chi_0} \sum_{j=0}^{\infty} \sum_{k=0}^{\infty} \frac{(-\xi)^{j+k}}{j!k!(\xi+j)(\xi+k)(1+2\xi+j+k)} \quad (20) \\ &= \frac{M_0^2 \xi^2 e^{2\xi}}{\chi_0} h(\xi) \end{aligned}$$

Therefore

$$\text{h.i.} = h(\xi)/g^2(\xi) = 1 + \xi^2 + \dots \quad (21)$$

IV. NUMERICAL DISCUSSION

In this section we wish to discuss two topics: (1) the fraction of molecules with degree of polymerization in the range P and $P + dP$ (the differential distribution curve), and (2) the heterogeneity index versus η or ξ .

The number of molecules initiated between u and $u + du$ is

$$\int_u^{u+du} x(t)dt = x(u)du$$

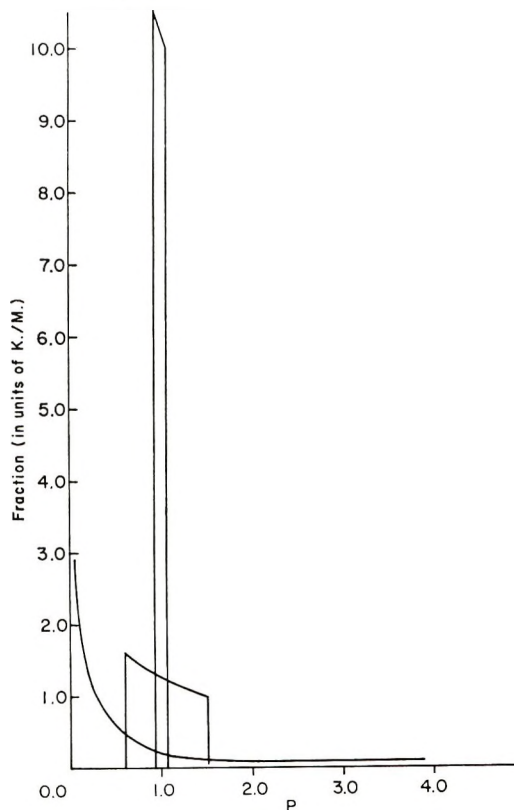


Fig. 1. Fraction vs. degree of polymerization for case II: (a) (narrowest) $\eta = 0.10$; (b) $\eta = 1.0$, (c) (broadest) $\eta = 10.0$. The fraction is in units of χ_0/M_0 and D.P. is in units of M_0/χ_0 .

and the fraction is simply $1/\chi_0$ times this. The molecules initiated between u and $u + du$ will have a degree of polymerization between $P(u)$ and $P(u + du) = P(u) + P'(u)du$. The fraction between $P(u)$ and $P(u) + dP(u)$ is

$$x(u)du = [x(u)/P'(u)]dP(u) \quad (22)$$

We shall discuss cases II and III separately.

Case II

Equation (22) can be written

$$x(u)/P'(u) = (\chi_0/M_0)(\eta \exp \{ \eta u^2/2 \}) \quad (23)$$

where u is a "dummy" parameter ($= t/\alpha$) which varies between zero and unity. Equation (23) is to be plotted against eq. (24):

$$P(\infty) - P(u) = M_0/\chi_0((\pi\eta/2)^{1/2}\Phi[(\eta/2)^{1/2}] + \exp \{ -\eta/2 \} - (\pi\eta/2)^{1/2}\Phi[(\eta/2)^{1/2}u]) \quad (24)$$

where u is the same as in eq. (23). Equations (23) and (24) give the fraction versus the degree of polymerization in parametric form and are plotted in Figure 1 for several values of η . Figure 2 gives the heterogeneity index for this case versus η .

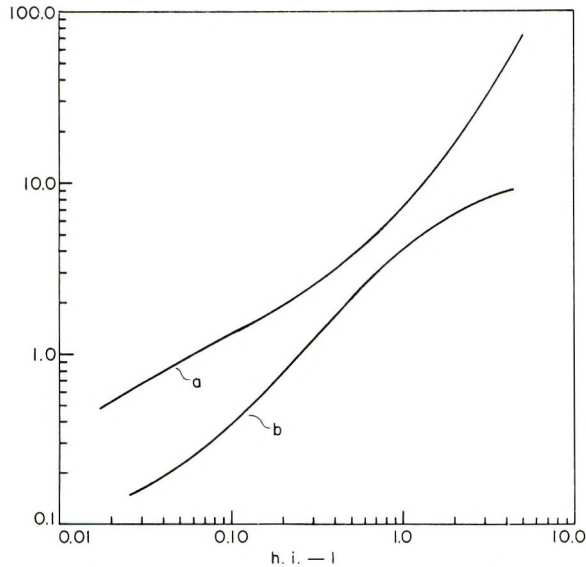


Fig. 2. Heterogeneity index vs. η : (a) case II; (b) case III.

Case III

The fraction of chains in the interval $P(u)$ and $P(u) + dP(u)$ is

$$x(u)du = \frac{\chi_0}{M_0} \left[\frac{\exp \{ u(\xi - 1) \}}{\xi} \exp \{ \xi(e^{-1} - 1) \} \right] \quad (25)$$

where u in this case ($= \beta t$) varies from zero to infinity. This is to be plotted versus eq. (26):

$$P(\infty) - P(u) = \frac{M_0}{\chi_0} \left[\xi e^\xi \sum_{j=0}^{\infty} \frac{(-\xi)^j}{j!(\xi + j)} \exp \{ -(\xi + j)u \} \right] \quad (26)$$

This infinite series may be reduced to a simple well-tabulated function. First write ξe^{-u} as m ,

$$\sum_{j=0}^{\infty} \frac{(-m)^j}{j!(\xi + j)} = \frac{1}{m^\xi} \sum_{j=0}^{\infty} \frac{(-1)^j m^{j+\xi}}{j!(\xi + j)} \quad (27)$$

The right-hand series is known as the incomplete gamma function,²¹ $\gamma(\xi, m)$,

$$\gamma(\xi, m) = \int_0^m e^{-t} t^{\xi-1} dt = \sum_{j=0}^{\infty} \frac{(-m)^{j+\xi}}{j!(\xi + j)}$$

It is easy to show by repeated integration by parts that, for integral ξ ,

$$\gamma(\xi, m) = \Gamma(\xi) [1 - e^{-m} e_{\xi-1}(m)]$$

where $e_{\xi-1}(m)$ is the truncated exponential function,²¹ i.e.,

$$e_{\xi-1}(m) = \sum_{j=0}^{\xi-1} m^j/j!$$

Simple manipulation gives

$$\gamma(\xi, m) = \Gamma(\xi) \sum_{j=\xi}^{\infty} m^j e^{-m}/j! = \Gamma(\xi) P(\xi, m) \quad (28)$$

where $P(\xi, m)$ is the extensively tabulated summed Poisson distribution.²² If ξ is not an integer, there do exist tables of incomplete gamma functions which can be used.²¹ Equation (26) may then be written

$$P(\infty) - P(u) = (M_0/\chi_0) [\Gamma(\xi + 1) e^{\xi/\xi} P(\xi, m)] \quad (29)$$

Figure 3 shows eq. (25) plotted versus eq. (29) for several values of ξ .

The numerical evaluation of h.i. for this case is considerably more difficult, and the final result is given (see Appendix) for integral ξ by eq. (30):

$$h(\xi) = \frac{\Gamma^2(\xi)}{\xi^{2\xi+1}} \left[\xi - 2 \sum_{j=1}^{\xi} P(j, \xi) + \frac{1}{2} \sum_{j=1}^{\xi} P(j, 2\xi) + \frac{1}{2} \sum_{n=\xi}^{2(\xi-1)} P(n+1, 2\xi) \sum_{j=n-(\xi-1)}^{\xi-1} \binom{1/2}{j} C_j^n \right] \quad (30)$$

where the $P(j, x)$ are the same functions as before and C_j^n are binomial coefficients. The quantities $\binom{1/2}{j} C_j^n$ are also well-tabulated,²² and so the last summation consists simply of adding a column of numbers from a table. The heterogeneity index is then

$$\text{h.i.} = \xi e^{2\xi} h(\xi) \quad (31)$$

This is plotted versus ξ in Figure 2.

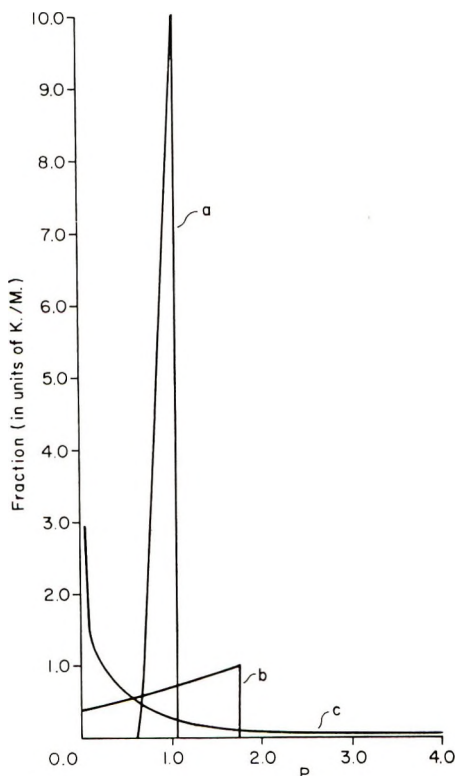


Fig. 3. Fraction vs. degree of polymerization for case III: (a) $\eta = 0.10$; (b) $\eta = 1.0$; (c) $\eta = 10.0$. The fraction is in units of χ_0/M_0 and D.P. is in units of M_0/χ_0 . The fraction is in units of χ_0/M_0 and D.P. is in units of M_0/χ_0 .

In Figure 2, the heterogeneity index is plotted for the range of 1.01 to 10. While it is true that values as low as 1.01 have not, as yet, been achieved, values of ca. 1.05 have. Whether this is due to mixing problems or to statistical fluctuations is not really clear, what is important is that this probably represents the lower limit of our calculations, and that this, therefore, is most probably our limit of accuracy.

To clarify the orders of magnitude involved in calculations of this type, we give one illustrative example. We wish to prepare a sample of polystyrene of heterogeneity index 4.0 and a P_n of 1000 by adding the initiator at a constant rate. The concentration of monomer in the original THF solution is 1.0 mole/l., which means that the total (final) initiator concentration χ_0 must be 10^{-3} mole/l. We take the rate constant for the propagation reaction to be $k_p = 250$ l./mole-sec. From Figure 2, we see that a heterogeneity index of 4.0 (h.i. - 1 = 3.0) requires the product of k_p , χ_0 , and α , the total time of addition of initiator, to be 25. Thus, we calculate α to be $25/250 \times 10^{-3} = 100$ sec. Therefore, if the initiator solution is added over a period of 100 sec. to the monomer solution, the final polymer should have an h.i. of 4.0.

In summary, we have described a technique for the anionic synthesis of polymers with tailored heterogeneity indices, if the rate constant for the polymerization reaction and the rate of initiator addition are known. Conversely, from a knowledge of the rate of addition of initiator and of the heterogeneity index, it becomes possible to estimate the rate constant for the propagation reaction.

Finally, we wish to stress that in view of the assumptions outlined in section II, the present treatment is only an approximation. In particular, it should be recalled that the apparent rate constant for chain propagation is not absolutely constant, but varies with initiator concentration as was shown by Szwarc et al.¹⁹ due not only to the dissociation of ion-pairs²⁴ but also to the formation of triple ions.^{25,26} Furthermore, the calculations were performed for single-ended polymers, while materials initiated by sodium naphthalene are usually two-ended, i.e., possessing "living" anions at both ends of the molecule. Also, the distribution may be altered by having both active and dormant ends rather than only active ends.²⁷ The extent to which the approximations made here affect the results of the calculations is now being tested experimentally.

APPENDIX

Recall that

$$\text{h.i.} = h(\xi)/g^2(\xi) \quad (32)$$

where

$$g(\xi) = \sum_{j=0}^{\infty} \frac{(-\xi)^j}{j!(\xi+j)(\xi+j+1)} \quad (33)$$

$$h(\xi) = \sum_{j=0}^{\infty} \sum_{k=0}^{\infty} \frac{(-\xi)^{j+k}}{j!k!(\xi+j)(\xi+k)(1+2\xi+j+k)} \quad (34)$$

We consider $g(\xi)$ first. By partial fractions,

$$g(\xi) = \sum_{j=0}^{\infty} \frac{(-\xi)^j}{j!(\xi+j)} - \sum_{j=0}^{\infty} \frac{(-\xi)^j}{j!(\xi+1+j)} \quad (35)$$

$$= (1/\xi^\xi)\gamma(\xi, \xi) - (1/\xi^{\xi+1})\gamma(\xi+1, \xi) \quad (36)$$

On using the recursion formula for the incomplete gamma function,²¹

$$\gamma(a+1, x) = a\gamma(a, x) - x^a e^{-x} \quad (37)$$

$g(\xi)$ becomes

$$g(\xi) = e^{-\xi}/\xi \quad (38)$$

We consider now $h(\xi)$. Equation (34) may be written

$$\begin{aligned} h(\xi) &= \sum_{j=0}^{\infty} \sum_{k=0}^{\infty} \frac{(-1)^{j+k}}{j!k!(\xi+j)(\xi+k)} \frac{1}{\xi^{2\xi+1}} \int_0^{\xi} y^{j+k+2\xi} dy \\ &= \frac{1}{\xi^{2\xi+1}} \int_0^{\xi} dy \left(\sum_{j=0}^{\infty} \frac{(-y)^{j+\xi}}{j!(j+\xi)} \right)^2 \\ &= \frac{1}{\xi^{2\xi+1}} \int_0^{\xi} dy [\gamma(\xi, y)]^2 \end{aligned} \quad (39)$$

Now for integer values of ξ ,

$$\gamma(\xi, y) = \Gamma(\xi) [1 - e_{\xi-1}(y)e^{-y}] \quad (40)$$

so

$$\begin{aligned} h(\xi) &= \frac{\Gamma^2(\xi)}{\xi^{2\xi+1}} \left[\int_0^{\xi} dy - 2 \int_0^{\xi} e^{-y} e_{\xi-1}(y) dy \right. \\ &\quad \left. + \int_0^{\xi} e^{-2y} e_{\xi^2-1}(y) dy \right] \end{aligned} \quad (41)$$

We now consider these two integrals:

$$\begin{aligned} \int_0^{\xi} e^{-y} e_{\xi-1}(y) dy &= \sum_{j=0}^{\xi-1} (1/j!) \int_0^{\xi} e^{-y} y^j dy \\ &= \sum_{j=0}^{\xi-1} \gamma(j+1, \xi) / j! \\ &= \sum_{j=1}^{\xi-1} P(j+1, \xi) = \sum_{j=1}^{\xi} P(j, \xi) \end{aligned} \quad (42)$$

By eq. (28) we have:

$$\begin{aligned} \int_0^{\xi} e^{-2y} e_{\xi^2-1}(y) dy &= \sum_{j=0}^{\xi-1} \sum_{k=0}^{\xi-1} \frac{1}{j!k!} \int_0^{\xi} e^{-2y} y^{j+k} dy \\ &= \frac{1}{2} \sum_{j=0}^{\xi-1} \sum_{\eta=j}^{\xi-1+j} \frac{\gamma(\eta+1, 2\xi)}{2^{\eta} j! (\eta-j)!} \\ &= \frac{1}{2} \sum_{\eta=0}^{\xi-1} \sum_{j=0}^{\eta} P(\eta+1, 2\xi) \frac{\eta!}{2^{\eta} j! (\eta-j)!} \\ &\quad + \frac{1}{2} \sum_{\eta=\xi}^{2(\xi-1)} \sum_{j=\eta-(\xi-1)}^{\xi-1} P(\eta+1, 2\xi) (1/2)^{\eta} C_j^{\eta} \\ &= \frac{1}{2} \sum_{j=1}^{\xi} P(j, 2\xi) + \frac{1}{2} \sum_{\eta=\xi}^{2(\xi-1)} \\ &\quad \times P(\eta+1, 2\xi) \sum_{j=\eta-(\xi-1)}^{\xi-1} (1/2)^{\eta} C_j^{\eta} \end{aligned} \quad (43)$$

Substitution of eqs. (42) and (43) into eq. (41) gives eq. (30).

One of us (A.E.) is indebted to the Petroleum Research fund for financial assistance in the course of this work.

We also wish to thank Professor M. Szwarc for a very helpful communication after submission of the manuscript.

References

1. Szwarc, M., *Nature*, **178**, 1168 (1956) and many subsequent publications.
2. Worsfold, D. J., and S. Bywater, *J. Polymer Sci.*, **26**, 299 (1957).
3. McCormick, H. W., *J. Polymer Sci.*, **25**, 488 (1957).
4. Tobolsky, A. V., A. Rembaum, and A. Eisenberg, *J. Polymer Sci.*, **45**, 345 (1960).
5. Bamford, C. H., W. G. Barb, A. D. Jenkins, and P. F. Onyon, *The Kinetics of Vinyl Polymerization by Radical Mechanisms*, Academic Press, New York, 1958.
6. Eisenberg, A., and A. Rembaum, *J. Polymer Sci. B*, **2**, 157 (1964).
7. Moacanin, J., and A. Rembaum, *J. Polymer Sci. B*, **2**, 979 (1964).
8. Ottolenghi, A., and A. Zilkha, *J. Polymer Sci. A*, **1**, 687 (1963).
9. Flory, P. J., *J. Am. Chem. Soc.*, **62**, 1561 (1940).
10. Brown, W. B., and M. Szwarc, *Trans. Faraday Soc.*, **54**, 416 (1958).
11. Flory, P. J., *Principles of Polymer Chemistry*, Cornell Univ. Press, Ithaca, N. Y., 1953.
12. Gold, L., *J. Chem. Phys.*, **28**, 91 (1958).
13. Nanda, V. S., and R. K. Jain, *J. Chem. Phys.*, **39**, 1363 (1963).
14. Szwarc, M., and M. Litt, *J. Phys. Chem.*, **62**, 568 (1958).
15. Orofino, T. A., and F. Wenger, *J. Chem. Phys.*, **35**, 532 (1961).
16. Coleman, B. D., F. Gornick, and G. Weiss, *J. Chem. Phys.*, **39**, 3233 (1963).
17. Nanda, V. S., *Trans. Faraday Soc.*, **60**, 949 (1964).
- 17b. Figini, R. V., *Z. Physik Chem.*, **38**, 341 (1963).
18. Wenger, F., *J. Am. Chem. Soc.*, **82**, 4281 (1960).
19. Szwarc, M., *Adv. Chem.*, **34**, 96 (1962).
20. von Hostalka, H., R. V. Figini, and G. V. Schulz, *Makromol. Chem.*, **71**, 198 (1964).
21. Erdelyi, A., Ed., *Higher Transcendental Functions*, McGraw-Hill, New York, 1953.
22. Burrington, R. S., and D. C. May, *Handbook of Probability and Statistics*, Handbook Publishers, Sandusky, Ohio, 1953.
23. *Tables of the Incomplete Gamma Function*, K. Pearson, Ed., Cambridge Univ. Press, Cambridge, 1951.
24. Bhattacharyya, D. N., C. L. Lee, J. Smid, and M. Szwarc, *Polymer*, **5**, 54 (1964).
25. Bhattacharyya, D. N., J. Smid, and M. Szwarc, *J. Am. Chem. Soc.*, **86**, 5024 (1964).
26. Bhattacharyya, D. N., C. L. Lee, J. Smid, and M. Szwarc, *J. Phys. Chem.*, **69**, 608, 612, 624 (1965).
27. Szwarc, M., and J. J. Hermans, *J. Polymer Sci. B*, **2**, 815 (1964).

Résumé

On a déduit des équations pour la courbe différentielle de distribution du poids moléculaire et pour l'indice d'hétérogénéité de plusieurs types d'addition successive d'initiateur dans une polymérisation anionique. Tous les résultats sont rigoureux et facilement utilisables, et dépendent seulement du produit de la constante de vitesse de la réaction de propagation, de la concentration totale en initiateur et d'un paramètre représentatif de la vitesse d'addition de l'initiateur. Les résultats sont portés en graphique en fonction du produit mentionné ci-dessus de telle sorte que l'on peut déterminer l'indice d'hétérogénéité auquel on peut s'attendre dans un large domaine de variables.

Zusammenfassung

Gleichungen für die differentielle Molekulargewichtsverteilungskurve und für den Heterogenitätsindex bei verschiedenartig durchgeführtem verzögertem Starterzusatz bei der anionischen Polymerisation werden abgeleitet. Alle Ergebnisse werden in geschlossener und leicht anwendbarer Form erhalten und hängen nur vom Produkt aus der Geschwindigkeitskonstanten der Wachstumsreaktion, der gesamten Starterkonzentration und einem für die Geschwindigkeit des Starterzusatzes charakteristischen Parameter ab. Die Ergebnisse werden gegen das genannte Produkt aufgetragen und so der unter einem grossen Bereich an auftretenden Variablen zu erwartende Heterogenitätsindex bestimmt.

Received December 28, 1964

Revised April 19, 1965

Prod. No. 4750A

Polyoxazolidones Prepared from Bisurethans and Bisepoxides

YOSHIO IWAKURA, SHIN-ICHI IZAWA, and FUSAKAZU HAYANO,
*Department of Synthetic Chemistry, Faculty of Engineering, University of
Tokyo, Tokyo, Japan*

Synopsis

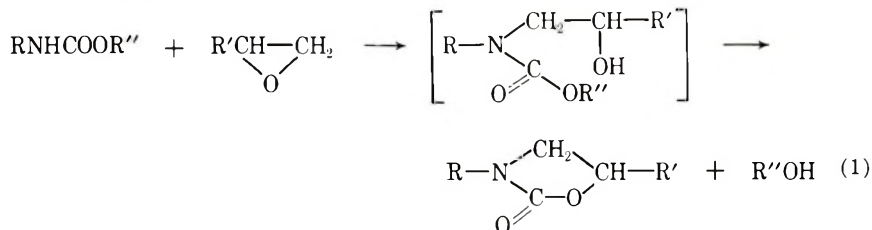
Linear polymers containing oxazolidone rings in the main chain were prepared from difunctional urethans and epoxides by the synthetic method previously used for reaction of monofunctional urethans and epoxides. The similarity of the infrared spectra of polymers and model compounds, bisoxazolidones, showed the presence of oxazolidone rings in a polymer chain. The solubility and softening temperatures of the polymers varied with the urethan unit but not with the bisepoxide structure. Polymers prepared from *p*-phenylenedimethylurethan and variable bisepoxides were insoluble or partially soluble in dimethylformamide, dimethyl sulfoxide, and *m*-cresol and had higher softening temperatures. Polymers from *m*-phenylenediethylurethan or toluenediethylurethan and bisepoxides were soluble in the organic solvents mentioned above, and had lower softening temperatures.

INTRODUCTION

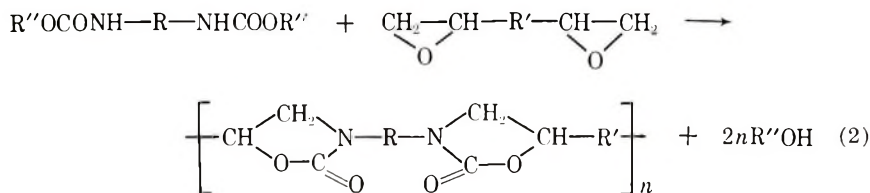
The polymerization of *N*-vinyl- and *N*-propenyloxazolidones has been studied and polymers having pendant oxazolidone rings have been described in recent literatures.¹⁻⁴ However, the preparation of polymers containing oxazolidone rings in the main chain have not been studied in detail. Speranza and Peppel obtained a polyoxazolidone from 2,4-toluene diisocyanate and vinylcyclohexene diepoxide in the course of their investigation of reaction between isocyanate and epoxide using quaternary ammonium salt as a catalyst.⁵ However, a detailed study of the polymer was not made. Oda and his co-workers also obtained polyoxazolidones by the reaction of *p*- and *m*-phenylenediglycidyl ethers and aliphatic diisocyanates using tetraethylammonium bromide as catalyst.⁶ These polymers prepared from diisocyanate and bisepoxide were insoluble in organic solvents and infusible, presumably because the polymers were partially crosslinked.

In a previous paper⁷ dealing with the addition condensation between *N*-aryluurethans and epoxides, it was shown that an intramolecular exchange of alcohol to form 2-oxazolidones occurred, and that tertiary amines and quaternary ammonium salts were effective catalysts for this reaction [eq. (1) on following page].

In this investigation, addition condensation between difunctional ure-



thans and difunctional epoxides was carried out and linear polymers containing oxazolidone rings in the main chain were obtained [eq. (2)].



EXPERIMENTAL

Monomers

Bisurethans and bisepoxides were prepared by the same method described in a previous paper⁷ dealing with monofunctional urethans and epoxides. The bisepoxides were found to be more than 99.5% pure by titration with hydrochloric acid-dioxane.

Bisoxazolidones

A typical preparation was as follows. A mixture of 0.448 g. (0.002 mole) of *p*-phenylenediglycidyl ether and 0.604 g. (0.004 mole) of phenylmethyleurethan was heated at 100°C. until miscible and then 0.1 g. of triethylenediamine was added. As the reaction proceeded, evolution of alcohol was observed, and the mixture became solid at the end of reaction. It was kept at 100°C. for 1 hr. more, and then recrystallized from dimethylformamide; m.p. 216–217°C.

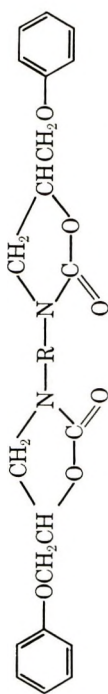
When the urethan and epoxide were immiscible in one at the reaction temperature, dimethylformamide was used as a solvent.

Polyoxazolidones

An example is as follows. A mixture of 1.26 g. (0.005 mole) of *m*-phenylenediethylurethan and 1.11 g. (0.005 mole) of *p*-phenylenediglycidyl ether in 1 ml. of dimethylformamide was heated at 90°C., and then 0.1 g. of triethylenediamine was added. After heating the mixture at 90–100°C. for 30 hr. it was poured into 100 ml. of acetone, and the precipitated polymer was collected by filtration. The isolated polymer was washed with acetone in a Soxhlet extractor for 20 hr. and dried to give 1.81 g. (95% yield) of polyoxazolidone.

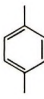
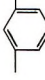
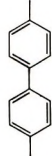
ANAL. Calcd. for $\text{C}_{20}\text{H}_{18}\text{O}_6\text{N}_2$: N, 7.33%. Found: N, 7.09%.

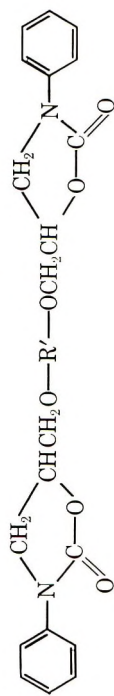
TABLE I
Bisoxazolidones



R	Melting point, °C.	C, %		H, %		N, %	
		Calcd.	Found	Calcd.	Found	Calcd.	Found
	249-253	67.81	67.60	5.25	5.49	6.08	6.25
	198-202	67.81	68.00	5.25	5.32	6.08	5.93
	185-187	71.98	71.55	5.49	5.26	5.09	5.16
	(not crystallized)						

TABLE II
Bisoxazolidones

R'	Melting point, °C.	C, %		H, %		N, %	
		Calcd.	Found	Calcd.	Found	Calcd.	Found
	216-217	67.81	67.58	5.25	5.04	6.08	5.83
	201-204	67.81	67.33	5.25	5.33	6.08	6.04
	247-251	71.63	70.88	5.26	5.28	5.22	5.21



RESULTS AND DISCUSSION

Bisoxazolidones

In order to obtain model compounds, the reactions of bisurethan and phenyl glycidyl ether, and of bisepoxide and phenylmethyleurethan were undertaken at first. *p*-Phenylenedimethylurethan, *m*-phenylenediethylurethan, *p,p'*-diphenylmethanedimethylurethan, and 2,4-toluenediethylurethan were used as difunctional urethans, and *p*-phenylenediglycidyl ether, *m*-phenylene diglycidyl ether, and *p,p'*-diphenylenediglycidyl ether as difunctional epoxides. The addition condensation was generally carried out by heating a mixture of urethan and epoxide at 90–100°C. for 2–4 hr. with triethylamine or triethylenediamine as a catalyst. Corresponding bisoxazolidones were obtained quantitatively in every case. Melting point and elemental analysis data are listed in Tables I and II.

Infrared spectra of bisurethans, bisepoxides, and some synthesized bisoxazolidones are shown in Figures 1 and 2. Samples were examined in Nujol. The most characteristic band shown by all bisoxazolidones was that at 1740 cm^{-1} (C=O stretching). The shift of the absorption band from 1700 cm^{-1} assigned to carbonyl in urethan monomers to 1740 cm^{-1} in bisoxazolidones is attributed to strain in the oxazolidone ring.⁸

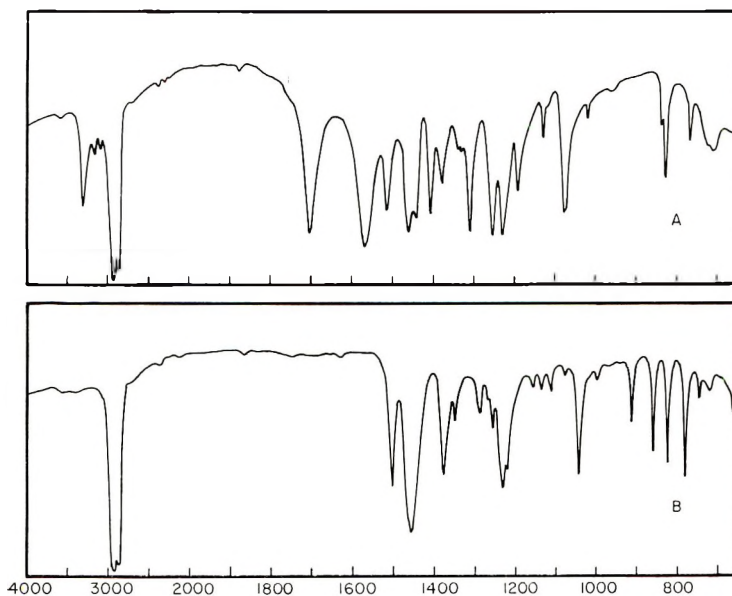


Fig. 1. Infrared spectra of bisurethan and bisepoxide:

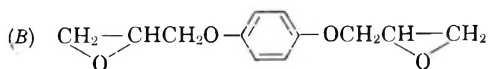
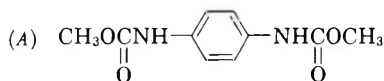
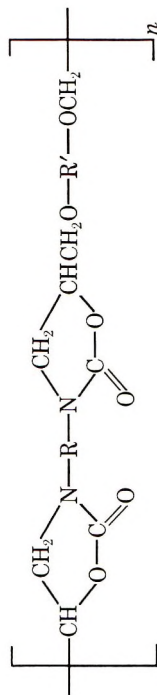
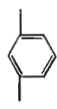
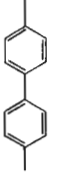
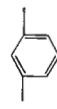
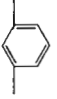

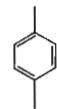

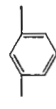
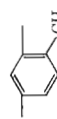
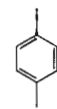
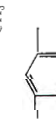
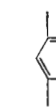


TABLE III
Polyoxazolidones

No.	Chemical Structure		Reaction temp., °C.	Time, hr.	State of the mixture at the end of reaction	Softening temp., °C. ^a	Solubility ^b			η_{inh} (30°C.) ^c
	R	R'					DMF	DMSO	<i>m</i> -Cresol	
1			100	5	Polymer precipit.	—	—	—	—	—
2			90	19	Polymer precipit.	275	—	±	±	—
3			90	27	Polymer precipit.	235	±	±	±	—
4			90	30	Viscous liq.	170	+	+	±	0.18



5			90	32	Liq.	130	+	+	±	0.11
6			90	25	Viscous liq.	165	+	+	±	0.16
7			90	12	Polymer precip.	192	±	±	±	0.09 ^d
8			90	28	Polymer precip.	150	±	±	±	0.11 ^d
9			90	32	Viscous liq.	170	+	+	±	0.10
10			90	28	Viscous liq.	170	+	+	±	0.12

^a Determined on iron hot plate.

^b (+) soluble in cold solvent, (±) soluble in hot solvent, (-) insoluble.

^c Determined in DMF except as noted (*c* = 0.25 g./100 ml.).

^d Determined in *m*-cresol.

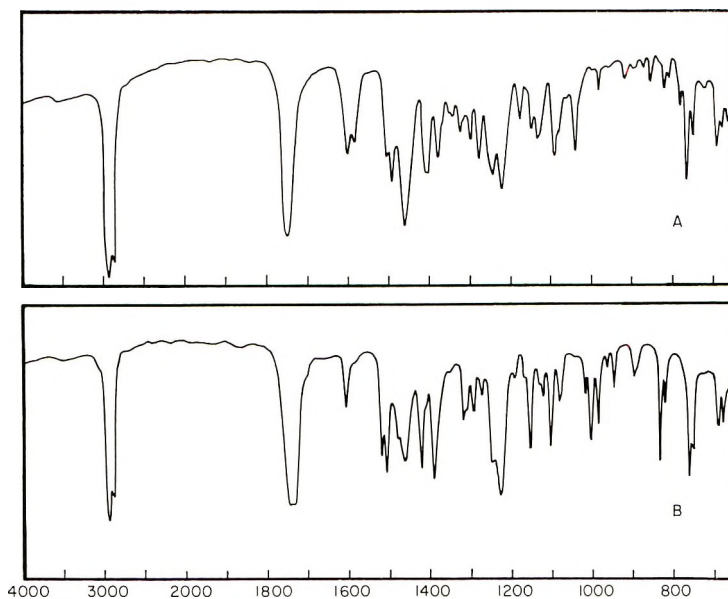
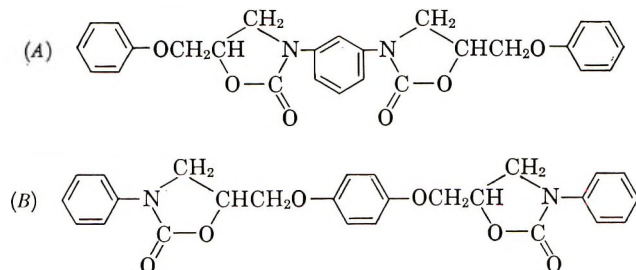


Fig. 2. Infrared spectra of bisoxazolidones:



Polyoxazolidones

Polyoxazolidones were prepared from bisurethans and bisepoxides as described above. Reaction conditions and some properties are listed in Table III.

Infrared spectra of polymers shown in Figure 3 were similar to those of bisoxazolidones. The presence of a band at 1740 cm^{-1} (C=O stretching) rather than at 1700 cm^{-1} indicates that there are oxazolidone rings in the polymer chain. No absorption band arising from O—H was recognized. These facts indicate that the same addition reaction of bisurethan and bisepoxide as that of monourethan and monoepoxide has occurred to form polyoxazolidones.

Examination of the data in Table III shows that the solubility and softening temperature of the polymers are affected by the structure of the urethan component. The polymers derived from *p*-phenylenedimethylurethan were scarcely soluble in organic solvents and had high softening temperatures. The polymer from *p*-phenylenedimethylurethan and *p*-phenylene diglycidyl ether was especially insoluble and had no softening temperature;

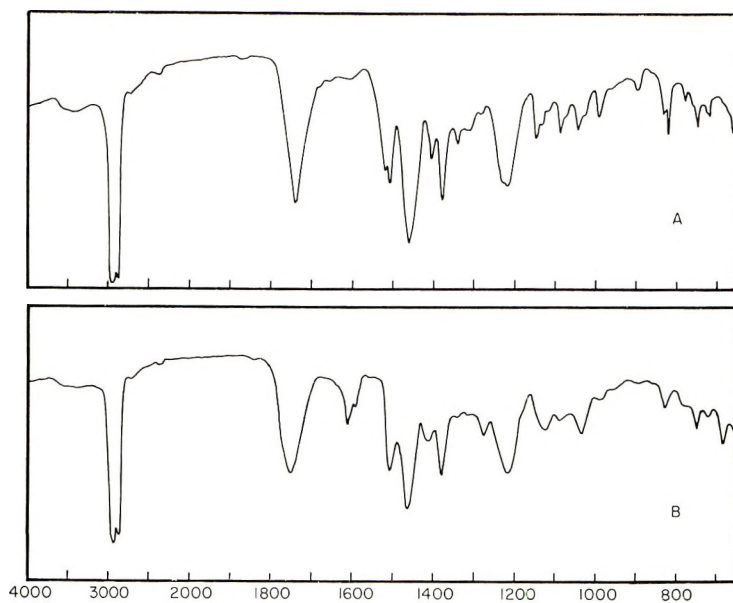
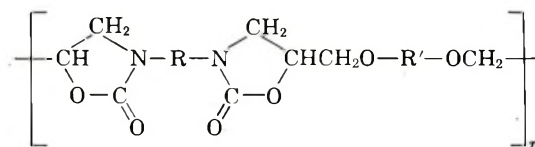


Fig. 3. Infrared spectra of polyoxazolones:odi



(A) R=R' = *p*-phenylene; (B) R = *m*-phenylene; R' = *p*-phenylene.

it gradually decomposed at 250–300°C. Consequently the polymer precipitated before a high molecular weight was reached. When *m*-phenylenediethylurethan, which contains an unsymmetrically substituted benzene ring, was substituted as the urethan component, the solubility in organic solvents increased and the softening temperature was lowered.

The epoxide component did not affect the properties of polymers. The reason for this is attributed to the structure of polymers formed: a benzene ring in the urethan component is attached directly on both sides to oxazolidone rings, whereas the benzene ring in the epoxide component is not.

TABLE IV
Effect of Molar Ratio of Monomers

Urethan/epoxide	Yield, % ^a	η_{inh} ^b
1.0/0.8	86	0.13
1.0/0.9	89	0.12
1.0/1.0	90	0.14
0.9/1.0	95	0.15
0.8/1.0	97	0.14
0.5/1.0	gelation	—

^a Calculated on monomer used.

^b Determined at a concentration of 0.5 g./100 ml. in dimethylformamide at 30°C.

These polymers were insoluble in common organic solvents, such as acetone, alcohols, and ethers.

In these polyaddition condensation reactions it is to be expected that the molar ratio of the monomers should affect the molecular weight, and that the maximum inherent viscosity should occur at the stoichiometric ratio. However, the results listed in Table IV do not show a peak in inherent viscosity. Furthermore, gelation occurred when one mole of bisurethan and two moles of bisepoxide were used. This fact suggests that self-polymerization of bisepoxide occurred when bisepoxide was used in excess.

References

1. Drechsel, E. K., *J. Org. Chem.*, **22**, 849 (1957).
2. Hart, R., *Makromol. Chem.*, **31**, 223 (1959).
3. Bork, J. F., and L. E. Coleman, *J. Polymer Sci.*, **43**, 413 (1960).
4. Bakke, W. W., W. E. Walles, and W. F. Tousignant (to Dow Chemical Co.), U. S. Pat. 2,993,031 (July 18, 1961).
5. Speranza, G. P., and W. J. Poppel, *J. Org. Chem.*, **23**, 1922 (1958).
6. Oda, R., S. Takiura, A. Miyasu, and M. Okano, *Kobunshi Kagaku*, **17**, 72 (1960).
7. Iwakura, Y., and S. Izawa, *J. Org. Chem.*, **29**, 379 (1964).
8. Pinchas, S., and D. Ben-Ishai, *J. Am. Chem. Soc.*, **79**, 4099 (1957).

Résumé

Des polymères linéaires contenant des cycles oxazolidones dans la chaîne principale ont été préparés au départ d'uréthanes difonctionnels et d'époxydes par une méthode synthétique préalablement utilisée basée sur la réaction d'un uréthane monofonctionnel et d'époxydes. La similarité des spectres infra-rouges des polymères avec ceux des dérivés modèles bisoxazolidoniques montrent la présence des cycles d'oxazolidones dans la chaîne polymérique. La solubilité, les températures de ramollissement des polymères varient avec la structure de l'unité uréthannique mais non pas avec la structure du bisépoxyde. Les polymères préparés au départ de *p*-phénylènediméthyluréthane et de divers époxydes sont insolubles et partiellement solubles dans le diméthylformamide, le diméthylsulfoxyde et le *m*-crésol, et ont des températures de ramollissement plus élevées. Les polymères au départ d'un *m*-phénylènediéthyluréthane ou toluènediéthyluréthane et de bisépoxydes sont solubles dans les solvants organiques mentionnés ci-dessus, et ont des températures de ramollissement plus basses.

Zusammenfassung

Lineare Polymere mit Oxazolidonringen in der Hauptkette wurden aus difunktionellen Urethanen und Epoxyden mit der früher für die Reaktion von monofunktionellen Urethanen mit Epoxyden benutzten synthetischen methode dargestellt. Die Ähnlichkeit der Infrarotspektren der Polymeren und der als Modellverbindungen verwendeten Bisoxazolidone liessen die Anwesenheit von Oxazolidonringen in der Polymerkette erkennen. Die Löslichkeit und die Erweichungstemperatur der Polymeren hingen vom Urethanbaustein, aber nicht von der Bisepoxydstruktur ab. Aus *p*-Phenylendimethylurethan und verschiedenen Bisepoxyden dargestellte Polymere waren nicht oder nur teilweise löslich in Dimethylformamid, Dimethylsulfoxyd aus *m*-Kresol und besaßen höhere Erweichungstemperaturen. Polymere aus *m*-Phenylendiäthylurethan oder Toluoldiäthylurethan und Bisepoxyden waren in den oben erwähnten organischen Lösungsmitteln löslich und besaßen niedrigere Erweichungstemperaturen.

Received June 7, 1965
Prod. No. 4864A

Catalytic Polymerizations of Nitrobenzene and Aniline

PAUL SIGAL,* PHILIP MASCIANTONIO, and PAUL FUGASSI, *Coal Research Laboratory, Carnegie Institute of Technology, Pittsburgh, Pennsylvania*

Synopsis

Nitrobenzene refluxed over a variety of solid catalysts near its standard boiling point of 211°C. polymerizes to give compounds whose structure appears to be that of a triaryl amine polymer. Under similar conditions aniline gives polymers whose structure appears to be a mixture of diaryl and triaryl amine bonds.

INTRODUCTION

In an attempt to substantiate a suggested coalification reaction involving aromatic condensation,¹ the polymerization of nitrobenzene was undertaken. Preliminary work indicated that the nitrobenzene polymerization did not proceed by diaryl bond formation with elimination of hydrogen, but rather with the formation of aryl-nitrogen linkages. However, since polymer chain backbones containing phenylene linkages are thought to impart useful physical properties to the polymer,² a great deal of work has been done in an attempt to develop such polymers. For this reason, and because no high molecular weight, linear polymers containing only one atom between phenylene linkages have been reported in the literature, a further study of the nitrobenzene polymer was deemed desirable. This paper presents a study of the polymerization of nitrobenzene over a series of solid catalysts and the characterization of the products of the polymerization. A study of the catalytic polymerization of aniline, performed in conjunction with the nitrobenzene polymerization experiments, is also presented.

EXPERIMENTAL

Preparation of Monomer and Catalyst

The standard nitrobenzene polymer was prepared by distillation of Fisher certified reagent grade nitrobenzene at atmospheric pressure. A 0.5°C. boiling range fraction was taken and kept in a storage buret protected from water vapor.

* Present address: Department of Chemistry, University of Detroit, Detroit, Michigan.

The aniline polymerizations were carried out with National Aniline Co. high purity material which was kept stored under nitrogen.

The catalysts used in the form of salts were prepared in gel form by shock precipitation where possible. Elemental metal catalysts were usually used in the purest and most finely divided form commercially available.

Catalyst Study

In order to determine a suitable catalyst for the preparation of nitrobenzene polymer, the catalytic efficiency of a series of metals and metal salts (oxides, sulfides, ferro- and ferricyanides) was examined. The series included copper, iron, gold, potassium, manganese, lead, zinc, cobalt, and platinum metals and certain of their compounds.

Nitrobenzene was polymerized over each of the catalysts under standardized conditions. In each case a catalyst-monomer weight ratio of 0.08 was used. The systems were kept at reflux at atmospheric pressure for 14 days. The unreacted nitrobenzene was then separated from the crude reaction mixtures by distillation and the residual polymeric materials weighed.

Aniline was polymerized in the presence of a number of catalysts including iron, cobalt, nickel, copper, manganese, and platinum compounds under conditions similar to those used in the nitrobenzene experiments. After separation, the polymeric materials were weighed. Whenever the yields permitted, infrared spectra of the nitrobenzene and aniline polymers were taken.

Closed-System Polymerizations

After determination of the most efficient catalyst for each system, a set of polymerizations was performed under helium in a closed system at reflux (1 atm.) so that all evolved by-products and intermediates could be trapped. The reaction vessel was equipped with an air condenser followed by a cold trap kept at ice temperatures. Any materials not condensed in the cold trap were collected in a eudiometer bulb. Evolution of noncondensable gases was followed as a function of time. Materials collected in the cold trap during the course of the polymerizations were identified by melting point and infrared spectrum. Noncondensable gases collected in the eudiometer tube were identified by mass spectral analysis. Conversions were limited to a fraction of 1% based on the total amount of condensable materials.

The nitrobenzene polymerizations were catalyzed by a cupric ferrocyanide gel and aniline by Adam's catalyst, $\text{PtO}_2 \cdot \text{H}_2\text{O}$.

The crude nitrobenzene polymeric mixtures remaining in the closed-system reaction flasks were subjected to vacuum distillation, fractions taken and identified, where possible, by infrared spectrum and melting point. The nondistillable black nitrobenzene polymer was subjected to a series of fractional extraction schemes with the usual organic solvents. The extracts were dried and infrared spectra taken.

In the aniline experiments, the crude mixture remaining in the closed-system reaction flask was steam distilled to effect removal of the unreacted aniline. The residue was vacuum distilled through a spinning band column and infrared spectra of all fractions taken. The nondistillable fraction was subjected to a series of solubility tests.

Molecular weights of the soluble nitrobenzene polymer fraction were determined cryoscopically in nitrobenzene. Molecular weights of the aniline polymer fractions were determined by cryoscopic and ebullioscopic methods in benzene.

Elemental analyses of the nitrobenzene and aniline polymers were done by the usual methods. Nuclear magnetic resonance spectra of the nitrobenzene polymer were taken in deuteriochloroform with tetramethylsilane as internal standard.

Model Compounds

Each of the six members of the ring, ring-prime dinitrobiphenyl series was obtained and polymerized over the cupric ferrocyanide gel. Infrared spectra of each polymer was taken and compared with that of the nitrobenzene polymer.

Diphenylamine, benzidine, carbazole, and *N,N'*-diphenyl-*p*-phenylenediamine were polymerized over Adam's catalyst. Infrared spectra were taken and compared with that of the aniline polymer.

Nitrobenzene-Aniline Polymer Correlation

A sample of the nondistillable nitrobenzene polymer was extracted with benzene and reduced under 5 atm. of H_2 at room temperature over Adam's catalyst. Removal of the catalyst and solvent yielded a product which was partially soluble in concentrated HCl with formation of a green solution. Neutralization of the solution with KOH gave a purple precipitate. The infrared spectrum of the precipitate was taken and compared to that of the total aniline polymer.

RESULTS AND DISCUSSION

Catalyst Study

Cupric ferricyanide and cupric ferrocyanide gels gave the largest yield of nitrobenzene polymer, about 50%. Ferrocyanides of the other metals gave yields of less than 5% and zinc cobalticyanide gave no conversion. Polymerization of aniline proceeded to conversions of 1-20%, with copper and iron compounds producing the higher yields. In most cases a typical purple polymer was obtained.

A sample of the nitrobenzene monomer was refluxed for 31 days in the absence of catalyst with only slight discoloration and no detectable amount of polymer resulting. A sample of the aniline monomer was refluxed for 100 days without catalyst with the formation of 0.2% of solid polymeric material.

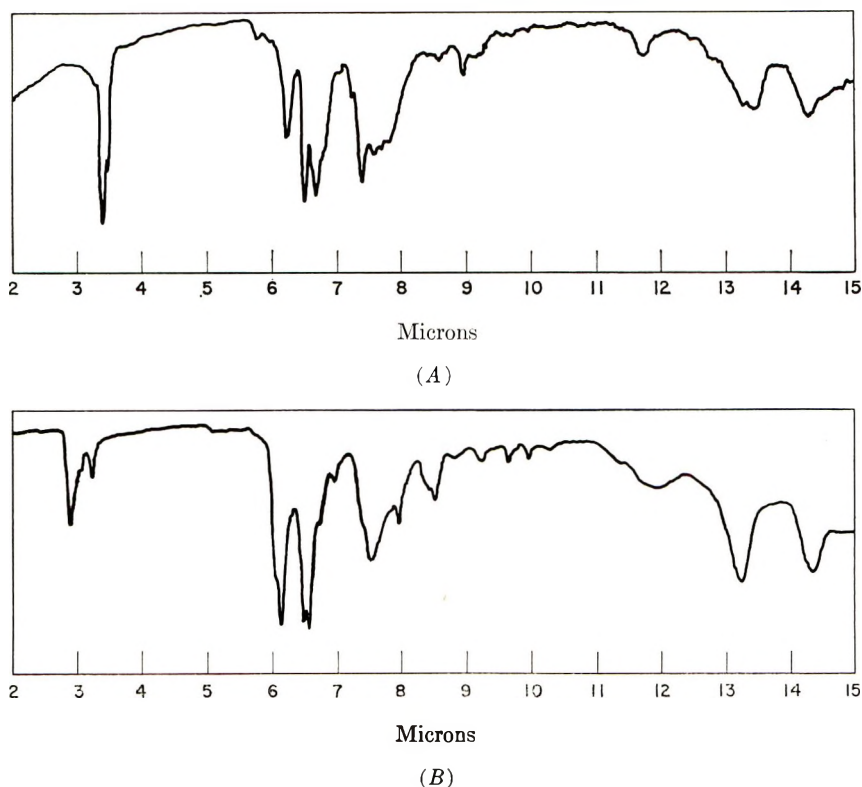


Fig. 1. Infrared spectra of (A) nitrobenzene polymer and (B) aniline polymer.

The infrared spectra of the nitrobenzene polymers appeared to be nearly identical regardless of the catalyst used. A typical spectrum is shown in Figure 1. The infrared spectra of the typical purple polymers of aniline also appeared independent of catalyst. These are shown in Figure 1

Closed Systems

The polymerization of nitrobenzene was accompanied by the formation of nitrosobenzene and a material tentatively identified as β -phenylhydroxylamine. The noncondensable gases collected in the eudiometer bulb were identified as CO_2 and N_2 in approximately 2:1 mole ratio. The rate of gas evolution was 1.7×10^{-4} mole/hr. and was found to be independent of catalyst-monomer ratio and time. However, a sharp break always appeared in the gas evolution rate curve at a point corresponding to nearly complete conversion of the catalyst cyanide to CO_2 and N_2 . Trace amounts of benzene, ammonia, and water were also detected in the off-gases.

Upon vacuum distillation of the crude reaction mixture, small amounts of nitrosobenzene evolved below 100°C . Above 100°C , the unreacted nitrobenzene distilled over. From 175 to 225°C , a yellow sublimate identified as phenazine appeared. At 190°C , a red oil began to distill out of the

residue and continued to appear as the temperature was raised. Evolution of the red oil and phenazine continued for about 20 hr. The nondistillable black residue corresponded to about 50% conversion. The red oil and phenazine yields were estimated to represent about 1% conversion. The infrared spectrum of the red oil showed slightly greater resolution than, but was otherwise identical to, the spectrum of the black polymeric residue. Both spectra were identical to the spectra of the total nitrobenzene polymers shown in Figure 1.

The black nitrobenzene polymer was subjected to a series of fractional extraction schemes with the usual organic solvents. Only chloroform, pyridine, quinoline, and nitrobenzene were found to be capable of dissolving more than a few per cent of the polymer. About 30–40% of the polymer was soluble in chloroform, and about 60–70% was soluble in nitrobenzene, the best solvent. However, a saturated chloroform solution contained only about 8% by weight. Infrared spectra of all dried extracts were identical.

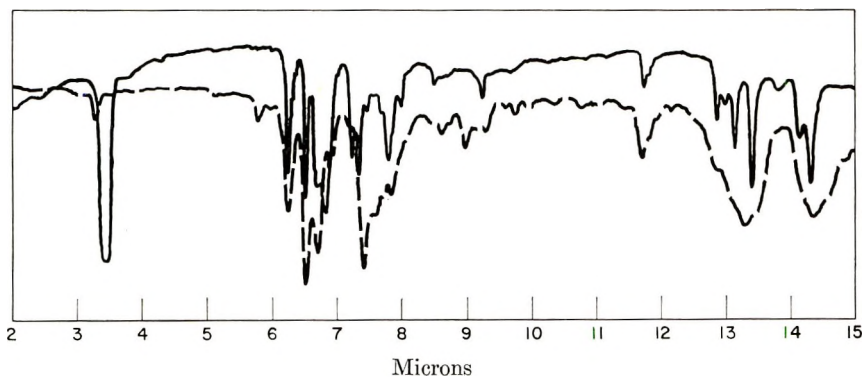


Fig. 2. Infrared spectra of (—) 2-nitrotriphenylamine (Nujol mull), and (---) red oil nitrobenzene polymer (pure film).

The average molecular weight of the chloroform-soluble fraction of the nitrobenzene polymer was found to be about 1500. The molecular weights of the other fractions could not be determined because of their low solubility. Elemental analyses of the nitrobenzene polymers did not yield consistent results. Values for hydrogen varied from 3.4 to 3.9%; for carbon, from 67 to 72%; for nitrogen, from 8 to 14%. The nitrogen assays were probably low due to the usual difficulty in determining nitro nitrogen. The carbon:hydrogen atomic ratios, however, did group about 6:4, indicating a disubstituted aromatic structure.

Each of the six ring, ring-prime dinitrobiphenyl model compounds was found to polymerize over the cupric ferrocyanide gel. The infrared spectrum of each of the polymers was similar to that of its monomer. However, little correlation existed between any of these polymer spectra and the nitrobenzene polymer spectrum.

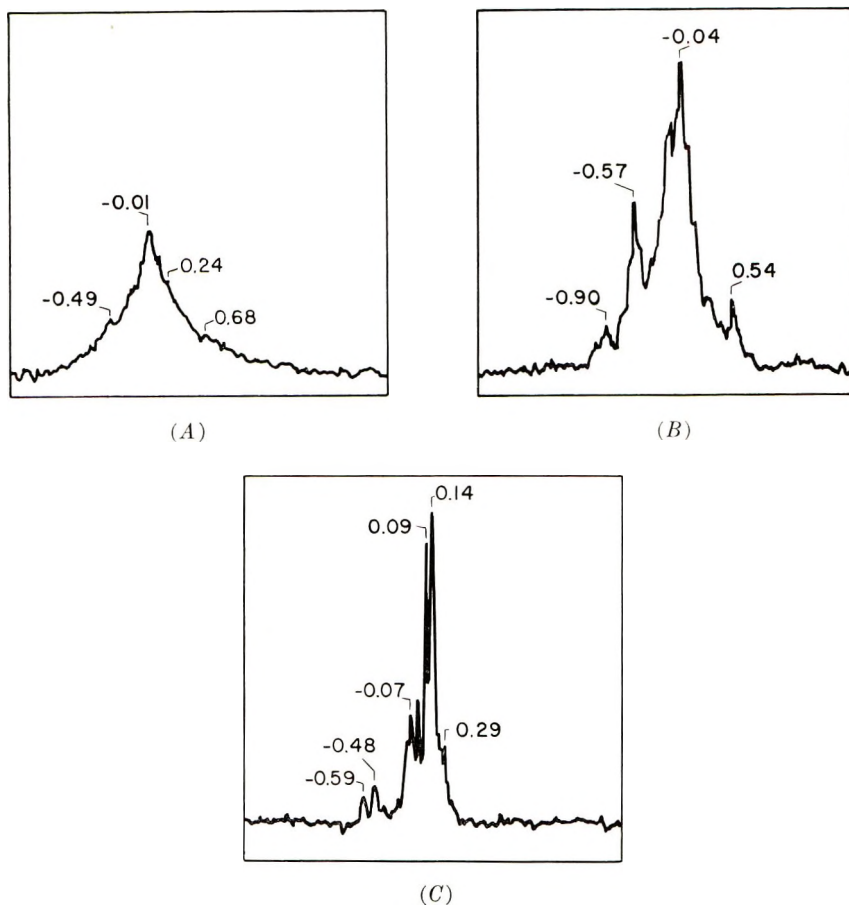


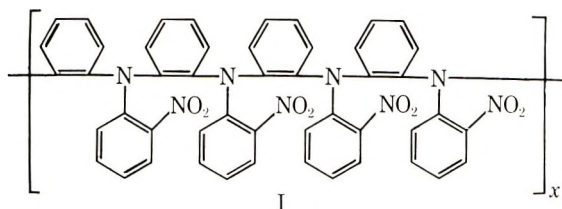
Fig. 3. NMR spectra of (A) black nitrobenzene polymer, (B) red oil nitrobenzene polymer, and (C) 2-nitrotriphenylamine.

The infrared spectra of a number of nitro-substituted aromatic amines were obtained and compared to that of the black nitrobenzene polymer and lower molecular weight red oil. The spectrum of 2-nitrotriphenylamine was found to fit almost perfectly within the envelope described by the nitrobenzene red oil polymer spectrum (see Fig. 2), which in turn fit within the more poorly resolved envelope of the black nitrobenzene polymer spectrum. Correspondence between the spectra of the nitrobenzene polymers and 4-nitrotriphenylamine was poor.

The aromatic portion of the proton resonance spectra of the chloroform soluble nitrobenzene polymers are shown in Figure 3, along with the spectrum of 2-nitrotriphenylamine. Numbers attached to the lines are chemical shifts in parts per million referred to benzene as zero. The salient features are as follows.

The black polymer spectrum shows a line at +6.05 ppm (not shown) which represents only about 6-7% of the total hydrogen of the polymer.

This is probably due to some hydroaromatic hydrogen arising from ring reduction. The rest of the hydrogen of the polymer is aromatic. The aromatic pattern shifts downfield in the order 2-nitrotriphenylamine, black polymer, and red oil polymer. Nitro groups are known to cause a large downfield shift. If the structure I



is postulated for the black polymer, and the red oil is a low molecular weight fraction, then the aromatic patterns are found in the correct relative positions.

The line at -0.57 ppm in the red oil polymer spectrum is probably due to protons *ortho* to nitro groups. The number of such protons per molecule is largest in the case of the postulated red oil polymer structure and diminishes through the postulated black polymer structure to the 2-nitrotriphenylamine. The intensity of the *ortho* proton lines (relative to the total aromatic proton pattern) should then decrease in the same order. Examination of the spectra shows this to be the case.

Polymerization of aniline over Adam's catalyst in the closed system was accompanied by the formation of diphenylamine (ca. 1%). Only trace amounts of gas were evolved and identified as CO_2 and ammonia. A very small amount of molecular hydrogen was detected.

The crude reaction mixture, steam-distilled to effect removal of the unreacted aniline and the diphenylamine, yielded a purple residue corresponding to 6% conversion. Vacuum distillation of the purple polymer through a spinning band column gave a series of yellow and red oils with a black residue remaining as the major fraction. The infrared spectrum of the black residue was nearly the same as that of the total aniline polymer.

The purple aniline polymer was found to be soluble in most organic solvents including benzene and alcohols. However, if the catalyst-monomer ratio (usually about 0.001) used in preparation of the aniline polymer was raised, the products were found to exhibit poor solubility behavior similar to the nitrobenzene polymers.

The average molecular weight of the purple aniline polymer was found to be about 500. Analysis of the aniline polymers gave a nitrogen content which decreased with increasing molecular weight to 8-9%. The nitrogen content of the aniline monomer is 15.1%.

Diphenylamine, benzidine, carbazole, and *N,N'*-diphenyl-*p*-phenylenediamine were found to polymerize over Adam's catalyst. *N,N'*-diphenyl-*p*-phenylenediamine yielded a purple polymer whose infrared spectrum (see Fig. 4) was similar to that of the aniline polymer.

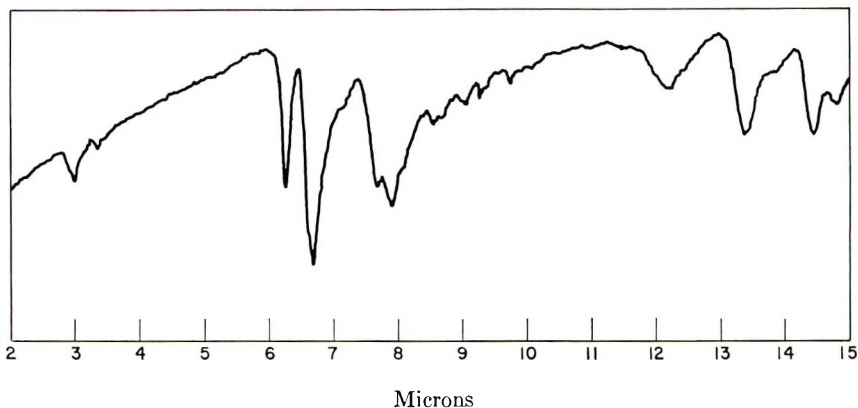


Fig. 4. Infrared spectra of purple polymer from *N,N'*-diphenyl-*p*-phenylenediamine.

Nitrobenzene-Aniline Polymer Correlation

The infrared spectrum of the purple precipitate obtained by reduction of the nitrobenzene polymer was found to be similar to the infrared spectrum of the purple aniline polymer. Both the precipitate and the purple aniline polymer were partially soluble in concentrated HCl with the formation of a green solution.

DISCUSSION AND CONCLUSIONS

The postulated structure for the nitrobenzene polymer, a nitro-substituted triaryl amine, is consistent with infrared and NMR data and with elemental analyses. This structure is similar to that of aniline black.^{3,4} The occurrence of phenazine and possibly β -phenylhydroxylamine as intermediates in earlier work on aniline black and as distillation products in our work also tends to support the above structure.⁵⁻⁷

The most efficient catalyst for nitrobenzene polymer formation is probably not cupric ferrocyanide gel but a copper-iron compound formed *in situ*, since other ferrocyanides and other copper compounds show low catalytic efficiency.

Formation of the same polymer over any of a number of catalysts suggests that the polymer structure is thermodynamically favored. The preferred nature of the structure is also indicated by the formation of only a single repeating unit; the infrared spectra of all polymer fractions are identical.

The evidence does not indicate any single structure for the aniline polymer. The phenylenediamine work supports a structure of the diaryl amine type. The similarity of the reduced nitrobenzene and aniline polymers, however, suggests a structure of the triaryl amine type. The formation of aniline black by hydrogenation of aniline over a colloidal platinum catalyst has been previously reported.⁸ It is probable that both

di- and triaryl amine structures are present in the purple aniline and phenylenediamine structures.

The solubility behavior of both the nitrobenzene and aniline polymers is notable. At molecular weights above 1500 the nitrobenzene polymer shows a low solubility characteristic of much higher molecular weight alkyl polymers. This behavior is probably not due to the effect of the nitro group alone, since the aniline polymer also becomes almost totally insoluble in the usual solvents at similar molecular weights. The observed facility with which the nitrobenzene polymer goes into a colloidal state, along with its anomalous solubility behavior, suggests that it exists as a tightly curled macromolecule.

The authors wish to acknowledge the financial support and assistance given to them by the Coal Research Board, Commonwealth of Pennsylvania, under Contract No. CR-27.

References

1. Fugassi, J. P., and R. Trammell, *Chem. Ind. (London)*, **1959**, 654.
2. Edgar, O. B., and R. Hill, *J. Polymer Sci.*, **8**, 1 (1952).
3. Fritzsche, J., *J. Prakt. Chem.*, **20**, 453 (1840).
4. Lightfoot, A., Brit. Pat. 151 (1863).
5. Green, A. G., and S. Wolff, *Ber.*, **46**, 33 (1916).
6. Mann, P. J., and B. C. Sanders, *Proc. Roy. Soc. (London)*, **B119**, 47 (1935).
7. Justin-Mueller, E., *Bull. Soc. Chim. France* [5], **1**, 1055 (1934).
8. Kahl, G., and E. Biesalski, *Z. Anorg. Allgem. Chem.*, **230**, 88 (1936).

Résumé

Le nitrobenzène refluxé sur une grande variété de catalyseurs solides près du point d'ébullition à 211°C polymérise pour former des composés dont la structure est semblable à des polymères de triarylamines. Dans des conditions semblables, l'aniline forme des polymères dont la structure semble correspondre à un mélange de liens amines diaryliques et triaryliques.

Zusammenfassung

Nitrobenzol polymerisiert beim Kochen unter Rückfluss über verschiedene feste Katalysatoren in der Nähe seines Standardsiedepunktes von 211°C unter Bildung von Verbindungen, deren Struktur diejenige eines Triarylaminpolymeren zu sein scheint. Unter ähnlichen Bedingungen liefert Anilin Polymere, deren Struktur offenbar aus einer Mischung von Diaryl- und Triarylaminebindungen zu bestehen scheint.

Received December 15, 1964

Revised April 23, 1965

Revised June 26, 1965

Prod. No. 4867A

γ -Irradiation of Siloxane Polymers in Air and Vacuum at Several Temperatures

ROBERT JENKINS,* *Northrop Space Laboratories, Hawthorne, California*

Synopsis

The effects of γ -irradiation on two polysiloxanes in environments of air and vacuum at several selected temperatures were studied. The physical property monitored during the γ -irradiation of the two polysiloxanes was the change in dynamic modulus which, in turn, is proportional to the change in the number of elastically effective chains in the polymer network. The measurements were accomplished by recording *in situ* the free-end response of the polymeric cantilever reeds in forced resonance at and near their fundamental frequency of resonance. The apparent energy of activation of crosslinking for the polydimethylsiloxane polymer was found to be 0.56 kcal./mole in vacuum over a limited temperature range, and 3.5 kcal./mole in air. For the polydimethyl-diphenylsiloxane polymer, the apparent energy of activation was found to be about 1.3 kcal./mole in vacuum, whereas in air the polymer response was complex, displaying both scissioning and crosslinking reactions so that a value could not be obtained. The ability of the pendant phenyl groups to reduce the effective crosslinking rate was found to be sensitive to both temperature and environment.

INTRODUCTION

It is generally concluded that the apparent crosslinking rates of polysiloxanes when irradiated *in vacuo* are enhanced as compared to irradiations performed in air;^{1,2} in addition, increased irradiation temperatures promote increased crosslinking rates,³⁻⁵ whereas substitution of diphenyl pendant groups in exchange for dimethyl in polysiloxanes reduces the crosslinking rate due to the stabilization of the unpaired electron by the phenyl energy sink.^{4,6-8} The purposes of this investigation were (1) to determine the energy of activation of two polysiloxanes, polydimethylsiloxane (PDMS) and polydimethyldiphenylsiloxane (PDMDPS), from their apparent crosslinking rates when irradiations were conducted in air and *in vacuo* at several temperatures and (2) to determine the efficiency of the substituted phenyl groups in reducing the crosslinking rate of the PDMS polymer at several temperatures and to determine if the crosslinking efficiency is temperature dependent.

The kinetic theory of elasticity that relates the stress-elongation-temperature behavior of polymers in their rubbery plateau region offers a convenient equation to follow the change of modulus with changes in either

* Present address: 6061 Sydney Drive, Huntington Beach, California.

the effective elastic chains in the polymer network ν or with temperature changes, providing the strain is small.⁹

$$E = \nu RT [2(L/L_0)^2 + (L_0/L)] [1 - (\bar{M}_c/\bar{M}_n)] \quad (1)$$

where E is Young's modulus of elasticity, ν is the number of moles of elastic chains per unit volume of polymer, R is the gas constant and T is the absolute temperature. L_0 is the unstretched length of the polymer sample, L is the stretched length, \bar{M}_c is the number-average molecular weight between crosslinks, and \bar{M}_n is the number-average molecular weight of the polymer at zero crosslink density. However, for crosslinked bulk polymers as studied in this investigation, $\bar{M}_c/\bar{M}_n \ll 1.0$ and $L_0 \simeq L$, so that eq. (1) is written as

$$E'_{\text{dyn}} \sim 3RT\rho/\bar{M}_c \quad (2)$$

where ρ is the density of the polymer. Equation (2) yields only an approximate relationship for the dynamic modulus, E'_{dyn} , since a static equilibrium condition is not obtained during the measurements. In addition, Tobolsky and others^{9,10} have shown that the stress-strain temperature behavior of rubberlike polymers, above their transition temperatures, are dependent upon a fairly large internal energy contribution at low elongations, whereas eq. (1) was derived from consideration of chain entropy only. Therefore, a front factor is introduced into eq. (2) that includes allowances for both these difficulties.

$$E'_{\text{dyn}} = 3\phi RT\nu \quad (3)$$

Comparison of ν values obtained by both the dynamic modulus and swelling techniques on identically γ -radiation-crosslinked siloxane samples yields a value of about 3.3 for ϕ .¹¹ This value assumes that the equilibrium swelling technique yields a closer approximation to the actual concentration of elastic bonds in the polymer network than does the dynamic method.

The dynamic modulus and swelling techniques allow one to follow the overall effects of both crosslinking and scissioning events which occur simultaneously during the irradiation of the polysiloxanes but does not allow assignments of individual rates for either process.

APPARATUS AND EXPERIMENTAL TECHNIQUE

The polymers examined were commercial gum products consisting of polydimethylsiloxane (PDMS) and polydimethyldiphenylsiloxane (PDMDPS) containing about 7 mole-% of diphenyl units. The gums were lightly crosslinked in sheets $1/8$ -in. thick by about 5.5 Mr γ -radiation from a 5000-c. Co⁶⁰ source. The sheets were then cut into reeds $5/16$ in. wide and 2 in. long and stored at 5°C. for further use.

Reeds (one each of PDMS and PDMDPS) were mounted in a miniaturized vibrating reed apparatus and the dynamic modulus of each determined.¹² The specimen temperatures were held constant by use of a heating element controlled by a thermocouple imbedded in a control

PDMS sample located between the two polymeric reeds. The vacuum was obtained by using a 15-ft.³/min. mechanical pump connected directly to a stainless steel canister containing the vibrating-reed apparatus. The dynamic vacuum system with continuous pumping was preferred over a static system, since any degassing of the polymeric reeds during irradiation will be swept from the system, thus preventing secondary reactions that may retard or accelerate the crosslinking rate.¹³⁻¹⁵

Prior to irradiation, the system was degassed for about 3 hr. at 38°C. Following the degassing the system was lowered into the gamma flux of about 2.6×10^5 r/hr. and the fundamental frequencies of vibrations of the two polymeric reeds recorded at the desired time intervals by sweeping the reeds through a small frequency range of about 20-100 cps. Once the crosslinking rate at 38°C. had been established, the temperature was increased to 66, then 93, and finally 121°C. At each temperature level, the rate of crosslinking was established before proceeding to the next temperature level. A pressure of about 10μ was held during the vacuum irradiations.

The same procedure and apparatus were utilized for the irradiations in air, thus insuring identical exposure conditions with the exception that the canister system was left open to the atmosphere.

RESULTS AND DISCUSSION

Thermal Stability in Air and Vacuum without Radiation

Before any conclusions could be drawn of the combined effects in air, vacuum, temperature, and radiation, the behavior of the polymers as a function of temperature-air and temperature-vacuum had to be determined. Samples of γ -cured PDMS and PDMDPS (90 hr. irradiation in air) were exposed to a temperature of 121°C. for approximately 1 week, first in vacuum (10μ) then in air. The modulus was constant for both polymers during their exposures indicating thermal stability in these environments. At higher temperatures, 149 and 177°C., both polymers exhibited modulus changes. In vacuum, the polymers appeared to crosslink, as evidenced by an increase in modulus, whereas in air a decrease in modulus occurred, indicating an apparent scissioning reaction of the main siloxane chain.

In this investigation it is significant that temperatures of 121°C. or less in either vacuum or air do not cause a change in modulus. Therefore, the comparison of the γ -induced crosslinking rates at the various temperatures and atmospheric environments yields information on the kinetics of the free-radical reactions.

Irradiations in Vacuum and Air Environments at Several Temperatures

Figures 1 and 2 present the results of the change in modulus with γ -radiation exposure at several temperatures of PDMS and PDMDPS in air and

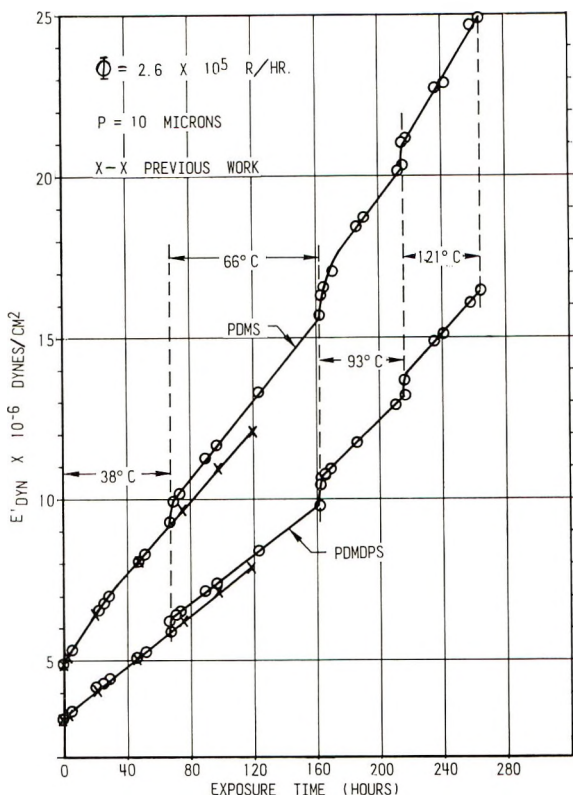


Fig. 1. Change of dynamic modulus with γ -ray exposure at several temperatures in vacuum.

vacuum. The change in moduli with γ -exposure of the samples in vacuum at all temperatures were found to be linear except for the initial portion of the PDMS curve from 0 to 30 hr., where the crosslinking rate was slightly higher than the major portion of the curve. This change of slope appears to be real since reproducibility of this portion of the curve is good, as seen in Figure 1 where the change of modulus with exposure, from a previous investigation, is plotted with the results obtained in this investigation at the 38°C. level.

The changes in modulus with γ -exposure of the siloxanes when irradiated in air at various temperatures show that the PDMS modulus change with exposure time is also linear at all temperature levels studied, whereas the PDMDPS polymer exhibited an initial induction period from 0 to 3 hr. of irradiation. At each temperature change, both polymers exhibited a change of modulus governed by:

$$(dE'/dT)_{\bar{M}_c} = 3\phi\rho R/\bar{M}_c \quad (4)$$

This property change is controlled by \bar{M}_c . The calculated crosslinking rate k , defined as the change in modulus per megareoentgen exposure $dE'_{\text{dyn}}/$

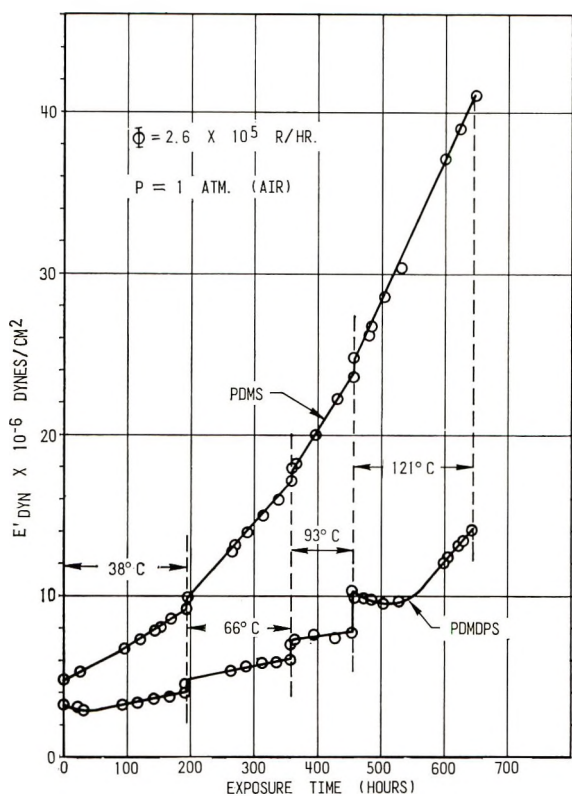


Fig. 2. Change of dynamic modulus with γ -ray exposure at several temperatures in air.

$d(M_r)$ of these polymers in both vacuum and air exposures at various temperatures is presented in Table I. In addition, the ratios of k_{vac}/k_{air} as a function of temperatures are also given. It is significant that, as the irradiation temperature is increased, the k_{vac}/k_{air} ratio of PDMS approaches unity, whereas at lower temperatures the rates diverge and the comparison

TABLE I
Ratios of Vacuum Crosslinking Rates to Air Crosslinking Rates at Several Temperatures

Polymer	Temperature, °C.	$k_{vac} \times 10^{-4}$, dyne/cm. ² /Mr	$k_{air} \times 10^{-4}$, dyne/cm. ² /Mr	Ratio k_{vac}/k_{air}
PDMS	38	21.5	10.2	2.11
	66	23.85	16.15	1.48
	93	24.8	22.7	1.09
	121	32.1	33.4	0.96
PDMAPS	38	15.2	3.84	3.95
	66	14.42	2.69	5.35
	93	18.46	2.11	8.74
	121	20.8	—	—

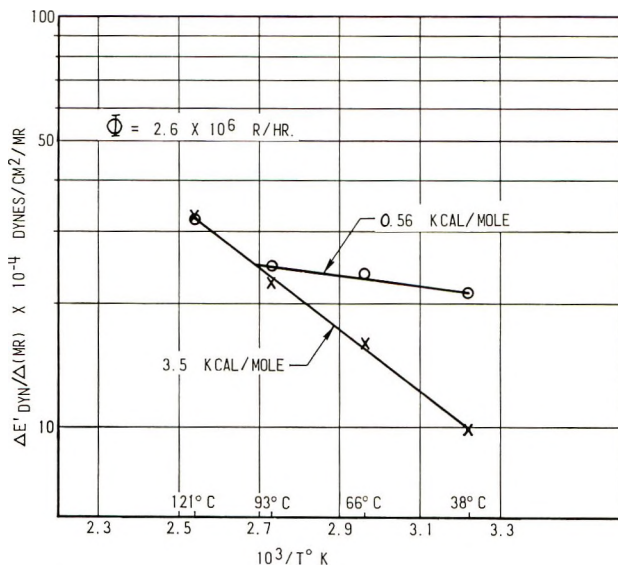


Fig. 3. Crosslinking rate k as a function of $1/T$ for PDMS: (●) in vacuum; (×) in air.

of irradiation effects in an oxygen-containing atmosphere with a vacuum environment become pronounced. The PDMDPS polymer exhibited a complex behavior which will be discussed later.

Figure 3 presents the results of these data as a curve of $\log k$ versus $1/T$ for the PDMS in both air and vacuum environments. It is interesting to note that both curves intersect at about 99°C., at which point the slopes appear to coincide. The change of the crosslinking rate of PDMS at 99°C. agrees with the observation made by Miller⁵ that some type of change in the reaction mechanism does occur at about 100°C. Miller observed a decrease in the apparent crosslinking yield at elevated temperatures when he irradiated liquid PDMS with electrons and postulated that the decrease was due to an ionic rearrangement of the siloxane backbone. The results of this investigation indicate an increased apparent crosslinking rate at temperatures greater than 100°C. The difference in results may be attributed to the polymer's state during irradiation where a moderate amount of crosslinks in the bulk polymer prevent ionic rearrangement. It is interesting to note that Miller's data of gas yields versus irradiation temperatures fit the results of this investigation much better than do his gel yields.

The calculated apparent activation energy of crosslinking for the PDMS in vacuum was found to be 0.56 kcal./mole up to 99°C.; at higher temperatures, the value appears to be 3.5 kcal./mole. This value of 3.5 kcal./mole is also the calculated value found for the PDMS when irradiated in air. The apparent energy of activation of 0.56 supports the value obtained by Koike⁴ of 0.65. Koike suggested that the value of 0.65 most

nearly represented the energy required for rotation of the methyl group about its triad axis to position the free radicals for crosslinking, rather than segmental motion of the main chain. The literature values for the methyl rotational and segmental motion barriers are, respectively, 1.3 and 3.5 kcal./mole.^{16,17}

The mechanism of crosslinking for the PDMS polymer when irradiated in air is not understood. Miller¹ in a recent paper studied the crosslinking yields of PDMS when irradiated under O₂ pressure and tentatively proposed that both $\equiv\text{Si}-\dot{\text{C}}\text{H}_2$ and $\equiv\dot{\text{S}}_i$ radicals are rapidly scavenged by O₂ to form the corresponding peroxy radicals of $\equiv\text{Si}-\text{CH}_2-\text{O}-\text{O}\cdot$ and $\equiv\text{S}_i-\text{O}-\text{O}\cdot$. The $\equiv\text{S}_i-\text{O}-\text{O}\cdot$ radicals, especially at elevated tem-

peratures, are converted to $\equiv\text{S}_i-\text{C} \begin{array}{l} \diagup \text{O} \\ \diagdown \text{OH} \end{array}$, while $\text{S}_i-\text{O}-\text{O}\cdot$ is an inter-

mediate in a reaction forming crosslinks. Miller also ruled out the formation of peroxide $-\text{O}-\text{O}-$ crosslinks due to thermal instability of these bonds. The results of this investigation indicate that the segmental motion of the polymer is probably the principal mechanism by which the free radicals gain position to crosslink, as is evidenced by a calculated activation energy of crosslinking of 3.5 kcal./mole. However, the role of O₂ is obscure.

Figure 4 presents the results of the plot of $\log k$ versus $1/T$ for the PDMDPS when irradiated in air and vacuum. It is apparent from Figures 2 and 4 that the effects produced by irradiation of a phenyl-containing polysiloxane in air are complex. An equilibrium exists between $k_{\text{crosslink}} \rightleftharpoons k_{\text{scission}}$ during irradiation, the position of which is dependent upon temperature, atmosphere, and pendant groups. When irradiations are conducted in vacuum, and the temperature is increased, the crosslinking reaction is highly favored over scissioning reaction. When the irradiations are conducted in an oxygen-containing atmosphere, increased temperatures promote the scissioning reaction, thus causing a subsequent decrease in the rate of change of modulus with radiation exposure. The apparent energy of activation for the PDMDPS polymer when irradiated in vacuum was calculated at about 1.3 kcal./mole. This value does not confirm Koike's results of 0.3 kcal./mole found when he irradiated a 5 mole-% PDMDPS in the liquid state.⁴ The value of 1.3 kcal./mole does suggest that the methyl rotation influences the crosslinking rate to a considerable extent.

Table II compares the crosslinking efficiencies of PDMDPS as compared to PDMS in vacuum and air at several temperatures where the efficiency E is defined as $k_{\text{PDMDPS}}/k_{\text{PDMS}}$. It is tacitly assumed that the crosslinking efficiency of PDMS in vacuum is 100% at each temperature level studied, whereas it is known¹ that the $k_{\text{scission}}/k_{\text{crosslink}}$ ratio for this polymer is about 0.1 at room temperature in the liquid phase and may not be the same ratio at higher temperatures. It is seen that for irradiations conducted in vacuum from 38 to 121°C., the efficiency is constant yielding a value of about 70%, thus revealing that the phenyl protection action in vacuum was

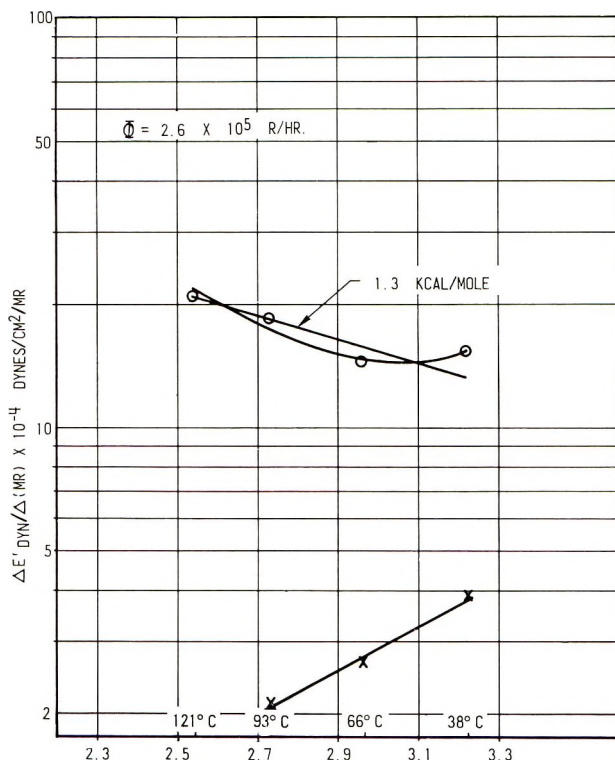


Fig. 4. Crosslinking rate k as a function of $1/T$ for PDMS: (O) in vacuum; (X) in air.

maintained during the course of this irradiation. However, once O_2 is introduced into the system, the crosslinking efficiency is rapidly reduced from about 38% to about 10% as the temperature is increased. These data indicate that the phenyl efficiency in air is temperature-sensitive and that a synergistic effect may exist between the phenyl group and O_2 , causing an increase in the scissioning reaction and/or forms a more efficient energy sink so that the crosslinking reaction is greatly reduced. This mechanism, which results in lowered reaction rates, appears to be more

TABLE II
Crosslinking Efficiency of PDMDPS as Compared to PDMS in
Vacuum and Air

Temperature, °C.	Crosslinking efficiency E , ($k_{\text{PDMDPS}}/k_{\text{PDMS}}$), %	
	Vacuum	Air
38	70.5	37.7
66	60.5	16.7
93	74.4	9.3
121	64.6	—

complex than that of the phenyl group acting only as an electron energy sink.

From Figure 2 for the PDMDPS, it is seen that up to temperatures of 93°C., the crosslinking rate, $k_{\text{crosslink}}$, steadily declines as the temperature is increased. At temperatures of 93°C. and greater, the reaction kinetics become extremely involved, with initial scissioning followed by rapid crosslinking. It is not possible to assign any mechanism at higher temperatures, since the data are so complex. Obviously, this temperature region for the PDMDPS when irradiated in air is in need of further study, as it appears that thermooxidative processes may occur by a synergistic effect of radiation, high temperature, and oxygen.

Color Development

Following the irradiation of both siloxanes in air at the various temperatures employed, it was observed that the PDMDPS had developed a dark brown color, whereas the PDMS had turned a light yellow. In addition, for the irradiations conducted in vacuum, the PDMDPS had discolored to a light yellow, whereas the PDMS remained almost clear but with a tinge of yellow. It is difficult to assign a mechanism for this discoloration of the PDMS polymer since it does not form crossconjugated systems to yield a chromophoric effect. For the PDMDPS irradiated in air, one may suggest that perhaps a quinosiloxane may be formed to yield the dark discoloration similar to the postulation advanced by Achhammer for the discoloration of polystyrene.¹⁸ However, we have not been able to verify a structure by infrared analysis at the present time due to the inherent difficulties in the differential KBR pellet technique. The mechanism for the discolorations that occur during the vacuum irradiations of this polymer is not understood or discussed.

CONCLUSIONS

Vacuum Exposures

Both polymers exhibited a relative linear relationship of $\log k \sim 1/T$ over portions of the selected temperature range investigated. The PDMS exhibited a change of slope of the $\log k \sim 1/T$ curve at about 99°C., indicating a different mechanism of crosslinking. The relative crosslinking efficiency of PDMDPS as compared to PDMS was essentially constant at about 70% over the temperature range studied.

Air Exposure

The PDMS polymer exhibited an approximate linear relationship of $\log k \sim 1/T$ for the temperature range studied. This curve intersected the $\log k \sim 1/T$ vacuum curve of the PDMS at about 99°C., yielding approximately equal apparent activation energies of 3.5 kcal./mole.

The PDMDPS polymer, for the initial temperature range studied, exhibited a positive slope for the $\log k \sim 1/T$ curve, indicating that the in-

creased temperatures were favoring the scissioning reaction. At radiation temperatures greater than 93°C. the polymer exhibited complex behavior of both rapid crosslinking and scissioning.

The crosslinking efficiency of the PDMDPS as compared to PDMS when irradiated in air was drastically reduced as the temperature was increased, indicating a complex synergistic effect between the pendant phenyl groups and available O₂.

It is obvious from this investigation that the effects of high temperature during the irradiation of polymers in air and vacuum are not well understood. It is encouraging that this method offers a possibility of exploring these phenomena *in situ* in moderately extreme environments, and if complemented by *in situ* stress-relaxation studies should help elucidate the mechanism of irradiation conducted at selected temperatures.

The author expresses his appreciation to the Northrop Space Laboratories of the Northrop Corporation for permission to publish this article and to L. Brown who fabricated the apparatus.

References

1. Miller, A. A., *J. Am. Chem. Soc.*, **83**, 31 (1961).
2. Charlesby, A., and P. G. Garratt, *Proc. Roy. Soc. (London)*, **A273**, 117 (1963).
3. Jenkins, R. K., *J. Polymer Sci. B*, **2**, 1147 (1964).
4. Koike, M., *J. Phys. Soc. Japan*, **18**, 3, 387 (1963).
5. Miller, A. A., *J. Am. Chem. Soc.*, **82**, 3519 (1960).
6. Miller, A. A., *Ind. Eng. Chem., Prod. Res. Develop.*, **3**, No. 3, 252 (1964).
7. Koike, M., *J. Phys. Soc. Japan*, **15**, 1501 (1960).
8. Jenkins, R. K., *J. Polymer Sci.*, in press.
9. Tobolsky, A. V., *Properties and Structures of Polymers*, Wiley, New York, 1960.
10. Shem, M. C., paper presented at the 1964 Pacific Southwest Regional Meeting, American Chemical Society, Costa Mesa, California (December 5, 1965).
11. Jenkins, R. K., *J. Polymer Sci. A-2*, **4**, 41 (1955).
12. Jenkins, R. K., *J. Polymer Sci., B*, **2**, 999 (1964).
13. Okada, Y., *J. Appl. Polymer Sci.*, **7**, 695 (1963).
14. Lyons, B. J., and M. Dole, *J. Phys. Chem.*, **68**, 526 (1964).
15. Okada, Y., and A. Amemiya, *J. Polymer Sci.*, **50**, S22 (1961).
16. Aston, J. G., R. M. Kennedy, and G. H. Messerly, *J. Am. Chem. Soc.*, **63**, 2343 (1941).
17. Kusumoto, H., I. J. Lawrenson, and H. S. Gutowsky, *J. Chem. Phys.*, **32**, 724 (1960).
18. Achhammer, B. G., M. J. Reiney, L. A. Wall, and F. W. Reinhart, *Natl. Bur. Std. Circ.*, **525**, 205 (1953).

Résumé

Les effets des irradiations gamma sur deux polysiloxanes à l'air et dans le vide à différentes températures ont été étudiés. La propriété physique suivie au cours de l'irradiation gamma des deux polysiloxanes étaient la modification de module dynamique que sa son tour est proportionnelle à la variation du nombre de chaînes élastiques effectives dans le réseau polymérique. Les mesures ont été effectuées en enregistrant *in situ* la réponse finale libre des batonnets de polymères en résonance forcée à leur fréquence de résonance fondamentale et au voisinage de celles-ci. L'énergie d'activation apparente de pontage pour le polymère polydiméthylsiloxanique a été trouvée égale à 0.56 Kcal/mole sous vide dans un domaine de température limité, et de 3.5 Kcal/mole à l'air.

Pour le polymère poly-diméthyl-diphénylsiloxanique, l'énergie d'activation apparente a été trouvée être environ égale à 1.3 Kcal/mole sous vide, tandis qu'à l'air la réponse du polymère est complexe, témoignant à la fois des ruptures et pontages, de sorte que la valeur n'a pas pu être obtenue. La capacité des groupes phényles latéraux de réduire la vitesse de pontage effective a été trouvée sensible à la fois à la température et à l'environnement.

Zusammenfassung

Der Einfluss der γ -Bestrahlung auf zwei Polysiloxane unter Luft und im Vakuum bei einigen ausgewählten Temperaturen wurde untersucht. Als physikalische Grösse wurde während der γ -Bestrahlung der beiden Polysiloxane die Änderung des dynamischen Moduls aufgezeichnet, welche ihrerseits der Änderung der Zahl der elastisch wirksamen Ketten im Polymernetzwerk proportional ist. Die Messungen wurden durch in-situ-Aufzeichnung der Reaktion des freien Endes von einseitig festgehaltenen Polymerstäbchen bei erzwungener Resonanz bei and nahe ihrer Grundresonanzfrequenz ausgeführt. Die scheinbare Aktivierungsenergie der Vernetzung wurde für das Polydimethylsiloxanpolymere im Vakuum in einem begrenzten Temperaturbereich zu 0,56 kcal/Mol und in Luft zu 3,5 kcal/Mol bestimmt. Für das Polydimethyldiphénylsiloxanpolymere betrug die scheinbare Aktivierungsenergie im Vakuum etwa 1,3 kcal/Mol, während in Luft das Polymere sich komplex verhält und gleichzeitig Spaltungs- und Vernetzungsreaktionen zeigte, sodass kein Wert für die Aktivierungsenergie erhalten werden konnte. Die Fähigkeit der anhängenden Phenylgruppen zur Herabsetzung der effektiven Vernetzungsgeschwindigkeit war von Temperature und Milieu abhängig.

Received June 14, 1965

Revised August 27, 1965

Prod. No. 4876A

Isothermal Kinetic Calorimeter Applied to Emulsion Polymerization

H. M. ANDERSEN, *Monsanto Company, St. Louis, Missouri*

Synopsis

A method for the direct measurement, by means of the heat of reaction, of essentially instantaneous polymerization rates is described. The polymerization is carried out isothermally, and the evolved heat is measured electrically over short time intervals. Applied to emulsion polymerization, the technique reveals several previously unobserved features.

INTRODUCTION

We present here a method for measuring the rate of polymerization by means of the heat evolved. Polymerization rates are ordinarily followed either gravimetrically or dilatometrically. These methods yield a conversion-time curve the "slope" of which has been accepted as the polymerization rate. In many cases, this procedure is entirely satisfactory, but if the polymerization does not necessarily follow a smooth curve, estimation of the rate from this slope is subject of serious error. This is true because considerable changes in rate will produce only minor changes in integral conversion, at least after any appreciable conversion has been reached. The problem is the classic one of evaluating small but important changes in large numbers, and the result is that the experimental methods are strained to yield data of sufficient accuracy.

Emulsion polymerization is an outstanding example in which the rate may change in a complex way during the process. Many studies have been made of the way in which soap, electrolyte, initiator, and other factors affect the polymerization rate, but there is still considerable disparity in the results. This problem has been reviewed by van der Hoff.¹ We suggest that the difficulties of accurately measuring rate changes by means of the usual conversion-time curves may have contributed to this problem. This would be especially true at higher polymerization rates and conversions.

The method described here circumvents these problems by measuring electrically the heat evolved by the polymerization over a short time interval (100 sec.), and repeating this measurement frequently (every 120 sec.), so that an almost continuous record of polymerization rate is obtained, independently of the conversion. The temperature of the reaction mixture

is maintained constant throughout. The total amount of heat evolved is also measured, and provides an index of conversion.

Munch² has reported a method similar in principle to ours. He was concerned primarily with measuring the total heat of reaction rather than rates, and did not work with polymerizations. His work was simultaneous with and independent of ours. Tong and Kenyon's vaporization calorimeter³⁻⁶ was designed primarily to measure heat of polymerization, although its speed of response permits some kinetic information to be obtained. Its specialized nature precludes its use for emulsion polymerization. A number of other polymerization calorimeters have also been described,⁷ but none is suitable for isothermal kinetic measurements.

EXPERIMENTAL

In brief, a constant reaction temperature and a constant heat flux out of the reaction flask are maintained. That part of the required heat not supplied by the polymerization is supplied by an immersion heater in the reaction mixture. By comparing the heater input during polymerization with that for no polymerization, the rate at which polymerization heat is generated can be measured. The cumulative total heat of polymerization is also measured.

Apparatus

Figure 1 shows the apparatus schematically. The reaction vessel, holding a volume of 700 ml., was immersed in a water thermostat at 26°C. The temperature of the reaction mixture was brought to 30°C. by means of the internal heater, controlled by the thermistor, bridge, and on-off control switch on the recorder. The input to the heater was set at a suitable value with the Variac, and was indicated by the wattmeter.

The "on-time" timer indicated the cumulative time the heater had been on (± 0.1 sec.), and the "off-time" timer the corresponding off time. The

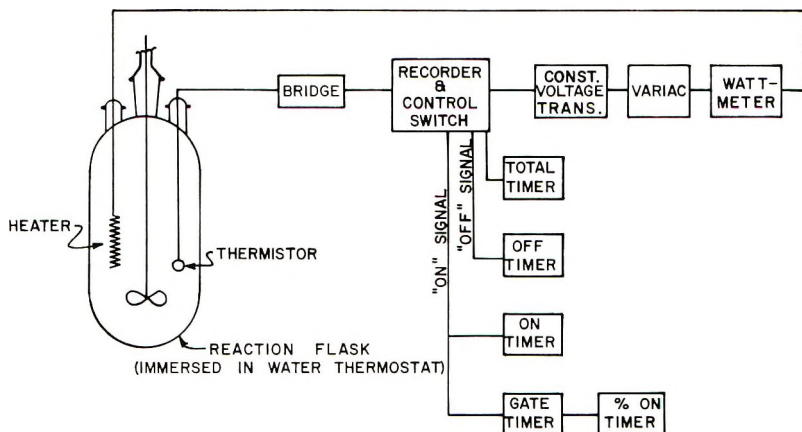


Fig. 1. Schematic diagram of isothermal kinetic calorimeter.

"total-time" timer ran continuously, indicating reaction time. These three timers provided a mutual check on one another because on-time plus off-time must equal total-time.

The reset timer opened a gate for a specified period, usually 100 sec., so that the "per cent-on" would run for that period when, and only when, the heater was on. Thus, for a gate of 100 sec., the "per cent-on" timer indicated directly that fraction of the wattmeter reading which was the average heating rate for the 100-sec. period. The reset timer reset itself automatically, and the per cent-on timer was reset manually after recording the reading. The total on-time value was also recorded. The gate was opened at 2-min. intervals by momentarily pressing a start button.

It was found essential to use a very low-lag heater. The one used consisted of 15 turns of bare no. 30 nichrome wire wound on a 16-mm. diameter glass tube, having a resistance of 18 ohms. The nichrome wire was welded to tungsten seal-throughs at each end, and the leads brought out through a $24/40$ joint at the upper end. This heater would cycle at a sufficient frequency, 10-15/100 sec., that the per cent-on time for such a period was an accurate measure of the heating rate. At the end of a run, polymer plate-out on the heater would tend to decrease the cycling frequency and therefore cause some, but not excessive, scatter in the data. The Variac setting was changed occasionally as required during the run to keep the on-time values between about 40 and 80%. This resulted in optimum control of temperature as well as accurate heat input measurement.

Reaction temperature was controlled to $\pm 0.01^\circ\text{C}$., except near the end of a run, when polymer fouling of the heater would increase the variations to about $\pm 0.04^\circ\text{C}$. Full scale on the recorder was set at 1.00°C . (on a 10-in. chart). Cumulative error in the timers was less than 5 sec. for a 60-min. run. The wattmeter used was accurate to $\pm 2\%$. Wattmeter settings were varied from 20 to 60 w., in 10-w. steps, as required. The temperature of the water bath in which the reaction flask was immersed was controlled to better than $\pm 0.01^\circ\text{C}$. with a Hallikainen Thermotrol. The reaction flask itself was a round-bottomed cylinder approximately 4 in. in diameter and 7 in. high, having five joints at the top to provide for the stirrer, heater, thermistor, condenser (not shown in the sketch), and reagent port.

Figure 2 gives the electrical circuit used. The wattmeter of appropriate range could be selected with a switch. A constant voltage transformer minimized line voltage variations. Printing timers and related devices could be incorporated to minimize manual operations.

A different, and theoretically preferable, electrical system was tried originally. A three-mode (proportional, reset, and rate) controller was used instead of the simple on-off system described above. The input to the heater was then continuously and automatically varied so as to maintain constant temperature. The heater input was monitored with a wattmeter, and continuously fed to a recorder via Hall device which gives a millivolt output proportional to power. This had the advantage of pro-

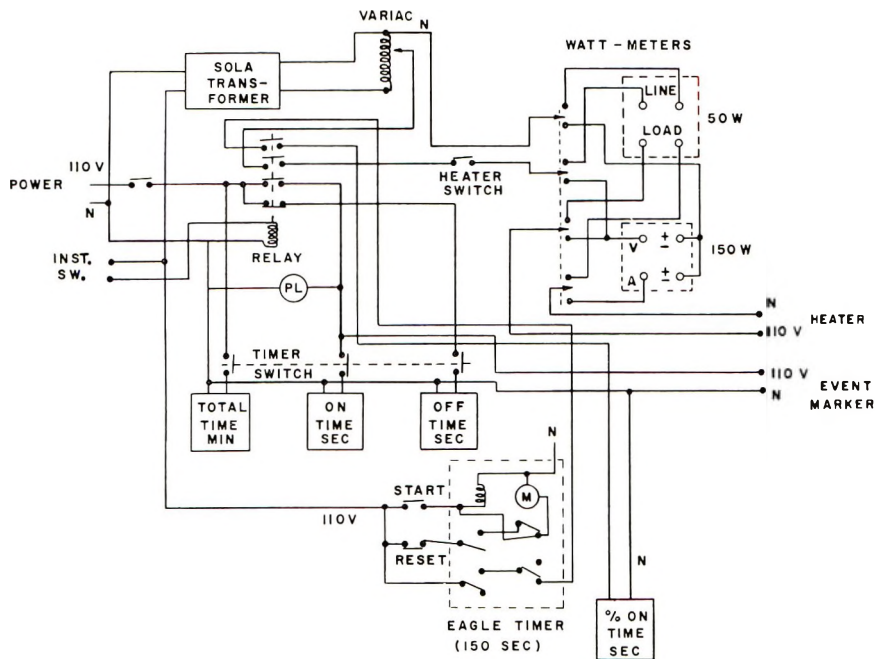


Fig. 2. Electrical circuit.

viding a truly instantaneous and continuous record, as well as saving a great many manual readings. Unfortunately, the heater in use at the time had too great a lag to allow the system to function properly. It is now being tried again with the low-lag heater described above.

Recipes

A redox emulsion polymerization of styrene was used to test the method. The "baseline" recipe was as follows: water, 500 ml.; sodium bicarbonate, 20 mmole; sodium pyrophosphate, 10 mmole; sodium alkylbenzenesulfonate, 10 g.; ferric ammonium sulfate, 0.5 mmole; tetrasodium ethylenediaminetetraacetate (EDTA): 1.0 mmole; sodium formaldehyde sulfoxylate (SFS), 10 mmole; ammonium persulfate (APS), 10 mmole; styrene, 200 ml.

The emulsifier and SFS were varied from the above values, as described below. The system was flushed with nitrogen, and a slight nitrogen pressure was maintained during a run.

Procedure

All components except the APS and SFS were added to the reaction flask, and brought to reaction temperature, 30°C., by means of the internal heater, with the bath at 24°C. The heat input required to maintain this temperature differential of 4°C. under these "no-reaction" conditions was then determined. A series of wattmeter and "per cent-on-time" readings

for 100 sec. intervals (one beginning every 2 min.) was measured for about 30 min., as was the cumulative heat input. Under these conditions, close to 50 w. was required.

When a satisfactory baseline was established, the APS (solid) was added. A small endotherm, about 0.1°C ., was observed while it dissolved, lasting about 0.5–1.0 min. The SFS was then added as a 1.0*M* solution (previously thermostatted at 30°C .) to start the reaction. Holding out both these reagents until starting the reaction prevented any prereaction. Readings of the 100-sec. heat inputs and the cumulative heat inputs were then continued at 2-min. intervals until the polymerization ceased.

RESULTS

The final rate of heat input after polymerization was less than the initial because of the change in specific heat in going from monomer to polymer. Initial heat input was close to 50 w., and the final close to 45 w. For this reason, the data were first plotted simply as rate of heat input versus time, a straight baseline drawn from the initial to final points, and the rate of

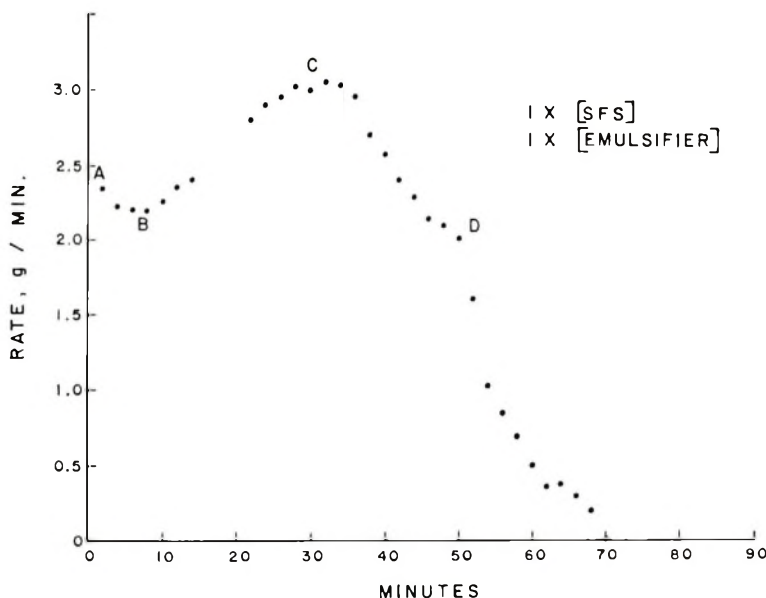


Fig. 3. Rate vs. time.

polymerization read as the difference between each point and the baseline. Although the "straight-line assumption" made here is not strictly correct, it introduces only a second-order error. If desired, a more exact calculation could eliminate it. Similarly, we have attempted no correction for the relatively small heat of solution of polymer in monomer.

Figures 3–5 give results for three typical runs. The rates, originally

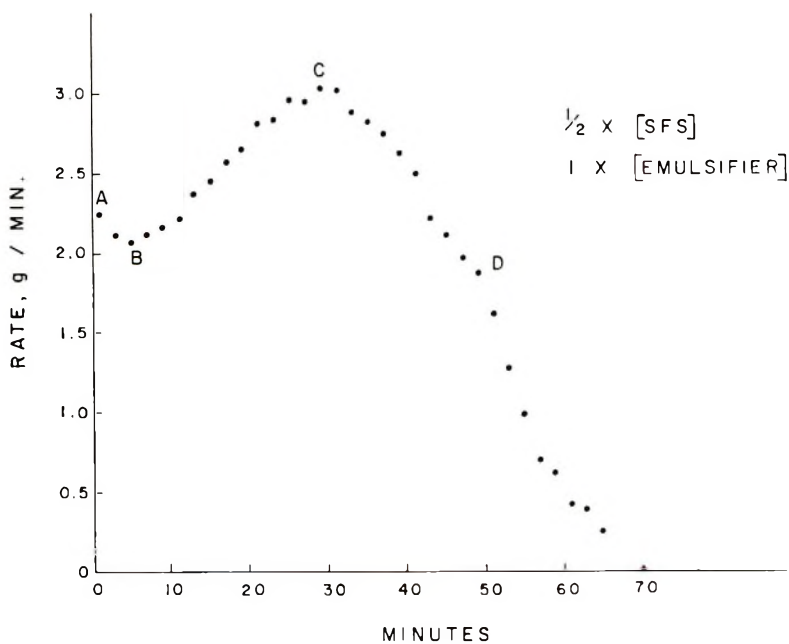


Fig. 4. Rate vs. time.

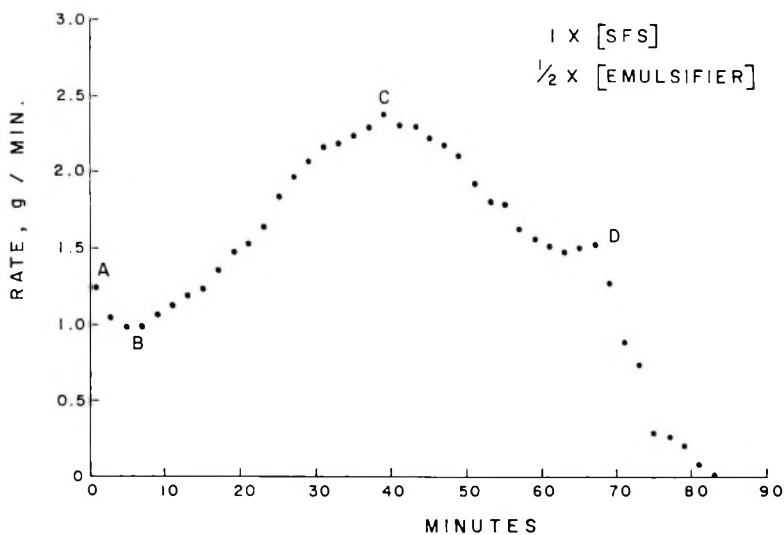


Fig. 5. Rate vs. time.

obtained in watts (from zero to about 30), were converted to grams of polymer formed per minute by the equation:

$$\frac{(\text{watts}) \times (14.33) \times (104)}{17,500} = \text{g./min.}$$

or

$$(\text{watts}) \times 0.0852 = \text{g./min.}$$

where 14.33 = conversion factor, watts to cal./min., 104 = molecular weight of styrene, and 17,500 = heat of polymerization of styrene, cal.⁷

Note that changing the SFS concentration by a factor of two had practically no effect on the rate curve, the two runs being almost superimposable, but changing the emulsifier concentration by a like amount had a

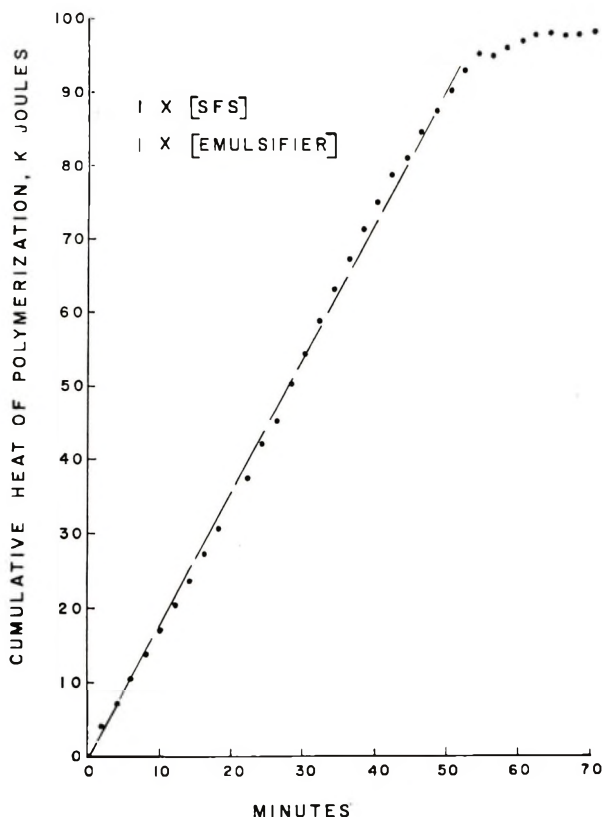


Fig. 6. Conversion vs. time.

major effect. This shows, obviously, that the limiting factor, in this case, was the number of micelles rather than the rate of radical generation. In all cases, the rate curves show the same general shape.

Figure 6 is a plot of the cumulative heat input versus time, for the same run shown in Figure 3, based on a point-to-point calculation comparing each cumulative reading with the "no-polymerization" baseline. This is equivalent to a conventional conversion-time plot. It has a slight sigmoidal curvature, but deviates only slightly from a straight line.

DISCUSSION

The primary object of this paper is to describe the experimental technique. Therefore, the quantitative analyses of these and other results in terms of theoretical significance is reserved pending additional work. We discuss here only a few qualitative observations.

Inspection of Figures 3-5 reveals several interesting features. The decrease in rate during the first 5-7 min., from A to B on the figures, is an apparently hitherto unreported phenomenon. It was present in all the runs made, and is believed not to be an artifact. Pending further work, we can only speculate regarding its cause. If, during this time the main locus of polymerization is molecularly dissolved styrene being consumed faster than it can dissolve from monomer droplets, the effect would be accounted for. At the end of this period, a sufficient number of micelles would be "started" so that the rate begins to increase.

The gradual increase in rate from B to C presumably represents the period of increasing concentration of active micelles and/or particles, in accordance with classic Smith-Ewart theory.¹ The steady-state plateau called for by this theory, however, is virtually absent. Only a well-defined maximum is present, followed by a decrease to D. A slower recipe might, however, result in more of a plateau. The sharp decrease beginning at D presumably marks the exhaustion of monomer droplets, after which the only monomer available for polymerization is that already imbibed by the particles. Obviously, any expression of the rate as a function of any reaction variable must include conversion and/or time.

Comparison of the cumulative heat-time curve (Fig. 6) with the rate curve (Fig. 3) aptly illustrates the advantage of measuring polymerization rate directly. We believe it would be quite impossible to derive rate data as detailed and informative as these by measuring the changes in slope of Figure 6. Careful inspection of the latter shows two inflection points, corresponding to the observed maximum and minimum in the rate. If the points of Figure 6 had been conversion-time points, however, the observer would have approximated the 0-50 minute section by the straight line, and accepted the slope of the latter as the rate of polymerization. The curvature of a conversion-time curve is determined very largely by the conversion previously attained, and therefore is influenced only slightly by changes in the current instantaneous rate. Although the present method does not measure the true instantaneous rate, the 100-sec. average is a sufficiently close approximation for most purposes. Improvement in the apparatus, as described under experimental, may make possible a truly instantaneous rate measurement.

The method is not, of course, limited to polymerizations. It should be applicable to any reaction evolving or adsorbing heat. By appropriate choice of the temperature differential between the bath and the reaction vessel, a wide range of reaction rates can be accommodated. Electrical equipment suitable for measuring even very small power inputs is available.

CONCLUSIONS

By the method described, through electrical measurement of the heat evolved over successive short time intervals, it is possible to gain a very detailed and informative record of the rate of polymerization.

When applied to emulsion polymerization in a few illustrative examples, the following previously unobserved features are apparent: a brief decrease in rate occurs during the first few minutes; there is little or no steady-state condition; and an abrupt decrease in rate occurs near the end, presumably marking exhaustion of free monomer droplets.

The assistance of Professor Raymond M. Fuoss of Yale University and of Mr. Stanley I. Proctor of Monsanto Company is gratefully acknowledged.

References

1. van der Hoff, B. M. E., in *Polymerization and Polycondensation Processes*, Advances in Chemistry Series, No. 34, American Chemical Society, Washington, D. C., 1962.
2. Munch, R. H., paper presented at St. Louis Society of Analysis Symposium, March 27, 1965.
3. Tong, L. K. J., and W. O. Kenyon, *J. Am. Chem. Soc.*, **67**, 1278 (1945).
4. Tong, L. K. J., and W. O. Kenyon, *J. Am. Chem. Soc.*, **68**, 1355 (1946).
5. Tong, L. K. J., and W. O. Kenyon, *J. Am. Chem. Soc.*, **69**, 1402 (1947).
6. Ekegren, S., S. Öhrn, K. Granath, and P. Kinell, *Acta Chem. Scand.*, **4**, 126 (1950).
7. Dainton, F. S., and K. J. Ivin, in *Experimental Thermochemistry*, Vol. II, H. A. Skinner, Ed., Interscience, New York, 1962, p. 251.

Résumé

Une méthode de mesure directe, au moyen de la chaleur de réaction, des polymérisations instantanées a été décrite. La polymérisation a été effectuée isothermiquement et la chaleur dégagée est mesurée électriquement sur des intervalles de temps très courts. Appliquée à la polymérisation en émulsion, cette technique révèle de nombreux phénomènes jusqu'ici non encore observés.

Zusammenfassung

Eine Methode zur direkten Messung von im wesentlichen momentanen Polymerisationsgeschwindigkeiten durch die Reaktionswärme wird beschrieben. Die Polymerisation wird isotherm durchgeführt und die entwickelte Wärme elektrisch über kurze Zeitintervalle gemessen. Bei Anwendung auf die Emulsionspolymerisation liefert die Methode einige neuartige Ergebnisse.

Received August 30, 1965
Prod. No. 4879A

Periodate Oxidative Decrystallization of Cotton Cellulose*

STANLEY P. ROWLAND and EDWIN R. COUSINS,† *Southern Regional Research Laboratory, Southern Utilization Research and Development Division, Agricultural Research Service, United States Department of Agriculture, New Orleans, Louisiana*

Synopsis

Cotton cellulose is decrystallized by periodate oxidation to essentially zero crystallinity index (CI) at 100% oxidant consumption. The decrease in CI is pseudo zero-order over 60% of the reaction and consistent with a diffusion-controlled mechanism. The attack on regions of high order is indicated to be 100% in the latter phase of oxidation and 13% in the initial phase. Data allow an estimate that approximately 60% of the structural segments of the cotton cellulose under investigation lies in highly ordered arrangements.

Davidson¹ showed that the x-ray powder diagram of cellulose becomes more diffuse as the degree of oxidation with periodic acid increases. Little other information is available on the crystallinity of periodate-oxidized cellulose, especially over the complete range of oxidation. Because this oxidation is selective for the vicinal hydroxyl groups in the cellulose structure,² because the product has been characterized extensively,³⁻⁵ and because the oxidation has proven valuable for determinations of accessibilities,^{6,7} it is important to have more quantitative information on the decrease in crystallinity in cellulose which is subjected to this oxidation. In the present work, the rate and course of decrease in crystallinity, as followed by crystallinity index, is examined preliminary to related studies of crosslinked cotton celluloses.

Experimental

Cotton cellulose was in the form of desized, scoured, bleached 80 × 80 print cloth weighing 3.3 oz./yd.² The oxidation of the cotton cellulose with 0.25*M* and 0.06*M* sodium metaperiodate solutions was conducted as described by Cousins et al.⁷ Oxidant consumption is expressed as per-

* Presented before the Division of Cellulose, Wood, and Fiber Chemistry, at 150th National Meeting, American Chemical Society, Atlantic City, N. J., September 12-17, 1965.

† Present address: U. S. Naval Weapons Station, Yorktown, Virginia.

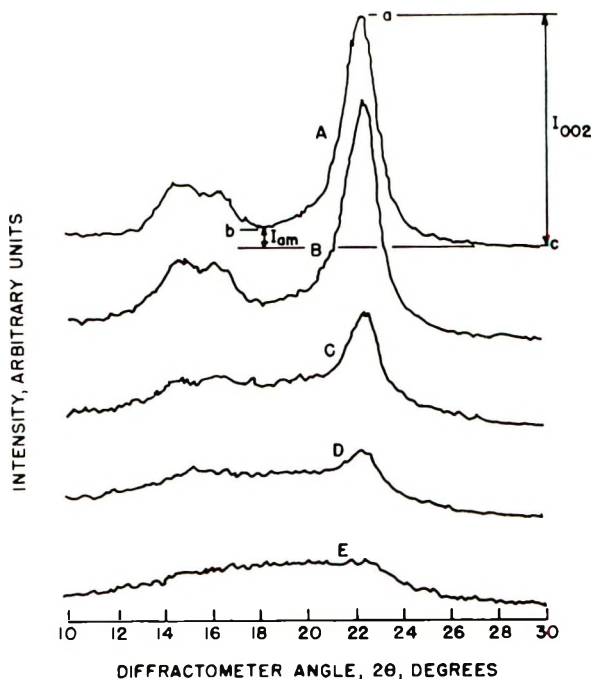


Fig. 1. X-ray diffractograms for periodate (0.25*M*)—oxidized cotton cellulose at various levels of oxidant consumption: (A) zero; (B) 28%; (C) 60%; (D) 80%; (E) 97%.

centage of the theoretical requirement to convert the cellulose to the dialdehyde structure.

X-ray diffractograms were obtained with a General Electric model XRD-5 x-ray diffractometer equipped with medium resolution Soller slits. The instrument employed a copper target and nickel filter to produce $K\alpha$ radiation and was operated at 50 k.v. and 10 or 15 ma. tube current with a 1° beam for one set of diffractograms. In a separate set of measurements, beam intensity was standardized by employing a polished brass plate in the target position and current intensity was adjusted (from 10 ma.) to maintain the initial intensity in each diffractogram. The latter set of diffractograms served as a check on the earlier set and was generally more satisfactory; these are the values reported here.

Thin platelets, 0.5 in. square, were prepared for x-ray diffraction studies by compressing 100-mg. quantities of cotton under 25,000 psi in an aluminum mold which served as the specimen holder. Samples of fabric cut into approximately 0.5 cm. squares and material ground in a Wiley mill to pass a 20-mesh screen were examined in the specimen holder. The former was preferred, since the ground material increased the amorphous scatter and is subject to the influences of several variable factors noted by Segal et al.⁸

Crystallinity indices (CI) were calculated from diffractograms by a method very similar to that of Segal et al.;⁸ the intensity in the diffracto-

gram at the position of the 002 peak ($2\theta = 22.6^\circ$ for cellulose I) and at suitable locations for the amorphous background ($2\theta = 18-20^\circ$) were substituted in the relation:

$$CI = 100(I_{002} - I_{am})/I_{002}$$

Specifically, I_{002} was measured by the vertical distance $a-c$ in Figure 1, where c is the baseline measured at $2\theta = 30^\circ$; I_{am} was measured by the vertical distance $b-c$ at the minimum between $2\theta = 18$ and 20° . At low levels of crystallinity the curve becomes convex in the $18-20^\circ$ region, and the maximum rather than the minimum is taken as the measure of the amorphous background.

Results and Discussion

We have observed a progressive decrease in crystallinity, as measured by crystallinity index (CI), during the periodate oxidation of cotton cellulose. X-ray diffractograms at selected stages of oxidation are shown in Figure 1; as noted earlier by Davidson¹ from powder diagrams, these diffractograms show no development of new crystalline lattice type. Under our experimental conditions involving excess of $0.25M$ periodate, the decrease in crystallinity index of cotton cellulose undergoing oxidation proceeds at a pseudo zero-order rate from a CI of 91.7 to a CI in the range of 35 (Fig. 2). Similar constancy in pseudo zero-order rate applies to the oxidation with $0.06M$ periodate over the range examined. Velocity constants are 0.62

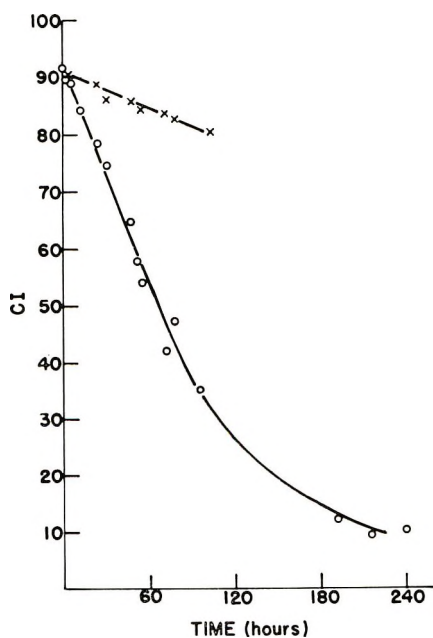


Fig. 2. Decrease in crystallinity index (CI) of cotton cellulose during course of periodate oxidations: (O) $0.25M$ periodate; (X) $0.06M$ periodate.

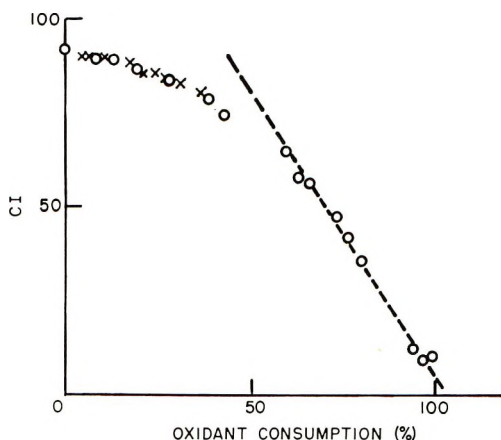


Fig. 3. Change of crystallinity index with consumption of oxidant: (O) 0.25*M* periodate; (X) 0.06*M* periodate.

and 0.11 CI/hr. for the oxidations with 0.25*M* and 0.06*M* periodate, respectively.

The relationship between CI and degree of oxidation, which is depicted in Figure 3, shows no significant difference for reactions conducted with 0.25*M* and 0.06*M* periodate, at least to approximately 40% oxidant consumption. It is evident that the decrease in CI per unit of oxidation is small (0.2) at the outset (initial 5% of oxidation), and large (1.5) and constant beyond approximately 60–70% oxidant consumption. These data are consistent with chain segments in amorphous regions or on surfaces undergoing rapid and predominant attack during the initial phase of the periodate oxidation, while the etching away of chain segments of crystalline regions constitutes the reaction in the latter stage. Thus, Figure 3 expresses a progressive oxidative decrystallization of cotton cellulose as a function of degree of consumption of oxidant. The constancy of decrease of CI per unit of oxidation over the latter portion of the oxidation is indicative of reaction occurring solely with polymeric chain segments of the highly ordered regions at this stage of oxidation. From the graphical slopes of the curve, the initial decrease of CI per unit of oxidation (to 5% oxidant consumption) is only 13% of that which characterizes the final 30–40% of the reaction; thus, the initial oxidation appears distributed 13% toward chain segments in highly ordered regions and 87% toward segments in noncrystalline regions.

The consistent decrease of 1.52 units of crystallinity index per unit of oxidation beyond 70% oxidant consumption suggests that oxidation of a totally crystalline cotton would undergo a change of 152 of these CI units during complete decrystallization. On this basis desized, scoured, bleached cotton having a crystallinity index of 91.7 (i.e., the cotton employed in this study) is indicated to have 60% of the anhydroglucose units (AGU) in highly ordered arrangements, which are associated with x-ray diffraction

patterns. This figure is generally consistent with accepted values of crystallinity.⁹⁻¹²

It must be noted that the value derived for apparent crystallinity of a sample of cellulose by this method is subject to inaccuracies to the extent that side reactions ("overoxidation") occur in addition to the simple oxidation of vicinal hydroxyl groups to aldehyde groups.^{2,3} Although attempts were made to minimize this in the current work,⁷ it is not unlikely that overoxidation occurred to the extent of a few per cent; the deviation of the oxidative decrystallization from crossing the abscissa at 100% oxidant consumption appears to be confirmation of this.

Earlier data on the periodate oxidation of cotton cellulose⁷ indicate that approximately one in 6-7 AGU (11.7-14.8%) is readily available for the oxidation, whereas current data show that approximately 2 in 5 AGU (40%) are not associated with apparent crystallinity: i.e., 3 in 5 AGU (60%) are intimately associated with the x-ray diffraction pattern which is characteristic of regions of high order. Thus, a single reagent finds a small fraction of the cellulose structure readily accessible and a larger fraction apparently noncrystalline. The extent of the readily accessible portion appears to vary with the concentration of reagent, constituting 29% (i.e., 11.7% accessibility⁷ divided by 40% noncrystallinity \times 100) of the noncrystalline fraction for 0.06*M* periodate and 37% (14.8% accessibility⁷ divided by 40% noncrystallinity \times 100) for 0.25*M* periodate. In either case the readily available fraction of vicinal hydroxyl groups is distinctly different from the fraction which is nonessential to the diffraction in x-ray patterns.

It is pertinent that Spedding and Warwicker¹³ interpret the changes occurring in the fine structure of cellulose during methylation with diazomethane (a reagent which has extreme difficulty in penetrating the crystalline lattice of cellulose and which contrasts sharply with periodate in this regard) as being more consistent with reaction at fibrillar surfaces followed later by reaction of the more accessible near-crystalline regions in the fibrils, rather than an alternate possibility of reaction in a crystalline-amorphous network. Whether the initial stages of the periodate oxidations occur primarily within noncrystalline regions (as pictured for the organization of cotton cellulose in terms of an assembly of crystalline and amorphous regions¹⁴) or on surfaces (as pictured for an arrangement of helically wound quasi single-crystal microfibrils¹⁵) is not clarified by our analysis. The fact that the readily accessible fraction varies with the concentration of reagent indicates that more than surfaces are involved in the very early phase of the reaction. The data, in fact, point out that crystalline regions (in addition to noncrystalline regions) are attacked and diminished from the very outset at a rate which remains constant throughout the major portion of the reaction. The periodate oxidation undergoes an interesting and gradual transition with increasing degree of oxidation from predominant reaction at noncrystalline regions in the initial stages to sole reaction at crystalline regions in the final stages.

We summarize (a) that cotton cellulose subjected to periodate oxidation undergoes decrease in crystallinity index at a pseudo zero-order rate indicative of a diffusion-controlled process over the major portion of the reaction, and (b) that initial reduction in crystallinity index at a given level of oxidation appears independent of the concentration of periodate reagent. We conclude (a) that constancy of decrease in CI per unit of oxidation in the latter portion of the oxidation reflects reaction with chain segments of highly ordered regions, (b) that initial oxidative attack is distributed approximately 13% with units of highly ordered regions and 87% with units of noncrystalline regions, (c) that the cotton cellulose under study is indicated to have approximately 60% of the AGU in highly ordered arrangements, and (d) that the AGU which are readily accessible to the reagent constitute only a fraction of those apparently present in noncrystalline arrangements.

The authors are indebted to Mr. D. Mitcham for x-ray diffractograms, to Dr. Mary L. Nelson and Dr. Leon Segal for suggestions and helpful discussions, and to Mr. G. I. Pittman for preparation of the figures.

Trade names have been used to identify materials or equipment used in this work, and such use does not imply endorsement or recommendation by the U. S. Department of Agriculture over other products not mentioned.

References

1. Davidson, G. F., *J. Textile Inst.*, **32**, T109 (1941).
2. Nevell, T. P., in *Methods in Carbohydrate Chemistry*, Vol. III, R. L. Whistler, Ed., Academic Press, New York, 1963, pp. 164-168.
3. Head, F. S. H., *J. Textile Inst.*, **44**, T209 (1953).
4. Nevell, T. P., *J. Textile Inst.*, **47**, T287 (1956).
5. Mack, C. H., and W. A. Reeves, *Textile Res. J.*, **31**, 800 (1961).
6. Timell, T., *Studies in Cellulose Reactions*, Royal Institute of Technology, Stockholm, 1950, pp. 30-43.
7. Cousins, E. R., A. L. Bullock, C. H. Mack, and S. P. Rowland, *Textile Res. J.*, **34**, 953 (1964).
8. Segal, L., J. J. Creely, A. E. Martin, and C. M. Conrad, *Textile Res. J.*, **29**, 76 (1959).
9. Mann, J., in *Methods in Carbohydrate Chemistry*, Vol. III, R. L. Whistler, Ed., Academic Press, New York, 1963, pp. 114-119.
10. Wakelin, J. H., H. S. Virgin, and E. Crystal, *J. Appl. Phys.*, **30**, 1654 (1959).
11. Smith, J. K., W. J. Kitchen, and D. B. Mutton, *J. Polymer Sci. C*, **2**, 499 (1963).
12. Jeffries, R., *J. Appl. Polymer Sci.*, **8**, 1213 (1964).
13. Spedding, H., and J. O. Warwicker, *J. Polymer Sci. A*, **2**, 3933 (1964).
14. Hearle, J. W. S., and R. H. Peters, *Fiber Structure*, Butterworths, London, 1963, pp. 209-234.
15. Manley, R. S. J., *Nature*, **204**, 1155 (1964).

Résumé

La cellulose de coton subit une décrystallisation par oxydation périodique jusqu'à atteindre un indice de cristallinité 0 à 100% de consommation en oxydant. La diminution en CI répond à une réaction apparente d'ordre 0 jusque 68% de conversion et s'accorde avec un mécanisme contrôlé par diffusion. L'attaque des régions d'ordre élevé est totale (100%) dans la dernière phase de l'oxydation, alors qu'elle n'est que de

13% dans la phase initiale. Les résultats permettent une estimation et indiquent que approximativement 60% des segments de structure de la cellulose de coton examinée se trouve dans un arrangement hautement ordonné.

Zusammenfassung

Baumwollzellulose wird durch Periodatoxydation bei 100% igem Verbrauch des Oxydationsmittels im wesentlichen bis zum Kristallinitätsindex (CI) Null de kristallisiert. Die Abnahme von CI ist über 60% der Reaktion von Pseudo-nullter Ordnung und entspricht einem diffusionskontrollierten Mechanismus. Der Angriff auf Bereich hoher Ordnung ist in der Schlussphase der Oxydation 100% und in der Anfangsphase 13%. Die Daten erlauben die Schätzung, dass etwa 60% der Kettensegmente der untersuchten Baumwollzellulose sich in einem hochgeordneten Zustand befinden.

Received June 7, 1965

Revised August 30, 1965

Prod. No. 4881A

Enhanced X-Ray Diffraction Patterns from Oriented Fibers

M. E. MILBERG, *Scientific Laboratory, Ford Motor Company, Dearborn, Michigan*

Synopsis

The difference x-ray diffraction pattern can reveal the presence of oriented, ordered material whose conventional diffraction pattern is masked by that of unoriented, disordered material. It is shown that this enhancement results from the fact that scattering from only oriented material contributes to the difference intensity, defined as the difference between the scattered intensity and its average over the polar angle in intensity space. Difference patterns of lightly crosslinked natural rubber, obtained as a function of elongation, show the development of crystallinity at smaller elongations than do the corresponding conventional patterns and indicate that nearly all the oriented material is crystalline. The difference and conventional patterns were obtained from the same diffractometer data. Photographically recorded diffraction patterns are intermediate between the conventional and difference diffractometer patterns in sensitivity to crystallinity. The difference diffraction pattern of a highly oriented atactic polystyrene fiber shows no evidence of crystallinity, the halos on the difference pattern being just as broad as those on the conventional pattern with no apparent tendency to break up into crystalline lines.

Introduction

A recent study of oriented sodium metaphosphate glass fibers¹ revealed the presence of oriented, ordered material whose conventional x-ray diffraction pattern had been masked by that of the preponderant disordered, nearly unoriented, material. The ordered material was detected by use of the difference diffraction pattern, defined for a cylindrically symmetric system as the difference between the conventional diffraction pattern and its average over the polar angle in intensity space, ϕ . The relevant coordinate system is shown in Figure 1. The effectiveness of the difference pattern in revealing the presence of what might be called poorly crystalline material results from the fact that it is the transform of the difference between the cylindrical and radial distribution functions and, as such, results only from those interatomic vectors which differ from the average angular distribution relative to the axis of cylindrical symmetry, i.e., the fiber axis.² Thus, if ordered material is oriented and the disordered is not, and if the ordered material consists of very small, poor or few crystallites, its diffraction pattern may be sufficiently masked by that of the amorphous material to result in an overall appearance of an oriented amorphous

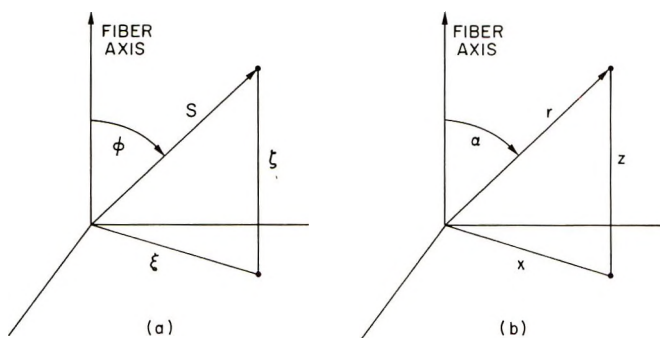


Fig. 1. Coordinate systems in (a) intensity and (b) direct spaces.

pattern. This appears to have been the case with sodium metaphosphate.^{1,3} However, the difference pattern, being sensitive only to the oriented material, can then reveal the presence of the ordered, or crystalline matter. The conventional and difference diffraction patterns of oriented sodium metaphosphate glass fibers can be seen in the previous report.¹ The difference patterns appear quite similar to the calculated diffraction pattern of very tiny diamond crystallites containing but 27 unit cells⁴ and quite different from conventional amorphous patterns, when due allowance is made for the fact that peaks in the difference pattern can be either positive or negative.

That the difference intensity $I'(S, \phi)$ is the transform of the difference between the cylindrical and radial distribution functions follows from the expansion of the cylindrical distribution function in spherical harmonics. The cylindrical distribution function can be written as⁵

$$D(r, \alpha) = \sum_{n=0}^{\infty} D_{2n}(r) P_{2n}(\cos \alpha) \quad (1)$$

where

$$D_{2n}(r) = (-1)^n 4\pi \int_0^{\infty} S^2 I_{2n}(S) j_{2n}(2\pi Sr) dS \quad (1a)$$

$$I_{2n}(S) = 1/2(4n + 1) \int_0^{\pi} I(S, \phi) P_{2n}(\cos \phi) \sin \phi d\phi \quad (1b)$$

P_{2n} and j_{2n} are, respectively, the Legendre polynomial and the spherical Bessel function of order $2n$, and r, α and S, ϕ are the spherical coordinates of a point in direct and intensity spaces, respectively, as shown in Figure 1. Note that $S = (2 \sin \theta)/\lambda$, where 2θ is the scattering angle and λ the wavelength. Now the first term in the series of eq. (1), $D_0(r)$, is just the radial distribution function,⁵ that is, the cylindrical distribution function averaged over the polar angle α . The remainder of the series gives the deviation from spherical symmetry. The difference intensity is defined as

$$I'(S, \phi) = I(S, \phi) - I_0(S), \quad (2)$$

where

$$I_0(S) = 1/2 \int_0^\infty I(S, \phi) \sin \phi d\phi \quad (2a)$$

It has been shown² that by substituting $I'(S, \phi)$ for $I(S, \phi)$ in eq. (1b) and then carrying through the calculation of the cylindrical distribution function, one obtains

$$D'(r, \alpha) = D(r, \alpha) - D_0(r) \quad (3)$$

which is the cylindrical distribution function with the first term omitted, or the difference between the cylindrical and radial distribution functions.

The cylindrical distribution function obtained for oriented NaPO_3 glass fibers³ demonstrated that at least some portion of the material was very highly oriented. The indication from the difference pattern that the oriented material was indeed crystalline or, at least, possessed order of a longer range than that usually associated with an amorphous material, suggested that the difference intensity might be very sensitive to incipient crystallization in oriented fibers. Therefore, an investigation of the difference diffraction patterns of natural rubber fibers as a function of elongation, and of highly oriented atactic polystyrene fibers, was undertaken. The investigation was aimed at establishing whether the difference diffraction pattern showed the development of crystallinity in natural rubber at elongations less than that at which it became evident in the conventional diffraction pattern and whether any indication of crystallinity could be detected in supposedly amorphous atactic polystyrene.

Experimental

Milled, unfilled natural rubber was compacted into glass tubing of about 2 mm. i.d. and lightly crosslinked by exposure to 25 Mrad of γ -radiation from ^{60}Co in an inert atmosphere. Samples were removed from the tubing for the recording of diffraction patterns. Samples of highly oriented atactic polystyrene were obtained from the Dow Chemical Company through the courtesy of Dr. Edward F. Gurnee. The sample used had a birefringence of about 2.5×10^{-2} . Many of its properties and the method of its preparation have been reported.⁶

Recording of the diffraction patterns was done by both counter and film techniques, though the counter method was used most extensively, since it is particularly suited to the calculation of the difference pattern. The samples were mounted on a G.E. goniostat for counter measurements so as to permit direct variation of S and ϕ ($90^\circ - \chi$ on the goniostat). The rubber samples were stretched *in situ*, all final measurements being made on one sample, increasing the elongation from one set of measurements to the next. The diffractometric rubber patterns were recorded by using zirconium-filtered molybdenum radiation, a pulse-height analyzer and a scintillation counter. The polystyrene patterns were recorded in the same manner, except that the radiation used was nickel-filtered copper.

Extreme care was taken to avoid serious scattering volume and absorption errors in the diffractometric measurements. It is clear that, except at zero scattering angle, the scattering volume for a fiber sample varies with χ when the goniostat geometry is employed, since the plane of χ bisects the scattering angle. With suitable choice of beam collimator, detector collimator, and sample sizes, the variation in scattering volume is a simple and straightforward function of the angles involved. It can be written as

$$V = \sec[\cos^{-1}(\cos^2 \chi + \sin^2 \chi \cos \theta)]V_0 \quad (4)$$

where V is the scattering volume at any value of χ and 2θ , and V_0 is the scattering volume when either χ or 2θ is zero. Account was taken of the variation in scattering volume by choosing conditions so that eq. (4) was applicable and multiplying the measured intensities by V_0/V . Note that

$$V_0/V = \cos^2 \chi + \sin^2 \chi \cos \theta \quad (5)$$

Except at very small scattering angles, the large change in path length in the fiber samples as χ is varied from 0 to 90° results in a substantial variation in x-ray absorption, unless either the sample diameter or the absorption coefficient is kept very small. Since the correction for absorption is difficult to make with the sample and diffraction geometry employed, sample size and radiation wavelength were so chosen as to make the absorption correction negligible. Fortunately, this condition was attainable, though just barely so, without leaving the range of validity of eq. (4).

Intensity measurements were made by scanning the desired range of scattering angle 2θ back and forth for a total of eight scans at each of eleven values of χ , while making a strip chart recording of the intensity through a ratemeter. All scanning was done automatically, including the change in χ each eight scans. Intensities were read from the charts each half degree in 2θ . The reading was done with a Benson Lehner Oscar K, so that digital computer cards punched with the intensities were automatically produced. The eight individual intensities for each point in intensity space were added together and the sum used to calculate $I'(S, \phi)$ from eq. (2), with the aid of a Philco 2000 digital computer.

The photographic diffraction patterns were obtained with the samples mounted in the goniostat and a flat film holder at the zero 2θ detector position of the diffractometer.

Results and Discussion

Plotted in Figure 2 are the diffractometric equatorial ($\phi = 90^\circ$) conventional and difference diffraction patterns of natural rubber for extensions varying from 300% to 550%. The equivalent patterns are plotted in Figure 3 for the meridian ($\phi = 0^\circ$). It is clear from Figure 2 that, on the equator, the conventional pattern appears noncrystalline at extensions less than 450%, while the difference pattern shows crystalline lines at 350%. Although the patterns for the meridian show the same effect in the vicinity

of the main amorphous halo, near $S = 0.2 \text{ \AA}^{-1}$, the diatropic crystalline (004) reflection⁷ at $S = 0.48 \text{ \AA}^{-1}$ shows up just as clearly on the conventional pattern as it does on the difference pattern. Figure 4, in which the conventional and difference patterns for both equator and meridian at 350% extension are superimposed, shows clearly the enhancement of the crys-

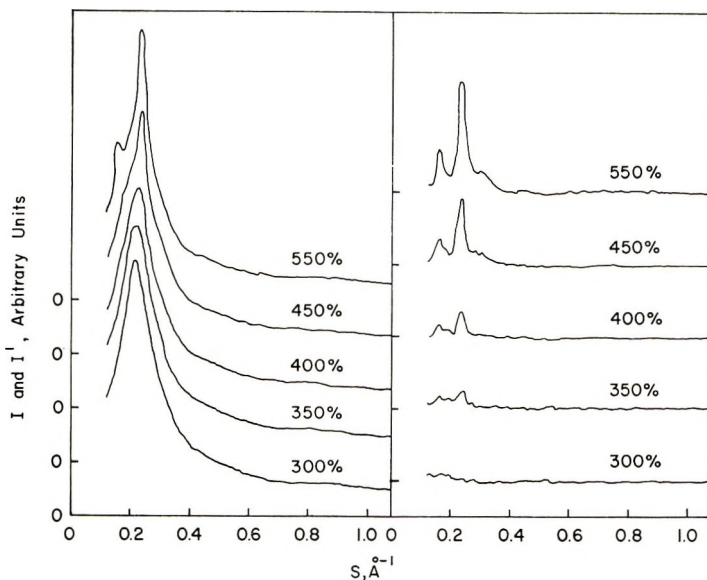


Fig. 2. Conventional (left) and difference (right) equatorial ($\phi = 90^\circ$) x-ray diffraction patterns for natural rubber at indicated extensions.

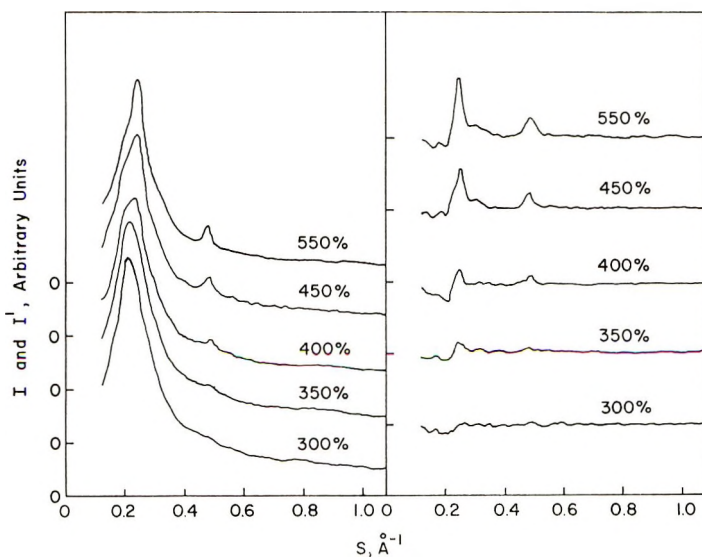


Fig. 3. Conventional (left) and difference (right) x-ray diffraction patterns along the meridian ($\phi = 0^\circ$) for natural rubber at indicated extensions.

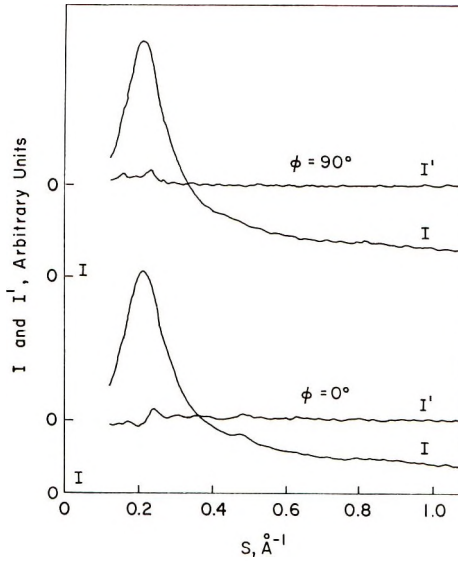


Fig. 4. Conventional (I) and difference (I') x-ray diffraction patterns of natural rubber at 350% extension. Zero for conventional patterns indicated by I .

talline lines in the difference pattern. Clearly, in this case, they are completely masked by the amorphous halo in the conventional pattern. The (004) line, which is in a region of only very slight amorphous scattering, is equally visible in both meridian patterns. Examination of the patterns for 300% extension in Figures 2 and 3 shows that where there are no crystalline lines, the difference intensity is nearly zero. This would seem to indicate that, as far as the x-rays are concerned, oriented amorphous material is nearly absent or, in other words, that which is oriented is ordered.

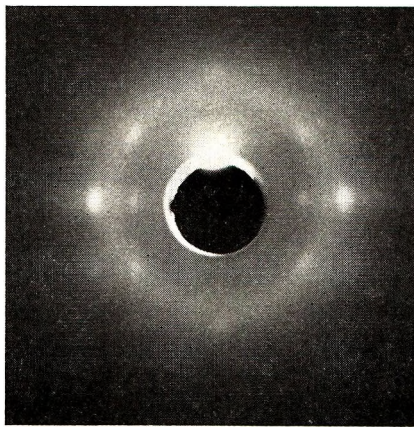


Fig. 5. Photographic x-ray diffraction pattern of natural rubber at 550% extension. Fiber axis is vertical.

The positive peak on the equatorial difference pattern at $S = 0.16 \text{ \AA}^{-1}$ appears to have a negative counterpart on the meridian and, therefore, to behave as expected of a paratropic reflection. This behavior is in agreement with Bunn's⁷ data, which include a strong (200) reflection at $S = 0.16 \text{ \AA}^{-1}$. The positive peak at $S = 0.235 \text{ \AA}^{-1}$ on the equator appears, at

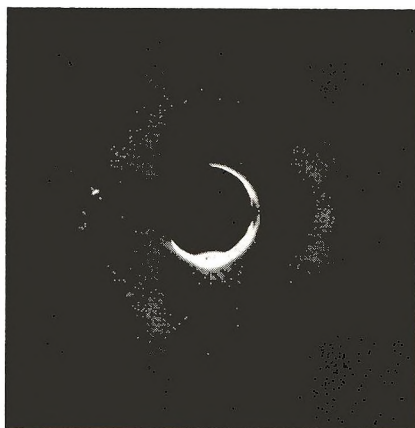


Fig. 6. Photographic x-ray diffraction pattern of natural rubber at 400% extension. Fiber axis is vertical.

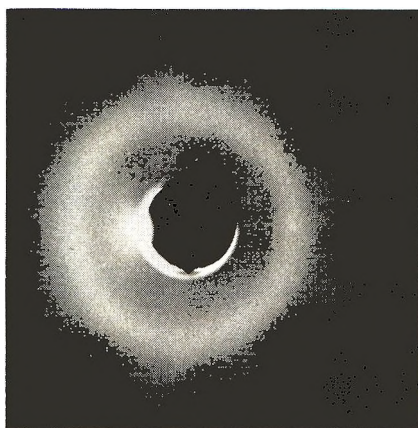


Fig. 7. Photographic x-ray diffraction pattern of natural rubber at 350% extension. Fiber axis is vertical.

first glance, to have a positive counterpart on the meridian. Close examination, however, reveals that the peak on the meridian is located at about $S = 0.25 \text{ \AA}^{-1}$ and is, presumably, different from the equatorial peak. Indeed, it seems likely that the equatorial peak at $S = 0.235 \text{ \AA}^{-1}$ is the paratropic (120) and the peak at $S = 0.25 \text{ \AA}^{-1}$ on the meridian is the diatropic (002), even though Bunn⁷ reports the (120) as very much more intense than the (002). The intensity discrepancy may possibly be accounted for by the difference in recording techniques, since the photographic

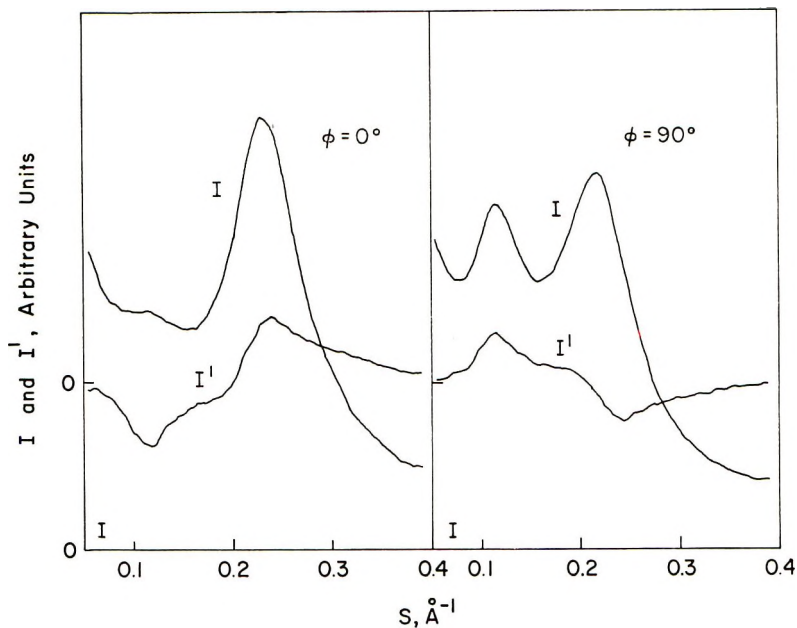


Fig. 8. Conventional (I) and difference (I') x-ray diffraction patterns for highly oriented atactic polystyrene fiber. Zero for conventional pattern indicated by I .

method employed by Bunn is intrinsically poor for recording diatropic reflections.

The photographic patterns appear to be a bit more sensitive to crystallinity than are the conventional diffractometric patterns, but less so than the difference patterns. This sensitivity probably results from the fact that the eye tends to see differences in intensity rather well. Figures 5, 6, and 7 show, respectively, the photographic patterns at 550, 400, and 350% extension. In these figures the fiber axis is vertical. The beginnings of crystallinity appear to be detectable at 400% extension.

Both the conventional and difference patterns for oriented atactic polystyrene are shown in Figure 8. Only the region of S including the two main halos is shown. It is clear that the difference pattern is no more detailed than the conventional pattern, that is, the peaks on the difference pattern are just as broad as those on the conventional pattern. Both the conventional and the difference diffraction patterns, then, indicate that oriented atactic polystyrene is noncrystalline.

Conclusions

It has been shown that the difference x-ray diffraction pattern of oriented fibers can reveal the presence of oriented, ordered material whose conventional diffraction pattern has been masked by that of the preponderant disordered material. This enhancement of the ordered diffraction pattern results from the fact that only oriented material contributes to the difference

intensity, which is the difference between the scattered intensity and its average over the polar angle in intensity space. That the enhancement occurs can be seen from the results obtained on stretched natural rubber, wherein the difference pattern revealed the development of crystallinity at smaller elongation than did the conventional pattern. The appearance of the difference patterns of natural rubber indicates that virtually all the oriented material is ordered.

The difference pattern of highly oriented, atactic polystyrene showed peaks just as broad as those on the conventional pattern. Nothing resembling a crystalline pattern was found. From this observation it is concluded that the oriented portion of this material is indeed noncrystalline. The range of any order which might be present probably does not exceed a very few unit cells.

The ability of the difference pattern to reveal the incipient crystallization of rubber and to show the presence of only oriented noncrystalline material in atactic polystyrene provides additional support for the validity of the results reported earlier¹ concerning crystallinity in oriented sodium metaphosphate glass fibers.

The invaluable work of Mr. H. D. Blair in obtaining and reducing the data is most gratefully acknowledged.

References

1. Milberg, M. E., *Phys. Chem. Glasses*, **5**, 150 (1964).
2. Milberg, M. E., *J. Appl. Phys.*, **33**, 1766 (1962).
3. Milberg, M. E., and M. C. Daly, *J. Chem. Phys.*, **39**, 2966 (1963).
4. Tiensuu, V. H., S. Ergun, and L. E. Alexander, *J. Appl. Phys.*, **35**, 1718 (1964).
5. Norman, N., Doctoral thesis, University of Oslo, 1954.
6. Andrews, R. D., *J. Appl. Phys.*, **25**, 1223 (1954).
7. Bunn, C. W., *Proc. Roy. Soc. (London)*, **A180**, 40 (1942).

Résumé

Le diagramme de diffraction de rayons-X par différence peuvent révéler la présence de matériaux ordonnés orientés dont le réseau de diffraction conventionnel est masqué par celui du matériau non orienté désordonné. On a montré que cette amélioration résulte du fait que la diffusion au départ uniquement de matériaux orientés contribue à l'intensité par différence, définie comme étant la différence entre l'intensité diffusée et sa moyenne sous un angle polaire dans l'espace. Les réseaux par différence de caoutchoucs naturels légèrement pontés, obtenus en fonction de l'élongation montrent un développement de cristallinité aux plus faibles elongations que les réseaux conventionnels correspondant et indiquent que' environ tout le matériau orienté est cristallin. Les réseaux par différence et conventionnels ont été obtenus au départ des mêmes données de diffractométrie. Les réseaux de diffraction en-réglés photographiquement sont intermédiaires entre les réseaux de diffractomètre conventionnel et par différence en ce qui concerne la sensibilité par rapport à la cristallinité. Le réseau de diffraction par différence de fibres de polystyrène hautement orientés atactiques ne montre aucune évidence de cristallinité, les halos se manifestant sur le réseau par différence étant justes aussi larges que ceux des réseaux conventionnels sans aucune tendance à s'interrompre sous forme de lignes cristallines.

Zusammenfassung

Das Differenzröntgenbeugungsdiagramm kann die Anwesenheit von organischem geordnetem Material erkennen lassen, dessen konventionelles Röntgenbeugungsdiagramm durch dasjenige von nicht orientiertem ungeordnetem Material überdeckt wird. Es wird gezeigt, dass dieser Umstand dadurch bedingt ist, dass nur die Streuung von orientiertem Material zur Differenzintensität beiträgt, welche als Differenz zwischen der Streuintensität und ihrem Mittelwert über den Polwinkel im Intensitätsraum definiert ist. Als Funktion der Dehnung erhaltene Differenzdiagramme von schwach vernetztem Naturkautschuk zeigen, die Kristallinitätsentwicklung bei kleineren Dehnungen als die entsprechenden konventionellen Diagramme und lassen erkennen, dass nahezu das gesamte orientierte Material kristallin ist. Differenzdiagramm und konventionelles Diagramm wurden aus den gleichen Diffraktometerdaten erhalten. Photographisch aufgezeichnete Beugungsdiagramme liegen in Bezug auf die Empfindlichkeit auf Kristallinität zwischen den konventionellen und den Differenzdiffraktometerdiagrammen. Das Differenzbeugungsdiagramm einer hochorientierten ataktischen Polystyrolfaser gibt keine Hinweise auf Kristallinität, da die Halos im Differenzdiagramm genauso breit sind wie die im konventionellen Diagramm und keine Tendenz zur Aufspaltung in kristalline Linien besitzen.

Received July 15, 1965

Prod. No. 4882A

Catalysis in the Polymerization of Silicic Acid

S. P. MOULIK* and D. K. MULLICK, *Department of Pure Chemistry, University College of Science, Calcutta, India*

Synopsis

Some aspects of the condensation polymerization of silicic acid have been discussed in a systematic manner. Empirical relationships between the time of gelation and the catalyzer concentration, with both H^+ and OH^- catalysis, have been suggested. These are found to be consistent with the observations of various authors. Also the activities of both the ionized and un-ionized species present in the system account for some anomalous observations and the pH optimum for the maximum time of gelation. The idea of a secondary salt effect, introduced by Brönsted, has been found to be helpful in understanding catalyst function.

INTRODUCTION

The catalyzing effect of both H^+ and OH^- ions on the polymerization of silicic acid has been studied by various workers.¹⁻¹⁰ In spite of the considerable amount of work being performed, no relationship, even in empirical form, was developed for the variation of time of gelation with concentration of H^+ and OH^- ions. Hurd and co-workers^{4,7} observed that in the most acidic region (pH -0.50 to +0.50) and in the alkaline region (or OH^- ion catalyzing region, pH 3.0-5.0 and 8.0-11.0) the logarithm of the time of gelation varied linearly with pH. However, it was reported only by Sen and Ghosh¹¹ that the time of gelation t followed an empirical relation of the type,

$$t = ke^{-k'(\text{pH}-x)^2}(\text{pH} - x)$$

where k and k' are constants and x is the pH at which the time of gelation is equal to zero. Also, the effectiveness of different acids used in preparing silicic acid from its salt and also the effect of different electrolytes upon the time of gelation have not been discussed in detail, if at all, in the earlier works.^{3,7,9,11,13,14}

In the present communication it has been attempted to correlate the variation of the time of gelation t with the concentration of H^+ and OH^- ions on the basis of two empirical relations taking into consideration the data of Hurd and co-workers,⁷ Sen and Ghosh^{10,11} and Moulik and Ghosh.¹² In addition, the catalytic effects of the ionized and un-ionized species present in the system have been used to explain the variation of pH for the maximum time of gelation in the cases of different acids.

* Present address; Department of Chemistry, University of Arizona, Tucson, Arizona.

RESULTS AND DISCUSSION

Empirical Relations

Iler⁵ and Alexander⁹ found that with acid catalysis the polymerization of silicic acid follows third-order kinetics while in base-catalyzed reactions the kinetics is second-order. The great difference in the values of the activation energy at these two regions¹⁵ (9.5 kcal./mole at pH -0.44 to 0.863 and 16.1 kcal./mole at pH 4.64) suggests that two different mechanisms of polymerization are operating. Therefore, the variation of the time of gelation with the variation of the concentration of the catalyst (either H^+ or OH^-) may follow two different relations. However, Hurd obtained only one such relation for the two cases. In the present calculation it has been found interesting that though in the base-catalyzed region $\log t$ varies linearly with $-\log C_{OH^-}$, in the region of acid-catalysis t^2 varies linearly with $-\log C_{H^+}$. This is illustrated in Figures 1-6. The above relationships are found to hold both in the case of preparation of silicic acid by mixing different acids to a silicate,^{7,10,11} where some inherent electrolytes were always present, and in the case of preparation of pure silicic acid by an ion-exchange method,¹² where the catalyst, either an acid or base, was added from an external source quantitatively. The plausibility of dif-

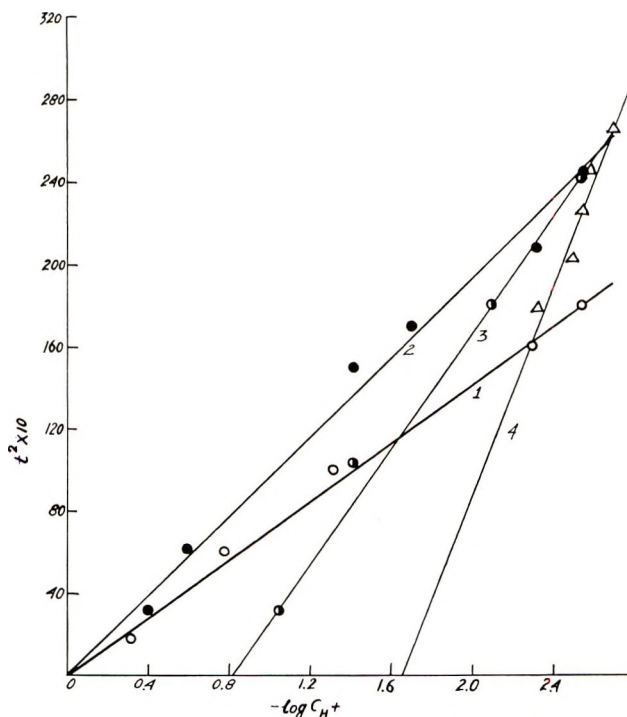


Fig. 1. Acid catalysis: (1) 1.85% SiO_2 in HCl , $34^\circ C.$; (2) 1.84% SiO_2 in H_2SO_4 , $30^\circ C.$; (3) 1.67% SiO_2 in H_3PO_4 , $32^\circ C.$; (4) 1.82% SiO_2 in CH_3COOH , $30^\circ C.$ Date of Moulik and Ghosh.¹²

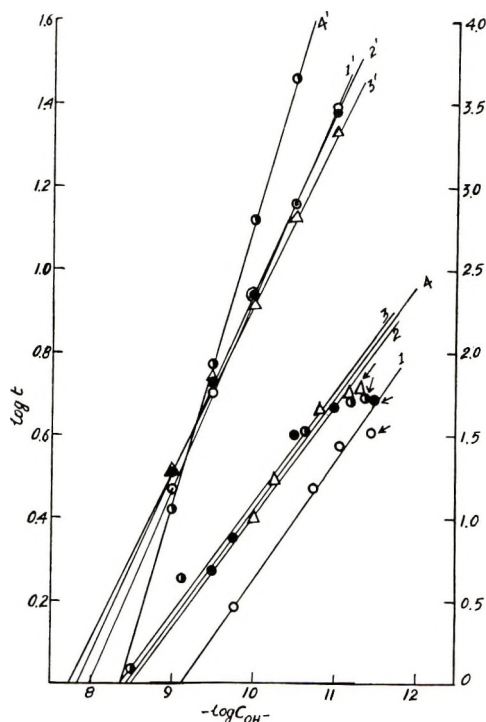


Fig. 2. Base catalysis: (1) 1.85% SiO_2 in NH_4OH , 34°C.; (2) 1.84% SiO_2 in NH_4OH , 30°C.; (3) 1.67% SiO_2 in NH_4OH , 32°C.; (4) 1.82% SiO_2 in NH_4OH , 30°C.; (1') in HCl , 24.9°C.; (2') in HNO_3 , 24.9°C.; (3') in H_2SO_4 , 24.9°C.; (4') H_3PO_4 , 24.9°C. The points marked with arrows correspond to the calculated OH^- ion concentration values of pure silicic acid. Data of Moulik and Ghosh for curves 1-4; data of Hurd et al.⁷ for curves 1'-4'.

ferent mechanisms is thus confirmed and probable empirical relations have been suggested in the following discussion.

Case I (Acid Catalysis). At a constant temperature and a constant SiO_2 concentration the rate of reaction increases with increasing concentration of H^+ ions.

Let an empirical relation of the type given in eq. (1) correlate the rate of change of the reaction velocity k_a with the H^+ ion concentration:

$$-d(1/k_a)^2/dC_{\text{H}^+} = A/C_{\text{H}^+} \quad (1)$$

where A is a constant.

On integration, eq. (1) becomes,

$$-(1/k_a)^2 = A \ln C_{\text{H}^+} + I_a \quad (2)$$

where I_a is the integration constant.

Again, the rate of reaction k_a is inversely proportional to the time of gelation¹² and therefore, $k_a = K/t$, K being the proportionality constant. On putting this value of k_a into eq. (2) it becomes.

$$-t^2/K^2 = 2.303A \log C_{\text{H}^+} + I_a \quad (3)$$

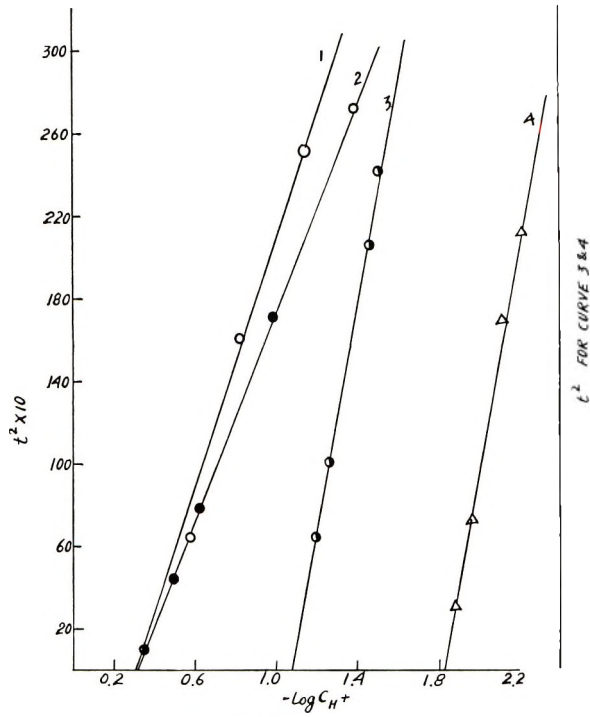


Fig. 3. Base catalysis for 3% SiO_2 at 55°C .: (1) in HCl ; (2) in H_2SO_4 ; (3) in H_3PO_4 ; (4) in ClCH_2COOH . Data of Sen and Ghosh.¹⁰

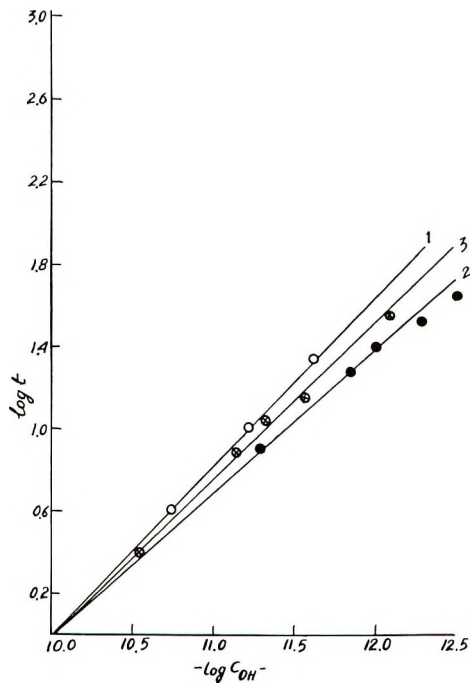


Fig. 4. Acid catalysis for 3% SiO_2 at 55°C .: (1) in HCl ; (2) in H_2SO_4 ; (3) in H_3PO_4 . Data of Sen and Ghosh.¹⁰

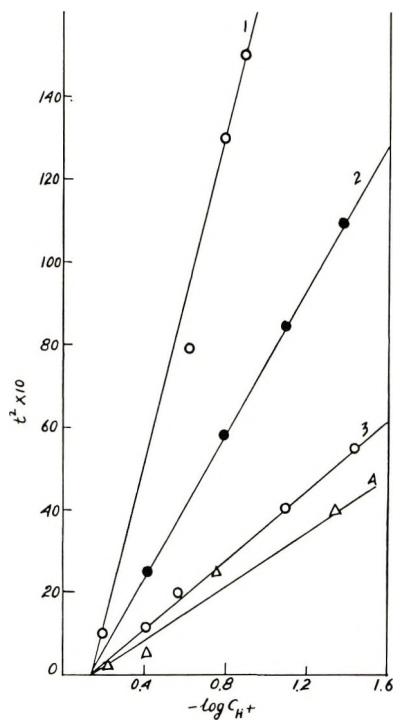


Fig. 5. Acid catalysis in the presence of added salt for 3% SiO₂ in HCl at 55°C.: (1) no salt; (2) 2N NaCl; (3) 2N CaCl₂; (4) 2N AlCl₃. Data of Sen and Ghosh.¹¹

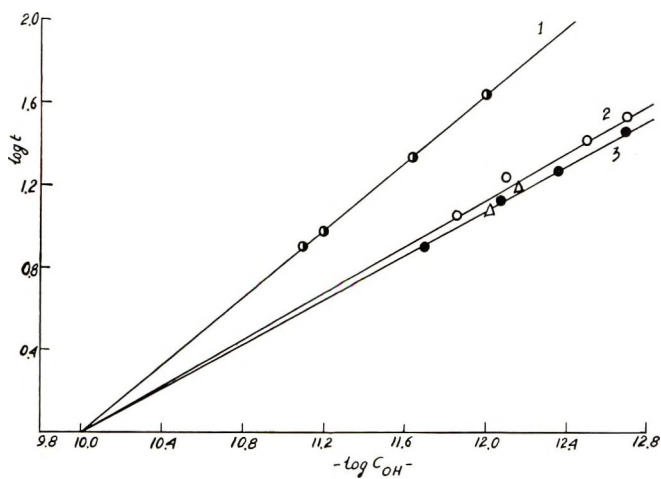


Fig. 6. Catalysis in the presence of added salt for 3% SiO₂ in HCl at 55°C.: (1) no salt; (2) 2N NaCl; (3) 2N CaCl₂; (4) 2N AlCl₃. Data of Sen and Ghosh.¹¹

or,

$$t^2 = -C_a - A' \log C_{H^+} \quad (4)$$

where, A' is a constant, $A' = 2.303 AK^2$, and $C_a = K^2 I_a =$ intercept.

Thus a plot of t^2 against $-\log C_{H^+}$ will yield a straight line having positive slope and negative intercept.

Case II (Base Catalysis). In this case also at a constant temperature and constant SiO_2 concentration the reaction velocity increases with increasing concentration of OH^- ions.

An empirical relation of the type given in eq. (5) may correlate the rate of change of the reaction velocity k_b with the OH^- ion concentration: as

$$-d \ln (1/k_b)/dC_{\text{OH}^-} = B/C_{\text{OH}^-} \quad (5)$$

where B is a constant.

On integration,

$$-\log (1/k_b) = B \log C_{\text{OH}^-} + I_b/2.303 \quad (6)$$

where I_b is the integration constant.

As before, the time of gelation t is related with the reaction velocity by $k_b = K_1/t$, where, K_1 is the proportionality constant. On putting the value of k_b in eq. (6) and rearranging it becomes,

$$\log t = (\log K_1 - I_b/2.303) - B \log C_{\text{OH}^-} \quad (7)$$

or

$$\log t = C_b - B \log C_{\text{OH}^-} \quad (8)$$

Accordingly, the variation of $\log t$ with $-\log C_{\text{OH}^-}$ will be linear.

The constants A and B in the cases of acid and base catalysis, respectively, may reflect the activation state attained, considering silicic acid molecules to form activated complexes^{16a} with the catalyzing species before undergoing polymerization.

Limitations of Eqs. (4) and (8). In eq. (4) when $C_{H^+} = 1$, i.e., $\log C_{H^+} = 0$, then $t^2 = -C_a$. In the cases of HCl and H_2SO_4 at $\log C_{H^+} = 0$, $t^2 = -C_a = 0$ (curves 1 and 2 of Fig. 1). For H_3PO_4 , CH_3COOH , ClCH_2COOH , etc., however, at $\log C_{H^+} = 0$, $t^2 = -C_a \neq 0$. In other words, the zero time of gelation is reached when $C_{H^+} < 1$ and the intercept has a negative value according to the condition of the eq. (4) (curves 3 and 4 of Fig. 1). This is due to the effects of un-ionized acid molecules and other species present in the system and will be discussed in the next section.

In eq. (8) at $C_{\text{OH}^-} = 1$, i.e., at $\log C_{\text{OH}^-} = 0$, $\log t = C_b$. From eq. (8) it is also evident that a zero time of gelation is theoretically impossible. Actually, it is a known fact that at pH 5.5 the time of gelation is minimum^{16b} (though not zero). Therefore, extrapolation of $\log t$ vs. $-\log C_{\text{OH}^-}$ curves at a pH less than 5.5, i.e., at $-\log C_{\text{OH}^-}$ less than 8.5, may result in some value of t which has no sense from the practical point of view. This value

of $-\log C_{\text{OH}^-}$ may also vary, depending upon the different species present in the solution for a particular SiO_2 concentration at a constant temperature.

Effects of Ionized and Un-ionized Species

In considering the catalyzing effects on the polymerization reaction of silicic acid the presence of various species, either ionic or nonionic, should be considered apart from the main catalyzing species, i.e., either H^+ or OH^- . Addition of neutral salts to a catalyst solution containing weak electrolytes (where acetic acid, monochloroacetic acid, citric acid, etc., are added to sodium silicate to prepare the silicic acid) may cause an accelerating effect, termed the secondary salt effect,¹⁷ which is due to the increased degree of the ionic dissociation of the weak acid as a result of the increased ionic concentration. The primary salt effect which is prominent in the case of acid-base catalysis of substrates which are ions¹⁸ is, however, insignificant in the present case because the substrate here is monosilicic acid, which is only very slightly ionic. Again, since the reaction in question may proceed with both acid and base catalysis, many different species may contribute to catalysis in the same solution and the observed change is the result of these effects. In the silicic acid system used by Hurd and co-workers^{4,7} or by Sen and Ghosh^{10,11} considerable acid (ionized or un-ionized) and salt were always present, and the rate was obviously the affected rate of reaction. Since the influence of the species produced *in situ* upon the velocity of reaction is linear¹⁹ it did not change any actual relationship that might exist between the time of gelation and the catalyst concentration. Having considered the data obtained with only acid or base catalysis of a pure silicic acid solution,¹² the present authors have observed that there are specific ions or un-ionized molecules which are responsible for the condensation polymerization process. Of the ionic functions, the effect of HCl is more prominent than that of H_2SO_4 , i.e., SO_4^{2-} ion is lower in activity than Cl^- ion, if of course we take account of the fact that same pH corresponds to same equivalent concentration of hydrogen ion for both these acids (curves 1 and 2 of Figs. 1 and 3). But in the cases of H_3PO_4 , CH_3COOH , ClCH_2COOH , etc. there is some accelerating effect, however, probably due to the un-ionized acid molecules (curves 3 and 4 of Figs. 1 and 3). The shift of the curves to the right also satisfies this condition as due to the effect of these acids in a short range of pH which is otherwise not favored with HCl and H_2SO_4 . Alexander,⁹ however, observed no effect of addition of $0.001M$ H_3PO_4 to a silicic acid prepared by the ion-exchange method. The fact that t^2 values do not pass through the origin in the cases of HCl and H_2SO_4 (curves 1 and 2 of Fig. 3) may be considered due to the effects of NaCl and Na_2SO_4 present in the system.

In base catalysis, the accelerating behavior decreases in the order $\text{H}_2\text{SO}_4 > \text{H}_3\text{PO}_4 > \text{HCl}$. Here the anions are required for catalysis (curves 1, 2, and 3 of Fig. 4). The lower activity of H_3PO_4 than H_2SO_4 may be attributed due to the singly charged anion of the monobasically dissociated

phosphoric acid. The works of Hurd and co-workers also reveal a less prominent effect in the case of H_3PO_4 (curves 1'-4', Fig. 2). The effect of OH^- ions only is best revealed in the work of Moulik and Ghosh,¹² where parallel lines are obtained with the variation of the concentration of the silicic acid and temperature (curves 1-4, Fig. 2). Along with the effect of NH_4^+ ions, the un-ionized NH_4OH present, should be considered.

The effect of addition of different salts from an external source to the gelling system is compared in Figures 5 and 6 for sodium silicate and HCl system both in the H^+ and OH^- catalysis regions. The linear plots of t^2 against $-\log C_{\text{H}^+}$ always show a decrease in the slope values with the addition of NaCl , CaCl_2 , and AlCl_3 , each at the same normality. This proves conclusively that cations have definite effects on the polymerization of silicic acid in the acidic region. With bases, however, the effect of NaCl , CaCl_2 , and AlCl_3 of the same normality has little effect on the time of gelation, as is evident from the more or less constant value of the time of gelation in presence of these salts. The reduction which has taken place in comparison to that where no salt has been added is a measure of the effect of the Cl^- ions only. The close similarity of gelation times in presence of salts having different valent cations further supports the slight effect of these cations.

Different values of the pH for the maximum time of gelation were reported by different authors. The variation was due to the probable presence of ionized and un-ionized species in the systems studied. For a pure silicic acid prepared by ion exchange it was found¹² that the pH for the maximum time of gelation depends only upon the concentration of SiO_2 in the system, because the addition of a very small amount of either acid or base always decreased the time of gelation. This observation is contrary to the idea of Sen and Ghosh¹⁰ that the pH for the maximum time of gelation depends upon the nature of the acid used to prepare the silicic acid and is independent of the SiO_2 concentration. According to Sen and Ghosh, the pH for the maximum time of gelation is greater the weaker the acid. In our discussion it has been pointed out with decreasing pH, the catalyzing power of undissociated acid molecules is greater, the weaker the corresponding acid. If the pH of such a buffered system is decreased by increasing the acid concentration, this raises the concentration of un-ionized acid molecules much more than it would for a strong, completely dissociated acid. This will evidently enhance the catalytic effect of un-ionized-acid molecules. Thus before the ideal pH (corresponding to the pure silicic acid having the same concentration) of gelation is reached, the effect is so pronounced that the time of gelation decreases somewhere before the ideal pH and a shift to higher pH direction of the maximum is observed. In this connection the observation of Iler⁵ that the pH of maximum time of gelation is in the range of 1-2, regardless of the type of acid used to prepare the silicic acid from sodium silicate, is interesting. The activity of fluoride ions present as an impurity, which has been considered by Iler to be the major factor in determining the optimum pH at the least

rapid stage of polymerization is then not the only factor, because with different acids the same quality and quantity of silicate, containing the same amount of fluoride ions, shows considerable variation in the optimum pH at the least rapid reaction stage. Unless one starts with a very pure silicic acid to which all catalyzing agents have been added from outside, it is very difficult to reach any conclusions, except on a qualitative level, concerning the pH optimum.

In observing the effect of electrolyte, Hurd³ found that the gelling time of sodium silicate plus an excess of acetic acid system at pH 5.09 was reduced by NaCl to a greater extent more than by Na₂SO₄. He was of the opinion that, although silicic acid is positively charged in the alkaline region and the effect of Na₂SO₄ should be greater than that of NaCl in the usual sense, the reverse finding proves the gelling to be something of a different process than is usual. This observation can, however, be brought into line with the general scheme by recourse to the secondary salt effect discussed previously. It can be shown that the dissociation constant of the weak acid in presence of added electrolyte is increased, according to relation,¹³

$$\log k_c = \log K + I^{1/2}(1 + I^{1/2})$$

where k_c , K , and I represent the concentration dissociation constant, thermodynamic dissociation constant, and the ionic strength, respectively. It is evident from this relation that k_c is increased by the addition of salt. Now NaCl and Na₂SO₄ at same strength will both increase the ionic strength, but the latter more than the former. Therefore, an increase in the value of k_c in the case of Na₂SO₄, compared to that with NaCl, will cause more dissociation of the weak acid (here the acetic acid) and a decrease in the OH⁻ ion concentration and hence an increase in the time of gelation. The difference in the effectiveness of NaCl and Na₂SO₄ in the usual sense is thus explained.

The authors express their thanks to the Council of Scientific and Industrial Research, Government of India, for financial assistance.

References

1. Willstater, R., H. Kraut, and K. Lobinger, *Ber.*, **58B**, 2426 (1925); *ibid.*, **61**, 2280 (1928); *ibid.*, **62**, 2027 (1929).
2. Brintzinger, H., and B. Trömer, *Z. Anorg. Allgem. Chem.*, **181**, 237 (1929).
3. Hurd, C. B., *Chem. Rev.*, **22**, 403 (1938).
4. Hurd, C. B., and R. W. Barclay, *J. Phys. Chem.*, **44**, 847 (1940).
5. Iler, R. K., *J. Phys. Chem.*, *ibid.*, **56**, 678 (1952); **57**, 604 (1953).
6. Kraut, H., *Ber.*, **64B**, 1709 (1931).
7. Hurd, C. B., and A. J. Marotta, *J. Am. Chem. Soc.*, **62**, 2767 (1940).
8. Ray, R. C., and P. B. Ganguly, *J. Phys. Chem.*, **34**, 352 (1930).
9. Alexander, G. B., *J. Am. Chem. Soc.*, **76**, 2094 (1954).
10. Sen, K. C., and B. N. Ghosh, *J. Indian Chem. Soc.*, **31**, 803 (1954).
11. Sen, K. C., and B. N. Ghosh, *J. Indian Chem. Soc.*, **33**, 209 (1956).
12. Moulik, S. P., and B. N. Ghosh, *J. Indian Chem. Soc.*, **40**, 907 (1963).
13. Merrill, R. C., and R. W. Spencer, *J. Phys. Colloid Chem.*, **54**, 806 (1950).

14. Baxter, S., and K. C. Bryant, *J. Chem. Soc.*, **1952**, 3021.
15. Penner, S. S., *J. Polymer Sci.*, **1**, 441 (1946).
16. Iler, R. K., *Colloid Chemistry of Silica and Silicates*, Cornell University Press, Ithaca, New York, 1955, (a) p. 45; (b) p. 48.
17. Brønsted, J. N., and C. E. Teeter, *J. Phys. Chem.*, **28**, 579 (1924).
18. Bell, R. P., *Advan. Catalysis*, **4**, 156 (1952).
19. Brønsted, J. N., *Z. Physik. Chem.*, **102**, 169 (1922).

Résumé

Les aspects de la réaction de polymérisation par condensation de l'acide silicique ont été discutés d'une manière plausible et systématique. Des relations empiriques entre le temps de gélation et la concentration en catalyseur aussi bien des catalyseurs acides et basiques H^+ et OH^- ont été suggérées. Ces relations sont en accord avec les observations de divers auteurs. En outre les activités des espèces ionisées et nonionisées et présentes dans le système rendent compte de certaines observations anormales de même que pour le pH optimum au temps maximum de gélation. L'idée d'un effet de sel secondaire, introduit par Brønsted, a été trouvée inutile pour comprendre la fonction des catalyseurs.

Zusammenfassung

Die Aspekte der Kondensationspolymerisationsreaktion von Kieselsäure wurden in plausibler und systematischer Weise diskutiert. Empirische Beziehungen zwischen der Gelbildungsdauer und der Katalysatorkonzentration in katalytisch wirksamen Bereich der H^+ - und OH^- -Ionen wurden angegeben. Sie stimmen mit den Beobachtungen verschiedener Autoren überein. Die Aktivität der ionisierten und der nichtionisierten im System vorhandenen Species kann gewisse anomale Beobachtungen sowie das pH-Optimum für das Maximum der Gelbildungsdauer erklären. Die von Brønsted eingeführte Annahme eines sekundären Salzeffekts erwies sich für das Verständnis der Katalysatorfunktion als nützlich.

Received June 7, 1965

Revised August 30, 1965

Prod. No. 4883A

Alternating Copolymerization of Ethylene with Maleic Anhydride*

SUEO MACHI, TAKASHI SAKAI, MASAO GOTODA, and TSUTOMU KAGIYA, *Japan Atomic Energy Research Institute, Takasaki Radiation Chemistry Research Establishment, Takasaki, Gumma, Japan*

Synopsis

The copolymerization of ethylene with maleic anhydride was carried out with γ -radiation and a radical initiator, i.e., 2,2'-azobisisobutyronitrile and diisopropyl peroxydicarbonate under pressure at various reaction conditions. The homopolymerization of neither monomer was observed in this system. In the γ -ray-initiated copolymerization the G value (polymerized monomer molecules per 100 e.v.) was shown to be between 10^3 and 10^4 . It was found that the dose rate exponent of the rate is approximately unity, and the rate is proportional to the amount of ethylene monomer. Apparent activation energies of 1.8 and 27.5 kcal./mole were obtained for γ -ray-initiated and AIBN-initiated copolymerization, respectively. Since the composition of copolymer is independent of monomer molar ratio and the molar ratio of ethylene to maleic anhydride in the polymer is approximately unity, the monomer reactivity ratios were obtained as $r_E \simeq 0$ and $r_M \simeq 0$ for γ -ray-initiated polymerization at 40°C. Alternating copolymerization was, therefore, concluded to occur. Infrared analysis of the copolymer is almost consistent with this. The copolymer in the solid state is amorphous. It is soluble in water, cyclohexane, and dimethylformamide and insoluble in lower alcohols, ether, and aromatic hydrocarbons. The aqueous solution of polymer gave a strong acid.

INTRODUCTION

The copolymerization of ethylene and maleic anhydride was first achieved by Hanford¹ with the use of benzoyl peroxide as an initiator. Few investigations of the copolymerization, however, have been made.

The purpose of this paper is to report an alternating copolymerization of ethylene with maleic anhydride by the use of γ -radiation and a radical initiator.

EXPERIMENTAL

The reaction vessel was an unstirred stainless steel autoclave of 100 ml. capacity. Ethylene used was 99.9% pure (free of CO and H₂S) containing 0.3 ppm O₂ and 21 ppm C₂H₂. Maleic anhydride was twice recrystallized from chloroform and dried in a vacuum desiccator. Acetone was dried

* Presented at the 14th Annual Meeting of the Society of Polymer Science, Japan, Tokyo, May 2, 1965.

TABLE I
Experimental Results for the Ethylene-Maleic Anhydride System^a

Run no.	Ethylene, anhydride, mole		Maleic anhydride, mole	Initial monomer mole ratio		Dose rate $\times 10^{-5}$, rad/hr.	Temp., °C.	Time, hr.	Copolymer formed, g.	G value $\times 10^{-20}$	Elementary analysis of copolymer				Final polymer mole ratio E/M
	Ethylene, mole	anhydride, mole		E/M	E/M						H, %	C, %	O, %	H/O	
13	0.15	0.30	0.30	0.5	0.5	3.9	40	2.0	1.19	6.6	54.31	4.29	32.92	0.149	1.29
3	0.50	0.50	0.50	1.0	1.0	1.4	40	2.0	2.39	5.7	51.23	5.00	42.09	0.119	0.93
12	0.79	0.30	0.30	2.6	2.6	1.8	40	16.0	21.70	4.5	56.13	5.14	34.08	0.151	1.31
7	0.70	0.10	0.10	7.0	7.0	3.0	40	1.0	2.83	11.0	55.31	4.60	34.76	0.132	1.08
6	1.32	0.16	0.16	8.3	8.3	1.4	65	2.0	4.27	10.6	53.37	5.28	36.88	0.143	1.21
8	0.91	0.10	0.10	9.1	9.1	3.0	40	1.0	3.76	13.5	55.98	4.86	37.41	0.130	1.06
4 ^c	1.28	0.21	0.21	6.1	6.1	—	65	3.0	5.58	—	53.85	4.68	37.76	0.124	0.99
11 ^d	0.79	0.30	0.30	2.6	2.6	—	30	19.5	5.47	—	53.34	4.70	36.95	0.127	1.02
M1 ^e	0	0.2	0.2	—	—	1.4	40	1.5	0	0	—	—	—	—	—
E1 ^e	1.6	0	0	—	—	1.4	40	1.5	7.2	26.5	—	—	—	—	—

^a Reactor volume is 100 ml., and 46 ml. acetone was used as solvent in experiments 3, 7, 8, 11, 12, and 13.

^b Number of polymerized monomer molecules per 100 e.v. absorbed in monomer and polymer.

^c Polymerization was initiated by azobisisobutyronitrile, 0.42 mmole.

^d Polymerization was initiated by diisopropyl peroxydicarbonate, of 0.44 mmole.

^e Homopolymerization of ethylene and maleic anhydride.

over sodium hydroxide and distilled. 2,2'-Azobisisobutyronitrile (AIBN) was recrystallized from acetone. Diisopropyl peroxydicarbonate was a commercial grade containing an equal amount of dioctyl phthalate as diluent.

All irradiations were performed with a 36,000 c. ^{60}Co source at Japan Atomic Energy Research Institute. The reaction temperature was automatically maintained constant within $\pm 1^\circ\text{C}$. in the course of a reaction. The polymerizations were carried out to low conversion not to deplete either of the monomers. The reaction was stopped by purging the unreacted ethylene and removing the ^{60}Co . The reaction mixtures were precipitated with dried methanol below 10°C . The polymers, obtained in a powdery form, were filtered, washed with ether, and dried to constant weight in a vacuum at room temperature. Since homopolymerization does not occur, no extraction of homopolymer was made. Infrared analysis was carried out by use of a Nippon-bunko Model DS-301 infrared spectrophotometer with NaCl optics. Elementary analysis for hydrogen, carbon, and oxygen was also made. The solution viscosity of polymer was measured in dimethylformamide at 30°C . in an Ubbelohde viscometer.

RESULTS AND DISCUSSION

Composition of Copolymer

The results obtained in the experiments where initial monomer molar ratio was varied are given in Table I. As shown in Figure 1, it is found that the polymer composition is independent of the composition of monomers, and the molar ratio of ethylene (E) to maleic anhydride (M) in the polymer is almost unity for both γ -ray-initiated and radical-initiated polymerization.

The data are examined by the copolymerization equation:²⁻⁴

$$e/m = E(r_E E + M)/M(r_M M + E) \quad (1)$$

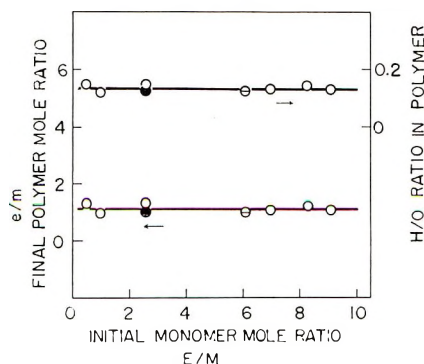


Fig. 1. Final polymer mole ratio and weight ratio of hydrogen to oxygen in polymer vs. initial monomer mole ratio: (O) γ -ray-initiated polymerization; (O with dot) AIBN-initiated polymerization; (●) IPP-initiated polymerization; \dagger reaction temperature 30 – 65°C .

where E and M represent the mole fractions of ethylene and maleic anhydride in monomer mixture, e and m are their mole fractions in copolymer, r_E and r_M are the ratios of propagation rate constants:

$$r_E = k_{EE}/k_{EM}$$

$$r_M = k_{MM}/k_{ME}$$

where k_{EE} and k_{EM} are the rate constants of the addition of ethylene and maleic anhydride to an ethylene free-radical chain end, k_{MM} and k_{ME} are the rate constants of the addition of maleic anhydride and ethylene to a maleic anhydride free-radical chain end.

Since maleic anhydride does not polymerize alone under our experimental conditions, as shown in Table I (Run no. M1), though the homopolymerization⁵ was carried out under severe conditions, k_{MM} vanishes and $r_M = 0$. Accordingly, eq. (1) becomes, in simplified form:

$$e/m = r_E(E/M) + 1 \quad (2)$$

Figure 1, a plot of e/m versus E/M , indicates that r_E is essentially zero. Since ethylene easily polymerizes alone, k_{EE} is not zero. Therefore, it is indicated that k_{EM} is much larger than k_{EE} . This and the fact that $r_M = 0$ indicate alternating copolymerization takes place in this system.

Polymerization Rate and Polymer Viscosity

The dependence of copolymerization rate and solution viscosity of polymer on the amount of ethylene and maleic anhydride in the reactor are shown in Figures 2 and 3, respectively. From these figures it is shown that both the polymerization rate and viscosity (corresponding to the degree of polymerization) are proportional to the amount of ethylene, while they are independent of the amount of maleic anhydride if less than equimolar. From these results it is presumed that the rate-determining step of propa-

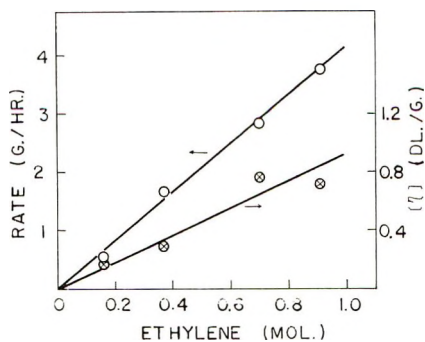


Fig. 2. Polymerization rate and intrinsic viscosity of polymer vs. amount of ethylene for γ -ray-initiated polymerization: (O) polymerization rate; (⊗) intrinsic viscosity. Reaction time 1.0 hr., temperature 40°C., dose rate 3.0×10^5 rad/hr., amount of maleic anhydride 0.1 mole, solvent acetone (46 ml.), reactor volume 100 ml.

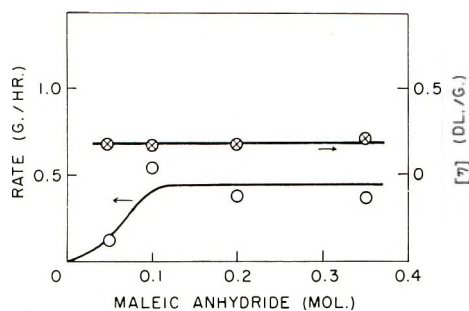


Fig. 3. Polymerization rate and intrinsic viscosity of polymer vs. amount of maleic anhydride for γ -ray-initiated polymerization: (O) polymerization rate; (\otimes) intrinsic viscosity. Amount of ethylene 0.16 mole; other reaction conditions are the same as shown in Fig. 2.

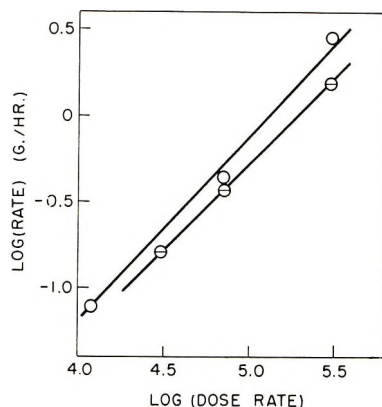


Fig. 4. Effect of dose rate on polymerization rate in γ -ray-initiated polymerization: (O) polymerization carried out in the presence of acetone, reaction temperature 40°C., amount of ethylene 0.7 mole, amount of maleic anhydride 0.1 mole, solvent acetone (46 ml.); (\ominus) polymerization carried out without solvent, temperature 65°C., amount of ethylene 0.8 mole, amount of maleic anhydride 0.16 mole; reactor volume 100 ml.

gation rate is the addition of ethylene to the maleic anhydride growing chain end.

The reaction rates were measured over a 25-fold variation in dose rate for γ -ray-initiated polymerization. Figure 4 shows that the dose rate exponent of the rate is almost unity for both solution and bulk polymerization. Considering copolymer precipitates in a polymerization medium, this high exponent may be associated with the heterogeneity of the system.

The temperature dependence of the polymerization rate was examined for γ -ray-initiated and AIBN-initiated copolymerization. Arrhenius plots are shown in Figure 5, from which we obtained apparent activation energies of 1.8 and 27.5 kcal./mole for γ -ray-initiated and AIBN-initiated polymerization, respectively. The overall activation energy of the polymerization is given by the simplified expression:

$$E = E_p + \alpha E_i - \alpha E_t \quad (3)$$

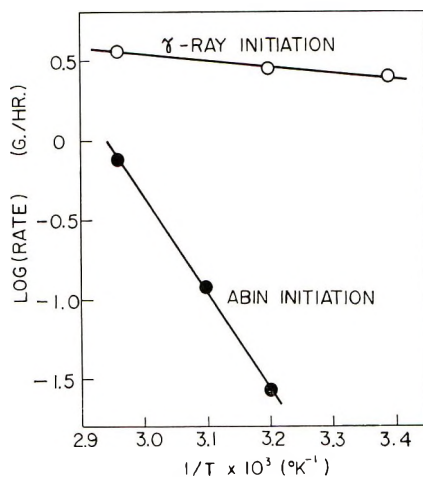


Fig. 5. Effect of temperature on polymerization rate: (O) γ -ray-initiated polymerization, dose rate 3×10^6 rad/hr.; (●) AIBN-initiated polymerization, amount of AIBN 0.42 mmole; amount of ethylene 0.7 mole, amount of maleic anhydride 0.1 mole, reactor volume 100 ml.

where the value of α lies between 1 and 0.5, depending on the relative amounts of first-order and second-order termination. In γ -ray-initiated polymerization, taking $\alpha = 1.0$, as shown by the dose rate exponent of the rate, $E_p + E_t - E_i = 1.8$ kcal./mole. If we assume first-order termination, E_i is found to be approximately 26 kcal./mole for AIBN-initiated copolymerization. This corresponds closely to the reported values for the thermal decomposition of AIBN,^{6,7} i.e., 31–34 kcal./mole. Though this correspondence should not be overstressed, it is shown that the activation energy of initiation makes a main contribution to the apparent overall activation energy, and that the difference in overall activation energy between AIBN-initiated and γ -ray-initiated polymerization is ascribed to the difference in that of initiation reaction.

Infrared Analysis and Some Properties of Copolymer

In Figure 6 an infrared spectrum of the copolymer obtained by γ -ray-initiated polymerization is given in comparison with that of γ -ray-polymerized polyethylene. The copolymer spectrum shows strong absorption peaks at 1860 and 1780 cm^{-1} which are assigned to the C=O vibration in cyclic anhydride. The 1230 cm^{-1} band is due to C—O single-bond vibration in the cyclic anhydride. Bands at 2960 and 2910 cm^{-1} arising from the methyl and methylene C—H stretching vibration and bands at 1460 and 1370 cm^{-1} arising from methylene C—H deformation vibration are also observed.

These features of the spectrum show that the copolymer is composed of the methylene from ethylene monomer, and the cyclic anhydride from maleic anhydride monomer. A weak absorption peak at 725 cm^{-1} which

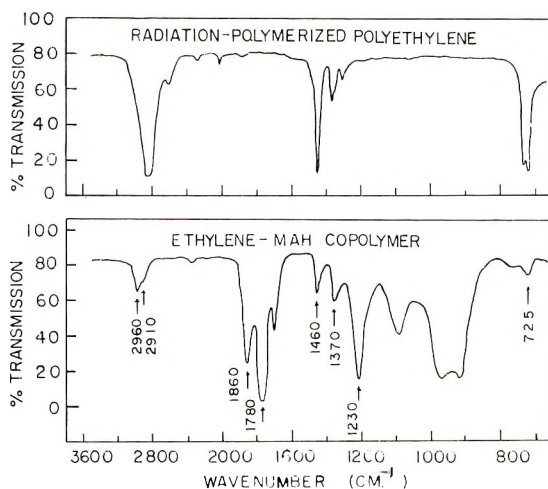


Fig. 6. Infrared spectra of an ethylene-maleic anhydride copolymer and polyethylene: copolymer sample polymerized under the conditions: temperature 2°C., dose rate 1.4×10^6 rad/hr., molar ratio of ethylene to maleic anhydride 5.0.

is due to the skeletal vibration of tetramethylene is also noted. This may indicate the sequence addition of more than two ethylene units takes place to some extent. However, considering the copolymer composition described before, the degree of sequence addition is believed to be small.

The copolymer is soluble in water, cyclohexane, dimethylformamide, and liquid maleic anhydride. It is insoluble in lower alcohols, ether, aromatic hydrocarbons, chloroform, and is almost insoluble in acetone, while polyethylene is not soluble in water and poly(maleic anhydride)⁵ is soluble in alcohol and ether. An aqueous solution of the copolymer gives a strong acid.

From the facts that the polymer obtained from reaction mixture is soluble in water and no polymer can be extracted by ether, it is indicated that homopolymerization of neither monomer takes place in the system.

References

1. Hanford, W. E., U. S. Pat. 2,378,629 (1945).
2. Alfrey, T., Jr., and G. Goldfinger, *J. Chem. Phys.*, **12**, 205 (1944).
3. Mayo, F. R., and F. M. Lewis, *J. Am. Chem. Soc.*, **66**, 1594 (1944).
4. Wall, F. T., *J. Am. Chem. Soc.*, **66**, 2050 (1944).
5. Lang, J. L., W. A. Pavelich, and H. D. Clarey, *J. Polymer Sci.*, **55**, S31 (1961); *J. Polymer Sci. A*, **1**, 1123 (1963).
6. Lewis, F. M., and M. S. Matheson, *J. Am. Chem. Soc.*, **71**, 747 (1949).
7. Overberger, C. G., M. T. O'Shaughnessy, and H. Shalit, *J. Am. Chem. Soc.*, **71**, 2661 (1949).

Résumé

La copolymérisation de l'éthylène avec l'anhydride maléique a été effectuée sous irradiation et en présence d'un radical initiateur, c.à.d. le 2,2'-aso-bis-isobutyronitrile et le

peroxydicarbonate de diisopropyle, sous pression et dans diverses conditions de réaction. L'homopolymérisation de ces monomères n'était pas observée dans le système. Dans la copolymérisation initiée aux rayons- γ , la valeur de G (le nombre de molécules polymérisées par 100 eV) était située entre 10^3 et 10^4 . On a trouvé que l'exposant de la vitesse de dose, en fonction de la vitesse, est approximativement unitaire, et la vitesse est proportionnelle à la quantité d'éthylène monomère. Une énergie d'activation apparente de 1.8 et 27.5 Kcal/mole a été obtenue pour la copolymérisation initiée par des rayons- γ et initiée par AIBN respectivement. Puisque la composition des copolymères est indépendante du rapport molaire de monomères et puisque le rapport molaire de l'éthylène sur de l'anhydride maléique dans le polymère est approximativement égale à 1, les rapports de réactivité monomérique sont $r_E = 0$ et $r_M = 0$ pour la polymérisation initiée aux rayons- γ à 40°C. La copolymérisation alternante était, de ce fait, admise. Analyse infra-rouge du copolymère est entièrement en accord avec ce point de vue. Le copolymère à l'état solide est amorphe. Il est soluble dans l'eau, le cyclohexane et le diméthylformamide; il est insoluble dans les alcools inférieurs, l'éther et les hydrocarbures aromatiques. Une solution aqueuse de polymère a une réaction d'acide fort.

Zusammenfassung

Die Copolymerisation von Athylen mit Maleinsäureanhydrid wurde mit γ -Strahlung und mit radikalischen Startern, wie z.B. 2,2'-Azobisisobutyronitril und Diisopropylperoxydicarbonat unter Druck und bei verschiedenen Reaktionsbedingungen ausgeführt. In diesem System wurde keine Homopolymerisation der Monomeren beobachtet. Bei der γ -Strahlinitiierten Copolymerisation lag der G -Wert (pro 100 eV polymerisierte Monomermoleküle) zwischen 10^3 und 10^4 . Der Exponent der Dosisleistung im Geschwindigkeitsausdruck ist etwa eins, und die Geschwindigkeit ist der Menge des Monomeren Athylens proportional. Scheinbare Aktivierungsenergien von 1,8 bzw. 27,5 kcal/Mol wurden für die γ -strahlinitiierte bzw. AIBN-gestartete Copolymerisation erhalten. Da die Zusammensetzung des Copolymeren vom Molverhältnis der Monomeren unabhängig ist und das Molverhältnis Athylen zu Maleinsäureanhydrid im Monomeren etwa eins beträgt, wurden die Reaktivitätsverhältnisse zu $r_E \sim 0$ und $r_M \sim 0$ für die γ -strahlinitiierte Polymerisation bei 40°C erhalten. Es tritt somit alternierende Copolymerisation auf. Die Infrarotanalyse des Copolymeren stimmt damit recht gut überein. Das Copolymer ist im festen Zustand amorph. Es ist in Wasser, Zyklohexan sowie Dimethylformamid löslich und in niedrigen Alkoholen, Äther und aromatischen Kohlenwasserstoffen unlöslich. Die wässrige Lösung des Polymeren lieferte eine starke Säure.

Received August 2, 1965

Prod. No. 4888A

Cyclobutane Polymers from Acrylonitrile Dimer

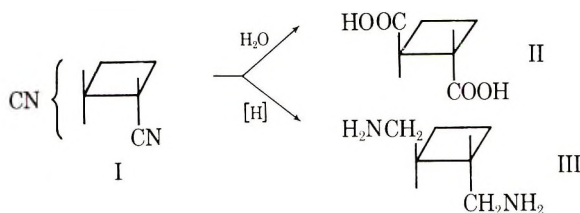
K. C. STUEBEN, *Research and Development Department, Plastics Division, Union Carbide Corporation, Bound Brook, New Jersey*

Synopsis

A wide variety of polyesters and polyamides was prepared from 1,2- and 1,3-disubstituted cyclobutane derivatives. In general, polyamides containing the *trans*-disubstituted cyclobutane ring were crystalline. Polyesters containing predominantly the *trans*-isomer tended to be crystalline but those containing mixtures of *cis-trans* isomers were amorphous. Mechanical properties have been determined wherever possible. Appreciable yields of cyclic dimers were isolated during the preparation of certain polyesters. These cyclic dimers readily polymerized when treated with dibutylzinc. Examination of acrylonitrile dimer (1,2-dicyanocyclobutane) by gas chromatography failed to reveal the presence of any 1,3-dicyanocyclobutanes.

INTRODUCTION

Polymers containing recurring cyclobutane rings in the backbone have been the subject of numerous investigations recently. Little has been published^{1,2} on linear condensation polymers containing the 1,2-disubstituted cyclobutane ring, however, in an area which was actively investigated several years ago in these laboratories. Acrylonitrile dimer³ (1,2-dicyanocyclobutane) provides a logical and economical entry to this class of polymers, particularly in view of the improvements which have been made in its synthesis^{4,5} recently. Although the dimerization of acrylonitrile produces a mixture of *cis* and *trans*-1,2-dicyanocyclobutanes,* isomerization to the *trans* form accompanies both hydrolysis and hydrogenation yielding the *trans*-diacid (II) and *trans*-diamine^{6,7} (III), respectively.

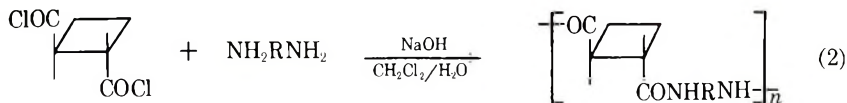


* Contrary to earlier assignments recent dipole studies⁵ have indicated that the lower-boiling isomer is the *trans* form.

RESULTS AND DISCUSSION

Polyamides

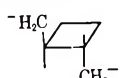
Conventional melt polymerization¹ is unsuitable for the preparation of polyamides derived from II because of the ease with which isomerization to the *cis* form and subsequent formation of terminating cyclic imides takes place.^{8,9} The milder conditions of interfacial polymerization were well suited here, and with this technique it was possible to obtain high molecular weight polyamides from the *trans*-diacid chloride and certain diamines [eq. (2)]



Examples of the polyamides prepared and their crystalline melting points are given in Table I.

One of the more characteristic features of these polyamides was the extreme ease with which they crystallized. Rapid quenching of a molded sample of VI, however, afforded coherent films for which the properties shown in Table II were determined.

TABLE I
Polyamides Prepared Interfacially

No.	Diamine (NH ₂ RNH ₂)	Yield, %	R.V. (25°C.) ^a	T _m , °C. ^b
IV	R = -(CH ₂) ₄ -	20	0.96	236
V	-(CH ₂) ₅ -	38	0.81	206
VI	-(CH ₂) ₆ -	31	1.91	212
VII	-(CH ₂) ₈ -	64	0.28	194
VIII	-(CH ₂) ₉ -	75	0.65	180
IX	-(CH ₂) ₁₀ -	79	0.33	175
X	Piperazine-	70	1.56	320
XI		38	0.28	190

^a Reduced viscosity (0.2 g. polymer in 100 ml. solvent) in phenol-tetrachloroethane (60-40 wt.-%).

^b Fisher Johns block.

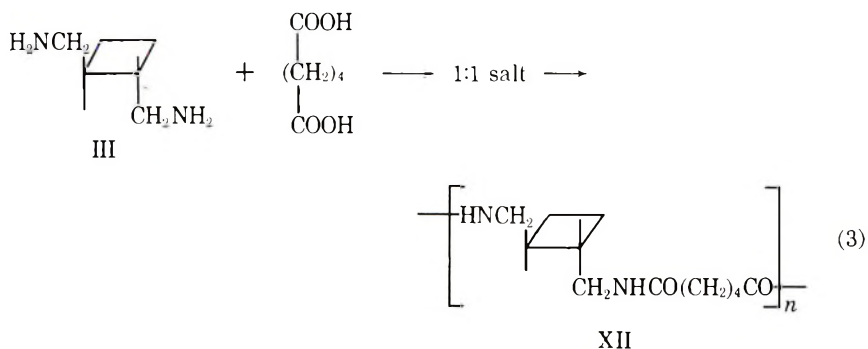
TABLE II
Tensile and Thermal Properties of
Poly(hexamethylene *trans*-1,2-cyclobutanedicarboxylic Acid Amide) (VI)

Glass transition temperature, °C.	65
Crystalline melting point, °C.	210
1% Tensile secant modulus at 25°C., psi	333,700
Tensile strength, psi	4,900
Elongation at break, %	2

By comparison, the hexamethylenediamine-derived polyamides from succinic acid, *trans*-1,2-cyclohexanedicarboxylic acid, and *trans*-1,2-cyclopropane-dicarboxylic acid melt at 210–212°C.,¹⁰ 238–242°C.,¹¹ and ca. 300°C.,¹² respectively.

The ease with which polyamide VI crystallized was somewhat unexpected in view of the existence of both D- and L-forms in the chain. Presumably, the cyclobutane rings project above and below the main chain axis and are thus accommodated in the crystal lattice.

The cyclobutanediamine (III) affords polyamides which are structurally very similar to those obtained from the diacid (II). In the diamine, however, the aminomethyl groups attached to the cyclobutane ring are not easily isomerized. Thus, the all-*trans* structure should be retained in the polymer, even under vigorous polymerization conditions. Several polyamides were prepared from the diamine by the standard melt technique as illustrated in eq. (3) with adipic acid.



The melt polymerizations proceeded readily and without signs of decomposition. The properties of the resultant polyamides are shown in Table III. Despite the close similarity in structure between polyamides VI and

TABLE III
Properties of Polyamides Derived from Diamine III

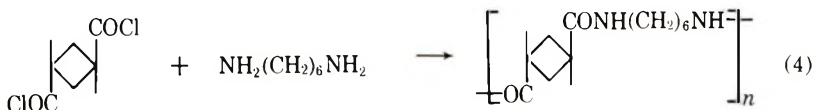
No.	Polymer	R.V. (25°C.) ^a	T_g , °C.	T_m , °C.	Tensile modulus, psi	Tensile strength, psi	Elonga- tion at break, %
XII	Adipamide	0.86	50	200	94,000– 210,000	2,000– 6,200	3–25
XIII	Sebacamide	1.28	25	160	280,000	6,600	
XIV	75% Adipic- 25% sebacic copolymer	1.34	25	150	260,000	6,400	4–26 15

^a Reduced viscosity (0.2 g. polymer in 100 ml. solvent) in phenol-tetrachloroethane (60–40 wt.-%).

XII, appreciable differences were noted in their ability to crystallize. As noted earlier, it was difficult to obtain polyamide VI in the amorphous state, even by quenching from the melt, while XII was readily quenched. The formation of the *cis* form of the diamine by isomerization and subsequent incorporation into the polyamide seems unlikely, since pyrrole¹³ formation would probably have occurred and made the attainment of high molecular weight difficult.

In contrast to the 1,2-disubstituted cyclobutane polymers, those derived from the 1,3-cyclobutane ring are capable only of geometric isomerization and therefore might display improved properties. Therefore, the polyamide derived from hexamethylenediamine and *trans*-1,3-cyclobutanedicarboxylic acid was prepared for comparison. The 1,3-dicarboxylic acid was synthesized by the route of Deutsch and Buchman.^{14,15} Certain modifications in their procedure were necessary, however, and the details are presented in the experimental section.

High molecular weight (reduced viscosity 1.39) polyamide (XV) was prepared by the interfacial polymerization of hexamethylenediamine and *trans*-1,3-cyclobutanedicarboxylic acid chloride [eq. (4)].



As expected, this polyamide melted much higher (ca. 305°d) than the 1,2-analog because of its increased symmetry. As prepared, it had only a low degree of crystallinity, however. Films cast from phenol displayed only feeble strength.

Polyesters

A number of polyesters containing recurring 1,2-disubstituted cyclobutane rings were prepared by conventional melt, solution, or interfacial techniques (Table IV). As a result of the vigorous conditions prevailing during conventional melt polymerization, high polymers derived from cyclobutane dicarboxylates are felt to be comprised of *cis* and *trans* isomers. Thus, the polyester (XVIII) prepared from diphenyl *trans*-1,2-cyclobutanedicarboxylate and bisphenol A was amorphous, while the *trans* product (XIX) prepared by the milder interfacial technique was crystalline. One of the polymers prepared, poly(ethylene 1,2-cyclobutanedicarboxylate) (XVI), displayed considerable tendency to form a 16-membered cyclic dimer during its preparation. This dimer readily repolymerized to a rubbery polymer when treated with a catalytic amount of dibutylzinc.

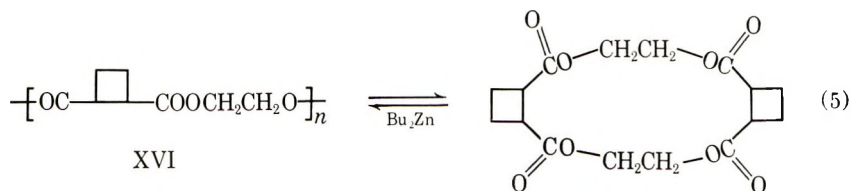
TABLE IV
Properties of 1,2-Disubstituted Cyclobutane Polyesters

No.	Structure	R.V. ^a	T_m , °C. ^b	Crystallinity
XVI	$\left[\text{OC} \begin{array}{c} \diagup \\ \square \\ \diagdown \end{array} \text{COOCH}_2\text{CH}_3 \right]_n$	0.41	25	No
XVII	$\left[\text{OC} \begin{array}{c} \diagup \\ \square \\ \diagdown \end{array} \text{COOCH}_2 \begin{array}{c} \diagup \\ \square \\ \diagdown \end{array} \text{CH}_2\text{O} \right]_n$	0.45	25	No
XVIII	$\left[\text{OC} \begin{array}{c} \diagup \\ \square \\ \diagdown \end{array} \text{COO} \begin{array}{c} \diagup \\ \square \\ \diagdown \end{array} \text{C}_6\text{H}_4 \begin{array}{c} \diagup \\ \square \\ \diagdown \end{array} \text{O} \right]_n$	0.60	118	No
XIX	$\left[\text{OC} \begin{array}{c} \diagup \\ \square \\ \diagdown \end{array} \text{COO} \begin{array}{c} \diagup \\ \square \\ \diagdown \end{array} \text{C}_6\text{H}_4 \begin{array}{c} \diagup \\ \square \\ \diagdown \end{array} \text{O} \right]_n$	0.1	Softened at 144-155	Low-medium
XX	$\left[\text{OCH}_2 \begin{array}{c} \diagup \\ \square \\ \diagdown \end{array} \text{CH}_2\text{OOC} \begin{array}{c} \diagup \\ \square \\ \diagdown \end{array} \text{C}_6\text{H}_4 \text{SO}_2 \begin{array}{c} \diagup \\ \square \\ \diagdown \end{array} \text{C}_6\text{H}_4 \text{CO} \right]_n$	0.49 ^c	Softened at 135-180	Low
XXI	$\left[\text{OCH}_2 \begin{array}{c} \diagup \\ \square \\ \diagdown \end{array} \text{CH}_2\text{OOC} \begin{array}{c} \diagup \\ \square \\ \diagdown \end{array} \text{C}_6\text{H}_4 \text{CO} \right]_n$	0.23	60	No

^a Reduced viscosity in chloroform at 25°C.

^b Fisher-Johns block.

^c Reduced viscosity in tetrachloroethane.



The highest melting polyester (XX) in this series was that prepared from *trans*-1,2-bis(hydroxymethyl)cyclobutane and 4,4'-diethylsulfonyl dibenzoate. This polyester was fiber forming and developed a low degree of crystallinity when annealed. This polymer and the related terephthalate (XXI) are relatively stable toward isomerization and are believed to be exclusively *trans*.

Several 1,3-disubstituted cyclobutane polyesters were also prepared during the course of this work (Table V). Because of their increased symmetry, these polyesters displayed higher glass transition temperatures and crystalline melting points than the 1,2 analogs. As in the cases above, conventional melt polymerization resulted in extensive isomerization with the formation of amorphous polyesters (XXII, XXIII, and XXV). Batzer and Fritz¹⁶ have shown, however, that the isomerization of cyclohexane-

TABLE V
Properties of 1,3-Disubstituted Cyclobutane Polyesters

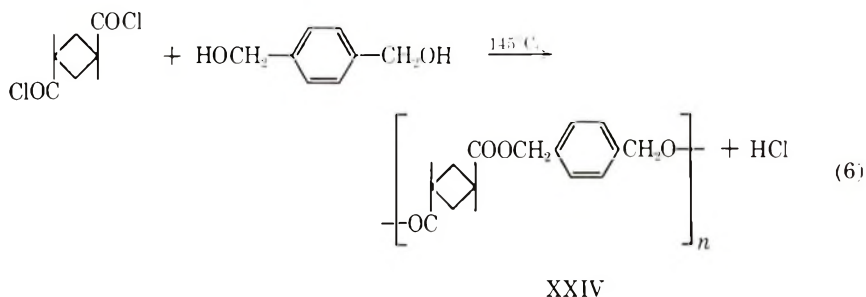
No.	Structure	R.V. ^a	T_g , °C. Crystallinity
XXII		1.46	ca. 25 ^b No
XXIII		1.78	60-70 ^b No
XXIV		0.21	T_m 87 ^c Low-medium
XXV		0.56	130 No
XXVI		0.26	T_m 180-220 ^b Low-medium

^a Reduced viscosity in chloroform at 25°C.

^b Fisher-Johns block.

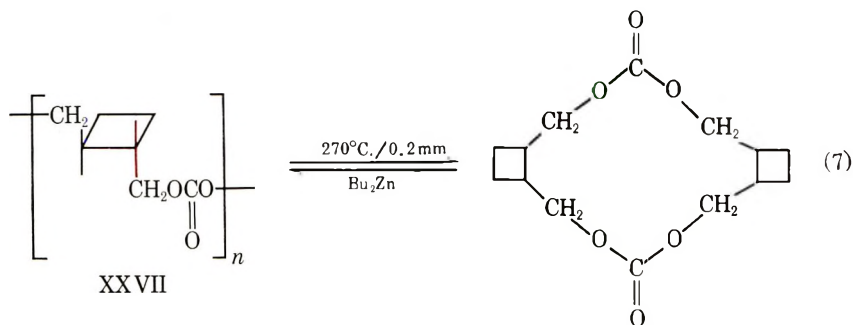
^c Polarizing microscope.

dicarboxylic acids is minimized if the conditions of polyesterification are mild. Thus, it was possible to prepare crystalline polyesters (XXIV and XXVI) by the reaction of *trans*-1,3-cyclobutanedicarboxylic acid chloride with *p*-xylylene glycol or bisphenol A under mild conditions [eq. (6)], while



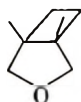
more vigorous conditions led only to amorphous materials.

A linear polycarbonate (XXVII) was prepared by melt polymerization of the *trans*-diol and diphenyl carbonate. The product was amorphous and had a glass transition at approximately room temperature. On heating to 270°C. *in vacuo*, the polymer depolymerized to a cyclic dimer in excellent yield. The dimer readily formed a rubbery high polymer (R.V. 0.83) on treating with dibutylzinc [eq. (7)].



Polyether

By using catalysts (PF_5 , SbCl_5) which are effective for the preparation of polyethers,¹⁷ some unsuccessful attempts were made to polymerize 6-oxabicyclo (3:2:0) heptane (XXVIII). The inability of this ether to



XXVIII

undergo polymerization is attributed to a lack of strain in the five-membered ring.

Acrylonitrile Dimer

The major products resulting from the thermal dimerization of acrylonitrile are known to be *cis*- and *trans*-1,2-dicyanocyclobutanes. Smaller amounts of other unidentified components have also been detected, their number and quantity depending upon the conditions used in the dimerization. Among some of the possible side products are the more symmetrical 1,3-dicyanocyclobutanes. Authentic samples of *cis*- and *trans*-1,3-dicyanocyclobutane were prepared from the corresponding dicarboxylic acid by conventional means. Crude acrylonitrile dimer prepared by the method of Coyner and Hillman³ was then examined by gas chromatography under conditions which readily distinguished among all of the four possible isomers and found to be devoid of the symmetrical 1,3 compounds.

EXPERIMENTAL

Monomers

***trans*-1,2-Cyclobutanedicarboxylic Acid.** *trans*-1,2-Cyclobutanedicarboxylic acid was prepared according to the method described by Coyner and Hillman.³

***trans*-Dimethyl-1,2-Cyclobutanedicarboxylate.** By using an improved method¹⁸ for the preparation of methyl esters, 20.5 g. (0.142 mole) of *trans*-1,2-cyclobutanedicarboxylic acid was dissolved in 80 ml. of chloroform-methanol (50:50 v/v) containing 3 ml. of concentrated sulfuric acid. After refluxing overnight into a Soxhlet containing 15 g. of anhydrous magnesium sulfate, the solvents were stripped off and the catalyst neutralized. The product was distilled *in vacuo*, b.p. 85.5–86°C./5.3–5.7 mm., n_D^{25} 1.4430 (lit.:¹⁹ b.p. 105–107°C./13 mm., n_D^{20} 1.4450); yield 82%. This product analyzed 98.7% pure by gas chromatography.

***trans*-1,2-Cyclobutanedicarboxylic Acid Chloride.** This compound was prepared in 92.5% yield by the usual method with thionyl chloride, b.p. 49.5–50.5°C./0.60–0.65 mm.

ANAL. Calcd. for C₆H₆Cl₂O₂: C, 39.81%; H, 3.43%; Cl, 39.17%; neut. equiv. 181.02. Found: C, 40.13%; H, 3.57%; Cl, 39.19%; neut. equiv. 181.0.

***trans*-1,2-Bis(hydroxymethyl)cyclobutane** was obtained by lithium aluminum hydride reduction of the acid chloride. The product had b.p. 122–124°C./5.8 mm., n_D^{26} 1.4717 (lit.:²⁰ b.p. 107–108°C./1.5 mm., n_D^{20} 1.4736).

Phenyl *trans*-1,2-Cyclobutanedicarboxylate. Phenol was allowed to react with the *trans*-1,2-cyclobutane dicarboxylic acid chloride in benzene according to the method given by Spassow.²¹ The crude product was recrystallized from ethanol to give 82.4% of the diphenyl ester, m.p. 87.5–89°.

ANAL. Calcd. for C₁₈O₁₆O₄: C, 72.96%; H, 5.44%. Found: C, 73.33, 73.42%; H, 5.31, 5.36%.

***trans*-1,2-Bis(aminomethyl)cyclobutane.**⁶ To a 3-liter stainless steel stirred autoclave were charged 500 cc. anhydrous *tert*-butanol. Raney nickel (80 g.) weighed as an aqueous sludge and then washed four times with 100 cc. portions of isopropyl alcohol (99%) and 400 g. (3.77 mole) of 1,2-dicyanocyclobutane. The free space was purged of air with hydrogen, after which liquid anhydrous ammonia (500 cc., 330 g.) was introduced, and the mixture was then heated to 100°C. Hydrogen was added to a total pressure of 1000 psig, following which the mixture was held at 100°C. at this pressure until the uptake of hydrogen ceased.

The product was filtered through a precoated (Hyflo) filter. Ammonia and *tert*-butanol were stripped from the total filtrate at 250 mm. through a column having an efficiency of about ten theoretical plates. Distillation of the residue through the same column at a reflux ratio of 5:1 yielded 324 g. (75.4%) of (I); b.p. 110–113°C./50 mm. A sample was distilled again and the fraction boiling at 111–112°C./50 mm. was collected and immediately analyzed.

ANAL. Calcd. for C₆H₁₄N₂: C, 63.1%; H, 12.37%; N, 24.5%; NH₃, 17.51%. Found: C, 63.5%; H, 12.20%; N, 24.3%; NH₃,²² 17.38%.

***cis*-3-Oxabicyclo(3:2:0)Heptane (XXVIII).** A solution of 23.25 g. (0.2 mole) of *cis*-1,2-bis(hydroxymethyl)cyclobutane²³ in 150 ml. of 18% sulfuric acid was refluxed for 25 min., during which time the solution changed from colorless to brown. After this treatment the product was steam distilled over and separated from the water by ether extraction. The extract was dried and distilled at atmospheric pressure giving 17.3 g. (88%), b.p. 119°C., *n*_D²⁶ 1.4473.

ANAL. Calcd. for C₆H₁₀O: C, 73.4%; H, 10.3%. Found: C, 74.03, 74.21%; H, 10.05, 10.11%.

The preparation of the *cis*- and *trans*-1,3-cyclobutanedicarboxylic acids is based largely on the work of Deutsch and Buchmann,^{14,15} the details of which recently appeared.²⁴ In certain aspects, our results and methods differed from his and are, therefore, reproduced here.

1,1,3,3-Cyclobutanetetracarboxylic Acid. A mixture of 29.2 g. (0.1 mole) of 7-phenyl-6,8-dioxaspiro (3,5)nonane-2,2-dicarboxylic acid²⁴ and 25 ml. of 2*N* nitric acid was heated to reflux for 5 min. All of the acid dissolved, and the benzaldehyde separated on top of the aqueous solution. The benzaldehyde was removed (its formation was quantitative) and the aqueous solution extracted twice with ether. The residual aqueous solution was boiled for a few minutes to expel the traces of ether. The aqueous solution was then added dropwise and with stirring to 100 ml. of concentrated nitric acid maintained at 25–30°C. over 45–75 min. (Use of hot nitric acid led to poor and erratic yields.) Following the addition, the reaction mixture was allowed to stir at room temperature for 1¹/₄–4 hr., during which time it became dark green and evolved oxides of nitrogen copiously. A final heating on the steam bath (internal temp. 90°C.) for ³/₄ hr. completed the reaction. The main bulk of the product could then be obtained

by cooling the solution in Dry Ice and filtering. However, appreciable product remained in the filtrate and so an alternate work-up was used involving rapid, low-temperature vacuum stripping of the excess nitric acid and treatment of the residue with formic acid to eliminate traces of oxidizing agent. Following removal of the formic acid, the residue was dissolved in ether and precipitated by addition of benzene and evaporation of the ether to give the product (70–79%).

The pure tetracarboxylic acid is not markedly soluble in ether, and in some runs most of the product failed to dissolve. Once recrystallized, it fails to dissolve in ether at all. The highest melting point obtained for the tetracarboxylic acid was 215–216°C. (dec.), but product melting near 200°C. (reported¹⁵ 205°C., dec.) was also satisfactory. Neutralization equivalents were higher than calculated values (63 versus 58) which might be due to incomplete oxidation or partial decarboxylation.²⁵

***cis* and *trans*-1,3-Cyclobutanedicarboxylic Acids.** 1,1,3,3-Cyclobutanetetracarboxylic acid (8.2 g., 0.0354 mole) was decarboxylated by heating in an oil bath at 220°–230°. When most of the solid had melted, the heating was continued for 15 min. longer, during which time carbon dioxide was evolved. The resultant light-brown syrup was cooled to room temperature and 10 ml. of acetyl chloride added. Following a 2-hr. reflux, the excess acetyl chloride and acetic anhydride were removed *in vacuo*, and the cyclic *cis*-anhydride of 1,3 cyclobutanedicarboxylic acid (1.9 g., 42.6%) sublimed out at 1–2 mm. and a bath temperature of 135°C. Recrystallization of the anhydride from benzene gave 1.64 g. (36.8%) of product, m.p. 148.5–152°C. An analytical sample was recrystallized twice more to give m.p. 152–153°C. (lit.:²⁴ m.p. 131–132°C.).

ANAL. Calcd. for C₆H₆O₃: C, 57.14%; H, 4.80%. Found: C, 56.92, 57.05%; H, 4.84, 5.01%.

The infrared spectrum of this compound in potassium bromide had the following absorptions (cm.⁻¹) 3000(w); 2970(w); 1825(s); 1810(s); 1775(s); 1445(w); 1323(m); 1300(m); 1280(m); 1258(s); 1218(m); 1178(s); 1077(m-s); 1005(m); 950(s, broad); 930(s); 902(m); 892(m); 748(m); 712(w).

Hydrolysis of the *cis*-Anhydride. A sample of *cis*-1,3-cyclobutanedicarboxylic acid anhydride (0.588 g., 0.00466 mole) was refluxed for 15 min. with 1.4 g. of 6*N* hydrochloric acid. The hydrochloric acid was evaporated on a steam bath *in vacuo* to give 0.56 g. (82.4%) of *cis*-1,3-cyclobutanedicarboxylic acid, m.p. 130–132.5°C. After two recrystallizations from a mixture of benzene and acetone with good recovery, the pure acid, m.p. 132.5–134.5°C., was obtained. (lit.:²⁴ m.p. 131°C.).

ANAL. Calcd. for C₆H₈O₄: C, 50.00%; H, 5.59%; neut. equiv., 72. Found: C, 50.14%; H, 5.85%; neut. equiv., 71.

***trans*,1,3-Cyclobutanedicarboxylic Acid.** This was isolated by the published procedure, m.p. 184–186°C. (lit.²⁴ m.p. 192–193°C.).

Isomerization of *cis*-1,3-Cyclobutanedicarboxylic Acid to the *trans* Isomer. A thick-walled pressure bottle was charged with 5 g. (0.0396 mole) of *cis*-1,3-cyclobutanedicarboxylic acid anhydride, 15 ml. of concentrated hydrochloric acid, and 5 ml. of water. The vessel was then closed and heated at 180°C. for 3 hr. and then cooled. The contents were rinsed out and concentrated *in vacuo* to give a crystalline solid, m.p. ca 155°C., which was a mixture of *cis* and *trans* isomers as indicated by its infrared spectrum (existence of peaks at 1082 and 1073 cm.^{-1}). The same mixture of isomers was obtained by combining the decarboxylation of the tetracarboxylic acid and the resultant equilibration in one step.

The crude product from five of the above equilibrations was combined and treated with acetyl chloride to convert the *cis*-isomer present to its cyclic anhydride. Sublimation of the product afforded 11.4 g. (45.6%) of the *cis*-anhydride. Workup of the pot residue yielded 9.4 g. (33.4%) of *trans*-diacid, m.p. 185–190°C.

Preparation of *trans*-1,3-Cyclobutanedicarboxylic Acid Chloride. A mixture of 9.4 g. (0.065 mole) of *trans*-1,3 cyclobutanedicarboxylic acid and 37.3 g. (0.294 mole) of oxalyl chloride was placed in a flask equipped with a reflux condenser and drying tube. After gentle warming, the reaction began, and the evolution of gas proceeded spontaneously for 20–30 min. The reaction was completed by refluxing for 2 hr. Excess oxalyl chloride was stripped off and then 11.35 g. (96.6%) of product distilled *in vacuo*, b.p. 72°C./0.6 mm.

ANAL. Calcd. for $\text{C}_6\text{H}_6\text{O}_2\text{Cl}_2$: C, 39.81%; H, 3.34%; Cl, 39.17%. Found: C, 39.67%; H, 3.23%; Cl, 39.39%.

Preparation of the 1,3-Dicyanocyclobutanes

Preparation of *trans*-1,3-Cyclobutanedicarboxamide. To a stirred solution of ammonium hydroxide (2 equiv.) in 2 ml. water maintained at ice temperatures was added 0.365 g. (0.002 mole) of the *trans*-diacid chloride. After standing awhile, the solid diamide was removed by filtration and dried to give 0.15 g. (52%), m.p. 284–286°C. (dec.). The amide was not analyzed but reacted directly in the next step.

Preparation of *trans*-1,3-Dicyanocyclobutane. A mixture of 0.15 g. (0.0015 mole) of the *trans*-diamide, 1 ml. of dry benzene, and 1 ml. of phosphorus oxychloride was refluxed for 1 hr. Following this treatment, the reaction mixture was added to crushed ice and stirred for several minutes to destroy the excess phosphorus oxychloride. The aqueous layer was extracted three times with benzene, and combined with the benzene layer. Drying and evaporation of this extract gave the crude product as a solid. Recrystallization from boiling heptane afforded the pure dinitrile, m.p. 94–94.5°C. (Kofler).

ANAL. Calcd. for $\text{C}_6\text{H}_6\text{N}_2$: C, 67.90%; H, 5.70%; N, 26.40%. Found: C, 6.80%; H, 5.73%; N, 26.10%.

***cis*-Methyl 1,3-Cyclobutanedicarboxylate.** An excess of ethereal diazo methane was allowed to react with 3.0 g. (0.0208 mole) of *cis*-1,3-cyclobutanedicarboxylic acid dissolved in 100 ml. of ether. When the reaction was complete the excess diazomethane was destroyed by the addition of some acetic acid and then the reaction mixture was extracted with bicarbonate solution and dried. The solvent was stripped off and an 84% yield of the *cis*-dimethyl ester, b.p. 132°C./25.3 mm. lit.:¹⁵ b.p. 132°C./30 mm.), n_D^{25} 1.4448 (lit.:²⁴ n_D^{25} 1.4443).

***cis*-1,3-Cyclobutanedicarboxamide.** To a cooled flask containing 2.72 g. (0.0157 mole) of the *cis*-dimethyl ester was added with stirring 3 ml. of concentrated ammonium hydroxide (0.045 mole) and then enough methanol to give an essentially clear solution. The mixture was stirred at ice bath temperature for 3 hr., at which point unreacted ester was still present. An additional 3 ml. of ammonium hydroxide was added and stirring continued overnight at room temperature. The reaction mixture which contained a white solid was concentrated down to dryness to give the crude product, m.p. 235–238°C. Recrystallization from methanol–water gave two crops: 1.4 g. (63%), m.p. 235–237°C., and 0.26 g. (12%), m.p. 224–231°C.

ANAL. Calcd. for $C_6H_{10}O_2N_2$: C, 50.69%; H, 7.09%; N, 19.71%; Found: C, 51.16%; H, 7.15%; N, 19.52%.

***cis*-1,3-Dicyanocyclobutane.** This compound was prepared from the *cis*-diamide by the same procedure used for the *trans* isomer. However, the product was a liquid, b.p. ca. 150°C./0.5 mm., which solidified on standing overnight. After recrystallization from benzene–heptane, the dinitrile melted at 53.5–54.5°C.

ANAL. Calcd. for $C_6H_6N_2$: C, 67.90%; H, 5.70%; N, 26.40%; Found: C, 67.77%; H, 5.68%; N, 26.29%.

***trans*-1,3-Phenyl Cyclobutanedicarboxylate.** This compound was prepared from the magnesium-catalyzed reaction of the diacid chloride with phenol by a procedure described previously. The yield of product was 90%, m.p. 84.5–86°C.

ANAL. Calcd. for $C_{18}H_{16}O_4$: C, 72.96%; H, 5.44%; Found: C, 73.13%; H, 5.52%.

Polymerizations

Polyamides

Interfacial Polymerization. The procedure described by Morgan et al.²⁶ was employed as illustrated below for poly(hexamethylene *trans*-1,3-cyclobutanedicarboxylic amide).

A solution of 3 g. of sodium chloride, 0.387 g. (0.00333 mole) of hexamethylenediamine, 0.35 g. (0.0033 mole) of sodium carbonate and 20 g. ice in 20 ml. of water was prepared and placed in a small Waring Blender. Stirring was started and a solution of 0.6 g. (0.00332 mole) of the *trans*-

diacid chloride in 50 ml. of methylene chloride added all at once. A gelatinous mass formed almost instantaneously and hindered stirring. The solvent was removed on the steam bath and the product isolated by filtration as a fibrous solid, 0.34 g. (51.6%), having a reduced viscosity of 1.39 in phenol-tetrachloroethane. The polymer melted with decomposition at about 305°C. in air. A film cast from phenol showed little strength and was found to be of low crystallinity. Attempts to anneal this material under argon at 250°C. caused rapid deterioration of color and appearance.

Melt Polymerization. Polyamides were prepared from *trans*-1,2-bis(aminomethyl) cyclobutane by standard melt techniques, an example of which follows. The stoichiometric 1:1 salt of adipic acid and *trans*-1,2-bis(aminomethyl) cyclobutane was prepared in absolute alcohol, m.p. 198–199°C.

A 3-g. sample of this salt was placed in an evacuated sealed tube and heated in a 215°C. bath for 2 hr. to give a low molecular weight prepolymer. The tube was opened and placed in a larger side-arm test tube equipped with a gas inlet tube. An argon atmosphere was maintained while the contents were heated at 270°C. for 45 min. Vacuum (0.3 mm.) was then applied and the heating continued for 1½ hr. The resultant light tan polymer was clear and very tough. It had a reduced viscosity of 1.23 in phenol-tetrachloroethane (60:40) at 25°C. The polymer was also soluble in ethanol-water (80:20) but insoluble in dimethylformamide. An ethanol-water solution of the polymer (from another run) was precipitated into acetone and dried (R.V. at 25°C. was 0.86 in phenol-tetrachloroethane).

Polyesters

Isolation of Ethylene 1,2-Cyclobutanedicarboxylate Dimer. Following a standard technique for the preparation of polyesters, a charge of 1.72 g. (0.01 mole) of *trans*-dimethyl 1,2-cyclobutanedicarboxylate and 1.86 g. (0.03 mole) of ethylene glycol was placed in a side-arm test tube fitted with a gas inlet tube. This mixture was heated at 120°C. and flushed with argon for 30 min., after which two drops of tetrabutyl titanate were added. The system was then heated to 155–185°C. for about 3¼ hr. and then brought slowly up to 240°C. over a 2-hr. period while vacuum was applied. It was heated at this temperature overnight under vacuum. The waxy sublimate which had formed weighed 1.5 g. and melted at 95–165°C. After recrystallization from chloroform-carbon tetrachloride and acetone, an analytical sample was obtained, m.p. 185–186.5°C.

ANAL. Calcd. for C₁₆H₂₀O₈: M. W. 340.3; C, 56.46%; H, 5.92%; Found: M. W. 340 ± 5; C, 56.76, 56.79%; H, 5.84, 6.08%.

Polymerization of Dimer with Dibutylzinc. In a small test tube flushed with argon was placed 0.3 g. of the cyclic dimer isolated above. The tube was lowered into an oil bath maintained at 205°C. and when melting was complete, 0.006 ml. of dibutylzinc in toluene (0.156 g./ml.) was added. Within

3 min. the fluid melt had become very viscous and the color had turned pale yellow. After heating an additional 20 min., the tube was cooled and the resultant solid polymer (opaque) removed. This material was a very tough, rubbery polymer which flowed under pressure at 75°C. and melted completely at 130–145°C., R.V. = 1.01 (CHCl₃).

Isolation of Cyclic Dimer Carbonate. In a large side-arm test tube were placed 13 g. (0.112 mole) of *trans*-1,2-bis(hydroxymethyl)cyclobutane, 25 g. (0.117 mole) of diphenyl carbonate, and a pinch of lithium hydroxide monohydrate. The reactants were heated to 200°C. in an inert atmosphere and phenol distilled off. The temperature was raised gradually to 258°C. over a period of 6½ hr. Vacuum (0.2–0.3 mm.) was applied and the heating continued. On raising the temperature to 270°C., the formation of sublimate became evident. In 2 hr., a total of 12.3 g. of waxy sublimate was isolated. After two recrystallizations from carbon tetrachloride, this afforded 7.4 g. (46.5%) of white needles, m.p. 205–208°C. An analytical sample had m.p. 209–210°C.

ANAL. Calcd. for C₁₄H₂₀O₆: C, 59.14%; H, 7.09%; Found: C, 59.17%; H, 6.82%.

The molecular weight of this substance in benzene was determined as 294 (theory is 284 for the dimer). It had a strong band at 1742 cm.⁻¹ (C=O) in the infrared.

Polymerization of Cyclic Dimer Carbonate with Dibutylzinc. A sample of 0.3 g. of the cyclic carbonate dimer (m.p. 208–209°C.) was placed in a small dry tube which contained an argon atmosphere. The solid was melted by immersing the tube in a bath at 222°C. By means of a microsyringe 0.001 ml. of a dibutylzinc solution in cyclohexane (0.153 g./ml.) was carefully added. The mixture was heated at 222°C. for 35 min. at which time an additional 0.009 ml. of the dibutylzinc solution was added. Within 2 min. the mixture was very viscous. After heating 8 min. longer, the viscous mass was cooled. The polymer stuck to a hot block of metal at 106°C. It had a reduced viscosity of 0.83 in chloroform and was amorphous by x-ray.

Poly(*p*-xylylene *trans*-1,3-Cyclobutanedicarboxylate) (XXIV). In a side-arm test tube under argon were placed 0.6729 g. (0.003717 mole) of the *trans*-diacid chloride and 0.5135 g. (0.003717 mole) of *p*-xylylene glycol. The mixture was warmed gently whereupon the evolution of hydrogen chloride began. The viscosity increased over a 1-hr. period. After 1 hr. in a 145°C. bath followed by 30 min. at this temperature *in vacuo*, the reaction was stopped. A colorless sticky polymer with a R.V. of 0.21 in chloroform was obtained. On standing at room temperature overnight, the sticky behavior disappeared and the polymer became opaque. The x-ray data indicated medium crystallinity. The crystallites were found to melt sharply at 87–87.5°C. The infrared spectrum of this polymer was indistinguishable from the *cis-trans* material.

Poly(bisphenol A *trans*-1,3-Cyclobutanedicarboxylate) (XXVI). In a carefully dried side arm test tube containing an argon inlet tube, was placed

0.8155 g. (0.004505 mole) of *trans*-1,3-cyclobutanedicarboxylic acid chloride, 1.0284 g. (0.004506 mole) of bisphenol A and 4 ml. of dry (distilled 3 times from P₂O₅) nitrobenzene. The mixture was heated from 75 to 103°C. over a 2-hr. period and then maintained at 103°C. for 3 hr. After cooling the nitrobenzene solvent was removed *in vacuo* and the resultant white solid heated at 125° for 2 hours longer. The product had a reduced viscosity of 0.26 (CHCl₃, 25°) and was crystalline by x-ray, m.p. 180–220°C. Even at this low molecular weight a film had appreciable strength.

Preparation of Poly(bisphenol A 1,2-Cyclobutanedicarboxylate)(XVIII). A mixture of 0.5707 g. (0.0025 mole) of bisphenol A and 0.7445 g. (0.0025 mole + 0.5% excess) of diphenyl *trans*-1,2-cyclobutanedicarboxylate was placed in a side arm test tube equipped with a gas inlet tube through which argon was led in. The mixture was heated from 202 to 240°C. for 3¹/₄ hr., during which time the liberated phenol distilled off. At this point the tube was cooled to 215°C. and vacuum applied. The temperature was gradually raised up to 250°C. over 8 hr. time. The extremely viscous mass which resulted was cooled and dissolved in chloroform, filtered, and precipitated into methanol. The solid polymer was dried and found to give a reduced viscosity in chloroform at 25°C. of 0.60.

Preparation of Poly(*p*-xylylene 1,2-Cyclobutanedicarboxylate) (XVII). A charge of 0.74 g. (0.0025 mole) of diphenyl *trans*-1,2-cyclobutanedicarboxylate, 0.365 g. (0.0025 mole + 5% excess) of *p*-xylylene glycol, and 10 mg. of manganous acetate were reacted in the melt at 175–220°C. for 2 hr. at atmospheric pressure and then at 216–262°C. for 4¹/₂ hr. *in vacuo*. The resultant pale yellow, tough polymer could be pulled into weak fibers. It flowed at room temperature and had a reduced viscosity of 0.45 in tetrachloroethane at 25°C. The polymer was amorphous by x-ray.

Poly(ethylene 1,3-cyclobutanedicarboxylate)(XXII). In a side-arm test tube equipped with a gas inlet tube 0.504 g. (0.0035 mole) of *cis*-1,3-cyclobutanedicarboxylic acid anhydride, 0.496 g. (0.008 mole) of dry distilled ethylene glycol, and 2 mg. of toluenesulfonic acid were placed. An inert atmosphere was maintained throughout and the mixture heated gradually from 143 up to 242°C. over 3³/₄ hr. Following this, the temperature was lowered to 156°C. and vacuum (0.1 mm.) applied gradually. The temperature was raised back up to 270°C. over 15 hr., during which time the light, tan melt became very viscous. At room temperature the polymer was rubbery. R. V. was 1.46 at 25°C. in CHCl₃.

Attempted Polymerization of *cis*-3-Oxabicyclo(3:2:0) heptane (XXVII). The monomer was purified by refluxing and distilling first from sodium hydroxide pellets and then from lithium aluminum hydride in an inert atmosphere. Approximately 1 ml. of the purified bicyclic ether was placed in a dry flask fitted with a gas inlet tube. The gas inlet tube was connected to two side-arm test tubes in series (PF5 generator) and then in turn to an argon source. The phosphorus pentafluoride obtained by decomposing 1.0 g. of monochlorobenzenediazonium hexafluorophosphate at 150–160°C. was swept into the reaction flask by means of the argon stream. As the cata-

lyst dissolved in the bicyclic ether, the color changed from water white to pale yellow to dark yellow. On standing overnight either at room temperature or in the cold, the reaction mixture turned brown. The reaction mixture

TABLE VI
Analyses of Cyclobutane Polymers

No.	(Formula) _n	Calculated			Found		
		C, %	H, %	N, %	C, %	H, %	N, %
IV	C ₁₀ H ₁₆ N ₂ O ₄	61.21	8.22	14.28	59.42	8.39	13.94
V	C ₁₁ H ₁₈ N ₂ O ₂	62.83	8.63	13.33	61.08	8.68	13.21
VI	C ₁₂ H ₂₀ N ₂ O ₂	64.25	8.99	12.49	63.37	9.05	12.03
VII	C ₁₄ H ₂₄ N ₂ O ₂	66.60	9.50	11.10	65.45	9.55	11.10
VIII	C ₁₅ H ₂₆ N ₂ O ₂	67.63	9.84	10.52	66.61	9.82	10.62
IX	C ₁₆ H ₂₈ N ₂ O ₂	68.53	10.06	9.99	67.54	10.14	10.04
X	C ₁₀ H ₁₄ N ₂ O ₂	61.84	7.27	14.44	58.98	7.26	13.37
XI	C ₁₂ H ₂₀ N ₂ O ₂	64.25	8.99	12.49	62.53	7.14	11.45
XII	C ₁₂ H ₂₀ N ₂ O ₂	64.25	8.99	12.49	62.61	8.80	12.09
XV	C ₁₂ H ₂₀ N ₂ O ₂	64.25	8.99	12.49	64.89	9.58	11.29
XVII	C ₁₄ H ₁₄ O ₄	68.28	5.73	—	67.85	5.79	—
XVIII	C ₂₁ H ₂₀ O ₄	74.98	5.99	—	75.10	5.84	—
XIX	C ₂₁ H ₂₀ O ₄	74.98	5.99	—	73.39	6.03	—
XX	C ₂₀ H ₁₈ O ₆ S	62.16	4.69	—	62.01	4.81	—
XXI	C ₁₄ H ₁₄ O ₄	68.28	5.73	—	68.32	5.83	—
XXII	C ₈ H ₁₀ O ₄	56.4	5.92	—	56.57	5.93	—
XXIV	C ₁₄ H ₁₄ O ₄	68.28	5.73	—	67.52	5.80	—
XXV	C ₂₁ H ₂₀ O ₄	74.98	5.99	—	74.70	5.94	—
XXVI	C ₂₁ H ₂₀ O ₄	74.98	5.99	—	74.95	5.94	—

was diluted with ethyl ether to give a clear solution and then washed with water, dried and distilled. A high recovery of the starting ether was obtained and identified by its infrared spectra and characteristic camphorlike odor.

Polymer Properties

Unless otherwise indicated, measurements of T_g and T_m were determined by measuring resiliency as a function of temperature by using the method described by Brown.²⁷ Determination of elongation, tensile strength, and tensile modulus were carried out in accordance with ASTM procedure D 638-58T. Elemental analyses of the polymers prepared are summarized in Table VI.

Gas Chromatographic Examination of Acrylonitrile Dimer

Once-distilled acrylonitrile dimer³ was examined by gas chromatography on a 2-m., 5% LAC 446 (diethylene glycol polyadipate) column at 225°C., helium flow of 50 cc./min. The resultant data together with the results on the 1,3-derivatives are given in Table VII.

TABLE VII

Component	Retention time, min.	Composition		
		Crude dimer, %	<i>trans</i> -1,3, %	<i>cis</i> -1,3, %
Unknown	1.1	0.23	—	—
"	1.2	0.12	—	—
"	1.6	—	—	0.07
"	2.2	2.70	—	0.91
<i>cis</i> -1,2- ^a	2.9	55.03	—	—
<i>trans</i> -1,3-	3.8	—	99+	15.65
<i>cis</i> -1,3-	6.0	—	trace	83.37
<i>trans</i> -1,2- ^a	8.05	41.92	—	—

^a Based on assignment of Coyner and Hillman.³

The author is indebted to Dr. C. N. Merriam for the determination of physical properties, to Miss O. Garty for the gas chromatography work, to Mr. W. Niegisch for the x-ray data, to Dr. G. H. Warner for the preparation of the 1,2-bis(aminomethyl)cyclobutane, and to Prof. E. R. Buchman for the details regarding the preparation of 1,3-cyclobutane monomers.

References

1. Armen, A., U. S. Pat. 3,074,914 (January 22, 1963).
2. Belg. Pat. 605,840 (to Farbwerke Hoechst) (Jan. 8, 1962).
3. Coyner, E. C., and W. S. Hillman, *J. Am. Chem. Soc.*, **71**, 324 (1949).
4. Sennewald, K., A. Götz, and G. Kalbrath (to Knapsack-Griesheim), Ger. Pat. 1,081,008 (May 5, 1960).
5. Lehn, W. L., and G. R. Nacci (to DuPont), French Pat., 1,275,705.
6. Warner, G. H., and F. Poppelsdorf, private communication.
7. Bayer, O., R. Schröter, W. Siefken, and K. Wagner, Brit. Pat. 896,324 (May 16, 1962).
8. Perkin, W. H., *J. Chem. Soc.*, **1894**, 572.
9. Fuson, R. C., *J. Am. Chem. Soc.*, **54**, 1120 (1932).
10. Korshak, V. V., and T. M. Frunze, *Dokl. Akad. Nauk SSSR*, **103**, 623 (1955).
11. Frunze, T. M., and V. V. Korshak, *Vysokomol. Soedin.*, **1**, 349 (1959).
12. Oda, R., T. Shono, A. Oku, and H. Takao, *Makromol. Chem.*, **67**, 124 (1963).
13. Hill, R., *Fibres from Synthetic Polymers*, Elsevier, Amsterdam-New York, 1953, p. 135.
14. Deutsch, D. H., and E. R. Buchman, *Experientia*, **6**, 462 (1950); paper presented at 119th Meeting of the American Chemical Society, Boston, Mass, 1951; *Abstracts*, p. 35M; Technical Report, California Institute of Technology, 1951.
15. Buchmann, E. R., private communication.
16. Batzer, H., and G. Fritz, *Makromol. Chem.*, **14**, 179 (1954).
17. Wittbecker, E. L., H. K. Hall, Jr., and T. W. Campbell, *J. Am. Chem. Soc.*, **82**, 1218 (1960).
18. Baker, B. R., *J. Am. Chem. Soc.*, **65**, 1577 (1943).
19. Shul'kina, Z. I., *Zhur. Obshch. Khim.*, **13**, 373 (1943); *Chem. Abstr.*, **38**, 3258a (1944).
20. Blomquist, A. T., and J. A. Verdol, *J. Am. Chem. Soc.*, **77**, 1806 (1955).
21. Spassow, A., *Ber.*, **75**, 779 (1942).
22. Critchfield, F. E., and J. B. Johnson, *Anal. Chem.*, **29**, 1174 (1957).
23. Bailey, W. J., and C. H. Cunor, *J. Am. Chem. Soc.*, **77**, 2787 (1955).
24. Allinger, N. L., and L. A. Tushaus, *J. Org. Chem.*, **30**, 1945 (1965).

25. Kerr, C., *J. Am. Chem. Soc.*, **51**, 614 (1929).
26. Beaman, R. G., P. W. Morgan, C. R. Koller, E. L. Wittbecker, and E. E. Magat, *J. Polymer Sci.*, **40**, 329 (1959).
27. Brown, A., *Textile Res. J.*, **25**, 891 (1955).

Résumé

Une grande variété de polyesters et polyamides ont été préparés au départ de dérivés cyclobutaniques 1,2 et 1,3 disubstitués. En général, le polyamide contenant des cycles-cyclobutaniques disubstitués *trans* sont cristallins. Les polyesters contenant principalement les isomères *trans* tendent à être cristallin, mais ceux contenant des mélanges d'isomères *cis* et *trans* sont amorphes. Les propriétés mécaniques ont été déterminées lorsque c'était possible. Les rendements appréciables en dimères cycliques ont été isolés au cours de la polymérisation de certains polyesters. Ces dimères cycliques polymérisent facilement lorsqu'ils sont traités au zinc dibutyle. L'examen du dimère acrylonitrrique (1,2-dicyanocyclobutane) au moyen de la chromatographie gazeuse n'a pas révélé la présence d'unités 1,3-dicyanocyclobutaniques.

Zusammenfassung

Eine grosse Vielfalt von Polyestern und Polyamiden wurde aus 1,2- und 1,3-disubstituierten Zyklobutanderivaten dargestellt. Im allgemeinen waren die Polyamide mit dem *trans*-disubstituierten Zyklobutanring kristallin. Polyester mit vorwiegend dem *trans*-Isomeren neigen zur Kristallinität, diejenigen mit Mischungen aus *cis*- und *trans*-Isomeren waren dagegen amorph. Wo immer möglich wurden mechanische Eigenschaften bestimmt. Bei der Darstellung gewisser Polyester wurden beträchtliche Ausbeuten an zyklischen Dimeren isoliert. Diese zyklischen Dimeren konnten durch Behandlung mit Dibutylzink leicht polymerisiert werden. Eine gaschromatische Überprüfung des Acrylnitrildimeren (1,2-Dicyanzyklobutan) lieferte keine Hinweise auf die Gegenwart von 1,3-Dicyanzyklobutan.

Received August 13, 1965

Revised September 12, 1965

Prod. No. 4889A

Macroreticular Redox Polymers. II. Further Synthesis and Properties of Some Redox Polymers

KENNETH A. KUN, *Research Laboratories, Rohm and Haas Company, Philadelphia, Pennsylvania*

Synopsis

A series of redox polymers was prepared by the addition of different redox groups to preformed, chloromethylated macroreticular styrene-divinylbenzene copolymers. These polymers contained the hydroquinone, hydroquinonesulfonic acid, methylhydroquinone, 2,5-dimethylhydroquinone, 2,5-dimethylhydroquinonesulfonic acid, 2,3,5-trimethylhydroquinone, *tert*-butylhydroquinone, chlorohydroquinone, benzyl mercaptan, anthraquinone, and the pyrogallol redox groups. Thus, a set of redox polymers is available having redox potentials that may range from approximately 150 to 700 mv.

INTRODUCTION

The use of chloromethylated styrene-divinylbenzene copolymers as matrices for the addition of functional groups provides a convenient procedure for the synthesis of oxidation-reduction (redox) polymers.^{1,2} Though the synthesis of specific monomers for specific redox polymers has the advantages that composition and structure of the polymers are known with increased certainty, addition of redox systems to preformed matrices allows flexibility, in the case of synthesis and with the physical properties of the polymers, that cannot be readily obtained by other known synthetic means. Redox polymers based upon the hydroquinone-quinone redox system were prepared by the addition of hydroquinone to preformed chloromethylated styrene-divinylbenzene copolymers.² Comparison of this redox system with conventional gel and macroreticular or macroporous matrices indicates the macroreticular redox polymers have greater reactivity and better stability than resins containing the same redox system on conventional gel-type structures.

Crosslinked macroreticular styrene-divinylbenzene copolymers were prepared by the polymerization technique of Meitzner and Oline,³ chloromethylated by the procedure of McBurney,⁴ and treated with hydroquinone to yield macroreticular hydroquinone redox polymers.^{1,2} The resulting polymers have a definite redox potential and are relatively hydrophobic. For possible applications involving the use of crosslinked redox polymers, particularly in nonaqueous fluids, these relatively hydrophobic resins may be useful. In aqueous systems, however, the hydrophobic characteristic can be a limitation to the utility of the resins. The hydroquinone redox

system provides redox polymers of a narrow redox potential range. By adding different redox groups to the preformed matrices, redox polymers with different redox potentials may be obtained.

This paper describes the synthesis of several redox polymers containing different redox groups and the conversion of relatively hydrophobic resins to the more hydrophilic redox ion-exchange polymers.

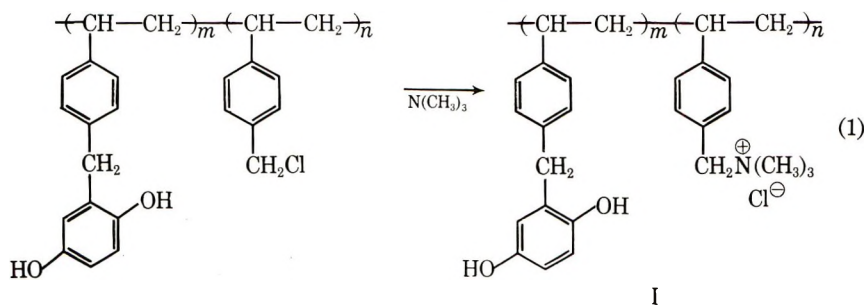
RESULTS AND DISCUSSION

Macroreticular Matrices

The redox groups described in this paper are on macroreticular poly-(styrene-divinylbenzene) matrices. Previous publications^{5,6} indicate that macroreticular resins contain significant fractional pore volumes and have characteristic pore size distributions, while conventional gel resins have no significant pore volume. For most of the synthesis described here, a lightly crosslinked copolymer was used; it had a surface area of approximately 20 m.²/g. and a pore volume of approximately 0.5 cc./g. (dry) resin. Some of the reactions described here were also run on highly crosslinked macroreticular matrices and on a conventional gel-type matrix. The structural properties of these matrices were discussed in a previous paper.² Methods for pore structure analysis also have been described^{5,6} and effects of changes in chemical and physical structural characteristics on redox polymer properties are the subject of this and the following paper.⁷

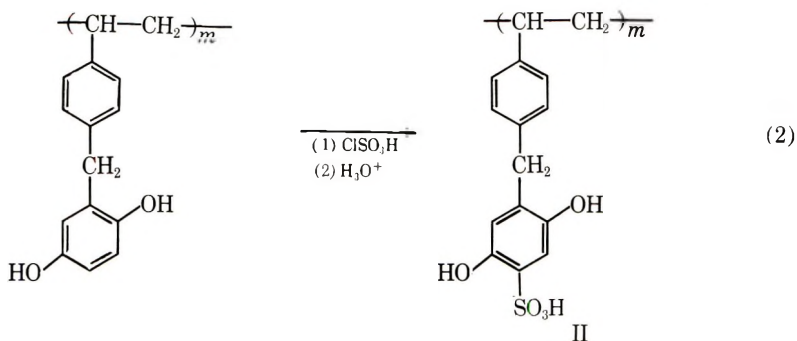
Hydrophilic Hydroquinone Redox Polymers

Crosslinked hydroquinone polymers are relatively hydrophobic; in aqueous systems this characteristic limits the rates of diffusion of reactants through the gel phase of the resin. Addition of hydrophilic functional groups to the polymer matrix increases the degree of hydration in the gel structure and thus increases the rates of diffusion of reactants through the gel phase. Redox polymers, prepared by the Friedel-Crafts addition of hydroquinone to chloromethylated poly(styrene-divinylbenzene) beads, were made hydrophilic by the incorporation of ion-exchange groups. By limiting the concentration of hydroquinone added to the polymeric matrix, significant concentrations of unreacted chloromethyl groups can be kept available for subsequent chemical treatment. Reaction of chloro-



methyl groups with amines yields hydrophilic redox polymers containing anion-exchange groups. Thus, treatment of a crosslinked redox polymers containing unreacted chloromethyl groups with trimethylamine, as shown eq. (1), produced redox polymers with strong base ion-exchange capacities (I). In a similar manner, redox polymers having weak base ion-exchange functionality were prepared by reacting primary or secondary amines, e.g., 2-methylaminoethanol and 2,2'-iminodiethanol respectively, with the available chloromethyl groups. These amination readily took place on both lightly crosslinked and highly crosslinked structures.

Besides adding hydrophilic groups to redox polymers via chloromethyl substituents, hydrophilic functionality can be added directly to the redox groups. Treatment of hydroquinone-containing polymers with chlorosulfonic acid places strong acid functional groups on the hydroquinone ring (II) as shown in eq. (2). This has the advantage of introducing hydro-



philic groups without lowering the maximum available redox capacity of the resins by using the chloromethyl sites for redox groups instead of hydrophilic groups.

The characteristics of some of these and other resins described in this paper are summarized in the experimental section for each resin. The effects of changes in chemical and physical structural characteristics on redox capacity, reaction rate, equilibria, and redox potential will be discussed in the following paper.⁷

Alkylated Hydroquinone Redox Polymers

A major portion of the work with redox polymers has involved the use of acidic or neutral solutions and, under these conditions, the hydroquinone redox system is stable. However, at high pH values the oxidized polymers, i.e., the quinone forms, are susceptible to further oxidation. Oxidation of hydroquinone to quinone can also cause dimerization.⁸⁻¹⁰ Both conditions, oxidation of quinone in alkaline solutions and dimerization, can be suppressed by the replacement of the hydrogen atoms on the quinone ring with functional groups that cannot be removed easily in the presence of mild oxidants. Quinone stability increases in basic solutions as the ring hydrogen atoms are replaced; fully substituted quinones are quite stable and cannot dimerize.^{11,12}

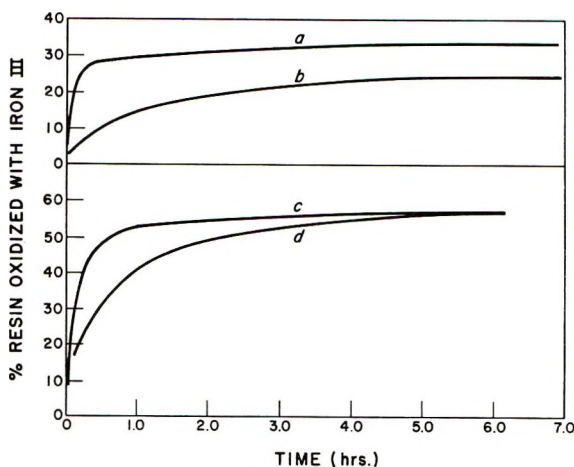


Fig. 1. Comparative reaction rates of hydroquinone and 2,5-dimethylhydroquinone redox polymers: (a) 2,5-dimethylhydroquinone redox polymer; (b) unsubstituted hydroquinone redox polymer; (c), (d) the sulfonic acid derivatives of (a) and (b), respectively.

Mono-, di-, and trimethylvinylhydroquinone polymers have been prepared by polymerization of the corresponding methylated monomers.^{11,12} Syntheses of these monomers were tedious and gave modest yields of polymers. By using the Friedel-Crafts reaction conditions described for the addition of dimethoxybenzene, hydroquinone and benzoquinone to chloromethylated styrene-divinylbenzene copolymers,^{1,2} dimethoxytoluene, 2,5-dimethylhydroquinone, 2,3,5-trimethylhydroquinone, *tert*-butylhydroquinone, 2,5-dimethylbenzoquinone, and 2,3,5-trimethylbenzoquinone were added to chloromethylated styrene-divinylbenzene copolymers. Redox polymers obtained from the hydroquinone additions gave cleaner and higher capacity products than corresponding benzoquinone additions.

Hydrophilic properties of these polymers were similar to that of the previously discussed hydroquinone adducts. By limiting the hydroquinone addition reaction, varying concentrations of unreacted chloromethyl groups can be made available for subsequent amination reactions. Or, if reactive sites are present in the hydroquinone ring, the sulfonic acid derivative may be prepared. Thus, treatment of the 2,5-dimethylhydroquinone adduct with chlorosulfonic acid gave the dimethylhydroquinone derivative of II, and, the ammonium *tert*-butylhydroquinone derivative of polymer I was obtained by the reaction of trimethylamine with the unreacted chloromethyl groups in the *tert*-butylhydroquinone redox polymer.

An increase in quinone stability is reflected by an increase in the reactivity of the corresponding hydroquinone. Comparative rates of reaction are shown in Figure 1 for the hydroquinone and the 2,5-dimethylhydroquinone redox polymers and for the sulfonated derivatives of these two resins. The four resins were prepared from the same lightly crosslinked, macroreticular chloromethylated copolymer. Rates of reaction appear

to be dependent upon the hydrophilic character of the resins and to a limited extent on the lower redox potential of the substituted hydroquinone.

Chlorinated Hydroquinone Redox Polymer

Another type of substituted hydroquinone redox polymer was prepared by the direct chlorination of the hydroquinone resin. Elemental analysis indicates the reaction product contains one chloro group per hydroquinone unit (found 12.78% Cl, calculated for one chloro group per vinylbenzylhydroquinone 13.6%; starting material contained 1.31% Cl from unreacted chloromethyl groups). Chlorine is probably reduced to chloride by the hydroquinone redox polymer, which, in turn, is oxidized to the quinone. The hydrogen chloride formed in this reaction can then react with the polymeric quinone to both add a chloro group and reduce the quinone. Redox capacity determinations at varying oxidant contact times indicate that chlorination caused no significant changes in the capacity and reactivity of the chlorohydroquinone redox polymer as compared to the precursor hydroquinone polymer. Since both resins are relatively hydrophobic and one was prepared from the other, the similarity in properties is to be expected. The chlorinated derivative, however, does decrease the possibilities of dimerization during an oxidation cycle and it should increase the stability of the redox function to strong oxidants.

Mercaptyl Redox Polymers

Mercaptyl or thiol redox polymers are described in the literature.¹³⁻¹⁶ Cassidy, in 1949, discussed the use of the sulfhydryl-disulfide redox system on a polymeric backbone as a synthetic redox polymer.¹³ Gregor¹⁴ and Overberger¹⁵ described the properties of some thiolstyrene polymers. Parrish¹⁶ and Trostyanshaya¹⁷ described the preparation of a polymeric vinylbenzyl mercaptan by the reaction of thiourea with conventional gel-type chloromethylated styrene-divinylbenzene copolymers and then hydrolysis of the resulting thiournium salt with alkali to give poly(vinylbenzyl mercaptan).

By using the synthetic route of Parrish and Trostyanshaya, conventional gel-type and macroreticular chloromethylated styrene-divinylbenzene copolymers were treated with thiourea to give the mercaptyl redox polymers where the bead matrices varied in crosslinker content, surface area, and porosity. The chemical and physical characteristics for each of these resins are described in the experimental section. It should be noted that the conventional gel resin was approximately 100-200 mesh while the macroreticular resins were in the range of 20-50 mesh. During the preparation of these mercaptyl resins, the poor physical stability, described for conventional gel mercaptyl redox polymers by Trostyanshaya, was observed. Conventional gel mercaptyl resins broke down to a granular powder; the macroreticular mercaptyl resins retained the spherical form found in bead polymers. This difference in physical stability was also observed after an oxidation-reduction cycle. The conventional mercaptyl

redox polymers continues to degrade physically while the macroreticular counterparts retained their original form and showed no sign of physical degradation.

Redox capacities given for the mercaptyl resins were determined by measuring the number of milliequivalents of iodine reduced per gram of (dry) resin.^{16,17} The oxidized form of the resin, i.e., the disulfide form, was easily reduced with 10% aqueous sodium bisulfite for a complete redox cycle.

Comparative reaction rates of the mercaptyl redox system on conventional and macroreticular matrices show the macroreticular mercaptyl resins to have significantly higher rates. Based on sulfur analysis (see elemental analysis of resins in the experimental section), the conventional gel matrix mercaptyl resin should have a higher redox capacity than the three macroreticular resins. After 48 hr. in contact with an aqueous iodine solution, the conventional matrix resin only reached a capacity of 2.40 meq./g. while the macroreticular redox resins reached this value within 15–30 min. after being added to the iodine solution. After 48 hr. of continuous contact with the iodine solution, the conventional redox polymer (100–200 mesh) still showed an increasing capacity while the reaction rates for the macroreticular redox polymers (20–50 mesh) reached full capacity and leveled off after 8 hr.

Anthraquinone Redox Polymers

Anthraquinone redox polymers are of interest in the preparation of hydrogen peroxide. Though these materials are prepared by a number of synthetic routes,¹⁸ the polymeric structures to which the redox groups are attached are sensitive to both pH and temperature or require synthesis procedures that are tedious. As part of the examination of macroreticular redox polymers, anthraquinone, 2-methylanthraquinone, and 2-ethylanthraquinone were combined with chloromethylated poly(styrene-divinylbenzene) by using the previously described Friedel-Craft reaction conditions. Initial results indicated a significant redox capacity for these resins; however, further evaluation showed a portion of the capacity was due to sorbed anthraquinone. The unreacted anthraquinones could be removed from the resin matrix only after very extensive hot alcohol extractions, e.g., wash resin with ethanol for 1 week in a Soxhlet extractor.

A hydrophilic anthraquinone redox polymer was prepared by the quaternization of 2-aminoanthraquinone with the chloromethylated copolymers. Nitrogen and chloride analysis indicated that 25% of the available chloromethyl groups reacted with the aminoanthraquinone.

Pyrogallol Redox Polymer

A pyrogallol redox polymer was prepared by the same method used for the hydroquinone polymers. Reaction of pyrogallol with a macroreticular chloromethylated styrene-divinylbenzene copolymer, using dioxane and zinc chloride, gave a material with a redox capacity of 3.48 meq./g. Ele-

mental analysis of the starting material and the reaction product indicated good conversion to the redox polymer, though the exact structure of this reaction product is not known. Extensive alcohol washings did not leach pyrogallol or its oxidation products, dibasic acids, from the resin. Initial evaluations indicate this resin will rapidly remove dissolved oxygen from water.

Redox Polymers as Specific Oxidizing and Reducing Agents

Redox polymers can be considered as specific oxidizing and reducing agents that are controlled by the redox potentials of the redox groups attached to the polymeric matrices and by the redox potentials of the reactants. Thus, it is possible to reduce one redox group in the presence of another with redox polymers of the appropriate redox potential. By using specific redox systems, redox potentials may be varied over a wide range.

The redox potentials of specific redox polymers may be approximated from monomeric redox units. Redox polymers described in this paper, for example, have redox potentials that may range from approximately 150 to 700 mv. On the basis of Clark's¹⁹ values for the corresponding quinones, the redox potentials of these redox polymers are approximately 150 mv. for the anthraquinone polymers, 470 mv. for the trimethylhydroquinone polymer, 530 mv. for the dimethylhydroquinone polymer, 590 mv. for the monomethylhydroquinone polymer, 650 mv. for the hydroquinone and chlorohydroquinone polymers, and 700 mv. for the sulfonated hydroquinone and the pyrogallol polymers. Polymers with different redox potentials may be obtained by using other redox groups. Model compounds have been used to approximate redox potentials of corresponding polymers.¹⁸ It must be remembered, however, that these values are only approximations, and that significant changes in redox potentials may be observed when the redox systems are placed on polymeric matrices and when they are in close association with each other.

EXPERIMENTAL

Experimental procedures for the synthesis of macroreticular styrene-divinylbenzene copolymers,³ the chloromethylation procedure,⁴ and the addition of hydroquinones to these chloromethylated copolymers^{1,2} are described in previous publications and, therefore, will not be repeated here.

Hydrophilic Hydroquinone Redox Polymers

The following are typical preparations for sulfonated and aminated hydroquinone redox polymers. Concentrations of reactants may be varied to give any proportions of redox and ion exchange capacities that may be desired.

Sulfonated Hydroquinone Redox Polymers. To a 3-liter round-bottomed flask, fitted with a stirrer, reflux condenser, and thermometer were added 93 g. of lightly crosslinked polyvinylbenzylhydroquinone and 800 ml. of ethyl-

ene dichloride. The copolymer swelled rapidly, and after 15 min. the slurry was cooled to 0°C. by using an ice-water bath. With continuous stirring 40.5 g. (0.3 mole) of chlorosulfonic acid was added dropwise, the temperature of the slurry being kept below 5°C. The reaction mixture was stirred for 2 hr. at 0°C., brought to room temperature over a period of 1 hr., then heated at 80°C. for 2 hr. The unreacted acid chloride was decomposed by the addition of cold water to the cold reaction mixture, and the product was isolated by filtration. The imbibed ethylene dichloride was removed from the resin by a steam distillation; the resin was washed free of acid with deionized water, drained, and stored in a hydrated state for further use.

A portion of this product was washed several times with anhydrous methanol and dried to constant weight at 50°C. *in vacuo*. This product contained 69.61% C, 5.92% H, 3.25% S, 1.59% residual Cl; it has a salt-splitting cation-exchange capacity of 1.14 meq./g. (dry) and a redox capacity of 4.88 meq./g. (dry) with Fe(III) in 1N H₂SO₄.

Aminated Hydroquinone Redox Polymer. To a 3-liter, round-bottomed flask fitted with a stirrer, reflux condenser, and thermometer were added 130 g. of lightly crosslinked polyvinylbenzylhydroquinone and 750 ml. of ethylene dichloride. The copolymer swelled rapidly, after 30 min. the excess ethylene dichloride was drained from the swollen beads. Then 100 g. of ice was added during cooling of slurry to 0°C. With continuous stirring, a slurry of 500 g. of 24.5% trimethylamine in water and 250 g. of ice were added to the beads at a rate that kept the reaction temperature below 15°C. The slurry was stirred for 5 hr., the temperature of the mixture being allowed to rise to room temperature at the end of the second hour. The reflux condenser was then replaced with a distillation condenser and a dropping funnel. Excess trimethylamine and residual ethylene dichloride were steam distilled from the polymer. Make-up water was added during the distillation to keep the liquid level of the slurry constant. The resin slurry was heated until the distillate temperature reached 100°C., and an additional 100 ml. of distillate was collected at 100°C. The slurry was drained of excess water and bottled for further use.

A portion of the wet resin was washed with methanol and dried to constant weight at 50°C. *in vacuo*. This product contained 71.43% C, 7.15% H, 1.96% N, and 6.47% Cl; it has an anion-exchange capacity of 1.53 meq./g. (dry) and a redox capacity of 2.53 meq./g. (dry) with Fe(III) in 1N H₂SO₄.

By replacing trimethylamine in the above synthesis with 2-methylaminoethanol and 2,2'-iminodiethanol amine, hydroquinone redox polymers were prepared containing 71.73% C, 6.78 H, 5.57% Cl, 2.80% N, and 74.32% C, 6.49% H, 4.34% Cl, and 1.74% N, respectively.

Alkylated Hydroquinone Redox Polymers. The alkylated hydroquinones and benzoquinones added to macroreticular chloromethylated styrene-divinylbenzene copolymers using the Friedel-Crafts reaction conditions were described previously.^{1,2} Detailed preparative procedures were given¹ for hydroquinone methylhydroquinone, 2,5-dimethylbenzoquinone, and 2,3,5-trimethylbenzoquinone redox polymers. The other alkylated hydroquinone

redox polymers were prepared exactly the same way. Thus, the addition of 2,5-dimethylhydroquinone to a lightly crosslinked macroreticular chloromethylated poly(styrene-divinylbenzene) gave a product containing 82.56% C, 6.58% H, and 0.94% residual Cl and having a redox capacity of 1.05 meq./g. (dry) with Fe(III) in 1N H₂SO₄. Sulfonation of this resin with chlorosulfonic acid, as described above, gave a product containing 63.52% C, 5.15% H, 4.53% S, and 1.95% residual Cl and having a redox capacity of 2.98 meq./g. (dry) with Fe(III) in 1N H₂SO₄.

Chlorinated Hydroquinone Redox Polymer. To a 500-ml. three-necked round-bottomed flask fitted with a stirrer, reflux condenser, and a thermometer, a slurry of 50 g. of a lightly crosslinked macroreticular hydroquinone redox polymer^{1,2} in 400 ml. of ethylene dichloride was added. Chlorine was bubbled through the slurry for 6 hr. at reflux temperature (approximately 80°C.). Hydrogen chloride was emitted. The reaction mixture was cooled slowly to room temperature (this run was allowed to stand overnight). The beads were drained off the chlorine-ethylene dichloride solution and then washed and drained three times with fresh ethylene dichloride. Addition of 500 ml. of water followed by a steam distillation of the slurry removed last traces of ethylene dichloride from the polymer. The beads were washed with water until the water washings were neutral to pH paper, excess water was drained from beads and the product was bottled for further use.

A portion was washed several times with methanol and dried to constant weight at 50°C. *in vacuo*. Elemental analysis of the starting material and final product are 79.41% C, 5.64% H, 1.31% Cl, and 70.03% C, 4.77% H, and 12.78% Cl, respectively. There is 13.6% Cl for a material containing one chloro group per vinylbenzylhydroquinone unit. Redox capacities for both materials were similar, 3.31 meq./g. (dry) for the starting material and 3.25 meq./g. (dry) for the chlorinated product with Ce(IV) in 1N H₂SO₄ for 4.3 hr.

Mercaptyl Redox Polymers

Resin A (Conventional Gel-Type Matrix). To a 5-liter, three-necked, round-bottomed flask fitted with a stirrer, reflux condenser, and thermometer, 200 g. of chloromethylated poly(styrene-divinylbenzene) containing 22.66% Cl. The beads were swollen for 15 min. with 560 ml. of dioxane and then a solution of 334.8 g. of thiourea in 840.0 ml. of ethanol was added. The resulting mixture was heated to reflux, with constant stirring, and refluxing continued for 24 hr. Reflux temperature was approximately 80–85°C. After cooling the reaction mixture, the dioxane-alcohol solution was moved by filtration and a solution of 60.0 g. of sodium hydroxide in 600 ml. of ethanol added. This mixture was refluxed, with stirring, for 8 hr. When the reaction mixture had cooled, the product was washed three times with 350-ml. portions of 10% hydrochloric acid. The beads broke down to a finely divided resin. Last traces of impurities were removed by treating the finely divided resin in a Soxhlet extractor for 16 hr. with hot water. The resin was dried to constant weight at 80°C. Analytical results for

this preparation showed the product to contain 72.40% C., 6.73% H, 20.51% S, 1.22% residual Cl, and 0.87% ash; it had a redox capacity of 2.40 meq./g. (dry) with I₂ in aqueous KI, and a surface area of <0.1 m.²/g.

Resin B. To a 3-liter, three-necked, round-bottomed flask fitted with a stirrer, reflux condenser and thermometer was added 200 g. of chloromethylated poly(styrene-divinylbenzene), copolymer. It contained 14.1% Cl, had a surface area of 59.2 m.²/g. and a porosity of 53%. The beads were swollen for 15 min. with 560 ml. of dioxane, and then a solution of 334.8 g. of thiourea in 840 ml. of ethanol was added. Synthesis and work-up continued as described for resin A. The final product contained 78.43% C, 7.28% H, 10.97% S, 0.42% residual Cl, and 0.32% ash and it had a redox capacity of 5.27 meq./g. (dry) with I₂ in aqueous KI.

Resin C. To a 5-liter, three-necked, round-bottomed flask fitted with a stirrer, reflux condenser, and thermometer was added 200 g. of chloromethylated poly(styrene-divinylbenzene) is added. It contained 13.1% chloride, had a surface area of 67.0 m.²/g., and a porosity of 38%. By using the synthesis procedure described for mercaptal resin A, a product was obtained containing 80.04% C, 7.34% H, 10.41% S, 1.48% residual Cl, and 0.10% ash and having a redox capacity of 4.48 meq./g. (dry) with I₂ in aqueous KI.

Resin D. To a 2-liter, three-necked, round-bottomed flask fitted with stirrer, reflux condenser, and thermometer was added 135 g. of chloromethylated poly(styrene-divinylbenzene). It contained 20.4% Cl, had a surface area of 19.2 m.²/g., and a porosity of 36%. By using the synthesis procedure described for mercaptal resin A, a product was obtained that contained 74.16% C, 7.10% H, 18.17% S, 0.61% residual Cl, and 0.24% ash; it had a redox capacity of 4.89 meq./g. (dry) with I₂ in aqueous KI.

Pyrogallol Redox Polymer

In a 500-ml. three-necked round-bottomed flask fitted with a stirrer, reflux condenser and a thermometer, a slurry of 76.3 g. of a lightly cross-linked macroreticular chloromethylated poly(styrene-divinylbenzene) beads in 400 ml. of dioxane was combined with 63.1 g. (0.5 mole) pyrogallol and 3 g. of freshly fused zinc chloride. The mixture was heated to reflux for 4 hr. Hydrogen chloride was emitted. Since pyrogallol is water-soluble and dioxane is miscible with water, the cooled reaction product was drained and washed free of dioxane and unreacted pyrogallol with deoxygenated deionized water. The beads were drained free of excess water and bottled for further use.

A portion of the polymer was washed several times with methanol and dried at 40°C. *in vacuo*. Elemental analyses of the starting material gave 72.42% C, 5.97% H, 21.37% Cl, and no ash; the pyrogallol redox polymer contained 75.87% C, 5.87% H, 1.64% residual Cl, 0.03% ash, and 16.68% O (by difference). There should be 18.4% O for a material containing one pyrogallol group per chloromethyl group. This material had a redox capacity of 3.48 meq./g. (dry) and readily removed oxygen from water.

The author gratefully acknowledges the technical assistance of Mr. William Freund.

The author also wishes to express his appreciation to Dr. Robert Kunin, Dr. Isadore Rosenthal, and Mr. Francis McGarvey for their helpful discussions and advice during the course of this work.

References

1. Kun, K. A., U. S. Pat. 3,173,892 (1965).
2. Kun, K. A., *J. Polymer Sci. A-1*, **3**, 1833 (1965).
3. Meitzner, E. F., and J. A. Oline, Union S. Africa Pat. Appl. 59/2393.
4. McBurney, C. H., U. S. Pat. 2,629,710 (1953).
5. Kun, K. A., and R. Kunin, *J. Polymer Sci. B*, **2**, 587, 839 (1964).
6. Kun, K. A., and R. Kunin, paper presented at the International Symposium on Macromolecular Chemistry, Prague, Czechoslovakia, Aug. 30-Sept. 1, 1965.
7. Kun, K. A., and R. Kunin, *J. Polymer Sci. A-1*, **4**, 859 (1966).
8. Erdtman, H., M. Granath, and G. Schultz, *Acta Chem. Scand.*, **8**, 1442 (1954).
9. Dean, F. M., A. M. Osman, and A. Robertson, *J. Chem. Soc.*, **1955**, 11.
10. Giza, Y-H.C., K. A. Kun, and H. G. Cassidy, *J. Org. Chem.*, **27**, 679 (1962).
11. Kun, K. A., and H. G. Cassidy, *J. Polymer Sci.*, **56**, 83 (1962).
12. Manecke, G., and G. Bourweig, *Chem. Ber.*, **95**, 1413 (1962).
13. Cassidy, H. G., *J. Am. Chem. Soc.*, **71**, 402 (1949).
14. Gregor, H. P., D. Delar, and G. K. Hoeschele, *J. Am. Chem. Soc.*, **77**, 3675 (1955).
15. Overberger, C. G., and A. Lebovits, *J. Am. Chem. Soc.*, **77**, 3675 (1955); *ibid.*, **78**, 4792 (1956).
16. Parrish, J. R., *Chem. Ind. (London)*, **1956**, No. 18, 137.
17. Trostyanshaya, E. B., and A. S. Tevlina, *Zh. Anal. Khim.*, **15**, 461 (1960).
18. Cassidy, H. G., and K. A. Kun, *Oxidation-Reduction Polymers*, Interscience, New York, 1965, Chap. 2.
19. Clark, W. M., *Oxidation-Reduction Potentials of Organic Systems*, Williams and Wilkins, Baltimore, Maryland, 1960.

Résumé

Une série de polymères redox a été préparée par addition de groupes oxydoréducteurs différents à des copolymères préformés, de styrène-divinylbenzène, chlorométhylés et réticulés. Ces polymères contenaient de l'hydroquinone, de l'acide hydroquinone-sulfonique, de la méthylhydroquinone, de la 2,5-diméthylhydroquinone, de la 2,5-diméthylhydroquinone-sulfonique, de la 2,3,5-triméthylhydroquinone, de la tertiaire butylhydroquinone, de la chlorohydroquinone, du benzyl-mercaptan, de l'antraquinone et des groupes pyrogalliques. De fait, tout un système de polymères oxydoréducteurs est disponible qui ont des potentiels oxydoréducteurs qui peut varier d'environ 150 à 700 mv.

Zusammenfassung

Eine Reihe von Redoxpolymeren wurde durch die Addition verschiedener Redoxgruppen an präformierte, chlormethylierte, vernetzte Styrol-Divinylbenzolkopolymere dargestellt. Diese Polymeren enthielten folgende Redoxgruppen: Hydrochinon, Hydrochinonsulfonsäure, Methylhydrochinon, 2,5-Dimethylhydrochinon, 2,5-Dimethylhydrochinonsulfonsäure, 2,3,5-Trimethylhydrochinon, *tert*-Butylhydrochinon, Chlorhydrochinon, Benzylmercaptan, Anthrachinon und Pyrogallol. Es ist so eine Reihe von Redoxpolymeren mit Redoxpotentialen im Bereich von etwa 150 bis 700 mV zugänglich.

Received August 3, 1965

Revised September 20, 1965

Prod. No. 4893

Macroreticular Redox Polymers. III. Characterization of Some Hydroquinone-Quinone Redox Polymers

KENNETH A. KUN and ROBERT KUNIN, *Research Laboratories,
Rohm and Haas Company, Philadelphia, Pennsylvania*

Synopsis

A series of hydroquinone-quinone redox polymers on highly and lightly crosslinked macroreticular styrene-divinylbenzene matrices was characterized for redox capacity, reactivity, equilibria, and redox potential. The effects of cerium(IV), iron(III), and oxygen on determinations of redox capacity are described.

INTRODUCTION

Previous publications^{1,2} describe a convenient, general synthetic process for the preparation of oxidation-reduction (redox) polymers by the addition of specific redox systems to preformed chloromethylated styrene-divinylbenzene copolymers. By using hydroquinone or a hydroquinone derivative, where the hydroxyl groups were protected by the formation of ester or ether groups, polyvinylbenzylhydroquinones were obtained.¹ These relatively hydrophobic polymers can be converted to a more hydrophilic redox-ion exchanger by the addition of anionic or cationic functional groups.² For example, treatment of polymeric vinylbenzylhydroquinone with chlorosulfonic acid yields the corresponding sulfonated redox-cation exchanger, or the addition of trimethylamine to chloromethyl groups on the redox polymer matrix gives terpolymers of vinylbenzylhydroquinone, vinylbenzyltrimethylamine, and divinylbenzene.

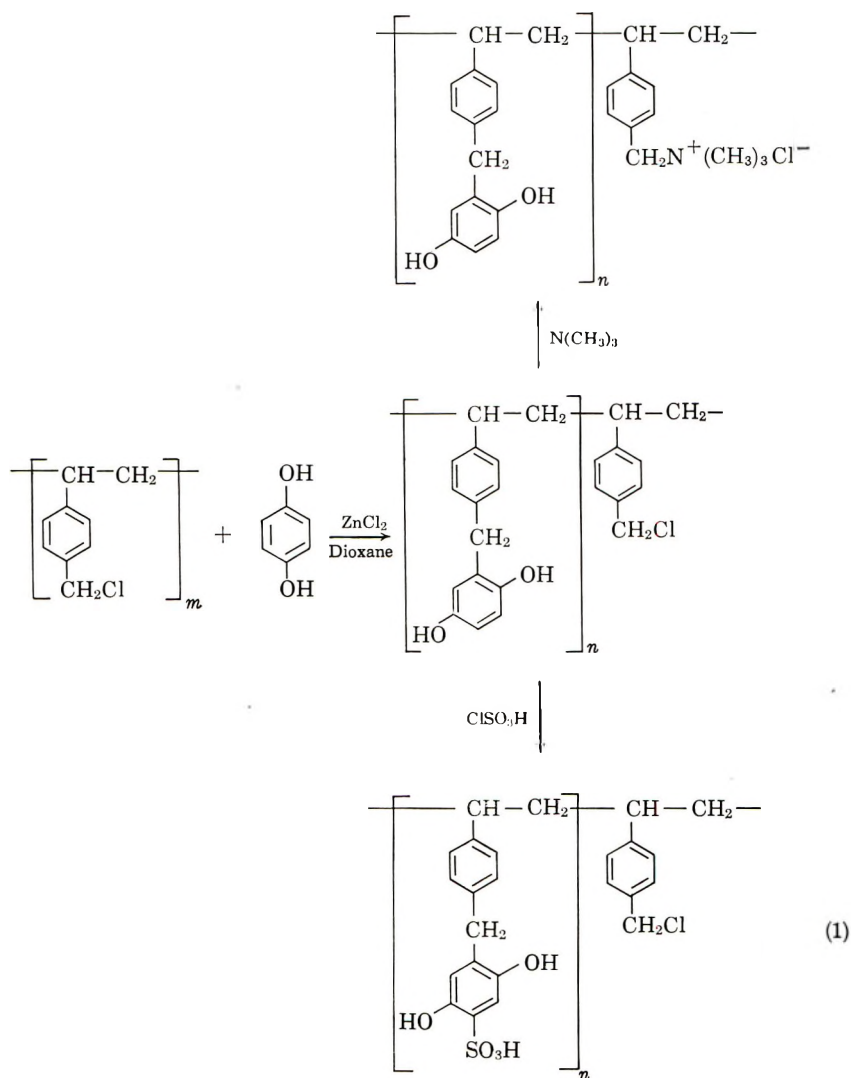
By utilizing copolymers having macroreticular structures, hydroquinone redox polymers were obtained that showed greater reactivity and better stability than resins having the conventional gel-type structures. These macroreticular copolymers are characterized by having significant fractional extra-gelular pore volumes in addition to the normal gel porosity (microreticular) where the pore structures are based upon distances between polymer chains. The nongel pore structure of macroreticular copolymers consists of voids or open spaces between agglomerates of randomly packed microspheres.³

This paper describes the effects of physical and chemical modifications of hydroquinone redox polymers on redox capacity and reaction rate.

RESULTS AND DISCUSSION

Synthesis of Crosslinked Redox Polymers

The redox polymers examined in this study are based upon hydroquinone and were prepared by a Friedel-Crafts addition of hydroquinone to macroreticular chloromethylated poly(styrene-divinylbenzene) copolymers.¹ Treatment of the hydroquinone polymers with chlorosulfonic acid or with trimethylamine gave the respective cationic and anionic redox polymers.² Equation (1) summarizes the synthetic routes used. Detailed preparative procedures have been presented^{1,2} and therefore will not be discussed here.



Oxidants

Properly to determine the utility and potential areas of application for redox polymers, the redox capacity, the redox potential, and the relative rates of reaction should be known. Luttinger and Cassidy,⁴ Manecke,⁵ and Sansoni⁶ evaluated a variety of oxidants and reductants for use in redox capacity determinations on crosslinked and soluble redox polymers. Each investigator reached the same general conclusions. Bromine, iodine, cerium(IV), iron(III), and hydrogen peroxide were considered good oxidants, and reduction of the oxidized resin could be obtained with titanium(III), potassium iodide, sodium sulfite, sodium bisulfite, and sodium dithionite; recently, metal hydrides have been used. Under the appropriate reaction conditions, the above oxidants are useful for potentiometric titrations of soluble redox polymers where structures and compositions are known. Soluble redox polymers, during a titration, are in contact with very dilute solutions of oxidant and, as aliquots of oxidant are added, the hydroquinonyl groups are rapidly oxidized. This technique gives both the redox capacity and the redox potential of the material being examined.

Attempts to use this method on crosslinked polymers were not successful. Redox capacities were approximated by treating the polymers with excess oxidant; but, excess oxidant caused side reactions. Bromine, as expected, oxidized the hydroquinone groups; it then brominates the resulting quinone. Iodine also oxidized hydroquinonyl groups to quinone. While it does not halogenate the polymer, it does form complexes with aromatic compounds. Its use requires careful treatment to recover all the unreacted iodide from the resin or to titrate the hydriodic acid formed during this redox reaction. Cerium(IV), in aqueous sulfuric acid, is a useful oxidant; however, excesses are consumed irreversibly. Oxidations with iron(III) are described with various degrees of success. In general, attempts to determine redox properties on crosslinked structures have given anomalous results.

Oxidation with Cerium(IV)

An evaluation of hydroquinone redox polymers on highly and lightly crosslinked polystyrene matrices and the aminated and sulfonated derivatives of these materials indicates the apparent redox capacities obtained with excesses of cerium(IV) have no significant relationship to the structures of the polymers. Cerium(IV) consumption is fastest for the sulfonated hydroquinone resins; reaction with lightly crosslinked resin is faster than with highly crosslinked resin. The aminated derivatives do not react with cerium(IV) as fast as the sulfonated analogs; however, the aminated derivatives are more reactive than the hydrophobic hydroquinone resins.

Attempted determinations of redox potentials by discontinuous titration techniques with cerium(IV) in 1*N* sulfuric acid showed that both the reduced and oxidized forms of the redox resins were reacting with excesses of oxidant. This reaction with the oxidant continued until all the cerium(IV) was reduced to cerium(III) for the sulfonic derivatives. The ami-

nated and the hydrophobic redox resins followed this same pattern. Consumption of excess cerium(IV) appears to be independent of the oxidant concentration.

Oxidation with Iron(III)

An examination of the redox potentials of a variety of oxidants indicated that iron(III) should readily oxidize hydroquinones at pH of 2 or less. Redox capacities of the two sulfonated redox polymers showed that at room temperature iron(III) oxidized the hydroquinonyl group but did not touch the polymer matrix. Table I gives the cerium(IV) capacities and the iron(III) capacities for the sulfonated redox polymers through several redox cycles. The calculated redox capacities are maximum values based on elemental microanalysis of the hydroquinone adducts. For this set of samples the redox capacities were determined from the residual or unreacted chloride found in the hydrophobic resin and, therefore, are maximum values. The cerium(IV) values show no significant relationship to the calculated redox capacities for the samples described in Table I, while the series of iron(III) capacities on the same set of samples are below the cal-

TABLE I
Redox Capacities of Hydroquinone Redox Polymers

	Sulfonate redox polymers		Animated redox polymers		Hydroquinone adduct	
	High	Low	High	Low	High	Low
Degree of crosslinking in the matrix	High	Low	High	Low	High	Low
Calcd. redox capacity based on residual % Cl, meq./g. dry resin ^a	1.92	6.19	1.84	4.98	1.91	5.14
Cerium(IV) redox capacity, meq./g. resin ^b						
10 min. contact time	1.78	1.65	0.99	2.00	—	—
1 hr. contact time	3.65	3.90	1.80	3.94	—	—
24 hr. contact time	9.81	14.3	4.63	9.71	3.00	3.35
Ion exchange capacity, meq./g. resin						
Anion exchange	—	—	1.70	1.53	—	—
SSCE	1.35	1.14	—	—	—	—
Iron(III) redox capacity, meq./g. resin						
1 liter/eluate 24 hr.	1.03	3.26	0.66	2.17	0.64	1.20
1 liter eluate/24 hr.	0.25	0.49	0.12	0.22	0.06	0.10
1 liter eluate/24 hr.	0.12	0.21	0.03	0.04	0.03	0.10
0.5 liter eluate/7 hr.	0.06	0.16	0.03	0.10	0.02	0.05
Total ^c	1.46	4.12	0.84	2.53	0.75	1.45
% of theoretical capacity found	76.0	63.2	45.6	50.8	39.3	26.2

^a These are maximum values based on elemental microanalysis of the hydroquinone adducts.

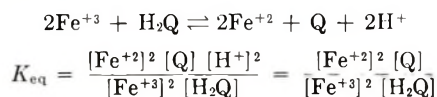
^b 0.1N cerium(IV) in 1N H₂SO₄

^c 1.0N iron(III) in 1N H₂SO₄.

culated capacities. In fact, the cerium(IV) capacity values are far in excess of the theoretical capacities, further indicating that this oxidant cannot be used. Iron(III) capacities indicate that the oxidation is slow, with the major portion of the available capacity being obtained with the first liter of oxidant. Subsequent additions of oxidant continue to give a measure of the available redox capacity but these values are only 10-25% of the initial value and appear to be dependent upon the structure of the redox polymer; i.e., crosslinker content, surface area, ion-exchange substituent, and the relative degree of hydration of the resin. It is of interest to note that, in the case of the capacity measurements with iron(III) as the oxidant, the utilization of the theoretical capacity increases with the increase in the hydrophilic nature of the polymer.

Attempts to increase the rate of reaction of the sulfonated redox polymers with iron(III) by increasing the reaction temperature to approximately 90°C. indicated that iron(III) attacked the resins, with results similar to that found with cerium(IV) at room temperature.

The oxidation of hydroquinones to quinones by iron(III) in 1*N* sulfuric acid is a favorable reaction based upon the standard oxidation reduction potentials for these materials. The potential of the Fe⁺²/Fe⁺³ system is 0.74 v., while that of H₂Q/Q system is 0.70 v. Determination of the equilibrium constant indicates that the reaction conditions for the iron(III) oxidations are not favored by working in 1*N* acid and by increases in iron(II) concentration. This is true for approximately equimolar solutions under equilibrium conditions. However, the redox capacity determination used is not a static system; resins having capacities of approximately 1-6 meq./g. are being treated with aliquots of 100 meq. of oxidant where the iron(II) that is formed is constantly being removed. The large excesses of iron(III) in the rate studies also tend to drive the reaction to completion.



in 1*N* acid.

Effect of Oxygen

The effect of oxygen on redox polymers is an important factor. Under acidic conditions, the oxidation of hydroquinone by oxygen is very slow; therefore, oxygen does not have to be excluded from the reaction system when iron III in 1*N* sulfuric acid is used as the oxidant. To establish the point, the following experiments were run. Air was bubbled through a 0.1*N* ferric sulfate solution in 1*N* sulfuric acid that contained 0.0138*N* ferrous sulfate. The ferrous sulfate concentration did not change after 24 hr. of this treatment and, therefore, it is assumed that once the iron(III) is reduced to iron(II), it will not reoxidize under the conditions of the evaluation. A redox capacity determination with freshly reduced sulfonated hydroquinone resin on the lightly crosslinked matrix, in an oxygen-free

atmosphere, with oxygen-free acid to remove last traces of reductant and oxygen-free ferric sulfate solution gave a value of 5.42 meq./g. while the control, run in the presence of oxygen, gave a value of 5.32 meq./g. The samples were run for a period of 46 hr. with 1.5 liters of oxidant. Thus, for macroscale determinations with crosslinked resins, under acidic conditions, oxygen is not a serious problem because the differences in redox capacities due to oxygen are no larger than the differences found in the reproducibility of the material being tested. The effects of oxygen, however, are reported to be very significant, and great care must be taken to remove it when working with soluble redox polymers at the micro scale.⁷

Redox Kinetics

The kinetics of the redox polymers were studied by measuring, by means of batch contact, the conversion of iron(III) to iron(II) as a function of time. Effects of matrix structures and functional groups are readily observed. By using the redox capacities determined with iron(III) as the maximum available capacity for each resin, the percentage of each resin oxidized by iron(III) was determined at room temperature (25°C.). Figures 1-3 show the percentages of available redox capacity oxidized, during a 7-hr. period, for the six types of redox polymers. The hydrophobic hydroquinone polymers having high and low degrees of crosslinking have total redox capacities of 0.75 and 1.45 meq./g. dry resin, respectively. The rates of oxidation, as shown in Figure 1, indicate that approximately 15% of the available redox capacities are realized during 7-hr. periods and the major portion of this degree of utilization of the capacity is obtained within the first 2 hr. Continuing the contact time for a total of 70 hr. increased the degree of oxidations to approximately 25-30%. As expected, the larger particle size (-16 + 20 mesh) beads are less reactive than the smaller (-30 + 40 mesh) beads which indicates that a diffusional process is controlling the rate.

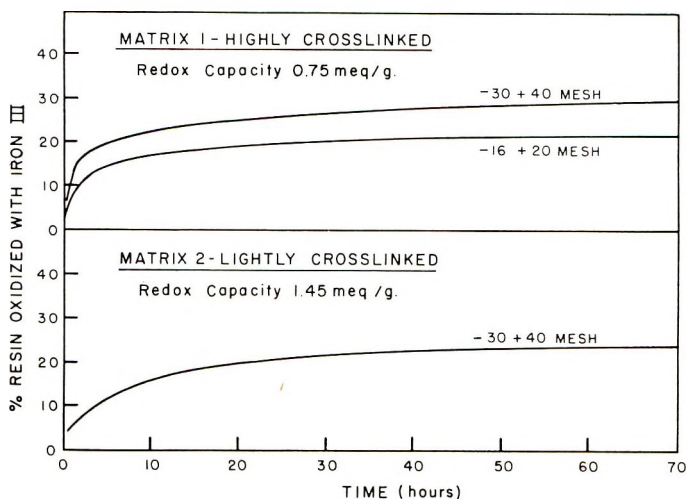


Fig. 1. Oxidation of macroreticular hydroquinone redox polymers with 0.1*N* iron(III) as a function of time.

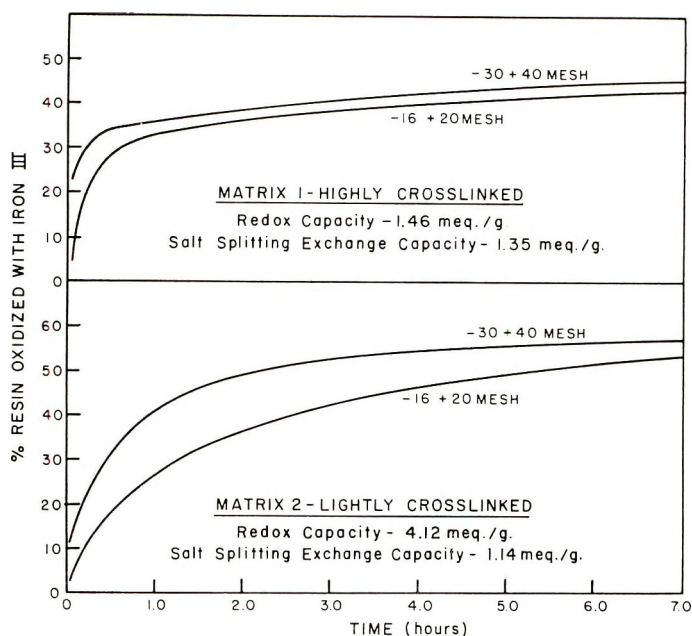


Fig. 2. Oxidation of macroreticular sulfonated hydroquinone redox polymers with 0.1N iron(III) as a function of time.

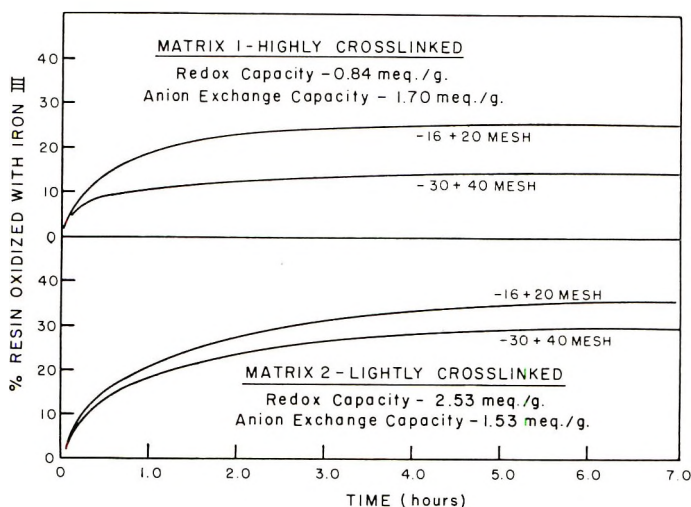


Fig. 3. Oxidation of macroreticular amine-hydroquinone redox polymers with 0.1N iron (III) as a function of time.

By increasing the hydrophilic character of the resins, the reaction rate and the available redox capacities are significantly increased. Figure 2 shows the relationship between reaction time and per cent oxidation of the sulfonated hydroquinone redox polymers. These sulfonic acid derivatives have an available redox capacity of 1.46 meq./g. dry resin for the highly crosslinked matrix and 4.12 meq./g. dry resin for the lightly crosslinked matrix. After 2 hr. of contact of the $-30 + 40$ mesh fractions with the

oxidant, the percentage of resin oxidized increased (over the hydrophobic resins) by 56% for the highly crosslinked resin and 145% for the lightly crosslinked resin. Here also, the -30 +40 mesh fractions were more reactive and showed higher capacities than the larger -16 +20 mesh fractions, and the lightly crosslinked resins were more reactive than the highly crosslinked resins.

Amination of unreacted chloromethyl groups in the hydrophobic hydroquinone resins also increases the hydrophilic character of the polymers. Figure 3 indicates that amination with trimethylamine to give the corresponding quaternary derivative did increase the reactivity and the available redox capacity of the resins though not to the extent that was obtained by sulfonation. The effective increase in available redox capacities for the amine-hydroquinone systems is 12% on the highly crosslinked matrix and 95% on the lightly crosslinked matrix. Reaction of the oxidant with resin shows a slight increase with highly crosslinked resins and a substantially greater increase with the lightly crosslinked resin. However, examination of the rate curves in Figure 3 shows that the larger (-16 +20 mesh) beads are more reactive than the smaller size beads (-30 +40). This is an inversion of the effect of particle size as observed with the hydroquinone and the sulfonated hydroquinone resins.

The reaction of iron(III) with the hydroquinone polymers showed that particle size affects reaction rate (Fig. 1) and this relationship is attributed to diffusion of soluble reactants through the gel structure of the polymer. Thus, the larger particle has a larger radius, and the soluble reactant must diffuse through more of the polymeric phase for an equivalent percentage of reaction within the bead. Although the macroreticular nature of redox polymers increases the difficulty for one to interpret the kinetic data quantitatively, the low rates and the marked effect of the introduction of ionic groups indicate the rate-controlling step to be particle diffusion rather than film diffusion.

The effect of particle size on reactivity also follows the expected diffusion effect with the sulfonated hydroquinone resins, as shown in Figure 2. In the case of the synthesis of the amine-hydroquinone resins, the amination involved the unreacted chloromethyl groups not utilized during the earlier step introducing the hydroquinone groups. Diffusion through the polymeric gel structure was also probably rate controlling as the hydroquinone reacted with the chloromethylated copolymer. The hydroquinone concentration on the polymer matrix would be greatest on the outer surface of the beads, and the concentration would decrease towards the center of the beads. For a given reaction time, hydroquinone would diffuse approximately the same distance into the larger and the smaller size beads. Since the hydroquinone addition is not permitted to go to completion, the unreacted chloromethyl groups are towards the center of the individual beads; the larger beads would have more unreacted chloromethyl groups than the smaller size beads. Amination of these materials gives products where the larger beads have a higher concentration of quaternary groups than the smaller beads. Thus, the larger beads would

be more hydrophilic and more reactive to oxidants in aqueous solutions. With the quaternary amine groups located primarily toward the center of the resin particles, it is not unexpected to find the redox capacities and rates of reactions of these materials to be more like those of the unsubstituted hydroquinone resins than like those of the sulfonated derivatives. The amine-hydroquinone redox polymer beads have a shell of relatively hydrophobic hydroquinone resin with a center of hydrophilic amine resin. Comparisons of redox capacities and rates of reaction clearly show these effects.

EXPERIMENTAL

Redox Capacity Determination

Redox polymer (1 g. dry weight) was charged into a $\frac{1}{2}$ in. sintered-glass tube and the hydrated resin treated with 500 ml. of 1*N* sulfuric acid. This was followed by treatment of the sample with 1 liter of 0.1*N* titanium(III) in 1*N* sulfuric acid to insure complete reduction of the polymer. The reduced sample was washed with 500 ml. of 1*N* sulfuric acid to remove the reductant. Acid washings were continued until the effluent would not reduce a dilute cerium(IV) solution. The redox polymer in acid was allowed to stand for $\frac{1}{2}$ hr., and the acid was drained from the beads and tested for reductant. If there was reductant in the acid, washings were continued; if the resin was free of reductant, 1 liter of 1*N* ferric sulfate in 1*N* sulfuric acid was passed through the resin bed very slowly. An aliquot of the effluent was titrated with standardized 0.08*N* ceric sulfate in 1*N* sulfuric acid, with *o*-phenanthroline as the indicator, to determine the concentration of iron(II) formed. A blank was run on the original ferric solution for ferrous and subtracted from each titer. (We usually ran the first liter of oxidant through the resin overnight.) A second and a third liter of ferric sulfate solution were passed through the resin as described for the first liter and the ferrous concentrations determined. (We found that the major portion of available redox capacity was detected in the first liter of oxidant; approximately 10–25% of the first ferrous concentration was found in the second liter of oxidant and capacities of about 0.1 to 0.3 meq./g. in the third liter of oxidant for the sulfonated redox polymers. Proportionally lower values were found in the aminated and hydrophobic resins.) Aliquots of oxidant were added to the resin until the ferrous concentration in the effluent gave a redox capacity value of less than 0.05 meq./g.

The number of aliquots of oxidant used, the volume and concentration of the ferric solutions, and the contact time of the oxidant with the redox polymer are dependent upon the redox polymer being evaluated. While polymeric structures and types of functional groups are being varied, the reaction conditions for the redox capacities should be adjusted to the individual materials. When one or more structures are selected for a more detailed evaluation or if a control procedure is required for synthesis studies, the reaction conditions for this capacity test can be standardized.

Rate of Reaction

A 1-g. portion of redox polymer (+20–30 or +30–40 mesh cut) hydrated in 25 ml. of 1*N* sulfuric acid was added to a three-necked, round-bottomed flask, fitted with a stirrer, a thermometer, and a pair of electrodes (calomel and platinum) connected to a potentiometer, containing 300 ml. of standardized 0.1*N* ferric sulfate in 1*N* sulfuric acid. Periodically 5-ml. aliquots of the ferric solution were removed and the ferrous content was determined by titration with standardized ceric sulfate in 1*N* sulfuric acid. The potential of the solution was measured when samples were removed; changes in potential during the redox reaction is a convenient indicator to determine when aliquots should be removed. (We have found that time intervals of every 15 min. for the first hour, every $\frac{1}{2}$ hr. for the second hour and every hour for approximately 7 hr. are convenient. We also took a sample approximately 24–33 hr. after the reaction was initiated.) The rate data were plotted and interpreted in the usual manner.

The authors gratefully acknowledge the technical assistance of Mr. Alfred G. LeSieur, Jr. and Mr. Edgar M. Cloeren.

References

1. Kun, K. A., *J. Polymer Sci. A1*, **3**, 1833 (1965).
2. Kun, K. A., *J. Polymer Sci. A1*, **4**, 847 (1966).
3. Kun, K. A., and R. Kunin, *J. Polymer Sci. B*, **2**, 587 (1964); *ibid.*, **2**, 839 (1964).
4. Luttinger, L., and H. G. Cassidy, *J. Polymer Sci.*, **20**, 417 (1956).
5. Manecke, G., in Houben-Weil, *Methods in Organic Chemistry*, Praxis I, Teil I, Thieme, Stuttgart, 1958.
6. Sansoni, B., *Chem. Tech. (Berlin)*, **10**, 580 (1958).
7. Cassidy, J. G., and K. A. Kun, *Oxidation-Reduction Polymers*, Interscience, New York, 1965.

Résumé

Une série de polymères oxydoréducteurs hydroquinone–quinone fixés sur une matrice soit hautement soit faiblement pontée à base de copolymères styrène divinylbenzène réticulés a été caractérisée par sa capacité redox, sa réactivité, ses constantes d'équilibre et son potentiel oxydoréducteur. Les effets du cerium(IV), du fer(III) et de l'oxygène sur la capacité oxydoréductrice sont décrites.

Zusammenfassung

Eine Reihe von Hydrochinon-Chinon-Redoxpolymeren auf stark und schwach vernetzten Makronetz-Styrol-Divinylbenzolmatrizen wurde in Bezug auf ihre Redoxkapazität, Reaktivität Gleichgewicht und Redoxpotential charakterisiert. Der Einfluss von Cer(IV), Eisen(III) und Sauerstoff auf die Bestimmung der Redoxkapazität wird beschrieben.

Received August 17, 1965

Revised September 20, 1965

Prod. No. 4894A

Cationic Polymerization of Cyclic Olefins

A. MIZOTE, T. TANAKA, T. HIGASHIMURA, and S. OKAMURA,
Department of Polymer Chemistry, Kyoto University, Kyoto, Japan

Synopsis

The polymerization and the polymerizabilities of indene, benzofuran, and 1,2-dihydronaphthalene are discussed from the point of view of ring strain, ring stabilization, and steric hindrance in the transition state. Monomer reactivities of these olefins were estimated from copolymerization with styrene and from the rate of addition of iodine bromide in acetic acid. Rates and degrees of polymerization are compared with monomer reactivities and resonance energies of indene, 1,2-dihydronaphthalene, and benzofuran as a measure of ring strain and stabilization. It is found that indene is 1.5-2.0 times more reactive than styrene. This high reactivity of indene is attributed to the ring strain in the monomer state and to the low amount of steric hindrance in the transition state of the coplanar five-membered cyclic olefin. 1,2-Dihydronaphthalene is strained and therefore reactive, but propagation to higher molecular weight products is impeded due to the steric hindrance. The reactivity of benzofuran is decreased by conjugative stabilization of C=C double bonds at the reaction site.

INTRODUCTION

Indene¹⁻³ and benzofuran⁴ are well known cyclic olefins which can be easily polymerized with conventional cationic catalysts. Few quantitative studies on reactivities of these cyclic olefins, especially in the pure state, have been carried out to date. Natta and his co-workers⁵ recently reported interesting results on reactivities and behavior of aliphatic cyclic olefins in coordinated stereoregular polymerization. In contrast to aliphatic cyclic olefins, aromatic cyclic olefins, such as indene⁶ and benzofuran,⁷ do not give crystalline polymers.

The main purpose of this paper is to establish relationships between structures and reactivities of aromatic cyclic olefins in homogeneous cationic polymerization. The reactivities of indene, benzofuran, and 1,2-dihydronaphthalene have been quantitatively determined and compared with those of styrene and β -methylstyrene.

It has been thought^{8,9} that cyclic olefins are related to α,β -disubstituted olefins and consequently tend to give only low molecular weight polymers due to steric repulsion of the substituents in the transition state for the propagation reaction. However, recent studies of Sigwalt¹⁰ and Mizote et al.¹¹ revealed that indene and benzofuran can be polymerized to fairly high molecular weight products under controlled reaction conditions.

Indene, benzofuran, and 1,2-dihydronaphthalene are convenient mono-

mers for comparing reactivities of cyclic olefins from the point of view of structure, ring size, and steric aspects. In the case of polymerization of five-membered cyclic olefins, both the monomer and the propagating carbonium ion have coplanar structures including the α - and β -carbon in the monomer unit, and there is no appreciable steric repulsion between the propagating chain end and incoming monomer.

In the case of six-membered cyclic olefins, e.g., 1,2-dihydronaphthalene, homopolymerization gives only low molecular weight products.¹² However, copolymerization experiments with styrene show that the monomer reactivity of 1,2-dihydronaphthalene is quite similar to that of styrene. This situation may be explained by the steric repulsion in the transition state of self-addition reaction. Since 1,2-dihydronaphthalene is planar, the origin of steric repulsion could be due mainly to the structure of the chain end, including the carbonium ion, and possibly due to the penultimate units.

EXPERIMENTAL

Materials

Benzofuran. Benzofuran was prepared by decarboxylation of coumarilic acid. The decarboxylation was achieved smoothly by heating coumarilic acid in the presence of small amounts of quinoline and copper dust. Coumarilic acid was prepared from coumalin according to Fuson.¹³ The crude benzofuran was washed with dilute hydrochloric acid, followed by washing with water, alkali, and water. After being dried with anhydrous sodium sulfite overnight, the material was fractionally distilled at reduced pressure under nitrogen atmosphere just before use; b.p. 43.5°C./6 mm. Hg, n_D^{25} 1.5637; (lit.¹⁴ b.p. 62–63°C./15 mm. Hg, $n_D^{22.7}$ 1.5645).

1,2-Dihydronaphthalene. 1,2-Dihydronaphthalene was prepared by direct reduction of naphthalene by gradual addition of metallic sodium into an absolute ethyl alcohol solution of naphthalene under reflux, followed by slow steam distillation through a long fractionating column. The distillate was extracted with benzene, and the benzene extract was washed with aqueous alkaline and then with water, followed by drying over anhydrous calcium chloride and fractional distillation; b.p. 66°C. 5.5 mm. Hg, $n_D^{22.6}$ 1.5690 (lit.¹⁵ b.p. 89°C. 24 mm. Hg, n_D^{25} 1.5789, d_4^{20} 0.9911).*

β -Methylstyrene. β -Methylstyrene^{16,17} was prepared by refluxing allylbenzene with equal volume of 20% potassium solution of butyl alcohol and fractional distillation. The refractive index showed that purified product was a mixture of *trans* and *cis* isomers (approximately 70% *trans* isomer); b.p. 176–177°C.; n_D^{26} 1.5450, d^{20} 0.9110 (lit.¹⁸ b.p. 71°C./25 mm. Hg, n_D^{25} 1.5480, d_4^{20} 0.902).

* 1,2-Dihydronaphthalene used here contains 17% tetralin (by gas chromatography), which may act as a hydrocarbon solvent and does not affect the copolymer composition. As it was hard to remove the tetralin, we used this material without further purification and accordingly, the monomer concentrations are corrected in our experimental results.

Other Monomers. Indene and styrene were obtained by purifying commercial reagent grade materials. Purification of indene was carried out by the method of Schmitt.⁶

Solvent and Catalysts. These were purified by conventional methods. Reagent grade trichloroacetic acid was used as cocatalyst without further purification.

Preparation of IBr Solution in Glacial Acetic Acid. IBr solution was prepared²² by dissolving equimolar amounts of bromine and iodine (both reagent grade materials) into glacial acetic acid and warming to 40°C. for several minutes.

Technique

Polymerizations were carried out at 30°C. The rate of polymerization of styrene, indene, and benzofuran was measured dilatometrically; for 1,2-dihydronaphthalene, the rate was estimated by determining the residual monomer concentration by gas chromatography.

Copolymer compositions were determined by infrared spectroscopy (KBr disk). The samples were obtained at less than 10% conversion. Initial monomer concentration was corrected for samples whose conversion exceeded 5% according to Overberger²³ when monomer reactivity ratios were estimated by the intersection method.

The molecular weights of the polymers were determined with a vapor pressure osmometer (Mechrolab Co.). Intrinsic viscosity measurements were carried out in benzene solution at 30°C.

Rate measurements of IBr²² addition to olefins in glacial acetic acid were carried out at 30°C. Olefins were added to the IBr glacial acetic acid solution (olefin concentration, 0.037 mole/l. IBr concentration 0.07 mole/l.), and aliquots of the reaction mixture were withdrawn at arbitrary intervals and put into the excess of KI aqueous solution. The liberated free iodine was titrated with aqueous 0.1*N* sodium hyposulfite solution.

Polymer yields given refer to methanol-insoluble polymer.

Heats of combustion of indene, benzofuran, and 1,2-dihydronaphthalene were determined with an adiabatic calorimeter (Shimazu Seisakusho Co. Ltd.) at 15°C.

Ultraviolet absorption spectra were obtained in ethyl alcohol solution.

RESULTS AND DISCUSSION

Rate of Homopolymerization

The rate equations¹¹ for homopolymerization of indene, benzofuran, and styrene are summarized in Table I.

Table II shows polymerization yield for indene, benzofuran, styrene, 1,2-dihydronaphthalene, and β -methylstyrene in ethylene dichloride with stannic chloride-trichloroacetic acid catalyst after 30 min. of reaction. On comparing the overall rate constants of styrene and indene in Table I, the rate for indene is found to be 1.5–2.0 times that for styrene. Benzo-

TABLE I
Rate of Polymerization of Indene, Benzofuran, and
Styrene in $(\text{CH}_2\text{Cl})_2$ at 30°C.

Monomer	Rate, mole/l.-min.	Catalyst
Indene	$R_p = 22.4 [M]^2[C]$	$\text{BF}_3 \cdot \text{OEt}_2$
Styrene	$R_p = 15.0 [M]^2[C]$	$\text{BF}_3 \cdot \text{OEt}_2$
Benzofuran	$R_p = 1.62 [M]^2[C]$	$\text{SnCl}_4 \cdot \text{CCl}_3\text{COOH}$

TABLE II
Comparison of Polymerization Yields^a

Monomer	Yield, % ^b	
	$\text{BF}_3 \cdot \text{OEt}_2$ (7.0 mmole/l.)	$\text{SnCl}_4 \cdot \text{CCl}_3\text{COOH}$ (100 mmole/l.)
Indene	80	100 (nil)
Styrene	60	100 (nil)
Benzofuran	0	60 (nil)
1,2-Dihydronaphthalene	0	10 (60)
β -Methylstyrene	0	0 (30)

^a Monomer concn., 10 vol.-%; solvent, $(\text{CH}_2\text{Cl})_2$; reaction time, 30 min.; 30°C.

^b Values in parentheses denote yields of methanol-soluble material.

furan can be hardly polymerized with $\text{BF}_3 \cdot \text{OEt}_2$. The rate of polymerization of benzofuran was determined with stannic chloride-trichloroacetic acid catalyst.

Table II shows yield data obtained after 30 min. of reaction. If the polymerization time is extended over 30 min., the yield of indene, styrene, and benzofuran is increased to close to 100%. However, 1,2-dihydronaphthalene and β -methylstyrene yield only methanol-soluble materials under our experimental conditions.

Figure 1 shows time-conversion curves for 1,2-dihydronaphthalene obtained by determining residual monomer concentration. The overall rates

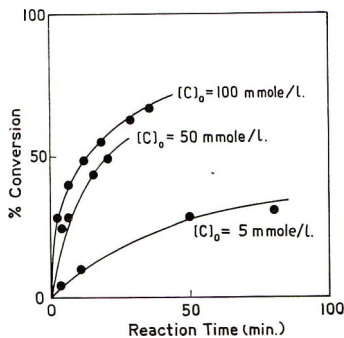


Fig. 1. Time-conversion curves of 1,2-dihydronaphthalene. Monomer concentration, 0.7 mole/l.; solvent, $(\text{CH}_2\text{Cl})_2$; catalyst, $\text{SnCl}_4 \cdot \text{CCl}_3\text{COOH}$; temperature, 30°C.

of polymerization thus decrease in the order: indene > styrene \gg benzofuran \geq 1,2-dihydronaphthalene \geq β -methylstyrene.

Degree of Polymerization

A comparison of the degrees of polymerization for indene, styrene, and benzofuran under identical experimental conditions is shown in Figure 2. \overline{DP} of polyindene is higher than that of styrene. In the case of benzofuran, $[\eta]$ of polybenzofuran varies with conversion, as is shown in Figure 3. The upswinging end of the $[\eta]$ -conversion curves might possibly be due to cross-linking by the reaction between propagating carbonium ion and ether linkages in polybenzofuran at high conversion.¹¹ The effect of conversion on \overline{DP} of polybenzofuran is less marked at lower monomer concentrations (less than 0.4 mole/l.) and at lower conversions (less than 40%). The benzofuran data in Figure 2 were obtained under these conditions. The \overline{DP} of the methanol-insoluble fraction of 1,2-dihydronaphthalene remained nearly constant (around tetramer), independent of monomer concentration ($[M] = 0.6$ – 2.4 mole/l., $\text{SnCl}_4 \cdot \text{CCl}_3\text{COOH}$ 0.1 mole/l., in ethylene dichloride 30°C .). No methanol-insoluble polymer was obtained from

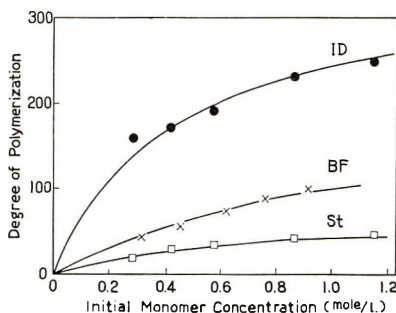


Fig. 2. Comparison of DP of (●) indene, (×) benzofuran, and (□) styrene. Solvent, $(\text{CH}_2\text{Cl})_2$; catalyst, $\text{SnCl}_4 \cdot \text{CCl}_3\text{COOH}$; temperature, 30°C .

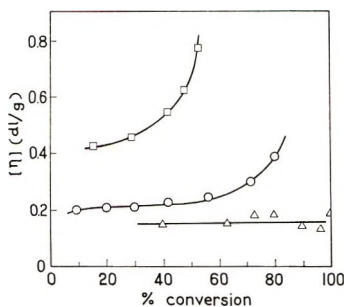


Fig. 3. Relation of $[\eta]$ of polybenzofuran vs. conversion: (○) monomer concn. 0.92 mole/l., 30°C .; (△) monomer concn. 0.42 mole/l., 30°C .; (□) monomer concn. 0.92 mole/l., 0°C . Solvent, $(\text{CH}_2\text{Cl})_2$; catalyst, $\text{SnCl}_4 \cdot \text{CCl}_3\text{COOH}$; catalyst concentration, 0.1 mole/l.

β -methylstyrene under these experimental conditions ($[M] = 10$ vol.-%, $\text{SnCl}_4 \cdot \text{CCl}_3\text{COOH}$ 0.1 mole/l., in ethylene dichloride, 30°C).

Thus the \overline{DP} of polymers of indene, styrene, benzofuran, 1,2-dihydronaphthalene, and β -methylstyrene obtained under identical conditions decreases in the order: indene $>$ benzofuran \geq styrene \gg 1,2-dihydronaphthalene \geq β -methylstyrene.

Copolymerization

Indene, benzofuran, 1,2-dihydronaphthalene, and β -methylstyrene²⁴ were copolymerized with styrene. Relative monomer reactivities of these olefins toward styrene carbonium ion were determined. The steric hindrance which impedes the homopolymerization of these monomers is not operating when they are copolymerized with styrene.

Copolymer composition curves obtained in $(\text{CH}_2\text{Cl})_2$ with $\text{BF}_3 \cdot \text{OEt}_2$ at 30°C . are shown in Figure 4.

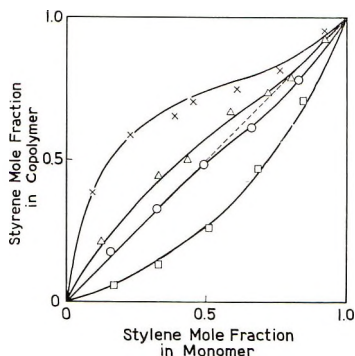


Fig. 4. Copolymer composition curves of styrene (M_1) and cyclic olefins: (\square) indene; (\circ) benzofuran; (Δ) 1,2-dihydronaphthalene; (\times) β -methylstyrene. Monomer concentration, 10 vol.-%; solvent, $(\text{CH}_2\text{Cl})_2$; catalyst, $\text{SnCl}_4 \cdot \text{CCl}_3\text{COOH}$; temperature, 30°C .

Monomer reactivity ratios are listed in Table III. Relative monomer reactivities toward styrene carbonium ion decrease in the order: indene $>$ benzofuran \geq styrene \approx 1,2-dihydronaphthalene \geq β -methylstyrene. The relative monomer reactivity of benzofuran is higher than that of styrene in copolymerization, while according to the homopolymer-

TABLE III
Summaries of Monomer Reactivity Ratios^a

	Indene	Benzofuran	1,2-Dihydronaphthalene	β -Methylstyrene
r_1	0.6 ± 0.1	0.80 ± 0.1	1.0 ± 0.3	1.8 ± 0.3
r_2	3.7 ± 0.2	0.95 ± 0.1	0.4 ± 0.2	0.07 ± 0.02

^a $M_1 =$ styrene, $M_1 + M_2 = 10$ vol.-% in $(\text{CH}_2\text{Cl})_2$, $\text{BF}_3 \cdot \text{OEt}_2$, 30°C .

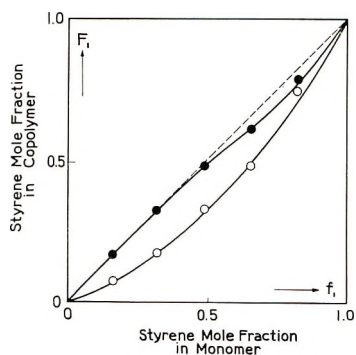


Fig. 5. Copolymer composition curves of styrene (M_1) and benzofuran (M_2) obtained in (O) toluene and (●) ethylene dichloride. Monomer concentration, 10 vol.-%; catalyst, $\text{BF}_3 \cdot \text{OEt}_2$; temperature, 30°C .

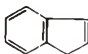

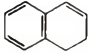
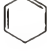
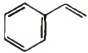
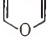
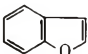
ization rate data this monomer is markedly less reactive than styrene. This difference in the rate of homopolymerization and relative monomer reactivity might be explained by a slower rate of initiation and/or larger solvation power of benzofuran monomer. The ether oxygen in the benzofuran will preferentially solvate the carbonium ion, so that the local concentration of benzofuran around the propagating styrene carbonium ion would be higher. Thus benzofuran would be incorporated preferentially into the copolymer. This interpretation is in agreement with the observation¹¹ that benzofuran is incorporated preferentially into the copolymer when styrene and benzofuran are copolymerized in nonpolar solvents like toluene. This interpretation of the change in copolymer composition with solvents by preferential monomer solvation has been proposed by Overberger et al.²⁵ for a similar system.

Figure 5 shows copolymer composition curves for the styrene–benzofuran system obtained in ethylene dichloride and toluene solvents.

While the rates of homopolymerization of 1,2-dihydronaphthalene and β -methylstyrene are much slower than that of styrene, the relative reactivities of these monomers in copolymerizations are not much different from that of styrene as reflected in their r_1 values. This might be explained by the removal of steric hindrance and not by preferential solvation, since the solvating power of these olefins is expected to be similar. The fact that the reactivity ratios are largely dissimilar for the styrene–1,2-dihydronaphthalene and styrene– β -methylstyrene systems could be construed as evidence for steric hindrance to incorporation for the homopolymerization of 1,2-dihydronaphthalene and β -methylstyrene. Since the structure of propagating carbonium ions in these systems is very similar, it could be expected that $r_1 r_2 = 1$. However, this is not the case, i.e., $r_1 r_2 = 0.4$ for the 1,2-dihydronaphthalene system and $r_1 r_2 = 0.12$ for the β -methylstyrene system; consequently, it may be assumed that steric hindrance plays a paramount role in determining the homopolymerization rate of these monomers.

Important factors which determine monomer reactivities of these materials are ring strain and conjugative stabilization of C=C bonds at the reaction site. This theory was tested by determining resonance stabilization energies of indene, benzofuran, and 1,2-dihydronaphthalene. These values were obtained by measurements of heat of combustion by use of Pauling's bond energies.²⁶ Results are listed in Table IV together with ultraviolet spectra and ring strain energies for cyclopentadiene, cyclohexadiene, and furan calculated by Cox,²⁷ and these compounds are related to olefinic part of indene, 1,2-dihydronaphthalene, and benzofuran, respectively. The molar extinction coefficients of indene and 1,2-dihydronaphthalene at nearly identical wavelengths are quite similar to that of styrene, but the molar extinction coefficient of benzofuran is larger by one order of magnitude than that of indene. These results show that benzofuran monomer is apparently stabilized by conjugation.

TABLE IV
Estimation of the Ring Strain and Conjugative
Stabilization of Cyclic Olefins

Olefin	Resonance energy, kcal./mole	Ultraviolet spectra		Cyclic diene	Ring strain energy, kcal./mole
		λ_{\max}	ϵ_{\max}		
	38 ± 5	248.0	13,200		+5
		279.5	580		
		285.5	318		
	(52 ± 5)	(260)	(10,000)		+4
	46 ± 5	287	320		
	70 ± 5	280.7	2,560		-8

Furthermore, to estimate the reactivities of these cyclic olefins, the rate of addition of IBr to the olefins was determined. IBr dissociates into I^+ and Br^- in polar solvents like acetic acid, and the addition of IBr to olefins is ionic. The attacking cation I^+ is much smaller than the propagating carbonium ion. Consequently, the rate of addition of IBr to the olefin would be a measure of relative reactivities without steric hindrance. The rates of addition of IBr to olefins in acetic acid at 30°C. are shown in Figure 6.

According to Figure 6, the rates are decreased in the order: 1,2-dihydronaphthalene > indene > styrene > benzofuran. This indicates that releasing the ring strain in 1,2-dihydronaphthalene and indene promotes the opening of the C=C double bond and, as a result, the reactivities of C=C double bonds are enhanced compared with styrene. The different

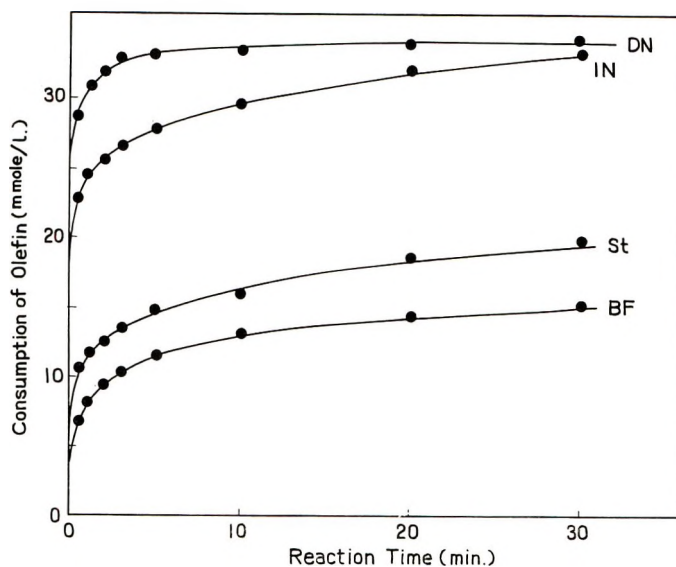
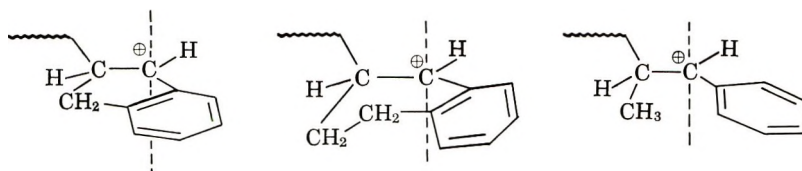


Fig. 6. Rate of addition of IBr to olefins in acetic acid at 30°C. Initial olefin concentration, 0.037 mole/l.; initial IBr concentration, 0.070 mole/l.

order in the rate of IBr addition and the ring strain for indene and 1,2-dihydronaphthalene might be attributed to the stabilization of the resulting cation, i.e., the indene cation is strained and the 1,2-dihydronaphthalene cation is less strained. The lower rate of IBr addition to benzofuran is probably due to the conjugative stabilization of the C=C double bond exceeding the ring strain as mentioned above.

Earlier²⁴ we discussed the steric effect of the β -methyl group in the polymerization of β -methylstyrene. Similar considerations might be applied to the polymerization of cyclic olefins.



Indene, 1,2-dihydronaphthalene, and benzofuran monomers have planar structures. However, the indene and benzofuran propagating cations have coplanar structures including five-membered rings. The 1,2-dihydronaphthalene cation is not coplanar, and one of the $-\text{CH}_2-$ groups in the alicyclic ring could create steric hindrance just like the β -methyl group in the β -methylstyrene cation.

A summary of the reactivities of indene, 1,2-dihydronaphthalene, and benzofuran is given in Table V. The order of reactivities is not always consistent. The larger polymerizability of indene could be due to the strained five-membered cyclic olefin part of the molecule. Since the

TABLE V
 Summaries of Reactivities

	Order
Rate of polymerization	Indene > styrene >> benzofuran \geq 1,2-dihydronaphthalene
Degree of polymerization	Indene > benzofuran > styrene >> 1,2-dihydronaphthalene
Monomer reactivity (by copolymerization)	Indene > benzofuran \geq styrene \geq 1,2-dihydronaphthalene
Rate of IBr addition	1,2-Dihydronaphthalene > indene > styrene > benzofuran
Ring strain and stabilization	Indene, 1,2-dihydronaphthalene (strained), styrene, benzofuran/stabilized)

monomer and the propagating cation have planar structures, there is no appreciable steric hindrance at the transition state of homopolymerization. Although benzofuran has the same skeletal structure as indene, it contains a furan ring, and is considered to be polar monomer, the actual polymerizability of benzofuran is less than that of styrene. This is attributed to the conjugative stabilization of the C=C double bond at the reaction site.

1,2-Dihydronaphthalene monomer itself is a fairly reactive olefin but due to steric hindrance the formation of high molecular weight polymer is difficult to achieve.

References

1. Krämer, G., and A. Spilker, *Ber.*, **23**, 3279 (1890).
2. Whitby, G., and M. Katz, *J. Am. Chem. Soc.*, **50**, 1160 (1928).
3. Staudinger, H., A. A. Ashdown, M. Brunner, H. A. Bruson, and S. Wehrli, *Helv. Chim. Acta*, **12**, 934 (1929).
4. Krämer, G., and A. Spilker, *Ber.*, **23**, 78, 3279 (1890).
5. Natta, G., G. Dall'asta, and G. Mazzanti, *Makromol. Chem.*, **61**, 178 (1963).
6. Schmitt, G. J., and G. Schuerch, *J. Polymer Sci.*, **49**, 287 (1961).
7. Natta, G., M. Farina, M. Peraldo, and G. Bressan, *Makromol. Chem.*, **43**, 68 (1961).
8. Schildknecht, C. E., *Vinyl and Related Polymers*, Wiley, New York, 1952.
9. Alfrey, T., Jr., J. J. Bohrer, and H. Mark, *Copolymerization*, Interscience, New York, 1952, p. 49.
10. Sigwalt, P., *J. Polymer Sci.*, **52**, 22 (1961).
11. Mizote, A., T. Tanaka, T. Higashimura, and S. Okamura, *Kobunshi Kagaku*, in press.
12. Von Braun and Kirschbaum, *Ber.*, **54**, 604 (1921).
13. Fuson, R. C., *Org. Syntheses*, **24**, 33 (1944).
14. Auwers, K. V., A. Boennecke, F. Krollpfeiffer, and G. Peters, *Ann.*, **408**, 212 (1915).
15. Straus and Lemmel, *Ber.*, **46**, 232 (1913).
16. Hershberg, E. B., *Helv. Chim. Acta*, **7**, 351 (1934).
17. Campbell, T. W., and W. G. Young, *J. Am. Chem. Soc.*, **69**, 688 (1947).
18. Overberger, C. G., D. Tanner, and E. M. Pearce, *J. Am. Chem. Soc.*, **80**, 4566 (1958).
19. Kuwata, T., *Yozai (Solvents)*, Maruzen, Tokyo, 1957.
20. Fieser, L. F., *J. Am. Chem. Soc.*, **70**, 3165 (1948).

21. Higashimura, T., and S. Okamura, *J. Polymer Sci.*, **21**, 289 (1956).
22. Gero, A., J. J. Kershner, and R. E. Perry, *J. Am. Chem. Soc.*, **75**, 5119 (1953).
23. Overberger, C. G., L. H. Arond, D. Tanner, J. J. Taylor, and T. Alfrey, Jr., *J. Am. Chem. Soc.*, **74**, 4848 (1952).
24. Mizote, A., T. Tanaka, and T. Higashimura, *J. Polymer Sci. A*, **3**, 2567 (1965).
25. Overberger, C. G., and V. G. Kamath, *J. Am. Chem. Soc.*, **85**, 446 (1963).
26. Pauling, L., *The Nature of the Chemical Bond*, Cornell Univ. Press, Ithaca, N. Y., 1940, pp. 53, 131.
27. Cox, J. D., *Tetrahedron*, **19**, 1175 (1963).

Résumé

La polymérisation et les polymérisabilités de l'indène, du benzofurane, et du 1,2-dihydronaphthalène ont été discutés du point de vue de la tension du cycle, de la stabilisation du cycle et de l'empêchement stérique à l'état transitoire. Des réactivités de monomères correspondants à ces oléfines ont été estimées au départ de leur copolymérisation avec le styrène et au départ de leur vitesse d'addition de bromure d'iode dans l'acide acétique. Les vitesses et les degrés de polymérisation ont été comparés avec les réactivités des monomères et les énergies de résonance de l'indène, du 1,2-dihydronaphthalène et du benzofurane comme mesure de la tension annulaire et de la stabilisation. On a trouvé que l'indène est 1,5 à 2 fois plus réactionnel que le styrène. Cette réactivité élevée de l'indène est attribuée à la tension cyclique à l'état monomérique et au peu d'empêchement stérique dans l'état transitoire de l'oléfine cyclique à cinq atomes qui est coplanaire. Le 1,2-dihydronaphthalène est tendu et de ce fait réactionnel, mais la propagation pour former des produits de poids moléculaires élevés, est empêchée par suite des effets stériques. La réactivité du benzofurane est diminuée par stabilisation par conjugaison des doubles liaisons C=C à l'endroit de réaction.

Zusammenfassung

Die Polymerisation und Polymerisierbarkeit von Inden, Benzofuran und 1,2-Dihydronaphthalin wurde vom Gesichtspunkt der Ringspannung, der Ringstabilisierung und der sterischen Hinderung im Übergangszustand aus diskutiert. Die Monomerreaktivität dieser Olefine wurde durch Kopolymerisation mit Styrol und aus der Geschwindigkeit der Addition von Jodbromid in Essigsäure bestimmt. Polymerisationsgeschwindigkeit und Polymerisationsgrad wurden mit der Monomerreaktivität und der Resonanzenergie von Inden, 1,2-Dihydronaphthalin und Benzofuran als Mass der Ringspannung und -stabilisierung verglichen. Inden ist 1,5 bis 2,0 Mal reaktionsfähiger als Styrol. Diese hohe Reaktivität von Inden wird auf die Ringspannung im Monomeren und auf die geringe sterische Hinderung im Übergangszustand des koplanaren 5-gliedrigen zyklischen Olefins zurückgeführt. 1,2-Dihydronaphthalin ist gespannt und daher reaktionsfähig, wegen der sterischen Hinderung findet jedoch kein Wachstum zu hohe molekulargewichtigen Produkten statt. Die Reaktivität von Benzofuran wird durch die Konjugationsstabilisierung der C=C-Doppelbindungen am Reaktionsort herabgesetzt.

Received July 1, 1965

Revised September 21, 1965

Prod. No. 4895A

Chain Transfer in Ethylene Polymerization

GEORGE A. MORTIMER, *Hydrocarbons and Polymers Division,
Monsanto Company, Texas City, Texas*

Synopsis

Chain transfer constants in the homogeneous free-radical polymerization of ethylene at 1360 atm. and 130°C. have been determined for over 50 compounds, including nearly 30 hydrocarbons. The effects of substitution, unsaturation, and ring strain in the transfer agent molecule on the reactivity of its C—H bonds in chain-transfer reactions with a polyethylene growing chain are analyzed. Qualitatively, these trends parallel those found for simple radicals attacking simple molecules. However, the principle that the reactivity of a compound is the sum of the reactivities of all reactive bonds, which is well established for simple radicals and transfer agents, is found not to be true in ethylene polymerization. It is postulated that the deviations from this principle are due to steric factors which become very important when the free radical is bulky. The transfer constants measured in ethylene polymerization are also compared with transfer constants in other systems. A strong correlation is found between the transfer constants in ethylene and published data on rates of abstraction of hydrogen atoms by methyl radicals.

INTRODUCTION

The literature on polyethylene contains a number of patent references to polyethylene regulators or modifiers whose major function is that of chain transfer. Yet, a search of the nonpatent literature for details of the behavior and function of these materials uncovers surprisingly few references. In one study, carried out in benzene solution at 83°C. under an ethylene pressure which was probably in the neighborhood of 50–150 atm., the chain-transfer constants for ethylene and benzene were determined.¹ In a later, but similar, study conducted at 70°C. under an ethylene pressure of 100 atm., the chain-transfer constants of ethylene, benzene, and heptane were determined.² Very recently, Hill and Doak³ have cited unpublished work of Little and co-workers in which the transfer constants for a series of compounds were determined in benzene solution at 70°C. under an ethylene pressure of 340 atm.⁴

Hill and Doak³ have recently reviewed chain transfer in bulk polymerization at high pressures and temperatures, which is the area of most commercial and patent interest, and compiled a number of chain-transfer constants. These authors have done an excellent job of extracting numerical values from the meager data available to them. However, the inadequacy of the data imposes three serious limitations on the usefulness of their compilation. First, for more than half of the values they report, the temperature was ill defined. Second, many of the values could only be approximated from the

TABLE I
Chain Transfer Data for Homogeneous Reaction

Transfer agent	C_s	Feed composition ^a				Reaction system	Melt index ^b
		Ethylene, mole-%	Propane, mole-%	Transfer agent, mole-%			
Ethylene (Base point)	0.00000 ± 0.00003 ^c	85.42	14.43		1	0.162	
"		"	"		1	0.131	
"		"	"		2	0.410	
"		"	"		2	0.553	
"		"	"		2	0.502	
Tetramethylsilane	0.0000	84.32	"	0.59	1	<0.1	
"		"	"	1.10	1	<0.1	
Cyclopropane	0.0000	74.26	18.86	6.72	1	0.134	
"		"	"	"	1	1.76	
Sulfur hexafluoride	0.0000	83.24	14.43	2.17	2	0.219	
"		83.12	"	2.30	2	0.476	
Methane	0.0000 ± 0.0002 ^d	82.03	14.37	3.47	2	0.775	
<i>tert</i> -Butanol	0.0002 ± 0.0005	81.97	14.43	3.47	2	0.635	
Perfluoropropane	0.0004 ± 0.0007	83.44	"	1.98	2	0.684	
"		82.79	14.16	2.89	2	0.626	
Deuteriobenzene	0.0005 ± 0.0003	80.25	14.43	5.30	2	1.22	
"		"	"	"	2	1.21	
Ethane	0.0006 ± 0.0005	78.37	"	7.05	1	0.324	
"		78.13	"	7.29	1	1.32	
Ethylene oxide	0.0007 ± 0.0001	79.08	"	6.36	2	1.07	
"		71.96	"	13.48	2	6.36	

2,2-Dimethylpropane		83.13	"	2.29	1	0.370
		82.18	"	3.23	1	0.655
		81.46	"	3.95	1	0.410
		"	"	"	1	0.800
Benzene		79.93	"	5.49	1	0.474
		77.94	"	7.48	1	0.895
		77.60	"	7.98	2	3.07
		"	"	"	2	2.75
Dimethyl sulfoxide		84.42	"	1.00	2	0.670
		80.44	"	4.98	2	1.35
		"	"	"	2	4.51
		84.38	"	1.17	1	0.244
Methanol		83.21	"	2.34	1	0.383
		"	"	"	1	0.658
		82.04	"	3.51	1	0.572
		80.87	"	4.68	1	1.54
Propane		86.86	12.98		1	0.040
		83.12	16.72		1	1.09
		82.80	17.05		1	0.625
		81.68	18.17		1	1.34
		79.78	20.06		1	4.08
		78.47	21.37		1	6.19
		75.85	23.99		1	12.2
		87.02	12.82		2	0.111
		82.74	17.10		2	3.75
		"	"		2	3.87
	"	"		2	1.70	
	"	"		2	2.37	
	79.65	20.20		2	6.08	
	79.16	20.68		2	11.3	
	77.03	22.82		2	22.6	

(continued)

TABLE I (continued)

Transfer agent	C_s	Feed composition ^a				Reaction system	Melt index ^b
		Ethylene, mole-%	Propane, mole-%	Transfer agent, mole-%			
<i>n</i> -Butane	0.004 ± 0.001	82.46	14.43	2.96	1	2.70	
		80.71	"	4.70	1	0.523	
Isobutane	0.005 ± 0.001	79.09	"	6.32	1	14.7	
		77.23	"	8.19	1	25.1	
		83.92	"	1.50	1	0.745	
		83.87	"	1.54	1	0.178	
		83.03	"	2.39	1	1.36	
		82.42	"	3.00	1	22.7	
2,2,4-Trimethylpentane	0.0064 ± 0.0015	82.38	"	3.04	1	0.417	
		81.04	"	4.38	1	8.75	
		77.55	"	7.86	1	39.7	
		84.11	"	1.44	1	0.557	
		83.55	"	2.00	1	0.775	
		"	"	"	1	1.55	
		"	"	"	1	3.22	
		"	"	"	1	1.85	
		83.28	"	2.16	2	4.30	
		"	"	"	2	4.93	
<i>n</i> -Hexane	0.0068 ± 0.0008	83.20	"	2.22	1	2.07	
		"	"	"	1	2.86	
Ethanol	0.0069 ± 0.0009	85.23	"	0.32	1	0.193	
		85.01	14.32	0.64	1	0.350	
<i>n</i> -Heptane	0.008 ± 0.002	84.58	14.43	0.97	1	0.730	
		84.26	"	1.29	1	1.01	

Cyclohexane	0.008 ± 0.001	85.11	14.43	0.47	1	0.295
		84.73	14.37	0.87	1	0.577
Methylcyclohexane		84.68	14.43	0.87	1	0.430
		84.24	"	1.31	1	1.38
		83.76	"	1.79	1	1.46
		83.42	14.37	2.18	1	3.04
		82.15	14.43	3.27	2	21.8
		"	"	"	2	19.0
1,2-Dichloroethane	0.011 ± 0.002	84.26	"	1.29	1	1.64
		"	"	"	1	2.13
Acetonitrile	0.011 ± 0.002	84.55	"	0.89	2	2.61
		"	"	"	2	2.02
<i>n</i> -Decane	0.011 ± 0.001	84.07	"	1.35	2	5.05
		"	"	"	2	4.38
Cyclopentane	0.012 ± 0.001	83.99	"	1.45	2	6.37
		"	"	"	2	6.28
Toluene	0.0127 ± 0.0007	82.91	"	2.50	2	20.7
		"	"	"	2	24.9
<i>n</i> -Tridecane	0.0129 ± 0.0009	83.33	"	2.21	1	10.0
		"	"	"	1	10.8
Isopropanol	0.014 ± 0.002	84.39	14.32	1.16	2	4.32
		84.44	14.27	"	2	4.85
Propylene	0.014 ± 0.002	84.19	14.43	1.23	1	3.48
		"	"	"	1	2.27
Hydrogen	0.015 ± 0.003	84.13	"	1.29	1	3.33
		96.20	0.00	3.64	1	0.144
		96.63	"	3.08	1	"
		95.29	"	4.42	1	"
		94.23	"	5.43	1	"
	0.016 ± 0.001	83.80	14.43	1.64	2	14.0
		83.96	14.27	"	2	13.0

(continued)

TABLE I (continued)

Transfer agent	C_s	Feed composition ^a				Reaction system	Melt index ^b
		Ethylene, mole-%	Propane, mole-%	Transfer agent, mole-%			
Trimethylamine	0.018 ± 0.003	85.44	14.32	0.08	2	0.557	
		85.20	14.11	0.54	2	1.63	
Isobutylene	0.021 ± 0.002	84.47	14.37	1.00	2	9.67	
		84.40	14.43	1.02	2	3.95	
		85.22	"	0.20	2	3.36	
		85.48	14.16	0.20	2	0.651	
Butene-2	0.025 ± 0.001	87.05	10.69	2.11	2	21.7	
		84.84	14.16	0.84	1	4.06	
<i>N,N</i> -Dimethylformamide	0.026 ± 0.002	84.41	14.43	1.01	1	6.20	
		84.56	14.37	0.91	2	11.5	
Tetrahydrofuran	0.0289 ± 0.0008	84.50	14.43	"	2	10.5	
		83.20	14.32	2.32	2	157.	
Acetone	0.029 ± 0.003	"	"	"	2	146.	
		85.23	14.43	0.32	1	0.263	
<i>p</i> -Xylene	0.030 ± 0.002	84.91	"	0.64	1	4.74	
		84.59	"	0.96	1	7.92	
		84.27	"	1.28	1	17.9	
		85.26	"	0.29	1	0.555	
<i>p</i> -Dioxane	0.032 ± 0.003	84.96	"	0.57	1	2.38	
		84.69	"	0.86	1	6.63	
		84.40	"	1.15	1	15.1	
		84.78	"	0.64	1	4.08	
		"	"	"	1	3.92	

Octene-1	0.036 ± 0.002	85.12	"	0.30	1	0.920
		"	"	"	1	1.12
		84.51	"	0.90	1	17.3
Methylene chloride		"	"	"	1	10.6
	0.036 ± 0.005	85.23	"	0.19	1	0.440
		84.86	"	0.56	1	3.81
2-Methylbutene-2	0.047 ± 0.003	84.74	"	0.67	1	12.1
		"	"	"	1	14.6
		84.53	"	0.86	1	18.8
Ethylbenzene	0.048 ± 0.005	84.45	"	"	1	15.6
		84.07	"	1.35	1	131.
		84.84	"	0.58	2	22.2
Cumene	0.048 ± 0.003	"	"	"	2	20.0
	0.05 ± 0.01	85.25	"	0.17	2	2.76
		"	"	"	2	1.35
<i>n</i> -Butyronitrile		"	"	"	2	1.60
	0.052 ± 0.003	84.74	"	0.68	2	26.7
		"	"	"	2	25.0
2-Methylbutene-1	0.053 ± 0.003	84.87	"	0.55	2	14.7
		84.76	"	0.66	2	26.4
		84.62	"	0.80	2	33.3
Butene-1	0.056 ± 0.002	"	"	"	2	28.2
		85.15	"	0.26	2	4.89
	0.060 ± 0.007	85.26	14.32	"	2	4.12
2-Butanone	0.084 ± 0.008	85.19	14.43	0.22	2	5.98
		"	"	"	2	6.50
		85.15	"	0.26	2	18.2
Isobutyronitrile	0.107 ± 0.017	85.26	14.32	"	2	11.7
		85.34	14.43	0.074	2	1.79
	0.12 ± 0.02	85.32	"	0.094	2	2.82
3-Methylbutene-1	0.19 ± 0.03	85.34	"	0.073	2	3.81
		85.40	14.37	"	2	3.09

(continued)

TABLE I (continued)

Transfer agent	C_p	Feed Composition ^a			Reaction system	Melt index ^b
		Ethylene, mole-%	Propane, mole-%	Transfer agent, mole-%		
Chloroform	0.29 ± 0.04	85.39	14.43	0.029	1	0.500
		85.27	"	0.15	1	10.2
		"	"	"	1	36.9
2-Ethylhexene-1	0.33 ± 0.03	85.64	14.05	"	1	35.6
		85.41	14.37	0.062	2	8.73
		85.51	14.27	"	2	5.87
Dimethyl phosphite	0.51 ± 0.04	85.37	14.43	0.051	2	12.7
		"	"	"	2	12.4
		85.40	"	0.012	1	0.580
Carbon tetrachloride	0.98 ± 0.08	85.38	"	0.037	1	13.5
		"	"	"	1	18.8
		"	"	"	1	

^a The balance of the feed, generally less than 0.2%, was benzene used as initiator solvent.

^b Measured as described by Mortimer et al.⁵

^c Calculated from the data of Woodbrey and Ehrlich²⁶ by the endgroup method of Boghetich et al.⁵

^d Calculated from the data in Table II.

^e Instead of using melt index, osmometric molecular weights were used. These were 43,400, 33,500, and 27,700, respectively.

limited data. Third, because of the widely varying reaction conditions under which the transfer constants were determined, and because the present state of understanding does not allow recalculation of these values to a consistent basis, the effects of the structure of the transfer agent on the transfer constant could only be grossly inferred. Thus, there is a real need for more extensive data obtained under well defined conditions.

The purposes of this report are twofold. The first purpose is to make available, for a wide variety of compounds, chain-transfer constants determined at the same set of carefully controlled conditions. Included in the tables are values for those few compounds for which values have been published previously.^{5,6} Some of these values have been recalculated on the basis of additional work. The second purpose is to present a coherent explanation of the behavior of chain-transfer agents in ethylene polymerization.

EXPERIMENTAL

Polymerization Procedure

Polymerizations were conducted in a high-pressure, steel vessel containing a magnetically driven agitator. Pressure and temperature measurements were made as previously described.⁵ The vessel was preheated to 130°C. with circulating hot oil. All gases other than ethylene which were used in the polymerization were distilled under pressure, in oxygen-free conditions, into tared containers which were then weighed and attached to the lines leading to the reactor. The reaction system was evacuated and purged with oxygen-free ethylene. All liquids, including a benzene solution of di-*tert*-butyl peroxide (DTBP), were put into a compartment with hypodermic syringes in such a way as to exclude air. This compartment was close to and attached to the reactor, but was isolated from it sufficiently that it could be maintained at room temperature while the reactor was at 130°C. The gases in the tared containers were then displaced into the reactor with ethylene and the reactor pressure was raised to about 500 atm. At this point, the liquids, including the initiator, were pressured into the reactor with ethylene. The time required to reach the reaction pressure of 1360 atm. after the addition of the initiator averaged about 2 min. The amount of polymerization during start-up was negligible. The DTBP concentration was 2.07×10^{-4} mole/l. in all runs.

Ethylene was added to the reaction as required to keep the pressure constant. The temperature was held constant during the reaction period and throughout the reaction zone by having a low initiator concentration so that the rate of polymerization was low and by having good agitation. Ethylene conversion was held at 10% or below, the run time generally being between 30 and 60 min. Prior testing showed that kinetic steady state was achieved under the conditions of these experiments, and that \bar{M}_n did not change with time below 10% conversion. DTBP depletion was calculated from half-life data to be less than 10% in all runs.⁷

TABLE II
 Methane Runs

Feed composition			$\bar{M}_n \times 10^{-3}$
Ethylene, mole-%	Acetone, mole-%	Methane, mole-%	
98.07	1.93	—	50.5
98.07	1.93	—	52.5
98.07	1.93	—	52.0
90.22	1.93	7.85	52.1
86.27	1.93	11.80	46.3
96.79	3.21	—	34.7
88.94	3.21	7.85	33.3

To terminate the experiment, the vessel was depressured. The polymer, which was completely soluble in hot xylene, was dissolved in xylene, precipitated with cold methanol, and dried in a vacuum oven at 60–80°C. prior to characterization. All data are given in Tables I and II.

Reactants

Initially, all liquids were distilled and stored under either nitrogen or argon until it was shown that this precaution was unnecessary if the liquids were sufficiently pure. All substances with doubtful purity were redistilled before use. A single batch of DTBP was used as received for all of the experiments. In most instances, the gases were Matheson Co. research grade. The propane was Phillips Co. instrument grade, which after deoxygenation by passage over an activated copper catalyst, was found to give the same results as research grade propane.

Reactor Systems

Although the same reactor was used in all experiments, a change in the piping to permit easier operation of the reactor resulted in an unexplained shift in the base condition (see Table I). The first system, 1, gave a slightly lower melt index than the second system, 2. All runs in Table I are identified as being performed in either system 1 or 2 so that they can be compared with the proper base runs. Results with propane, cyclohexane, and ethylbenzene indicated that, within experimental error, the same C_s values were obtained in both systems.

CALCULATION METHODS

Number-average molecular weights were calculated from the melt indexes (MI).⁸ This seemingly dubious way of obtaining \bar{M}_n data was used for the following reasons. First, the \bar{M}_n -MI correlation had essentially the same experimental uncertainty as the osmotic measurements themselves. Second, periodic checks of the correlation by osmometry always agreed with the calculated \bar{M}_n within experimental error. Finally, with

the same overall effort, twice as many data points could be obtained by using this faster method.

In order to be sure that these high-pressure gas-phase reactions were homogeneous, propane was added as a solvent in almost all runs.⁹ Ehrlich has previously demonstrated that the ethylene-propane-polyethylene system is homogeneous at 1360 atm. and 130°C. for the propane concentrations and polymer molecular weights employed in this study.¹⁰ In the absence of a solvent, the reaction system becomes heterogeneous as polymerization proceeds.¹¹ Attempts were made to get meaningful chain-transfer data in the absence of propane, but because of phase separation during the course of these polymerizations these attempts were usually unsuccessful. Data on methane (Table II) were obtained in a heterogeneous reaction and may be somewhat inaccurate for this reason. Data for propylene were obtained both with and without propane present with no apparent difference in the results. Possibly propylene is a good polymer solvent itself.

The feed composition was calculated from the measured amounts of additives, the P - V - T diagram for ethylene,¹² and the known mixing characteristics of ethylene and propane.¹³ The chain-transfer constants were calculated by least squares by using eq. (1) in the form suggested by Mayo,¹⁴ where \overline{DP} is the degree of polymerization, \overline{DP}_0 is the degree of polymerization in the absence of chain-transfer agent, $[S]$ is the concentration of chain-transfer agent, $[M]$ is the ethylene concentration, and C_s is the chain-transfer constant. By using a constant amount of initiator in all runs, the effects of initiation and termination were kept constant, and eq. (1) is valid.

$$(1/\overline{DP}) - (1/\overline{DP}_0) = C_{s1}([S_1]/[M]) + C_{s2}([S_2]/[M]) \quad (1)$$

Some of the substances used in this work, especially the olefins,⁵ retard the polymerization. Such retardation will alter the molecular weight and may lead to incorrect C_s values if a correction in the measured \overline{M}_n is not made. It can be shown that $1/\overline{DP}$ should be corrected by subtracting from the measured value a quantity $k_c[S\cdot]/k_p[M]$, where $[S\cdot]$ is the concentration of radicals derived from the transfer agent, k_c is the rate constant for cross termination between $S\cdot$ and polymer chains, and k_p is the ethylene propagation rate constant. The correction can be calculated if all quantities are known.

Kinetic data are available from which the required values may be at least approximately obtained. The polyethylene termination constant, k_t , has been measured to be about 10^9 l./mole/sec. at one set of conditions.¹ Making reasonable estimates of the activation volumes and energies, one concludes that 10^9 is also a good estimate for k_t at the conditions of this work. If the initiator efficiency is reasonable (0.3-1.0), then k_p can be calculated from the above values and the data of Symcox and Ehrlich¹³ to be about 10^4 l./mole/sec. On making the reasonable assumption that $k_t < k_c < 100 k_t$ and assuming steady-state conditions, $[S\cdot]$, and therefore

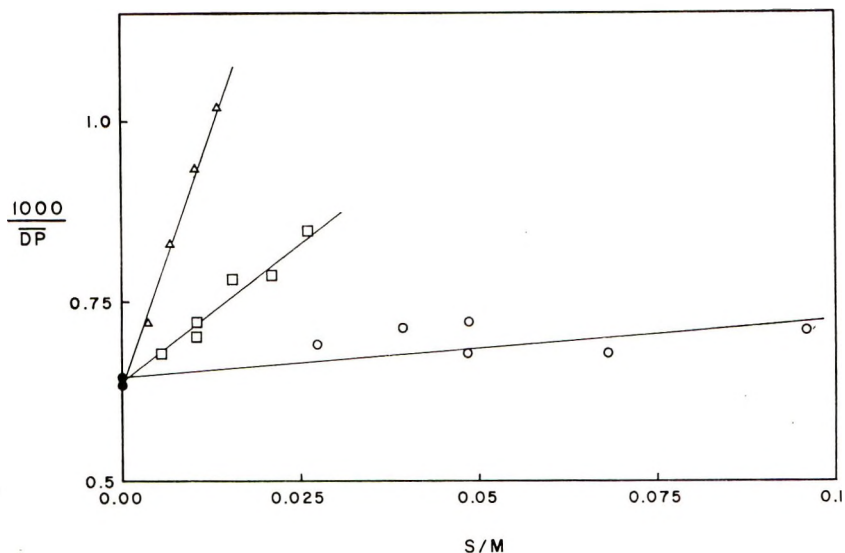


Fig. 1. Mayo-type plots of chain transfer activity at 1360 atm. and 130°C. for three representative compounds: (O) 2,2-dimethylpropane; (□) cyclohexane; (Δ) *p*-xylene; (●) base points.

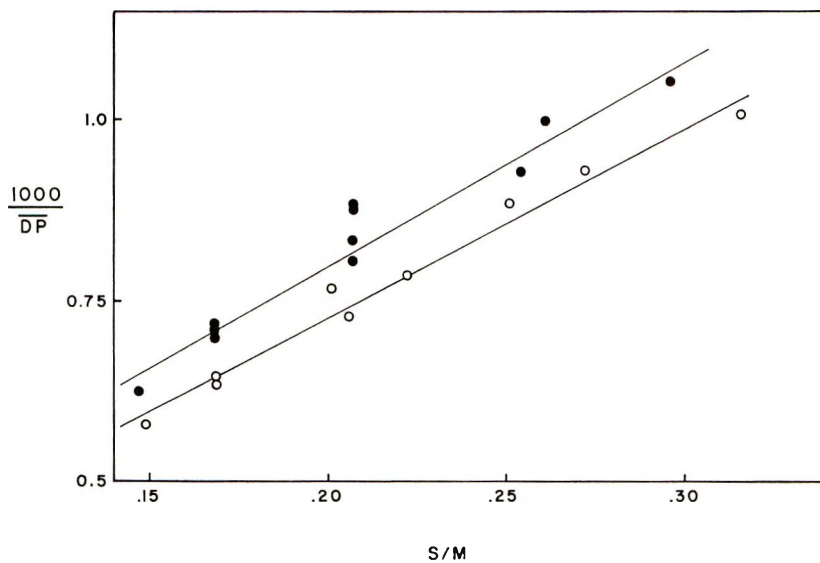


Fig. 2. Mayo-type plots of chain-transfer activity for propane at 1360 atm. and 130°C. in both reactor systems: (O) system 1; (●) system 2.

the correction, can be calculated for various values of k_c . When this is done, it is found that, within the limits and under the assumptions given above, the correction is of the order of 1% of the measured $1/\overline{DP}$ value when the polymerization rate is reduced to 50% of its unretarded value. Therefore, no correction for retardation was made, inasmuch as the lowest rate encountered in any of the runs was 30% of normal. It should be

pointed out that the startling insensitivity of \overline{DP} to retardation is a result of the high values of k_p and k_t for ethylene.

In most of the experiments, a constant weight of propane was used. This practice resulted in some variation of the $[S]/[M]$ ratio for propane. All results were corrected to a constant ratio for propane by using eq. (1) and the experimentally determined C_s value for propane. The data plotted in Figure 1 are so corrected.

The standard deviations reported in Table I were calculated in two ways. One way was to obtain them in the usual manner from the few data points being plotted for each C_s , as was done in the previously reported work.^{5,6} The other way was to use the relationships (2) and (3)¹⁵ for duplicate experiments, where $X = [S]/[M]$ and $Y = 1/\overline{DP}$ as calculated from the melt index.

$$\sum_{a=1}^{a=\mu} (Y_{1a} - Y_{2a})^2/2 = \mu\sigma_y^2 \quad (2)$$

$$\sigma_{C_s}^2 = \frac{\sigma_y^2}{\Sigma X^2 - (\Sigma X)^2/N} \quad (3)$$

From 47 pairs of duplicate runs ($\mu = 47$), σ_y was calculated to be $\left(\begin{smallmatrix} 2.4 & + & 0.6 \\ & & 0.3 \end{smallmatrix} \right) \times 10^{-5}$, which represents the standard deviation of reproducing a melt index value from a duplicate run. This method of obtaining standard deviations for C_s probably gives a truer approximation than the usual method. However, in Table I, the reported deviation is the larger of the values obtained by the two methods.

It should be mentioned that initially runs were made with several concentrations of transfer agent (as shown in Figs. 1 and 2). It was thus established that the linear relationship predicted from eq. (1) was indeed found. Once eq. (1) was validated, it was wasteful experimentally to continue to get points along the line, since a straight line is fixed by two points. Since the effect of random errors is minimized the further apart the points are spread, it became our practice to use the base runs of Table I as one point to fix the C_s line and usually a pair of runs which gave a reasonably high MI as the other point at the opposite extremity of the line. This practice generated the data necessary for use of eqs. (2) and (3) and also suggested their use. Where the original guess of the concentration of transfer agent to use proved to be low, that run was also included in the calculations. Some such instances can be seen in Table I.

Perhaps it should also be pointed out that all calculations, beginning with the calculation of the reaction feed concentrations from the reactor charging conditions, were done on a digital computer with a series of programs which took their input data directly from the previous program. Table I presents the rounded data obtained as output from the programs. Recalculation of the transfer constants from the rounded data may, in some instances, lead to minor differences due to rounding errors that were absent in the original calculation.

As the chain-transfer constant of a chain-transfer agent became very small it became necessary to add increasingly large amounts of the transfer agent to the reaction in order to see any effect. Quite often this procedure resulted in experimental difficulties in actually running the polymerization and in making sure that the reaction mixture remained homogeneous during the period of polymerization. Some errors in calculating feed composition could also creep in under these circumstances. Hence, for some compounds listed in the tables, a chain-transfer constant of zero is listed without a standard deviation, it being felt that the experimental difficulties did not justify assigning a standard deviation to the value in the usual way. It should be understood that the last significant zero is the best estimate that can be made, but that it contains an unknown error.

DISCUSSION

A cursory examination of the C_s values in Table I immediately discloses that chain-transfer constants are higher for these compounds in ethylene polymerization than in almost any other polymerization system.^{3,16} Therefore, the chain-transfer reaction is more important in ethylene polymerization than it is in the polymerization of almost all other monomers. If one examines the chain-transfer constants for the series ethane, propane, and isobutane, or propylene, butene-1, and 3-methylbutene-1, one sees immediately that tertiary hydrogens are more reactive (i.e., more easily abstracted) than secondary, which in turn are more reactive than primary. Furthermore, hydrogen atoms alpha to unsaturation are much more reactive than their saturated counterparts. It has previously been shown that olefins and alkyl benzenes undergo chain transfer at the α position.⁵ These trends are expected.

From classical studies of the reactions of small free radicals, such as halogen atoms,¹⁷ methyl radicals,¹⁸ phenyl radicals,¹⁹ and *tert*-butoxy radicals²⁰ with various alkanes, the view has become established that all primary hydrogen atoms are essentially alike, all secondary hydrogen atoms are also alike, and all tertiary hydrogen atoms are alike in their reactivity towards free radicals. From this point of view, we would expect an *n*-alkane with twice as many secondary hydrogen atoms to have approximately twice the chain-transfer activity of the smaller hydrocarbon. In hydrogen abstraction reactions of phenyl radicals, for example, this has been extensively demonstrated.¹⁹

Therefore, it is quite striking and remarkable that this is not seen in the chain-transfer constants with polyethylene. If one were to calculate an average reactivity per secondary hydrogen atom for a series of normal alkanes running from propane through tridecane, one would see that the average reactivity per hydrogen atom decreases continuously as the molecular weight of the chain-transfer agent increases. The same trend is seen among the α -olefins where, for example, octene-1 actually has a lower chain-transfer constant than butene-1, although both contain the same number of alkyl-type hydrogen atoms and octene contains many more alkyl-type secondary hydrogen atoms.

Although, to the author's knowledge such a gross departure from the expected pattern of reactivity of C—H bonds has not been reported heretofore, there is some precedent for the departure in hydrogen abstraction reactions of simple radicals with certain hydrocarbons. For example, both phenyl¹⁹ and *tert*-butoxy²¹ radicals show an abnormally low rate of hydrogen abstraction from certain tertiary carbon atoms where approach of the radical to the site is hindered by bulky surrounding groups or by the conformation of the molecule. Perhaps more analogous to the present work is the finding that the radical resulting from radical addition to the double bond of 2,4,4-trimethylpentene-1 reacts abnormally slowly with mercaptans, suggesting that a bulky radical attacks chain-transfer agents with difficulty.²²

In order to explain the chain-transfer constants obtained in this work, it is postulated that the growing polyethylene chain is a very bulky radical and that steric factors are very important in understanding its reactions. This postulate asserts that even the customary zigzag conformation of *n*-alkanes will present some steric hindrance to the approach of the polyethylene radical to certain of the hydrogen atoms, and that as the size of the chain-transfer agent increases, more of the hydrogen atoms are shielded from the bulky attacking free radical.

This postulate of steric hindrance can also be invoked to explain why cumene is less reactive than 3-methyl butene-1. It has previously been pointed out that a phenyl and a vinyl group should exert the same activating influence on α -hydrogen atoms,⁵ and indeed the pair propylene and toluene have essentially the same C_s value, as do the pair butene-1 and ethylbenzene. To explain the lack of expected reactivity of cumene, it is postulated that two methyl groups and a phenyl group hinder the approach of the growing chain.

The same type of reasoning can be used to explain why cyclopentane which has ten secondary hydrogen atoms, is considerably more reactive than cyclohexane, which has twelve. The concept of *I*-strain has been invoked to explain the increased reactivity of five-membered rings in reactions where the reactive center is transferred to the ring.²³ However, the increase in reactivity per hydrogen atom in cyclopentane is sufficient only to offset the statistical effect of a greater number of hydrogen atoms in cyclohexane, and both compounds show essentially the same reactivity with chlorine atoms¹⁷ or with phenyl radicals.¹⁹ With polyethylene, then, an additional explanation is necessary. If the normal zigzag conformation of a hydrocarbon chain presents some steric hindrance to chain transfer, then cyclohexane, which has this conformation, should be expected to show reduced reactivity. In cyclopentane, however, the hydrogen atoms are held out away from an almost planar ring and therefore are probably in a position of maximum availability to a bulky attacking radical. The combination of *I*-strain and steric hindrance can account for the observed C_s values.

It is certainly well established that the known reactivity of individual carbon-hydrogen bonds can be summed to obtain the overall reactivity

of a compound with small radicals.¹⁹ The assertion that the same can be done in polymeric systems²⁴ would now seem to require reexamination. As noted previously, the presence of small but detectible steric hindrance with the phenyl and *tert*-butoxy radicals is established. The results discussed above show clearly that with a polyethylene radical, the steric effects are no longer small.

In smaller rings, particularly in the three-membered ring, another effect shows itself. The hydrogen atoms on cyclopropane are strikingly inert. In cyclopropane the normal sp^3 carbon orbitals are severely distorted in order to form the ring, and those bonds which form the ring acquire more p character than sp^3 would predict. Conversely, the carbon-hydrogen bonds acquire more s character than normal. This increased s character in the carbon-hydrogen bond gives a stronger bond and therefore one which is less easily broken by an attacking radical. This effect of ring strain has been pointed out before,²³ and an unusually high energy of activation for hydrogen abstraction has been estimated for cyclopropane.²⁵ The apparent absence of chain transfer to cyclopropane is interesting in the degree to which the effect of ring strain is manifested.

Chain transfer to monomer, a familiar reaction in other monomer systems, is strikingly small with ethylene. The value in Table I was calculated from the vinyl data of Woodbrey and Ehrlich²⁶ assuming all vinyl endgroups to be the result of chain transfer. Even at 250°C., the C_s value for ethylene is only 0.00007 ± 0.00002 , for the same assumption. Since disproportionation termination will also give rise to vinyl groups, the actual extent of chain transfer is unknown but cannot be greater than this.

Among nonhydrocarbons we see many familiar trends. Carbon-oxygen single bonds, carbon-nitrogen single bonds, and carbon-halogen bonds activate the hydrogen atoms attached to the same carbon atom as the hetero atom. Carbon-oxygen double bonds and carbon-nitrogen triple bonds are like carbon-carbon double bonds, in that they activate the hydrogen atoms alpha to the functional group. Table I contains a series of alcohols, nitriles, and ketones in which primary, secondary, and tertiary hydrogen atoms are found. For each series, it is again seen that tertiary hydrogen atoms are more reactive than secondary, which in turn are more reactive than primary. From the data on chlorinated hydrocarbons, another expected trend is seen: increasing chlorine substitution leads to increased chain-transfer activity. It is interesting to note that silicon-carbon bonds and sulfoxide-carbon bonds have no detectible activating influence on adjacent hydrogen atoms; perhaps they even have a slight deactivating influence.

A few comments on some specific compounds might be appropriate. If one compares the chain-transfer activity of trimethylamine with that of dimethylamine, the conclusion that the nitrogen-hydrogen bond is quite reactive in chain-transfer reactions seems reasonable. By contrast, the oxygen-hydrogen bond of alcohols is unreactive.²⁷ The effect of ring strain in small-ring compounds is seen again in the low chain-transfer activity of

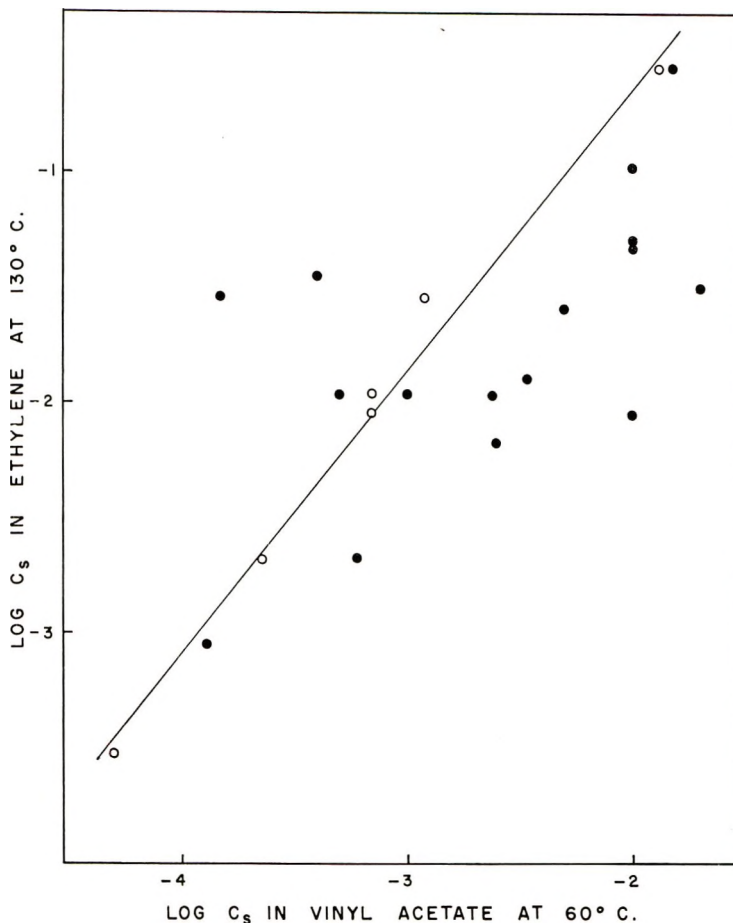


Fig. 3. C_s in vinyl acetate at 60°C. vs. C_s in ethylene at 130°C.: (O) data of Henrici-Olivé and Olivé;¹⁶ (●) data of Clarke et al.³³ The line is drawn through the open circles.

ethylene oxide which, except for the ring strain, would be expected to have about one-half the chain transfer activity of *p*-dioxane. It is also noteworthy that tetrahydrofuran, with a five-membered ring and only four hydrogens activated by an ether linkage, is about as reactive as *p*-dioxane, which has a six-membered ring and twice as many hydrogen atoms activated by ether linkages. Thus, both the effect of ring size and the steric considerations seem to hold not only for hydrocarbons but for all compounds which we have studied. This is understandable, since the bulky group which provides most of the steric hindrance is the polymer radical.

A comparison of the chain-transfer constants given here with related literature is in order. Values for C_s in ethylene polymerization or telomerization have appeared for carbon tetrachloride,^{4,28-30} cyclohexane,³¹ heptane,² benzene, ethylene,^{1,2} and other substances,⁴ all at lower pressures

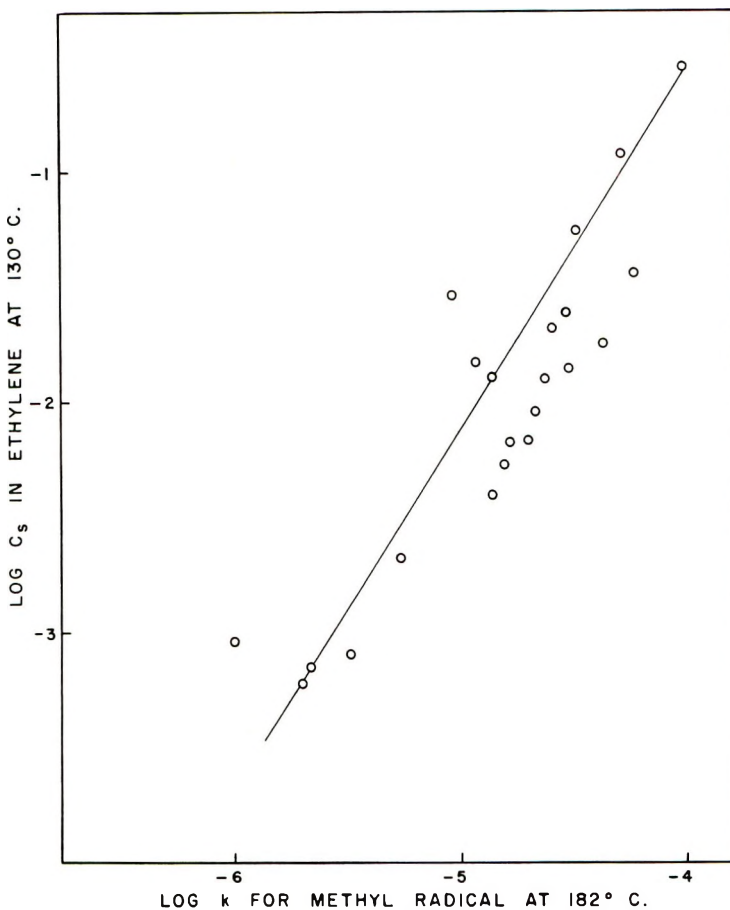


Fig. 4. C_s in ethylene at 130°C. vs. k for methyl radicals at 182°C. The k values are from Trotman-Dickenson,¹⁹ with the arithmetic average being used where more than one value is given.

than were used in this study. Although there is considerable scatter where several values are available, as for carbon tetrachloride, the previously published values are all higher than reported here.

The fact that C_s values are lower at the higher pressures used in this study is consistent with what is presently known of ethylene polymerization. The volume of activation of the propagation step has been determined to be -23 cc./mole,¹³ whereas -10 cc./mole would be an average value for the activation volume for chain-transfer reactions.³² Thus, C_s should be decreased as pressure increases. Possibly some of the scatter in the previously reported values is the result of pressure differences. Qualitatively at least, the C_s values given here are consistent with earlier work at lower pressures.

It is natural to compare the present C_s values with those obtained in vinyl acetate polymerization inasmuch as both monomers have much in common.

Figure 3 shows the correlation obtained when the present C_s values are plotted against published values for the same compounds in vinyl acetate. There is an excellent correlation between the present data and those C_s values which met the Olivé's critical standards,¹⁶ but a poor correlation with the more extensive data of Clarke, Howard, and Stockmayer.³³ It is not entirely clear why the data of the latter authors do not correlate.

Since the polyethylene growing chain is a hydrocarbon radical, it is also instructive to compare our results with gas-phase data for another hydrocarbon radical. Figure 4 presents a comparison of our C_s values with published data on rates of methyl radical abstraction of hydrogen atoms from a wide variety of compounds including aliphatic, olefinic, and aromatic hydrocarbons, chlorinated hydrocarbons, amines, alcohols, an ether, and a ketone.¹⁸ There is a strong correlation between the two sets of data, as would be expected.

The author gratefully acknowledges the laboratory assistance of L. C. Arnold, assistance with the statistical aspects of the calculations by P. W. Tidwell, helpful discussions of R. A. Mendelson, and number-average molecular weights by F. L. Finger.

References

1. Iaita, Z., and Z. Machacek, *J. Polymer Sci.*, **38**, 459 (1959).
2. Lyubetskiĭ, S. G., B. A. Dolgoplosk, and B. L. Erusalimskiĭ, *Vysokomolekul. Soedin.*, **3**, 734 (1961).
3. Hill, A., and K. W. Doak in *Crystalline Olefin Polymers*, Part 1, R. Raff and K. W. Doak, eds., Interscience, New York, 1964, pp. 285-291.
4. Little, J. R., L. W. Hartzel, F. O. Gunther, and F. R. Mayo, unpublished work, U. S. Rubber Co., cited in ref. 3.
5. Boghetich, L., G. A. Mortimer, and G. W. Daues, *J. Polymer Sci.*, **61**, 3 (1962).
6. Mortimer, G. A., and L. C. Arnold, *J. Am. Chem. Soc.*, **84**, 4986 (1962).
7. Steacie, E. W. R., *Atomic and Free Radical Reactions*, ACS Monograph No. 125, 2nd Ed., Reinhold, New York, 1954, Vol. I, pp. 234-236.
8. Mortimer, G. A., G. W. Daues, and W. F. Hamner, *J. Appl. Polymer Sci.*, **8**, 839 (1964).
9. Ehrlich, P., and E. B. Graham, *J. Polymer Sci.*, **45**, 246 (1960).
10. Ehrlich, P., private communication of unpublished experiments performed at the Springfield, Mass. laboratories of the Monsanto Co.
11. Ehrlich, P., *J. Polymer Sci. A*, **3**, 131 (1965).
12. Benzler, H., and A. V. Koch, *Chem. Ing. Tech.*, **27**, 71 (1955).
13. Symcox, R. O., and P. Ehrlich, *J. Am. Chem. Soc.*, **84**, 531 (1962).
14. Mayo, F. R., *J. Am. Chem. Soc.*, **65**, 2324 (1943).
15. Davies, O. L., *Statistical Methods in Research and Production*, Oliver and Boyd, London, 1957, p. 160.
16. Henrici-Olivé, G., and S. Olivé, *Fortschr. Hochpolymer.-Forsch.*, **2**, 496 (1961).
17. Russell, G. A., *J. Am. Chem. Soc.*, **80**, 4987, 4997 (1958).
18. Trotman-Dickenson, A. F., *Quart. Rev.* (London), **7**, 198 (1953).
19. Bridger, R. F., and G. A. Russell, *J. Am. Chem. Soc.*, **85**, 3754 (1963).
20. Walling, C., and W. Thaler, *J. Am. Chem. Soc.*, **83**, 3877 (1961).
21. Brook, J. T. H., *Trans. Faraday Soc.*, **53**, 327 (1957).
22. Huyser, E. S., and J. D. Taliaferro, *J. Org. Chem.*, **28**, 1676 (1963).
23. Brown, H. C., R. S. Fletcher, and R. B. Johannesen, *J. Am. Chem. Soc.*, **73**, 212 (1951).
24. Lazar, M., and J. Pavlinec, *Chem. Zvesti*, **15**, 428 (1961).

25. Gordon, A. S., and S. R. Smith, *J. Phys. Chem.*, **66**, 521 (1962).
26. Woodbrey, J. C., and P. Ehrlich, *J. Am. Chem. Soc.*, **85**, 1580 (1963).
27. Morton, M., J. A. Cala, and L. Piirma, *J. Am. Chem. Soc.*, **72**, 2213 (1950).
28. Karapetyan, Sh. A., B. A. Englin, and R. Kh. Freidlina, *Izv. Akad. Nauk SSSR, Ser. Khim.*, **1963**, 1346.
29. David, C., and P. A. Gosselain, *Tetrahedron*, **18**, 639 (1962).
30. Jaacks, V., and F. R. Mayo, *J. Am. Chem. Soc.*, **87**, 3371 (1965).
31. Huggett, C., T. R. Walton, and C. R. Midkiff, Jr., paper presented at 146th Meeting, American Chemical Society, Denver, January 1964; *Polymer Preprints*, **5**, No. 1, 106 (1964).
32. Walling, C., *J. Polymer Sci.*, **48**, 335 (1960).
33. Clarke, J. T., R. O. Howard, and W. H. Stockmayer, *Makromol. Chem.*, **44-46**, 427 (1961).

Résumé

Les constantes de transfert de chaînes dans la polymérisation radicalaire homogène de l'éthylène à 1360 atm. et 130°C, ont été déterminées à l'égard de 50 composés qui comportent environ 30 hydrocarbures. Les effets de la substitution, de l'insaturation et de la tension cyclique dans la molécule de l'agent de transfert sur la réactivité de sa liaison C—H au cours de réactions de transfert de chaînes avec une chaîne croissante de polyéthylène sont discutés. Qualitativement, les tendances sont semblables à celles trouvées pour des radicaux simples attaquant des molécules simples. Toutefois, le principe suivant lequel la réactivité d'un composé est la somme des réactivités de toutes les liaisons réactionnelles, principe que est bien établi pour les radicaux simples et les agents de transfert, n'est pas valable dans la polymérisation de l'éthylène. On admet que les déviations à l'égard de ce principe sont dues à des effets stériques qui deviennent très importants lorsque le radical libre est volumineux. Les constantes de transfert mesurées dans la polymérisation ont été ainsi comparées avec les constantes dans d'autres systèmes. Une corrélation intime a été trouvée entre les constantes de transfert de l'éthylène et les données publiées sur les vitesses d'arrachement d'atomes d'hydrogène au départ de radicaux méthyles.

Zusammenfassung

Kettenübertragungskonstanten bei der homogenen radikalischen Polymerisation von Äthylen bei 1360 atm und 130°C wurden für mehr als 50 Verbindungen, darunter nahezu 30 Kohlenwasserstoffe, bestimmt. Der Einfluss der Substitution, des ungesättigten Charakters und der Ringspannung im Überträgermolekül auf die Reaktivität seiner C—H—Bindungen bei Übertragungsreaktionen mit einer wachsenden Polyäthylenkette wird analysiert. Qualitativ sind die Verhältnisse ähnlich wie beim Angriff einfacher Radikale auf einfache Moleküle. Jedoch erweist sich das bei einfachen Radikalen und Überträgern gut begründete Prinzip, dass die Reaktivität einer Verbindung der Summe der Reaktivitäten aller reaktiven Bindungen gleich ist, bei der Äthylenpolymerisation nicht als richtig. Es wird angenommen, dass die Abweichungen von diesem Prinzip durch sterische Faktoren bedingt sind, welche bei einem freien Radikal mit grosser Raumbeanspruchung sehr wichtig werden. Die bei der Äthylenpolymerisation bemessenen Übertragungskonstanten werden mit Übertragungskonstanten in anderen Systemen verglichen. Es besteht eine gute Korrelation zwischen de Übertragungskonstanten bei Äthylen und veröffentlichten Daten über die Geschwindigkeit der Wasserstoffatomabstraktion durch Methylradikale.

Received June 25, 1965

Revised September 21, 1965

Prod. No. 4896A

Studies on Some Radical Transfer Reactions. Part I. Hydrogen Atom Abstraction from Some Organic Substrates by $\dot{\text{O}}\text{H}$ Radicals

BHAIRAB CHANDRA MITRA, SUBHASH CHANDER CHADHA,
PREMAMOY GHOSH,* and SANTI R. PALIT, *Indian Association for
the Cultivation of Science, Jadavpur, Calcutta, India*

Synopsis

Polymerization of methyl methacrylate was carried out in aqueous and nonaqueous media in the presence of some sulfonated and carboxylic organic compounds, hydroxyl radicals generated from hydrogen peroxide being used as initiators of polymerization. The occurrence of radical transfer reactions by way of hydrogen atom abstraction from the organic substrates by the $\dot{\text{O}}\text{H}$ radicals was demonstrated by the detection of sulfonate and carboxyl endgroups in the respective polymers. It was found that the radical transfer reactions were more favored in aqueous media than in nonaqueous systems.

INTRODUCTION

The oxidizing reactions of hydrogen peroxide are considered to take place primarily through the agency of hydroxyl ($\dot{\text{O}}\text{H}$) radicals, and oxidation of organic substrates often yields hydroxylated products preceded by the intermediate formation of substrate radicals, probably by hydrogen atom abstraction from the substrate molecules by the $\dot{\text{O}}\text{H}$ radicals in the medium. It is mostly difficult to detect and characterize the short-lived substrate radical intermediates generated by the above probable radical-transfer mechanism. Some polymerization experiments have been carried out with hydrogen peroxide as the initiator in the presence of some organic (sulfonated and carboxylic) compounds, and endgroups incorporated in the polymers have been investigated in order to get an idea about the occurrence of such radical-transfer reactions, since a radical derived from the organic substrate may participate in the polymerization process and thereby appear as an endgroup in the resultant polymer.

EXPERIMENTAL

The monomer used was methyl methacrylate (MMA). It was purified by the usual procedures.¹ Polymerization of MMA was carried out with hydrogen peroxide as the initiator in the presence of a number of organic

* Present address: Department of Applied Chemistry, University College of Science and Technology, Calcutta, India.

(sulfonated or carboxylic) substrates. Polymerization was generally carried out in aqueous medium with water-soluble substrates, and, in case they were soluble in MMA or in a suitable organic solvent, polymerization was also carried out in nonaqueous systems. The initiating OH radicals were generated by the photolysis of H_2O_2 ultraviolet light or by the redox reaction between Fe^{2+} and H_2O_2 in the dark.

PMMA samples prepared in aqueous or nonaqueous media were isolated, washed, and dried and then purified by the method of repeated precipitation.¹ The purified polymers are then tested for endgroups present in them by the application of dye techniques.² Hydroxyl endgroups normally present (H_2O_2 being the initiator) are as such not responsive to the dye tests, and hence any response to the dye tests given by the purified polymer is indicative of the presence of sulfonate ($-\text{SO}_3^-$) or carboxyl ($-\text{COO}^-$) endgroups in the appropriate polymers. The general methods for the analysis of carboxyl,¹ sulfonate,³ chloride,⁴ and hydroxyl⁵ endgroups have been reported earlier.

RESULTS AND DISCUSSION

In presence of low concentrations of the sulfonated substrates used herein, the induction period in polymerization and also the rate of polymerization remained more or less unchanged when compared with a blank polymerization experiment in absence of the substrate.

In presence of the carboxylic substrates at low concentrations, however, the induction period in MMA polymerization was generally found to be higher, and the rate of polymerization was slower, the effect being predominant in aqueous media but only very slight in nonaqueous systems.

Polymerization in Presence of Sulfonated Substrates

All the polymer samples prepared in presence of the sulfonated substrates with the use of H_2O_2 as the initiator give positive response for sulfonate endgroups (Table I). The incorporation of sulfonate endgroups in the polymers is indicative of the generation of sulfonate-bearing radicals in the medium, presumably by way of hydrogen-abstraction reactions involving OH radicals (derived from H_2O_2) and the sulfonated substrates, e.g.,



In view of the rate of polymerization being almost unaffected in presence of the sulfonated substrates, decomposition of H_2O_2 by reduction activation with the sulfonated substrates is precluded. At very low concentration of the sulfonated substrates (0.005–0.05M) in the aqueous medium, appreciable incorporation of sulfonate endgroups (0.2–0.7 per chain) has been observed, but in nonaqueous systems, use of relatively higher concentrations of the substrate (*p*-toluene-sulfonic acid) results in polymers of very low sulfonate endgroup content (0.03–0.1 per chain), H_2O_2 being the initi-

TABLE I
 Radical-Transfer Reaction Involving OH radicals and Sulfonated Substrates Demonstrated by Endgroup Analysis

Initiator	Initiator concentration, mole/l.	Organic substrate	Substrate concentration, mole/l.	Polymerization medium	Sulfonate endgroups per chain
H ₂ O ₂	0.03-0.06	C ₈ H ₈ SO ₃ Na	0.014-0.056	Aqueous	0.10-0.35
H ₂ O ₂	"	CH ₃ C ₆ H ₄ SO ₃ Na	0.005-0.05	"	0.25-0.68
Fe ⁺⁺	0.0025	CH ₃ C ₆ H ₄ SO ₃ Na	0.005-0.05	"	0.43-0.80
H ₂ O ₂	0.01				
H ₂ O ₂	0.07	CH ₃ C ₆ H ₄ SO ₃ H	0.062-0.250	Nonaqueous	0.03-0.08
AIBN	0.003	CH ₃ C ₆ H ₄ SO ₃ H	0.062-0.250	"	Negligible

ator in all cases. When H_2O_2 is replaced by AIBN as the initiator in the nonaqueous system, practically no sulfonate endgroup is detectable in the polymer. These observations preclude the possibility of sulfonate endgroup incorporation to measurable extents by transfer reaction involving a growing polymer chain and the sulfonated compound. They also indicate that the radical-transfer reaction involving the sulfonated substrates is favorable with $\dot{O}H$ radicals but not with radicals derived from AIBN and that the reaction with $\dot{O}H$ radicals is favored in aqueous systems and only goes to a very small extent in nonaqueous media. From the results of endgroup analysis it is also apparent that $\dot{O}H$ radicals react faster with *p*-toluene sulfonate than with benzene sulfonate since, in otherwise similar conditions in aqueous media, higher sulfonate incorporation is observed in polymers obtained in the presence of the toluene sulfonate. This is presumably due to hydrogen abstraction from the methyl group of the toluene sulfonate by $\dot{O}H$ radicals being more favored.

Polymerization in Presence of Carboxylic Substrates

All the polymers prepared by H_2O_2 initiation in presence of different carboxylic substrates, give in general positive response for carboxyl endgroups, faint or moderate, depending on the nature and concentration of the substrates. The prolongation of induction period and the progress of polymerization thereafter could be easily observed in aqueous polymerization, as the polymer was obtained in a separated phase. The retardation of polymerization was most prominent in the presence of acetic acid.

The presence of carboxylic endgroups (although the test is faint) in polymers obtained in presence of acetic acid or potassium acetate indicates the formation of $\dot{C}H_2COO^-$ radicals, at least in part by way of the hydrogen abstraction reaction under consideration, although the radical $CH_3CO\dot{O}$ may also possibly be formed in the medium by transfer of an electron from the anion CH_3COO^- to an $\dot{O}H$ radical. The formation of a $\dot{C}H_2COO^-$ radical, however, gets support from the suggested mechanism of Baxendale et al.⁶ With chloroacetic acid as the substrate, the resulting polymers are found to bear both chlorine atoms and carboxyl endgroups, the radical derived thus appears to be $Cl\dot{C}HCOO^-$. The test for carboxyl endgroups is relatively more intense with chloroacetic and phenylacetic acids than with acetic acid.

Higher amounts of carboxyl endgroups are incorporated in presence of lactic acid (α -hydroxypropionic acid) than in presence of propionic acid. Thus substituents (such as chlorine, phenyl, or hydroxyl) make the carboxylic acids more reactive with $\dot{O}H$ radicals. Formic acid also appears to take part in the radical-transfer reaction, and the radical derived from it is probably $\dot{C}OOH$ (carboxyl) at least in part, and hence a positive test for carboxyl endgroups is obtained. Incorporation of carboxyl endgroups is most pronounced in presence of tartaric acid or its salts.

As with the sulfonated compounds, the radical-transfer reactions with the carboxylic compounds are more favored in aqueous media than in non-

TABLE II
Radical-Transfer Reaction Involving OH Radicals and Carboxylic Substrates Demonstrated by Endgroup Analysis

Initiator	Initiator concentration, mole/l.	Organic substrate	Substrate concentration mole/l.	Polymerization medium	Carboxyl endgroups per chain
Fe ⁺⁺	5.1 × 10 ⁻⁴	Acetic acid	0.053-0.317	Aqueous ^a	0.03-0.076
H ₂ O ₂	0.0176	Acetic acid	0.053-0.317	Aqueous	0.026-0.146
H ₂ O ₂	0.0176	Potassium acetate	0.05-0.30	Aqueous	0.023-0.12
H ₂ O ₂	0.668	Acetic acid	0.04-0.17	Nonaqueous	Negligible-0.06
Fe ⁺⁺	5.1 × 10 ⁻⁴	Monochloroacetic acid	0.01-0.1	Aqueous ^a	0.09-0.13
H ₂ O ₂	0.0176	Monochloroacetic acid	0.03-0.10	Nonaqueous	0.02-0.06
H ₂ O ₂	0.0176	Lactic acid	0.06-0.26	Aqueous ^a	0.13-0.29
Fe ⁺⁺	5.1 × 10 ⁻⁴	Phenylacetic acid	0.02-0.07	Nonaqueous	0.21-0.32
H ₂ O ₂	0.668	"		Nonaqueous	Nil
AIBN	0.003	Sodium formate	0.014-0.147	Aqueous	0.124-0.43
H ₂ O ₂	0.0176	Potassium hydrogen tartarate	0.005-0.070	Aqueous	0.544-0.814
H ₂ O ₂	0.0176	Tartaric acid	0.003-0.013	Aqueous	0.27-0.47
H ₂ O ₂	0.334	Potassium hydrogen tartarate	0.08-0.16	Nonaqueous (DMF solution)	0.23-0.39
H ₂ O ₂	0.334	Tartaric acid	0.01-0.02	Nonaqueous (DMF solution)	0.28-0.42
AIBN	0.003	Tartaric acid or its salt as above		Nonaqueous (DMF solution)	Negligible
H ₂ O ₂	0.334	Potassium hydrogen tartarate	0.002-0.016	Nonaqueous (DMF solution)	0.19-0.55
AIBN	0.003	"	"	Nonaqueous (acetic acid)	Negligible

^a These polymerization experiments were done in dark. The rest were all carried out in presence of ultraviolet light.

aqueous systems, and this is clear from the results of endgroup analysis (Table II). Polymers obtained by initiation with AIBN in presence of the carboxylic acids, e.g., tartaric acid, in nonaqueous media give mostly negative or negligible response for carboxyl groups. This conclusively proves that the carboxyl incorporation in H_2O_2 -initiated polymers is largely due to the radical-transfer reactions under discussion and not to chain transfer with growing chains in any measurable extents. Conclusions made on the basis of endgroup analysis are in good agreement with those made by Dixon et al.⁷ based on electron spin resonance studies.

Thanks are due to the National Bureau of Standards (U.S.A.) for financial assistance to one of the authors (B. C. M.).

References

1. Palit, S. R., and P. Ghosh, *J. Polymer Sci.*, **58**, 1225 (1962).
2. Palit, S. R., *Chem. Ind. (London)*, **1960**, 1531.
3. Ghosh, P., S. C. Chadha, A. R. Mukherjee, and S. R. Palit, *J. Polymer Sci. A*, **2**, 4433 (1964).
4. Saha, M. K., P. Ghosh, and S. R. Palit, *J. Polymer Sci. A*, **2**, 1365 (1964).
5. Ghosh, P., P. K. Sengupta, and A. Pramanik, *J. Polymer Sci. A*, **3**, 1725 (1965).
6. Baxendale, J. H., and T. A. Wilson, *Trans. Faraday Soc.*, **53**, 344 (1957).
7. Dixon, W. T., R. O. C. Norman, and A. L. Buley, *J. Chem. Soc.*, **1964**, 3625.

Résumé

La polymérisation du polyméthacrylate de méthyle a été effectuée en milieu aqueux et non aqueux en présence de dérivés organiques sulfonés et carboxylés en utilisant des radicaux hydroxyles issus de l'eau oxygénée comme initiateur de polymérisation. L'occurrence de réaction de transfert radicalaire par abstraction de l'atome d'hydrogène au départ de substrats organiques par des radicaux OH a été démontrée par la détection de groupes terminaux sulfoniques et carboxyliques dans les polymères respectifs. On a trouvé que les réactions de transfert radicalaire sont plus fortement favorisées en milieu aqueux que dans des systèmes non-aqueux.

Zusammenfassung

Die Polymerisation von Methylmethacrylat mit Hydroxylradikalen aus Wasserstoffperoxyd als Polymerisationsstarter wurde in wässrigen und nicht wässrigen Medien in Gegenwart gewisser sulfonierter und Karboxylgruppen-hältiger organischer Verbindungen ausgeführt. Das Auftreten von Radikalübertragungsreaktionen mit Wasserstoffatomabstraktion vom organischen Substrat durch die ÖH-Radikale wurde durch den Nachweis von Sulfonat- und Karboxylendgruppen in den betreffenden Polymere nachgewiesen. Die Radikalübertragungsreaktionen waren in den wässrigen Medien gegenüber den nicht wässrigen Systemen begünstigt.

Received August 17, 1965
Prod. No. 4897A

Polymerization of β -Cyanopropionaldehyde*

HIROSHI SUMITOMO and KAZUKIYO KOBAYASHI, *Department of Chemical Technology, Faculty of Engineering, Osaka University, Higashinoda, Miyakojima-ku, Osaka, Japan*

Synopsis

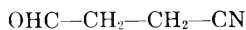
A new class of polyacetals, poly(cyanoethyl)oxymethylene, was obtained by the polymerization of β -cyanopropionaldehyde at -78°C . with use of ionic initiators including boron trifluoride diethyl etherate, diethylzinc, triethylaluminum, and triethylaluminum-titanium tetrachloride complexes. The influence of temperature, initiator, and solvent upon the polymerization was studied. Infrared spectra of polymers obtained from different initiators are also illustrated. An attempt was made to fractionate the polymer by means of solvent extraction. The acetone-soluble polymer is an elastomeric material having a low solution viscosity. The acetone-insoluble, dimethylformamide-soluble polymer obtained as a white powder was found to have extremely high solution viscosity. Some amounts of insoluble fraction could be also separated. The latter two fractions were observed to have a reasonable stability.

INTRODUCTION

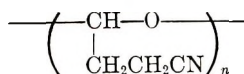
β -Cyanopropionaldehyde (CPA) (I) is an intermediate, now commercially available, used in the production of monosodium glutamate starting from acrylonitrile.¹⁻³

The present investigation was designed to obtain new high molecular weight polymers directly from CPA. Although considerable attention has been paid to the polymerizations of formaldehyde, acetaldehyde, chloral, higher aldehydes and such aldehydes,⁴⁻⁸ nothing is known about the polymerization of nitrile-containing aldehydes.

This note is concerned with the preparation of a new class of polyacetals, poly(cyanoethyl)oxymethylene (II), which has been attained by the low-temperature polymerization of CPA with the use of ionic initiators including boron trifluoride diethyl etherate, diethylzinc, triethylaluminum, and triethylaluminum-titanium tetrachloride complexes.



I



II

* This paper was presented at the 14th Annual Meeting of the Society of Polymer Science, Tokyo, Japan, May 1-3, 1965.

EXPERIMENTAL

Materials

β -Cyanopropionaldehyde dimethyl acetal (100 g.) was refluxed with water (500 ml.) for 4 hr. Water and methanol were removed by distillation and the residue was distilled under reduced pressure. A total of 36 g. (60% yield) of CPA was collected, b.p. 62–63°C./1 mm. Hg (Lit.:² b.p. 85.1–85.5°C./3 mm. Hg). The distillation of monomer, dried over anhydrous sodium sulfate, was repeated again prior to use.

Methylene chloride and tetrahydrofuran (THF) used as solvents were purified by distillation after drying over calcium hydride and after refluxing in the presence of sodium, respectively.

Commercial boron trifluoride diethyl etherate and titanium tetrachloride were used after distillation. Diethylzinc and triethylaluminum were also of commercial origin (Ethyl Corp.).

Polymerization

Cold CPA was added to an initiator solution in a glass ampule which had been cooled in a nitrogen-filled dry box. The ampule was sealed after an evacuation at the liquid nitrogen temperature and placed in a Dewar flask filled with solid CO₂.

Polymerization was stopped by either (1) the addition of a larger amount of cold methanol or (2) the addition of a small amount of pyridine–acetyl chloride mixture followed by washing with methanol, and the resulting polymer was collected, dried, and weighed.

Fractional Extraction of Polymer

In order to separate the insoluble polymer from the soluble one, the original polymer sample was first repeatedly extracted with acetone at room temperature. The fraction remaining undissolved and was removed by filtration and extracted again with dimethylformamide (DMF) until no more soluble material could be extracted. Some insoluble fraction still remained after the treatment described above. The acetone- and DMF-soluble fractions, respectively, were recovered by the additions of methanol as a precipitant to each of the extract solution obtained above and condensed under reduced pressure at room temperature. The fractions were dried under vacuum at room temperature.

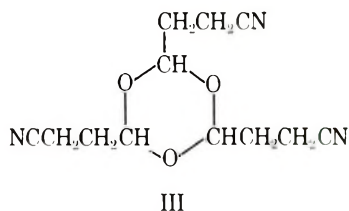
Viscosity Measurement

Reduced viscosity, η_{sp}/c , was measured in DMF at 25°C. with use of an Ostwald viscometer.

RESULTS AND DISCUSSION

The results of polymerization initiated by BF₃ etherate are given in Table I. The material formed at the higher temperature, 0°C., being

easily crystallized in needles, was found to be a cyclic trimer of CPA, 2,4,6-tris(β -cyanoethyl)-s-trioxane (III), from the molecular weight meas-



urement, nuclear magnetic resonance, infrared, elemental, and x-ray analyses;^{9,10} m.p. 129–130°C.

The white elastomeric material obtained at the lower temperature, -78°C . is soluble in acetone, DMF, and dimethyl sulfoxide. It seems that higher conversions and lower molecular weights are obtained with THF as solvent rather than methylene chloride.

Data for polymerization of CPA with diethylzinc are collected in Table II. The reduced viscosity for an acetone-soluble fraction seems to be increased by the addition of water as a cocatalyst in the polymerizing system. The acetone-soluble and insoluble fractions are a white elastomer and a white powder, respectively. The latter can be further separated into two parts on the basis of solubility in DMF. The results of fractionation of the polymer obtained in run 89 are given in the footnote to Table II. The DMF-insoluble fraction is also insoluble in almost all other organic solvents.

Table III contains data for the polymerization of CPA initiated by triethylaluminum. It appears that the rate of polymerization with triethylaluminum is somewhat higher than that obtained with BF_3 etherate or diethylzinc. The results of fractionation of products are shown in Table IV. It should be noticed that even an acetone-soluble fraction gives a rather higher value of reduced viscosity (0.46) and that a fraction insoluble in acetone but soluble in DMF shows extremely high viscosity (6.9 and 7.3).

In Table V are given the results of polymerization of CPA with use of triethylaluminum-titanium tetrachloride complexes prepared with a variety of molar ratios of aluminum to titanium.

Table VI shows the results of the separation of the products obtained above. Reduced viscosities of the fractions which are insoluble in acetone and soluble in DMF were not so high as those separated from the polymer prepared with the use of triethylaluminum alone as initiator.

Chemical Structure of Polymer

Infrared spectra of CPA monomer, its cyclic trimer, and some polymers obtained in the above experiments are shown in Figures 1–5. The monomer displays major absorptions of $\text{C}=\text{O}$ stretching at 1720 cm^{-1} and also of $\text{C}\equiv\text{N}$ stretching at 2250 cm^{-1} . In the spectra of the polymers new broad bands appear in the region between 940 and 1130 cm^{-1} instead of

TABLE I
Results of Polymerization Initiated by Boron Trifluoride Diethyl Etherate

Run no.	CPA, g.	$\text{BF}_3 \cdot \text{O}(\text{C}_2\text{H}_5)_2$, ml.	Solvent	Solvent, ml.	Temp., °C.	Time, days	Yield, g.	Conversion, %	η_{sp}/c^a
24	2	0.18 mg.	Methylene chloride	2.0	0	1	0.25	12.1	Trimer
52	10	0.35	"	10.3	-78	1	0.40	4.0	Viscous liquid
63	"	"	"	"	"	2	1.12	11.2	0.18
53	"	"	"	"	"	3	2.30 ^b	23.0	0.22
54	"	"	"	"	"	7	2.83	28.3	0.20
39	"	"	"	"	"	34	3.28	32.8	0.21
56A	7.8	"	THF	8.6	"	2	1.18	15.1	Viscous liquid
55	10	"	"	"	"	6	5.81	58.1	0.03

^a In DMF, $c = 0.2$ g./100 ml., 25°C.

^b Softening point, 74–78°C.

TABLE II
Results of Polymerization with Diethylzinc^a

Run no.	CPA, g.	$\text{Zn}(\text{C}_2\text{H}_5)_2$, g.	Cocatalyst	Cocatalyst, ml.	Solvent	Solvent, g.	Yield, g.	Conversion, %	Acetone-soluble fraction
89	20	1.4	—	—	Methylene chloride	20.6	6.94	34.7	$\frac{\eta_{sp}/c^b}{\%}$ 95.8 ^c
90	"	"	Water	0.2	"	"	6.69	33.5	96.2
83	10	0.7	Methanol	0.1	"	10.3	2.54	25.4	81.0
85	"	"	—	—	THF	8.6	2.96	29.6	98.5
86	"	"	Water	0.1	"	"	2.85	28.5	71.4

^a Temp., -78°C.; time, 4 days; terminated with pyridine-acetyl chloride.

^b In DMF, $c = 0.2$ g./100 ml., 25°C.

^c Fractionation shows 2.8% acetone-insoluble, DMF-insoluble material, 1.4% DMF-insoluble material. The acetone-insoluble, DMF-soluble material melted in the range 155–165°C.; elemental analysis showed C, 57.10%; H, 5.84%; N, 16.2% (calcd. for $\text{C}_4\text{H}_8\text{ON}$: C, 57.82%; H, 6.06%; N, 16.9%).

TABLE III
Results of Triethylaluminum-Initiated Polymerization at -78°C .

Run no.	CPA, g.	$\text{Al}(\text{C}_2\text{H}_5)_3$		Solvent	Amt. solvent		Time, days	Yield, g.	Conversion, %
		g.	mole-%/ monomer		g.	mole-%/ monomer			
48	6	0.0 ₈	1.0	Methylene chloride	1.5	25	3	0.97	16.2
50	10	0.1 ₄	"	"	10.2	100	"	1.74	17.4
49	"	"	"	"	20.5	200	"	2.03	20.3
56B	3	0.0 ₄	"	"	15.6	500	"	0.61	"
87	20	0.4 ₀	1.4	"	20.5	100	"	6.24	31.2
88	"	"	"	"	"	"	"	8.64 ^a	43.2
50	10	0.7 ₀	5.0	THF	8.6	"	6	6.72	67.2
91	20	0.3 ₀	1.0	"	17.2	"	3	13.93	69.7

^a Terminated with pyridine-acetyl chloride.

TABLE IV
Fractionation of Triethylaluminum-Initiated Polymers with Acetone and DMF as Solvents

Sample no. ^a	Acetone-soluble		Acetone-insoluble, DMF-soluble		DMF-insoluble, %
	%	η_{sp}/c^b	%	η_{sp}/c^c	
87	69.8	0.18	9.1	6.97	21.1
88	74.0	0.46	2.9	7.32	23.3
91	88.6	0.15	4.0	0.76	7.4 ^d

^a Sample numbers refer to products of runs listed in Table III.

^b In DMF, $c = 0.20$ g./100 ml., at 25°C.

^c In DMF, $c = 0.18$ g./100 ml., at 25°C.

^d Melting range 160–175°C.

TABLE V
Results of Polymerization with Use of Triethylaluminum-Titanium Tetrachloride Complexes^a

Run no.	CPA, g.	TiCl ₄ ,		Molar ratio of Al/Ti	Yield, g.	Conversion, %
		g.	mole-%/mole monomer			
58	4	0.0 ₉	1	1	0.97	24.3
57	"	"	"	2	2.07	51.8
59	"	"	"	3	2.02	50.5
46	"	0.1 ₉	2	2	2.92	73.0

^a In methylene chloride (1:1 mole); temp., -78°C.; time, 3 days.

TABLE VI
Results of Fractionation of Al(C₂H₅)₃-TiCl₄-Initiated Polymers with Acetone and DMF as Solvents

Sample no. ^a	Acetone-soluble, %	Acetone-insoluble, DMF-soluble		DMF-insoluble, %
		%	η_{sp}^b/c	
57	69.7	9.8	0.34	20.5
46	45.1	25.9	0.78	29.0

^a Sample numbers refer to products of runs listed in Table V.

^b In DMF, $c = 0.2$ g./100 ml., at 25°C.

the carbonyl bands; on the other hand, little change is observed in the nitrile band. This suggests that the aldehyde structure of the monomer changed to an ether structure after polymerization. Weak absorptions detected at 1760 cm.⁻¹ in Figures 3 and 4 are considered to be due to the terminal acetyl group which might be formed when the polymer was terminated by the treatment with pyridine-acetyl chloride. Differences which can be observed in detail in the spectra of the polymers are being further studied.

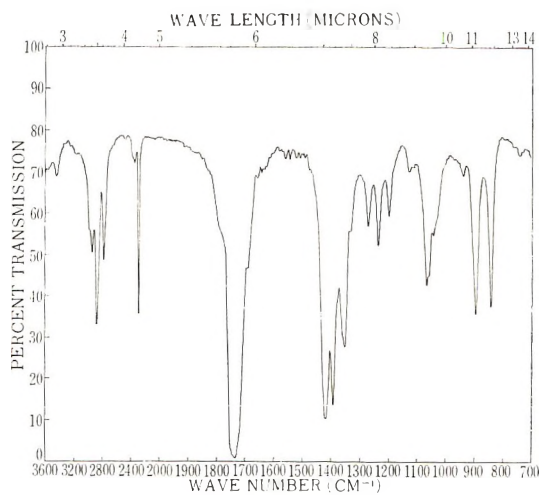


Fig. 1. Infrared spectrum of β -cyanopropionaldehyde.

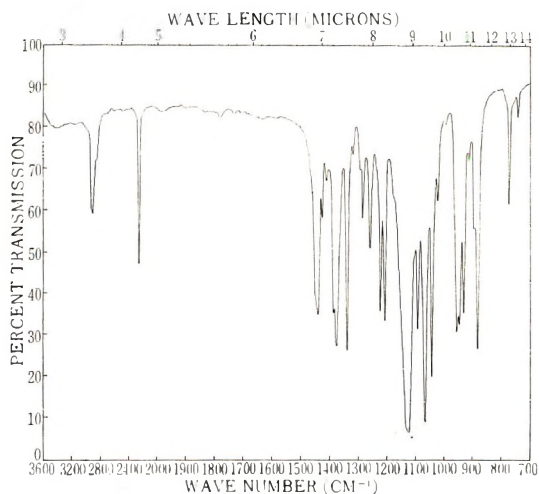


Fig. 2. Infrared spectrum of the cyclic trimer of β -cyanopropionaldehyde, III (KBr disk).

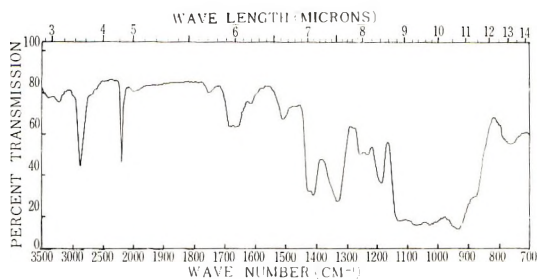


Fig. 3. Infrared spectrum of the polymer prepared with $\text{BF}_3 \cdot \text{O}(\text{C}_2\text{H}_5)_2$ initiator.

The treatment of the polymer with an acidic aqueous alcohol solution of 2,4-dinitrophenylhydrazine at boiling water temperature for about 1 hr. gave the hydrazone melting at 194–195°C. in about 95% yields. This

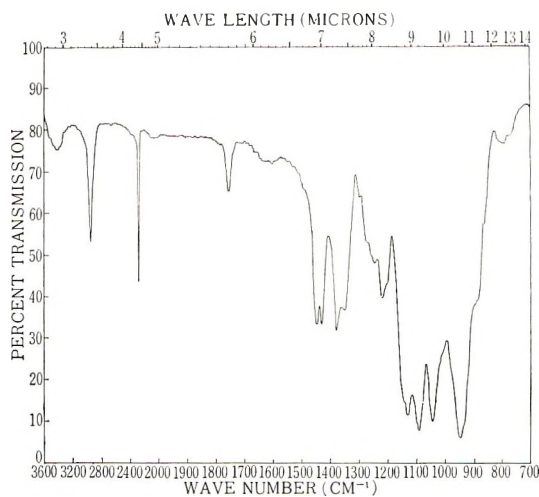


Fig. 4. Infrared spectrum of the acetone-soluble, DMF-insoluble fraction separated from the polymer (run 89) initiated with diethylzinc (KBr disk).

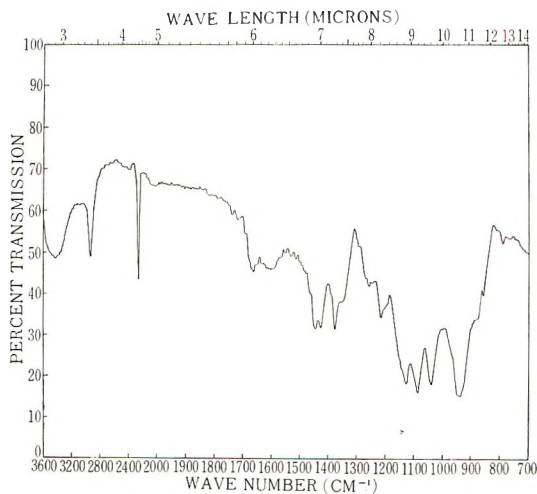


Fig. 5. Infrared spectrum of the DMF-insoluble fraction separated from the polymer (run 87) obtained by using triethylaluminum (KBr disk).

compound was found by mixed melting point determinations to be identical with that prepared from CPA monomer.

The experiments described above indicate that CPA polymerizes with ionic initiators at low temperature to form linear high molecular weight poly(cyanoethyl)oxymethylene.

The insoluble polymer was quite stable on being allowed to stand in the air at room temperature, although the acetone-soluble polymer appeared to be degraded under the same conditions, the formation of some colored products being noted.

We wish to express our gratitude to Emeritus Professor Y. Hachihama for his continued interest and encouragement in this work. The assistance of Messrs. K. Kawamura and T. Ohji in the experimental work has been most valuable. The sample of β -cyanopropionaldehyde dimethyl acetal was kindly supplied by Ajinomoto Co., Inc.

References

1. Kato, J., H. Wakamatsu, Y. Iwanaga, and T. Yoshida, *Kogyo Kagaku Zasshi*, **64**, 2139 (1961).
2. Kato, J., H. Wakamatsu, T. Komatsu, Y. Iwanaga, and T. Yoshida, *Kogyo Kagaku Zasshi*, **64**, 2142 (1961).
3. *Chem. Eng. News*, **43**, No. 12, Mar. 22, 1965.
4. Furukawa, J., and T. Saegusa, *Polymerization of Aldehydes and Oxides*, Wiley, New York, 1963.
5. Saegusa, T., *Kogyo Kagaku Zasshi*, **65**, 792 (1965).
6. Vogl, O., *J. Polymer Sci.*, **46**, 261 (1960).
7. Vogl, O., *Chem. Ind. (London)*, **1961**, 748.
8. Vogl, O., *J. Polymer Sci. A*, **2**, 4591 (1964) and following papers.
9. Sumitomo, H., and Y. Hachihama, paper presented at the 13th Annual Meeting of the Society of Polymer Science, Japan, Kyoto, June 5-7, 1964.
10. Nagashima, N., A. Nakamura, S. Ninagawa, and A. Okuda, paper presented at the 18th Annual Meeting of the Chemical Society of Japan, April 2-5, 1965.

Résumé

Une nouvelle classe de polyacétals, le poly(cyanoéthyl)oxyméthylène, a été obtenue par la polymérisation du β -cyanopropionaldéhyde à -78°C en utilisant des initiateurs ioniques contenant du trifluorure de bore sous forme de complexe éther diéthylique, diéthylzinc, triéthylaluminium et triéthylaluminium-tétrachlorure de titane sous forme de complexes. L'influence de la température, de l'initiateur et du solvant sur la polymérisation a été étudiée. Les spectres infra-rouges de polymères obtenus au départ de différents initiateurs sont également illustrés. Un essai a été effectué pour fractionner le polymère par extraction au solvant. Le polymère soluble dans l'acétone est un matériau élastomère ayant une viscosité faible en solution. Le polymère insoluble dans l'acétone mais soluble dans le diméthylformamide obtenu sous forme de poudre blanche a une viscosité très élevée en solution. Certaines quantités de fractions insolubles ont également pu être séparées; les deux dernières fractions ont une stabilité raisonnable.

Zusammenfassung

Eine neue Klasse von Polyacetalen, Poly(cyanoäthylloxymethylen), wurde durch die Polymerisation von β -Cyanopropionaldehyd bei -78°C mit ionischen Startern wie Bortrifluorid-Diäthylätherat, Diäthylzink, Triäthylaluminium, und Triäthylaluminium-Titantetrachloridkomplexen erhalten. Der Einfluss von Temperatur, Starter und Lösungsmittel auf die Polymerisation wurde untersucht. Infrarotspektren von mit verschiedenen Startern erhaltenen Polymeren werden gezeigt. Es wurde versucht, das Polymere durch Lösungsmittelextraktion zu fraktionieren. Das Aceton-lösliche Polymere bildet ein elastisches Material mit niedrigerer Lösungsviskosität. Das als weisses Pulver erhaltene Aceton-unlösliche und Dimethylformamid-lösliche Polymere besass

eine extrem hohe Lösungsviskosität. Auch ein gewisser Anteil an unlöslicher Fraktion konnte abgetrennt werden. Die letzteren beiden Fraktionen besaßen eine annehmbare Stabilität.

Received July 27, 1965

Revised September 17, 1965

Prod. No. 4902A

Polymers from Aryl Glycidyl Ethers

T. B. GIBB, JR., R. A. CLENDINNING, and W. D. NIEGISCH,
*Research and Development Department, Plastics Division, Union Carbide
Corporation, Bound Brook, New Jersey*

Synopsis

High molecular weight, linear polyethers were prepared by polymerizing a series of ring-substituted phenyl glycidyl ethers by using the ferric chloride-propylene oxide and dibutylzinc-water catalyst systems. The α -naphthyl, β -naphthyl, *p*-phenylphenyl, the *o*-, *m*-, and *p*-methyl, and the *o*- and *p*-chlorophenyl polymers resemble the parent polymer in that they are readily crystallizable polyethers which have melting points above 170°C. The other substituted poly(phenyl glycidyl ethers), including the *o*- and *p*-isopropyl, *p*-*tert*-butyl, *p*-octyl, and 2,4,6-trichloro derivatives show much less tendency to crystallize and are lower melting. The x-ray and electron diffraction data established that poly(*o*-chlorophenyl glycidyl ether) crystallizes in an orthorhombic unit cell; data obtained in a parallel study of unsubstituted poly(phenyl glycidyl ether) did not allow assignment of a specific structure.

Interest in the polymerization of cyclic ethers by organometallic compounds has been quite high in recent years. Continuing our recent study on the polymerization of phenyl glycidyl ether,¹ we wish to report additional physical data on this polyether and its ring-substituted derivatives.

It is significant that all of the polymers prepared, except the ones substituted with the larger *p*-alkyl groups (isopropyl, *tert*-butyl, and octyl) are high molecular weight, crystallizable polyethers from which films and monofilaments can be prepared. In contrast, it had been stated in earlier publications that polymers of the alkyl phenyl glycidyl ethers prepared by base catalysis range from low molecular weight oils to amorphous resins² while polymers of the *o*- and *p*-chlorophenyl glycidyl ethers prepared by triethylaluminum-based catalysts are low molecular weight polyethers containing only small amounts of a crystallizable fraction.³

The epoxides in Table I were prepared by reaction of the appropriate phenol with epichlorohydrin followed by ring closure to the epoxide.⁴ The highly purified monomers were polymerized in sealed glass tubes as outlined earlier.¹ The ferric chloride-propylene oxide catalyst was prepared by the procedure reported by Price and Osgan.⁵ Reduced viscosities were determined in *p*-chlorophenol at 47°C. after heating for 30 min. at 140°C. The α - and β -naphthyl glycidyl ether polymers required 1 hr. at 210°C. to effect solution. Melting points were determined in a capillary tube except for the last four polymers, which were determined with the aid of a Leitz hot stage polarizing microscope.

TABLE I
 Polymers from Aryl Glycidyl Ethers

$\begin{array}{c} \text{R in} \\ \diagup \quad \diagdown \\ \text{O} \\ \diagdown \quad \diagup \\ \text{ROCH}_2\text{CH}-\text{CH}_2 \end{array}$	Catalyst	Yield, %	Reduced viscosity	Melting point, °C.	Apparent crystallizability
C ₆ H ₅	Bu ₂ Zn-H ₂ O	97	10.2	200-204	High
<i>o</i> -CH ₃ C ₆ H ₄	FeCl ₃ -PO	76	2.5	189-191	High
<i>m</i> -CH ₃ C ₆ H ₄	"	83	2.2	165-169	Med.
<i>p</i> -CH ₃ C ₆ H ₄	"	74	3.1	207-212	Med.
<i>o</i> -(CH ₃) ₂ CHC ₆ H ₄	"	40	2.2	120-128	Low
<i>p</i> -(CH ₃) ₂ CHC ₆ H ₄	"	79	0.9	—	Low
<i>p</i> -(CH ₃) ₃ CC ₆ H ₄	"	20	1.6	—	Nil
<i>p</i> -C ₈ H ₁₇ C ₆ H ₄ ^a	"	5	0.7	—	Nil
<i>o</i> -ClC ₆ H ₄	"	71	4.7	195-200	High
<i>p</i> -ClC ₆ H ₄	"	50	2.4	170-176	High
α -C ₁₀ H ₇	Bu ₂ Zn-H ₂ O	97	6.0	233-235	Med.
β -C ₁₀ H ₇	"	99	3.7	297	High
2,4,6-Cl ₃ C ₆ H ₂	"	84	2.4	120-130	Low
<i>p</i> -C ₆ H ₅ C ₆ H ₄	"	2.6	Insol.	286-293	Med.

^a 1,1,3,3-Tetramethyl butyl phenyl.

As can be seen from Table I, introduction of an alkyl group or halogen on the aromatic ring of the phenyl glycidyl ether appreciably lowers the melting point slightly. As expected, the larger the alkyl group, the greater exception to this generalization is the *p*-methyl group, which raises the melting point slightly. As expected, the larger the alkyl group, the greater the melting point depression. Substitution of α -naphthyl, β -naphthyl, or *p*-phenylphenyl for phenyl in this series causes a sharp rise in the melting point of the polymer.

The crystallizability of the polyethers was determined qualitatively by the following method. Approximately 0.5 mg. of each polymer, excepting the naphthyl and *p*-phenylphenyl derivatives, was melted between 2 cm. cover glasses on a Fischer melting point block and transferred to an oven at 220°C. After 1/2 hr. the oven was permitted to cool to room temperature over a 4 hr. interval. Annealing of the bicyclic derivatives was started 10°C. above the respective melting points. The apparent crystallizability, judged by observing the size and number of spherulites in a polarizing microscope, is indicated in the last column of Table I. The polymers that are rated high in apparent crystallizability form well-developed spherulites. An illustration of a poly(phenyl glycidyl ether) spherulite is shown in Figure 1.

Since qualitative observations suggest that the nature and positions of substituents on the aryl ring have a major effect on the crystallizability of the polyethers, crystallographic studies of two of them were instituted.

X-ray and electron diffraction data established that poly(*o*-chloro phenyl glycidyl ether) crystallizes in an orthorhombic unit cell with $a = 12.6$ Å., $b = 9.90$ Å., and $c = 6.93$ Å. (the fiber repeat distance). The theoretical

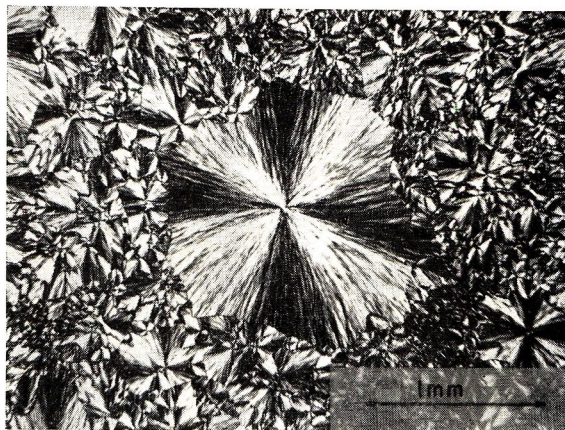


Fig. 1. Spherulitic melt-annealed film of poly(phenyl glycidyl ether).

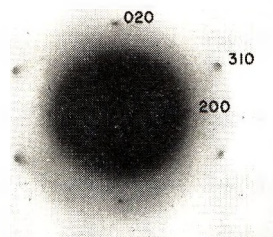


Fig. 2. Single-crystal electron diffraction pattern of poly(*o*-chlorophenyl glycidyl ether) in *hk0* projection. The pattern was obtained from a melt-annealed film that had been solution-cast onto a carbon substrate.

crystal density for four repeat units in the unit cell is 1.414 g./cc. at 25°C. This compares favorably with the measured density of 1.354 g./cc. at 23°C. for an annealed sample.

The key to the lattice symmetry was provided by a single crystal electron diffraction pattern (Fig. 2), which was obtained from a thin film that had been cast on a carbon substrate. It was then heated *in vacuo* to 210°C., cooled to 160°C., and held at this temperature for 2 hr. The projection corresponds to the zero layer line of the fiber diagram, thereby establishing the *a* and *b* dimensions of the lattice. The polymer chains must, therefore, be aligned normal to the plane of the film. Consequently, the polymer chains are folded, since the films of this high molecular weight polymer were not more than 200 Å. thick. The observed fiber repeat distance is identical to the value for an extended planar zigzag configuration of the ethylene oxide backbone.

Table II lists the observed interplanar spacings, d_{obs} , as derived from x-ray data recorded in a 114.6-mm. Norelco powder camera. Nickel filtered copper radiation was employed throughout this study. Also listed are the interplanar spacings, d_{calc} , which were calculated from the least-squares derived lattice constants reported above, and the zero layer-

TABLE II
 X-Ray Diffraction Data for Poly(*o*-chlorophenyl Glycidyl Ether)

d_{obs} , A.	Relative intensity, I^a	hkl	d_{calc} , A.	$\Delta \times 10^3$	$d_{(hkl)}$ fiber
6.299	w	200	6.315	16	
5.698	vw	011	5.679	19	
5.319	m	210	5.324	5	5.33
5.157	vwv	111	5.180	23	
4.962	w	020	4.951	11	4.99
4.622	w	120	4.610	12	4.64
4.252	vw	211	4.223	29	
4.036	w	021	4.029	7	
3.881	s	310	3.876	5	3.89
3.602	m	301	3.600	2	
3.391	m	221	3.397	6	
3.302	m	320	3.208	6	3.20
2.891	w	131	2.901	10	
2.759	vw	411	2.760	1	
2.604	vw	222	2.590	14	
2.481	vwv	421	2.485	4	
2.307	w	240	2.305	2	2.31
2.237	vwv	232	2.236	1	

^a v = very, w = weak, m = medium, s = strong.

line fiber data. The assignment of every reflection with low residuals, $d_{obs} - d_{calc} = \Delta$, supports the assignment. A special reading device was used to measure the powder patterns to ± 0.005 cm.

Poly(phenyl glycidyl ether) was examined by the same techniques. It was disconcerting to find that x-ray powder diffraction patterns of melt annealed samples of FeCl₃-propylene oxide-catalyzed polymer were different from those of samples that had no melt history but were annealed at 169–179°C. (Table III). The polymer was originally precipitated from a toluene solution into alcohol, affording a finely divided polymer. The diffraction patterns were reproducible, regardless of the annealing time. An added complication arose from the observation that the fiber data do not exactly correspond to either powder pattern, although some interplanar spacings are common to both (Table III). The measured fiber repeat distance is 5.41 Å. with an estimated error of at least 1%.⁶

Since this behavior is suggestive of polymorphism, the samples were examined by differential thermal analysis. In all cases, the samples melted at 195–200°C. and showed a cooling exotherm at 160–180°C. The absence of multiple crystal forms was confirmed by birefringent melting point determinations.

An additional complication is introduced by the fact that our diffraction patterns bear only a superficial resemblance to the data obtained by Takahashi and Kambara⁷ for poly(phenyl glycidyl ether) which had been polymerized with a AlEt₃/Ni(dimethyl glyoxime)₂ catalyst system. Their

TABLE III
 X-Ray Diffraction Data for Poly(Phenyl Glycidyl Ether)^a

Melted then annealed in solid state ^b		Annealed in solid state ^c		Fiber from melt		
<i>I</i>	<i>d</i> , A.	<i>I</i>	<i>d</i> , A.	<i>I</i>	<i>d</i> , A.	<i>hkl</i>
—	—	vw	16.3			
w	8.95	—	—			
w	8.21	vw	8.22			
—	—	vw	7.60			
mw	7.51	—	—			
mw	6.25	w	6.25			
—	—	—	—	w	5.59	<i>hk0</i>
ms	5.43	m	5.44	—	—	—
Broad, w	4.91	Broad, w	4.95	w	5.1	<i>hkl</i>
Broad, ms	4.58	m	4.59	s	4.55	<i>hkl</i>
—	—	v Broad, m	4.47	—	—	—
ms	4.14	w	4.16	—	—	—
—	—	s	4.02	s	4.04	<i>hk0</i>
s	3.90	ms	3.88	—	—	—
Broad, w	3.69	Broad, w	3.69	—	—	—
ms	3.32	Broad, m	3.32	vw	3.26	<i>hkl</i>
		vw	2.81	—	—	—
		vw	2.71	—	—	—
		w	2.00			
		w	1.94			

^a Powder recrystallized from pyridine.

^b Annealed 6 hr. at 165°C., pattern typical of all melted and annealed samples.

^c Pattern irrespective of annealing time (3 hr. at 169°C., 3 hr. at 179°C., 3 days at 170°C.)

value for the chain repeat distance was 5.48 Å. Our difficulties in correlating the diffraction data obtained in the present study may have been shared by Takahashi and Kambara.* The latter report that the amorphous specific volume of the polymer is 0.7860. We find that this corresponds to a density of 1.27 g./cc., which is in direct conflict with the published density range of 1.21–1.29 g./cc. reported by the same authors. Clearly the amorphous density should be equal to, or less than, the lowest reported value, since this polymer exhibits the usual relation between density and crystallinity. The density of our annealed samples was 1.25 g./cc. Furthermore, we find it impossible to fit an orthorhombic cell to our diffraction data, based either on the suggested parameters of Takahashi and Kambara or other values more consistent with either set of data reported in Table III.

It is quite probable that we are observing differences in stereoregularity of the polymer prepared by us and that prepared according to Takahashi and

* It has been called to our attention by a referee that another worker, Salvatore S. Stivala, Doctoral Dissertation, University of Pennsylvania, 1960, has reported x-ray data on poly(phenyl glycidyl ether) fibers, which had a melting point of 206°C. (by density change) and a chain repeat distance of 5.53 Å.

Kambara.⁷ Yet this does not account for the differences in the patterns of our polymer when annealed according to different schedules. A rational interpretation of this situation must await obtainment of additional experimental data.

References

1. Garty, K. T., T. B. Gibb, Jr., and R. A. Clendinning, *J. Polymer Sci. A*, **1**, 85 (1963).
2. Sorokin, M. F., L. G. Shode, and L. S. Mikhailova, *Lakokrasochnye Materialy i ikh Primenenie*, **1962**, No. 4, 10; *Chem. Abstr.* **58**, 1540 (1964).
3. Belgian Pat. 579,074 (to Hercules Powder Company), (May 27, 1959).
4. Gibb, T. B., Jr., and R. A. Clendinning, *J. Chem. Eng. Data*, in press.
5. Price, C. C., and M. Osgan, *J. Am. Chem. Soc.*, **78**, 4787 (1956).
6. Henry, N. F. M., H. Lipson, and W. A. Wooster, *The Interpretation of X-ray Diffraction Photographs*, MacMillan, New York, 1953, 5th Ed., p. 53.
7. Takahashi, A., and S. Kambara, *Makromol. Chem.*, **72**, 92 (1964).

Résumé

Des polyéthers linéaires de hauts poids moléculaires ont été préparés par polymérisation d'une série d'éthers glycidyle-phényles substitués dans le noyau utilisant le chlorure ferrique-oxyde propylène et le dibutyle zinc-eau comme systèmes catalytiques. Les polymères α -naphthyles, β -naphthyles, p -phénylphényl, les o -, m - et p -methyles, et les o - et p -chlorophényliques ressemblent aux polymères parents, en ce sens qu'ils forment des polyéthers facilement cristallisables de point de fusion au-dessus de 170°C. Les autres poly(phényl-glycidyl-éthers) substitués, y compris les o - et p -isopropyles, p - t -butyles, o -octyles, et dérivés 2,4,6-trichlorés montrent beaucoup moins de tendance à la cristallisation et présentent un point de fusion plus bas. La diffraction aux rayons-X et aux électrons indiquent que l'éther poly(o -chlorophényl glycidyl) cristallise dans une cellule périodique orthorhombique; les résultats obtenus dans une étude parallèle sur le poly(phényl glycidyl-éther) ne permet pas d'attribution de structure spécifique.

Zusammenfassung

Hochmolekulare lineare Polyäther wurden durch Polymerisation einer Reihe von ring-substituierten Phenylglycidyläthern mit Eisenchlorid-Propylenoxyd und Dibutylzink-Wasser als Katalysatorsystem dargestellt. Die α -Naphthyl-, β -Naphthyl-, p -Phenylphenyl-, die o -, m - und p -Butyl und die o - und p -Chlorophenylpolymeren ähneln insofern dem Stammpolymeren, als sie leicht kristallisierbare Polyäther mit Schmelzpunkten oberhalb 170°C sind. Die anderen substituierten Poly(phenylglycidyläther) nämlich die o - und p -Isopropyl-, p - t -Butyl-, p -Octyl- und 2,4,6-Trichlorerivate zeigen eine viel geringere Kristallisationstendenz und schmelzen niedriger. Röntgen- und Elektronenbeugungsdaten ergeben, dass Poly(o -chlorophenylglycidyläther) in einer orthorhombischen Elementarzelle kristallisiert; die mit unsubstituierten Poly(phenylglycidyläthern) erhaltenen Daten erlaubten keine Zuordnung einer spezifischen Struktur.

Received August 13, 1965

Revised September 23, 1965

Prod. No. 4903A

Stereospecific Polymerization of α -Methylstyrene by Friedel-Crafts Catalysts

Y. OH SUMI, T. HIGASHIMURA, and S. OKAMURA, *Department of
Polymer Chemistry, Kyoto University, Kyoto, Japan*

Synopsis

The relationship between stereoregularity and polymerization conditions of α -methylstyrene has been studied by means of NMR spectra. The effects of solvents and various Friedel-Crafts catalysts have been investigated. The stereoregularity of poly- α -methylstyrene increased with increased polymer solubility in the solvent used and with decreasing polymerization temperature. This behavior is completely different from the stereospecific polymerization of vinyl ethers and methyl methacrylate in homogeneous systems. This may be due to the strong steric repulsion exerted by the two substituents in the α -position of α -methylstyrene. For example, with $\text{BF}_3 \cdot \text{O}(\text{C}_2\text{H}_5)_2$ as catalyst at -78°C ., atactic polymer is obtained in *n*-hexane, a nonsolvent for α -methylstyrene, whereas highly stereoregular polymer is produced in toluene or methylene chloride, good solvents for the polymer. However, the polarity of the solvent and the nature of the catalyst hardly affect the stereoregularity of the polymer.

INTRODUCTION

In the cationic polymerization of α -methylstyrene (α MS) at low temperatures, stereoregular polymer was produced in *n*-hexane-chloroform mixed solvent, but not in pure *n*-hexane.¹ Poly- α -methylstyrene (P α MS) obtained in *n*-hexane (15 vol.-%)-chloroform (75 vol.-%) mixed solvent was hardly soluble in benzene at room temperature, and the x-ray diffraction pattern of this polymer was sharper than that of conventional P α MS.¹ This phenomenon is remarkable, since in the stereoregular polymerization of vinyl ethers,² methyl methacrylate (MMA),³ and styrene,⁴ the isotacticity of polymers decreases on addition of a polar solvent.

The reason for this behavior of these monomers should be clarified. The relationship between stereoregularity of P α MS and polymerization conditions has been examined. Fortunately, the steric structure of P α MS can be easily analyzed by high-resolution NMR spectroscopy,⁵⁻⁸ since the α -methyl protons are sensitive to the stereochemical configuration.

This paper discusses the relationship between polymerization conditions and steric structure of P α MS on the basis of high-resolution NMR spectroscopy. On the basis of these data, we discuss the mechanism of cationic polymerization of α MS.

It is found that the repulsive interactions between the two substituents in the α -positions of the attacking monomer and that of the polymer control

the steric structure of polymer. Therefore, in a homogenous system, i.e., under conditions when the entering monomer can attack a growing chain end from the position with the smallest steric hinderance, polymerization conditions, e.g., the nature of the catalysts or the polarity of the solvent, hardly affect the steric structure of P α MS.

EXPERIMENTAL

Procedure

Freshly distilled monomer and solvent were introduced into a 100-ml. reaction vessel. The reaction vessel was sealed with a rubber cap and brought to the polymerization temperature. After the reaction vessel reached thermal equilibrium, the catalyst was introduced with a syringe. At the end of the polymerization, the polymer was isolated from the reaction mixture by precipitation in excess methanol, washed, and dried *in vacuo* at 40°C.

NMR spectra of P α MS were determined in chloroform solution (15% w/v) in a sealed tube at 60 Mc./sec. with a Varian HR-60 instrument.

Materials

α MS (Tokyo Chemical Industry) was washed with aqueous 10% NaOH and water, dried over K₂CO₃, and distilled over calcium hydride before use.

Toluene was washed successively with concentrated sulfuric acid, water, aqueous 10% NaOH, and water, dried over CaCl₂, and distilled over metallic sodium.

Chloroform was washed with concentrated sulfuric acid, water, aqueous 10% Na₂CO₃, and water, dried over CaCl₂, and distilled over phosphorus pentoxide.

Methylene chloride was washed with aqueous 10% Na₂CO₃ and water, dried over CaCl₂, and distilled over phosphorus pentoxide.

Nitroethane was washed first with a 10% mixed aqueous solution of NaHSO₃ and NaHCO₃ and with water, dried over CaCl₂, and distilled over calcium hydride.

Nitrobenzene was washed with dilute sulfuric acid, water, aqueous 10% Na₂CO₃, and water, dried over CaCl₂, and distilled over calcium hydride.

BF₃·O(C₂H₅)₂, SnCl₄, TiCl₄ were distilled before use. Trichloroacetic acid (Guaranteed reagent) was used without further purification.

RESULTS

Determination of Steric Structure of P α MS

The three signals of α -methyl protons in the NMR spectrum of P α MS were assigned to isotactic, heterotactic, and syndiotactic triads on the basis of chemical shifts at $\tau = 9.82, 9.57,$ and $9.38,$ respectively.

These positions of the α -methyl proton signals agree with those reported by Brownstein et al.,⁵ Sakurada and Nishioka,⁶ and Braun et al.⁷ No

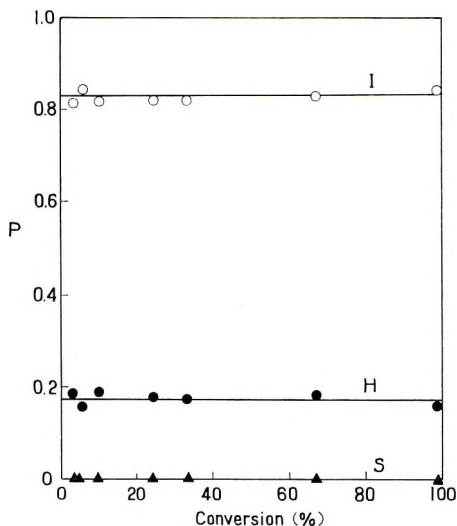


Fig. 1. Relationship between fraction P of three kinds of tacticity and conversion of α MS obtained by $\text{BF}_3 \cdot \text{OEt}_2$ in methylene chloride at -78°C .: (O) isotacticity; (●) heterotacticity; (▲) syndiotacticity. $[M]_0 = 20$ vol.-%; $[\text{BF}_3 \cdot \text{OEt}_2] = 0.024$ mole/l.

final interpretation of NMR spectra of $\text{P}\alpha\text{MS}$ has yet been decided on, but we tentatively adopted the interpretation of Sakurada and Nishioka, because these workers completely analyzed the crystalline structure of isotactic $\text{P}\alpha\text{MS}$ obtained cationically by the x-ray fiber diagram as described in our previous paper.^{8,9}

αMS was polymerized in methylene chloride by $\text{BF}_3 \cdot \text{O}(\text{C}_2\text{H}_5)_2$ at -78°C . The relationship between the steric structure of the polymer and conversion was investigated by NMR spectra. As shown in Figure 1, the isotacticity of the triads of all resultant polymers was independent of conversion over a wide range. Also, this result shows good reproducibility of NMR spectra and the stereoregularity of $\text{P}\alpha\text{MS}$ at constant polymerization conditions.

Effect of Solvent on Steric Structure of $\text{P}\alpha\text{MS}$

αMS was polymerized in a mixed solvent system with $\text{BF}_3 \cdot \text{O}(\text{C}_2\text{H}_5)_2$ as catalyst at -78°C . Toluene, chloroform, and methylene chloride were used as good solvents for the polymer and n -hexane as a nonsolvent. The relationship between the three kinds of tacticity of the polymer, the appearance of the polymerization system, and solvent composition are shown in Figures 2, 3, and 4, respectively.

Atactic $\text{P}\alpha\text{MS}$ was obtained in n -hexane, a non-solvent for the polymer. By addition of a good solvent, the polymerization became homogeneous and the isotactic fraction of $\text{P}\alpha\text{MS}$ increased, independently of the polarity of the solvent. On the other hand, in the homogeneous polymerization of vinyl ethers by cationic catalyst, the isotacticity of polymers decreases upon addition of a polar solvent.²

To study the effect of solubility of the polar species, that is, a catalyst and a growing chain end, on the steric structure of P α MS, nitroethane was used as a polymerization medium. Because *n*-hexane is a nonsolvent for P α MS and polar species, the polymerization was carried out in a mixed solvent of methylene chloride–nitroethane using $\text{BF}_3 \cdot \text{O}(\text{C}_2\text{H}_5)_2$ catalyst

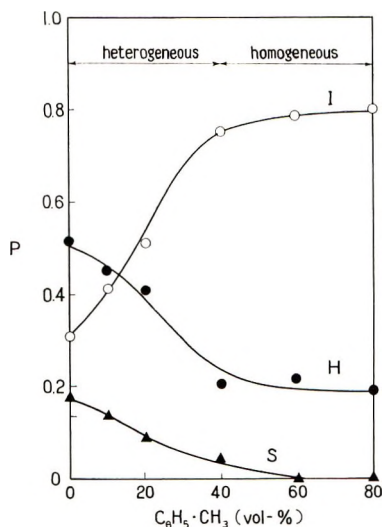


Fig. 2. Relationship between fraction *P* of three kinds of tacticity for P α MS and solvent composition in *n*-hexane–toluene at -78°C .: (O) isotacticity; (●) heterotacticity; (▲) syndiotacticity. $[\text{M}]_0 = 20$ vol.-%; $[\text{BF}_3\text{OEt}_2] = 0.024$ mole/l.; time of polymerization, 90 min.

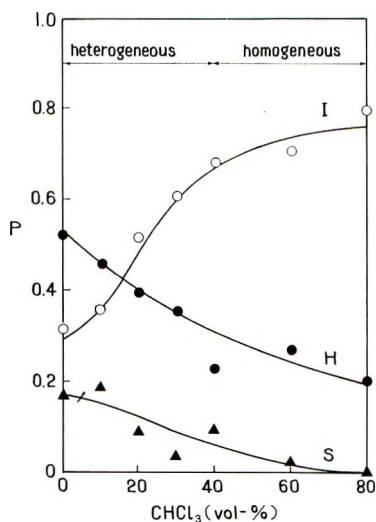


Fig. 3. Relationship between fraction *P* of three kinds of tacticity for P α MS and solvent composition in *n*-hexane–chloroform at -78°C .: (O) isotacticity; (●) heterotacticity; (▲) syndiotacticity. $[\text{M}]_0 = 20$ vol.-%; $[\text{BF}_3 \cdot \text{OEt}_2] = 0.024$ mole/l.; time of polymerization, 90 min.

at -78°C . The relationship between the steric structure of $\text{P}\alpha\text{MS}$ and solvent composition is shown in Figure 5. The polymers were isotactic over the entire solvent composition range.

Also polymerizations were carried out in *n*-hexane containing 2 vol.-% of nitrobenzene which seems preferentially to solvate the growing ion. The

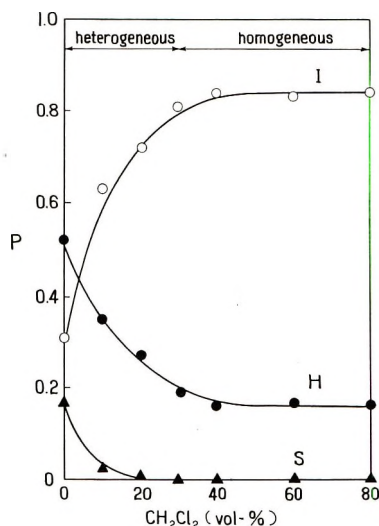


Fig. 4. Relationship between fraction P of three kinds of tacticity for $\text{P}\alpha\text{MS}$ and solvent composition in *n*-hexane-methylene chloride at -78°C .: (O) isotacticity; (●) heterotacticity; (▲) syndiotacticity. $[M]_0 = 20$ vol.-%; $[\text{BF}_3 \cdot \text{OEt}_2] = 0.024$ mole/l.; time of polymerization, 90 min.

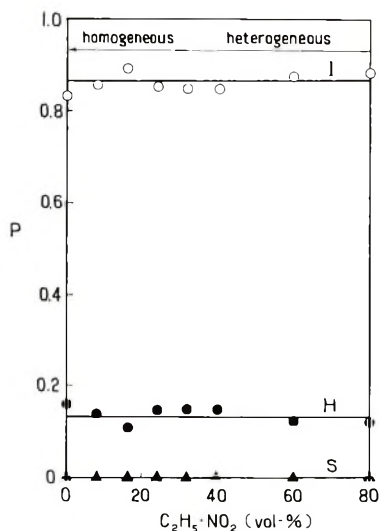


Fig. 5. Relationship between fraction P of three kinds of tacticity for $\text{P}\alpha\text{MS}$ and solvent composition in methylene chloride-nitroethane at -78°C .: (O) isotacticity; (●) heterotacticity; (▲) syndiotacticity. $[M]_0 = 20$ vol.-%; $[\text{BF}_3 \cdot \text{OEt}_2] = 0.024$ mole/l.; polymerization time, 90 min.

resultant polymer exhibited a more isotactic structure than that obtained in pure *n*-hexane. The isotactic content of the latter was about 30%, while that of the former was about 60%. These results seem to indicate that the solubility of the growing ion is an important factor in obtaining stereoregular polymers.

Effect of the Nature of the Catalyst on the Steric Structure of P α MS

The various catalysts used affected only slightly the steric structure of polymers obtained in toluene and in methylene chloride. As shown in Table I, the polymer obtained with $\text{BF}_3 \cdot \text{O}(\text{C}_2\text{H}_5)_2$ was found to have the most isotactic structure. The various catalysts gave almost identical

TABLE I
Effect of Catalysts on Tacticity of P α MS in Toluene and in Methylene Chloride at -78°C .^a

No.	Catalyst	Solvent	<i>I</i> , %	<i>H</i> , %	<i>S</i> , %
7-1	$\text{BF}_3 \cdot \text{O}(\text{C}_2\text{H}_5)_2$	Toluene	83.2	16.8	0
7-2	$\text{SnCl}_4 \cdot \text{TCA}^b$	"	82.4	17.6	0
7-3	$\text{AlBr}_3 \cdot \text{TCA}^b$	"	81.1	15.8	3.1
7-4	TiCl_4	"	78.4	17.7	3.9
11-1	$\text{BF}_3 \cdot \text{O}(\text{C}_2\text{H}_5)_2$	Methylene chloride	84.0	16.0	0
11-2	$\text{SnCl}_4 \cdot \text{TCA}^b$	"	83.6	16.4	0
11-3	$\text{AlBr}_3 \cdot \text{TCA}^b$	"	76.3	21.5	2.2
11-4	TiCl_4	"	77.8	18.9	3.3

^a $[M]_0 = 20$ vol.-%; $[\text{BF}_3 \cdot \text{OEt}_2] = 0.024$ mole/l., time of polymerization, 90 min.

^b TCA = trichloroacetic acid, mole ratio of $[\text{TCA}]/[\text{Cat}] = 0.7$.

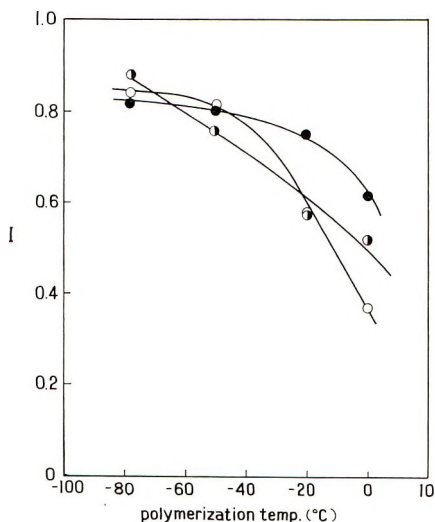


Fig. 6. Effect of polymerization temperature on isotacticity *I* of P α MS obtained with $\text{BF}_3 \cdot \text{OEt}_2$ in various solvents: (●) toluene; (○) methylene chloride; (◐) nitroethane. $[M]_0 = 20$ vol.-%; $[\text{BF}_3 \cdot \text{OEt}_2] = 0.024$ mole/l.; time of polymerization, 90 min.

products in toluene and in methylene chloride solvents. The increase of acidity of catalyst slightly decreased the isotacticity of polymer.

Effect of Polymerization Temperature on the Steric Structure of P α MS

The effect of polymerization temperature was studied in toluene, methylene chloride, and nitroethane. The isotacticity of the polymers decreased with increasing temperature, as shown in Figure 6. The decrease of isotacticity with increasing temperature in polar solvents, i.e., methylene chloride and nitroethane, was found to be stronger than that in nonpolar solvent, e.g., toluene.

As reported previously, the configuration of all P α MS obtained in this paper could be expressed by Bovey's single parameter σ .⁸

DISCUSSION

The experimental results indicate that the steric structure of the polymer is determined by (a) the physical state of the system, i.e., homogeneity or heterogeneity, and (b) temperature. Highly isotactic polymer is obtained in a homogeneous system (good solvent) and at low temperatures. On the other hand, polarity of the solvent and the nature of the catalyst did not considerably affect the stereoregularity of P α MS. This is in contrast to poly(isobutyl vinyl ether) and poly(methyl methacrylate) whose stereospecificity is strongly affected by the polarity of the medium and nature of the catalyst.

The catalyst affected only slightly the steric structure of the polymer. An increase of acidity of catalyst decreased the isotacticity. The dissociation of the ion-pair to growing end and counterion may increase with increasing acidity of the catalyst. With increasing distance between growing carbonium ion and counterion, the stereoregularity was expected to decrease, but the decrease of regularity was not as large as anticipated.

The steric structure was strongly affected by the physical state of the system, but not by the polarity of solvent.

Thus stereoregular P α MS was obtained in toluene and methylene chloride solvents in which the polymerization proceeds in the homogeneous phase. In contrast, in the cationic polymerization of alkyl vinyl ethers, polymer stereoregularity is little affected by the physical state of the polymer.

In homogeneous polymerizations, the interaction between counterion, the substituents of the growing end, and those of the attacking monomer determines the steric configuration of the resulting polymer. Thus in homogeneous systems the monomer attacks the growing end from the least hindered direction. α MS has two α -substituents so that, particularly in good solvents, the steric structure could be determined by the repulsive interaction between the α -methyl groups on the growing ion on the one hand and on the incoming monomer on the other. The details of a similar mechanism have already been reported in the case of vinyl ethers.¹⁰ This interpretation can also be used to explain the results obtained with α MS.

In poor solvents the polymer is forced out of solution, and the increasing monomer cannot attack from the least hindered direction because it encounters additional interference by other polymer segments in the neighborhood of the growing site. Therefore, atactic polymer is obtained in poor solvent. Experiments show that when small amounts of strongly polar solvent (nitrobenzene) are added to a medium containing large proportions as a poor solvent (*n*-hexane), isotactic polymer is formed. It could be that polar solvent which preferentially solvates the growing ion facilitates hindrance to free entry of incoming monomer, thus resulting in increased polymer stereoregularity.

The effect of temperature on stereoregularity was investigated. It was theorized that stereoregularity of P α MS will increase at lower temperature due to increased interaction of α -substituents. Experiments show that the effect of temperature is more pronounced in a polar medium, which could be attributed to decreased interaction between growing carbonium ion and counterion.

The authors thank The Research Institute of Kureha Spinning Co. Ltd. for the measurement of NMR spectra.

References

1. Okamura, S., T. Higashimura, and Y. Imanishi, *J. Polymer Sci.*, **33**, 491 (1958); *Kobunshi Kagaku*, **16**, 129 (1959).
2. Higashimura, T., T. Kodama, and S. Okamura, *Kobunshi Kagaku*, **17**, 163 (1960).
3. Braun, D., M. Herner, U. Johnsen, and W. Kern, *Makromol. Chem.*, **51**, 15 (1962).
4. Kern, R. J., *Nature*, **187**, 410 (1960).
5. Brownstein, S., S. Bywater, and D. J. Worsfold, *Makromol. Chem.*, **48**, 127 (1961).
6. Sakurada, Y., and A. Nishioka, *J. Polymer Sci. B*, **1**, 633 (1963).
7. Braun, D., G. Heufer, U. Johnsen, and K. Kolbe, *Ber. Bunsenges.*, **38**, 959 (1964).
8. Ohsumi, Y., T. Higashimura, and S. Okamura, *J. Polymer Sci. A*, **3**, 3729 (1965).
9. Sakurada, Y., Ph.D. Thesis, (1964); Japan Pat. 11540 (1962).
10. Higashimura, T., T. Yonezawa, S. Okamura, and K. Fukui, *J. Polymer Sci.*, **39**, 487 (1959).

Résumé

La relation entre la stéréorégularité et les conditions de polymérisation de l' α -méthylstyrène ont été étudiée sur la base de spectres NMR. Les effets de solvants et différents catalyseurs Friedel-Crafts ont été examinés. La stéréorégularité du poly- α -méthylstyrène croît avec une solubilité croissante du polymère dans le solvant utilisé et avec une diminution de température de polymérisation. Ce comportement est complètement différent de la polymérisation stéréospécifique d'éthers vinyliques et méthacrylates de méthyle dans des systèmes homogènes. Ceci peut être dû à la répulsion stérique élevée exercée par les deux substituants en position α de l' α -méthylstyrène. Par exemple, utilisant $\text{BF}_3 \cdot \text{O}(\text{C}_2\text{H}_5)_2$ comme catalyseur à -78°C , le polymère atactique est obtenu dans l'hexane normal, un non-solvant pour l' α -méthylstyrène, tandis que du polymère hautement stéréorégulier est produit dans le toluène ou le chlorure de méthylène, bons solvants pour le polymère. Toutefois, la polarité du solvant et la nature du catalyseur affectent fortement la stéréorégularité du polymère.

Zusammenfassung

Die Beziehung zwischen Stereoregularität und Polymerisationsbedingungen bei α -Methylstyrol, nämlich der Einfluss des Lösungsmittels und verschiedener Friedel-

Crafts Katalysatoren wurden an Hand der NMR-Spektren untersucht. Die Stereoregularität von Poly- α -Methylstyrol nahm bei erhöhter Löslichkeit des Polymeren im verwendeten Lösungsmittel und bei Erniedrigung der Polymerisationstemperatur zu. Dieses Verhalten ist völlig von demjenigen der stereospezifischen Polymerisation von Vinyläthern und Methylmethacrylat in homogenen Systemen verschieden. Dies kann durch die starke sterische Abstossung zwischen den beiden Substituenten an der α -Stellung von α -Methylstyrol verursacht sein. Zum Beispiel wird mit $\text{BF}_3 \cdot \text{O}(\text{C}_2\text{H}_5)_2$ als Katalysator bei -78°C in *n*-Hexan, einem nicht-Lösungsmittel für Poly- α -methylstyrol, ein ataktisches Polymeres erhalten, während in Toluol oder Methylenchlorid, guten Lösungsmitteln für das Polymere, hochgradig stereoreguläre Polymere entstehen. Die Polarität des Lösungsmittels und die Natur des Katalysators besitzen jedoch kaum einen Einfluss auf die Stereoregularität des Polymeren.

Received August 11, 1965

Revised September 20, 1965

Prod. No. 4904A

Diffusion of Water Vapor Through a Hydrophilic Polymer Film

THOMAS GILLESPIE, *Physical Research Laboratory*, and BILL M. WILLIAMS, *Plastics Fundamental Research, The Dow Chemical Company, Midland, Michigan*

Synopsis

Multifilm techniques have been used to measure the diffusion coefficient of water vapor in cellophane, and the data have been compared with the integral diffusion coefficient obtained in previous work with single films. The multifilm techniques lead to a much sharper resolution of the effect of concentration on diffusion, and the maximum integral diffusion coefficient. The diffusion coefficient for water vapor in cellophane peaks at a moisture content corresponding to about 70% R.H., which is presumably the "critical concentration" discussed in previous work on the thermodynamics of water sorption by cellophane.

INTRODUCTION

The permeability of a gas through a polymer film is defined¹ by the equation

$$\dot{Q} = (K/L)\Delta p \quad (1)$$

where \dot{Q} is the volume of gas transmitted per unit area per unit time, Δp is the pressure drop across the film, L is the thickness of the film, and K is the permeability. It is well known that K is not a constant if the solubility of the gas in the polymer is pressure-dependent. In a case like this, the permeability increases rapidly as the mean concentration of the gas in the polymer is increased. For example, cellophane, which is hydrophilic, is a reasonably good barrier to the passage of water vapor at low relative humidity; however, as the relative humidity is increased the solubility of water vapor increases rapidly, and the permeability also increases rapidly.

In analyzing experimental data from permeability experiments, it is the usual practice to start with the equation

$$\dot{Q} = -D (dc/dx) \quad (2)$$

where D is the diffusion coefficient and c is the concentration of the gas at a point x .

The gas concentration is related to the gas pressure P by Henry's law,

$$c = Sp \quad (3)$$

where S is the solubility. Substituting eq. (3) in (2) leads to

$$\dot{Q} = (1/L) \int_{p_1}^{p_2} D d(Sp) \quad (4)$$

where $p_2 - p_1$ is the pressure drop, Δp . It is common practice^{1,2} to carry out experiments in which p_1 is zero and to write

$$\dot{Q} = (\bar{D}S_2/L)p_2 \quad (5)$$

S_2 is the solubility of the gas in the polymer at pressure p_2 . D is the integral diffusion coefficient and may be defined² as

$$\bar{D} = (1/c) \int_0^c D dx \quad (6)$$

Comparing eqs. (1) and (5) leads to

$$K = \bar{D}S_2 \quad (7)$$

One particularly interesting result of experiments which have been analyzed with eqs. (5) and (6) is that although the permeability and the solubility increase continuously with p_2 , the integral diffusion coefficient may increase to a maximum and then decrease as p_2 is increased. Such variations in the diffusion coefficient strongly suggest the possibility of using diffusion data as a tool for learning more about the structure of polymeric materials. In this connection we felt that we would get a better resolution of the effect of concentration on diffusion if we were to measure the diffusion coefficient at a specific concentration, D , rather than the integral diffusion coefficient, \bar{D} .

If one considers the diffusion of a gas through a film to be similar to the flow of electricity in a circuit, then a relatively easy method of obtaining small values of dc/dx for substitution in eq. (2) would be to use a number of films in series in a permeability experiment and to measure the concentration of the gas in each film. This is what we have done.

In what follows the diffusion coefficients obtained by using multiple films to obtain relatively small concentration gradients of water vapor across cellophane films are compared with the integral diffusion coefficients obtained by using single films and relatively large concentration gradients.

As we expected, the resolution of the effect of concentration on the diffusion coefficient is considerably better in the experiments with multiple films.

Experimental

The cellophane used was obtained from du Pont de Nemours. The trade name was Dupont PT. It was 0.0012 in. thick.

In one set of experiments the permeability of the cellophane to water vapor was measured by a standard method in which the film was used to seal the top of a shallow dish containing calcium chloride and then the

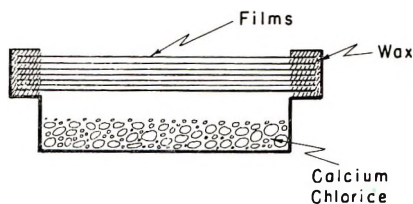


Fig. 1. Schematic diagram of the multiple film-dish apparatus.

sealed dish was placed in a cabinet at a constant relative humidity and constant temperature for 24 hr. The rate of transmission \dot{Q} was calculated from the gain in weight and the area of the cellophane film.

In a second set of experiments, a dish containing calcium chloride was covered with a number of films in series. The dish was first sealed with wax (60% paraffin, 40% beeswax) in the usual manner as illustrated in Figure 1. A thin layer of the wax was then applied to both sides of a second film in a strip bordering on the edge. This second film was then sealed in place over the first film. This procedure was then repeated with subsequent films until a multilayer of the desired number of films covered the dish.

The dish was then placed in the humidity cabinet and weighed at intervals until the rate of increase in weight reached a constant value, indicating equilibrium.

After equilibrium had been reached, the films were quickly removed by cutting out disks, about 2 in. in diameter, with a razor blade. The films were then weighed separately as quickly as possible. The films were dried over calcium chloride and then weighed again in order to be able to calculate the moisture content of each film during the moisture vapor transmission experiment.

In a third set of experiments, a special cell was constructed which consisted of a series of cellophane membranes separated by ring Teflon gaskets. Provisions were made for the insertion of relative humidity sensing elements between the films. The sensing system used was an electronic hygrometer controller obtained from HygroDynamics Inc., Silver Springs, Maryland (Catalog No. 15-3110). The experiments with this multiple cell were conducted in a room controlled at 23°C.

Experimental Results and Discussion

Figures 2 and 3 illustrate results obtained with the multicell apparatus in which the relative humidity between the films was measured. For the polystyrene film which is insoluble in water, one would expect a constant concentration gradient, and Figure 2 is in agreement with this expectation. For the hydrophilic cellophane film there is a marked variation in the concentration gradient (see Fig. 3).

The diffusion of gas through a polymer film is analogous to the flow of electricity in a circuit, with eq. (2) being comparable to Ohm's law. \dot{Q}

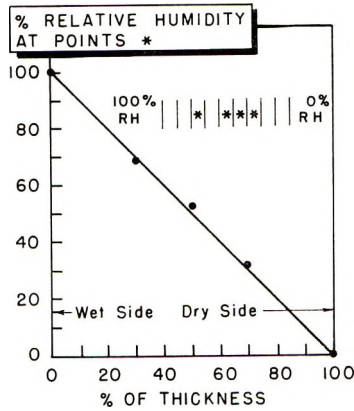


Fig. 2. Typical results obtained with the multicell apparatus with a hydrophobic film (polystyrene).

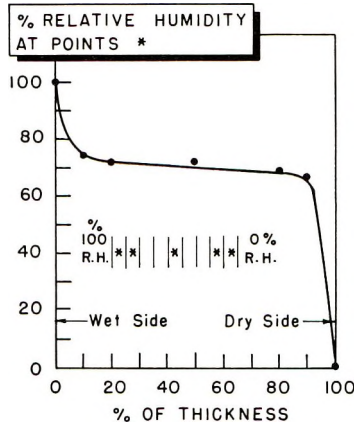


Fig. 3. Typical results obtained with the multicell apparatus with cellophane.

is analogous to the current, dc/dx is analogous to the potential gradient, and D is analogous to the conductance. Utilizing this analogy one can see from Figure 2 that the diffusion of water vapor through cellophane is relatively very rapid when the mean relative humidity is of the order of 70%.

In order to calculate the diffusion coefficients as a function of the concentrations of water in the cellophane film, we needed a curve relating the water concentration in cellophane to the relative humidity. The required data were obtained in a separate experiment by a weighing method and are given in Figure 4.

Figure 5 illustrates the results obtained with the dishes covered with several films of cellophane. These results are essentially the same as those which were obtained with the multicell apparatus. The data indicate again a marked change in the concentration gradient across the

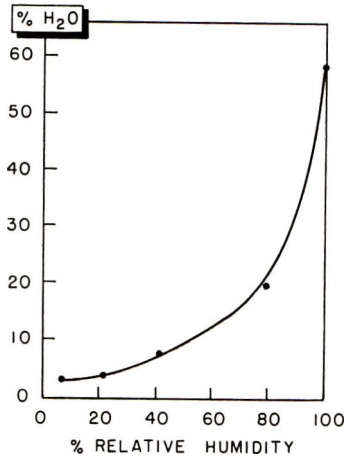


Fig. 4. Water sorption curve for cellophane.

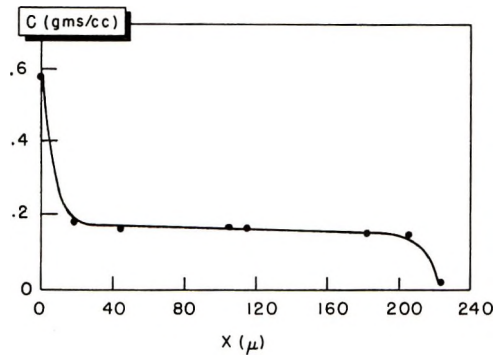


Fig. 5. Typical results obtained with the multiple film-dish apparatus with cellophane.

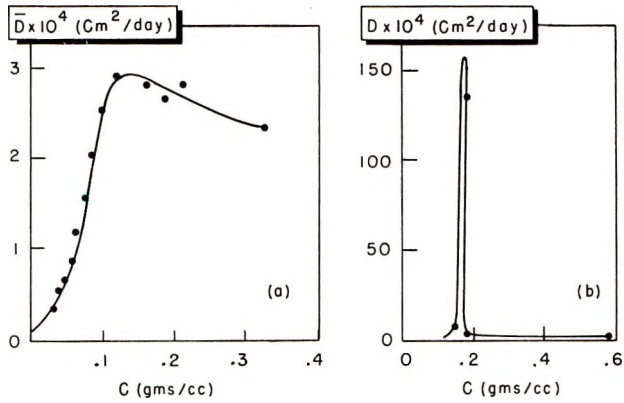


Fig. 6. Comparison of the diffusion coefficients calculated from eq. (2) and the integral diffusion coefficients.

system and the same relatively high diffusion rate at a water concentration corresponding to a relative humidity of about 70%.

In Figures 6*a* and 6*b*, the diffusion coefficients calculated from eq. (2) are compared with the integral diffusion coefficients. The resolution of the effect of concentration is much sharper with the multilayer method and the maximum diffusion coefficients is much larger.

Because of its sharper resolution of concentration effects, we expect that the multilayer method will be a very useful tool which will give us more insight into problems involving the structure of polymeric materials than we have been able to get in the past by the measurement of integral diffusion coefficients.

In this connection, and with particular reference to the cellophane-water system, the reader is referred to an article by Simril and Smith³ in which it is pointed out that at 30°C. there is a critical moisture content, corresponding to about 65%, at which a machine-cast sample of cellophane begins to free itself of strains imposed by drying under tension, as indicated by shrinkage in both the machine and transverse directions. These authors also state that at this humidity, the film first becomes permeable to water-soluble gases. While this statement is only true in a relative sense, there seems no doubt from the present work that there is a critical concentration at which the diffusion coefficient peaks.

A referee has suggested that it would be interesting to apply Rouse's method⁴ to our data for multiple films. Rouse's theory leads to

$$D = \frac{d}{dc} (\bar{D}c) \quad (8)$$

When this equation is applied to data such as those illustrated in Figure 6*a*, the values of D show a sharper dependence on concentration than that exhibited by \bar{D} . However, the dependence is not nearly as sharp as that illustrated in Figure 6*b*. Furthermore, the maximum D is considerably smaller and occurs at a lower concentration. We do not know why there should be these differences, but we suspect that swelling of the film may be a contributing factor.

References

1. Barrer, R. M., *Diffusion in and through Solids*, MacMillan, New York, 1941.
2. Sobolev, I., J. A. Meyer, V. Stannett, and M. Szwarc, *Ind. Eng. Chem.*, **49**, 441 (1957).
3. Simril, V. L., and S. Smith, *Ind. Eng. Chem.*, **34**, 226 (1942).
4. Rouse, P. E., *J. Am. Chem. Soc.*, **69**, 1068 (1947).

Résumé

Des techniques multifilms ont été utilisées pour mesurer le coefficient de diffusion de la vapeur d'eau dans la cellophane et les résultats ont été comparés avec le "coefficient de diffusion intégral," obtenu dans un travail antérieur avec des films simples. La technique multifilm permet d'obtenir des résolutions beaucoup plus grandes de l'effet de la concentration sur la diffusion et le coefficient de diffusion maximum est

beaucoup plus important que le coefficient de diffusion maximum intégral. Le coefficient de diffusion pour la vapeur d'eau dans la cellophane montre un maximum à une teneur en humidité correspondant à 70%, ce qui est vraisemblablement la "concentration critique," discutée dans un travail antérieur concernant la thermodynamique de la sorption d'eau dans la cellophane.

Zusammenfassung

Mehrfachfilmverfahren wurden zur Messung des Diffusionskoeffizienten von Wasserdampf in Zellophan verwendet und die Ergebnisse mit den in einer früheren Arbeit mit Einfachfilmen erhaltenen "integralen Diffusionskoeffizienten" verglichen. Mehrfachfilmverfahren ergaben eine bedeutend schärfere Auflösung des Konzentrationseinflusses auf die Diffusion und der maximale Diffusionskoeffizient ist bedeutend grösser als der maximale integrale Diffusionskoeffizient. Der Diffusionskoeffizient für Wasserdampf in Zellophan erreicht ein Maximum bei einem Feuchtigkeitsgehalt entsprechend einer relativen Feuchtigkeit von etwa 70%, welche wahrscheinlich der in der früheren Arbeit über die Thermodynamik der Wassersorption durch Zellophan diskutierten "kritischen Konzentration" entspricht.

Received June 17, 1965

Revised August 19, 1965

Prod. No. 4906A

Nuclear Magnetic Resonance and X-Ray Determination of the Structure of Poly(vinylidene Fluoride)*

J. B. LANDO,† H. G. OLF, and A. PETERLIN, *Camille Dreyfus
Laboratory, Research Triangle Institute, Durham, North Carolina*

Synopsis

In this study, wide-line NMR and x-ray diffraction have been used in conjunction to study the crystal structure of poly(vinylidene fluoride). Drawn poly(vinylidene fluoride) film was found to contain two crystal phases, the relative amounts of each depending on the draw temperature. Drawing at 50°C. yields a single phase, designated as phase I, while drawing at temperatures between 120 and 160°C. yields a mixture of phase I and a second phase (phase II). The fraction of phase II increases with increasing draw temperature, but this phase was never obtained without some phase I. A tentative orthorhombic unit cell is proposed for phase II. The structure of phase I has been determined from x-ray data. The unit cell is orthorhombic, space group $Cm2m$, having lattice constants $a = 8.47$, $b = 4.90$, and c (chain axis) = 2.56 Å. There are two polymer chains in this unit cell. The conformation of the polymer chains is planar zigzag. The details of this structure have been confirmed by experimentally determining at -196°C . the change in the NMR second moment with the angle between the magnetic field and the draw direction of phase I (drawn at 50°C.), and by comparing these results with a theoretical calculation of the second moments, based on the atomic positions obtained from the proposed structure.

INTRODUCTION

In this study of the crystal structure of poly(vinylidene fluoride), wide-line nuclear magnetic resonance has been used to lend additional support to the conclusions drawn from x-ray data. The usual application of NMR to the determination of crystal structures has been in the determination of the positions of the hydrogen atoms in the unit cell of crystals of low molecular weight,¹⁻³ a task which cannot usually be accomplished by the x-ray method because of the small scattering factor of hydrogen atoms.

The utility of NMR in the determination of the crystal structure of polymers is enhanced by two basic factors. Firstly, the number of x-ray reflections and the accuracy with which the relative intensities of these reflections can be measured are severely limited in many polymers by such factors as degree of crystallinity, small crystallite size, and the degree of

* Presented before the Division of Polymer Chemistry, 150th Meeting American Chemical Society, Atlantic City, New Jersey, September 15, 1965.

† Present address: Case Institute of Technology, Cleveland, Ohio.

orientation of the polymer chains. For example, in the case of poly(vinylidene fluoride) the fact that approximately 5% of the monomer units are reversed along the polymer chain has been established by high-resolution fluorine NMR.^{4,5} We have verified these results for the samples we have used and thus a limitation on the degree of crystallinity of poly(vinylidene fluoride) can be expected.

The second major factor enhancing the use of NMR in polymer structure determination is the fixed angular relationship between the hydrogen-hydrogen vector of a backbone methylene and the chain axis. That the NMR second moment is sensitive to differences in this angle has been established for polyethylene and polyoxymethylene.⁶ In that study the experimental dependence of the second moment on the angle between the draw direction of drawn polymer samples and the magnetic field was measured at -196°C ., a temperature at which the second moment no longer changes with decreasing temperature. The rigid lattice second moment was then calculated theoretically as a function of this angle with the aid of van Vleck's formula⁷ and the known polyethylene and polyoxymethylene unit cell parameters. The experimental results for the polyoxymethylene helix and the polyethylene zigzag were markedly different. However, the experimental values of each polymer agreed very well with the respective theoretical calculations.

Since the validity of this NMR method has been verified by the work, described above, on polymers of well established crystal structure, we have used this method to support the previously unreported structure, obtained from x-ray data, of poly(vinylidene fluoride) drawn at 50°C .

EXPERIMENTAL

Sample Preparation

Poly(vinylidene fluoride), melting point 171°C ., was obtained from the Pennsalt Chemical Corporation. Films were pressed from this material at 190°C . Samples of this film were drawn at temperatures from 50 to 160°C . at an extension rate of approximately 1 cm./min. to a draw ratio of about 4:1. Some of the drawn samples were rolled parallel to the draw direction at room temperature in an attempt to obtain biaxial orientation.

X-Ray Diffraction

All x-ray photographs were obtained with $\text{CuK}\alpha$ radiation, using a Weissenberg camera having a radius of 28.7 mm. Drawn samples were examined by taking x-ray photographs with the beam normal to the polymer film and with the draw direction (chain axis) parallel to the axis of the cylindrical camera. Reflections from planes perpendicular to the chain axis were obtained by taking 180° oscillation photographs with the draw direction aligned perpendicular to the camera axis (oscillation axis). Relative intensities of x-ray reflections from photographs taken with a

sample drawn at 50°C. were obtained by visual comparison to a standard set of intensity spots⁸ and by making the appropriate Lorentz-polarization, spot-size, and absorption corrections.^{9,10}

Weissenberg photographs were obtained from samples drawn at 120°C. and subsequently rolled, the draw direction being parallel to the oscillation axis.

Wide-Line Nuclear Magnetic Resonance

A modified⁶ Varian dual-purpose NMR spectrometer operating at 60 Mc./sec. was used to obtain the proton NMR spectra at -196°C. of poly(vinylidene fluoride) film, drawn at 50°C., at different values of the angle between the draw direction and the magnetic field. The peak to peak sweep amplitude used was 1.1 gauss. Experimental second moments were determined from these spectra.

RESULTS

X-Ray Diffraction

X-ray photographs of poly(vinylidene fluoride) samples drawn at temperatures between 50 and 160°C. are shown in Figure 1. These pictures were obtained with the beam normal to the polymer film and the draw direction parallel to the axis of the camera. It can readily be seen that the diffraction pattern changes with increasing draw temperature. The sample drawn at 50°C. was found to exist in a single crystalline phase, subsequently referred to as phase I. The samples drawn at higher temperatures are a mixture of phase I and another crystalline phase, designated phase II. The fraction of phase II increases with increasing draw temperature. Figure 1*e* shows that a sample drawn at 120°C. and subsequently rolled parallel to the draw direction at room temperature is converted almost completely to phase I.

Since drawn samples of poly(vinylidene fluoride) crystallized in phase II could not be obtained without the presence of considerable phase I and since many of the equatorial reflections of phase II appear very close to those of phase I, a complete x-ray analysis of phase II has not as yet been possible. However, it is possible to ascertain from the spacings of the first and second layer lines (Figure 1*d*) (4.64 and 2.32 Å., respectively) that the polymer chain should have a 2/1 helical conformation. An orthorhombic unit cell, having axes $a = 9.66$ Å., $b = 4.96$ Å., c (chain axis) = 4.64 Å. and a possible space group $Pna2_1$ (no. 33)¹⁰ has been tentatively assigned to phase II. These data would require two polymer chains and four monomer units in the unit cell and a density of 1.90 g./cc.

A complete analysis of the structure of phase I has been made from poly(vinylidene fluoride) film drawn at 50°C. Relative intensity data have been obtained from photographs such as that shown in Figure 1*a*, while the relative intensities of the (001) and (002) reflections were determined from

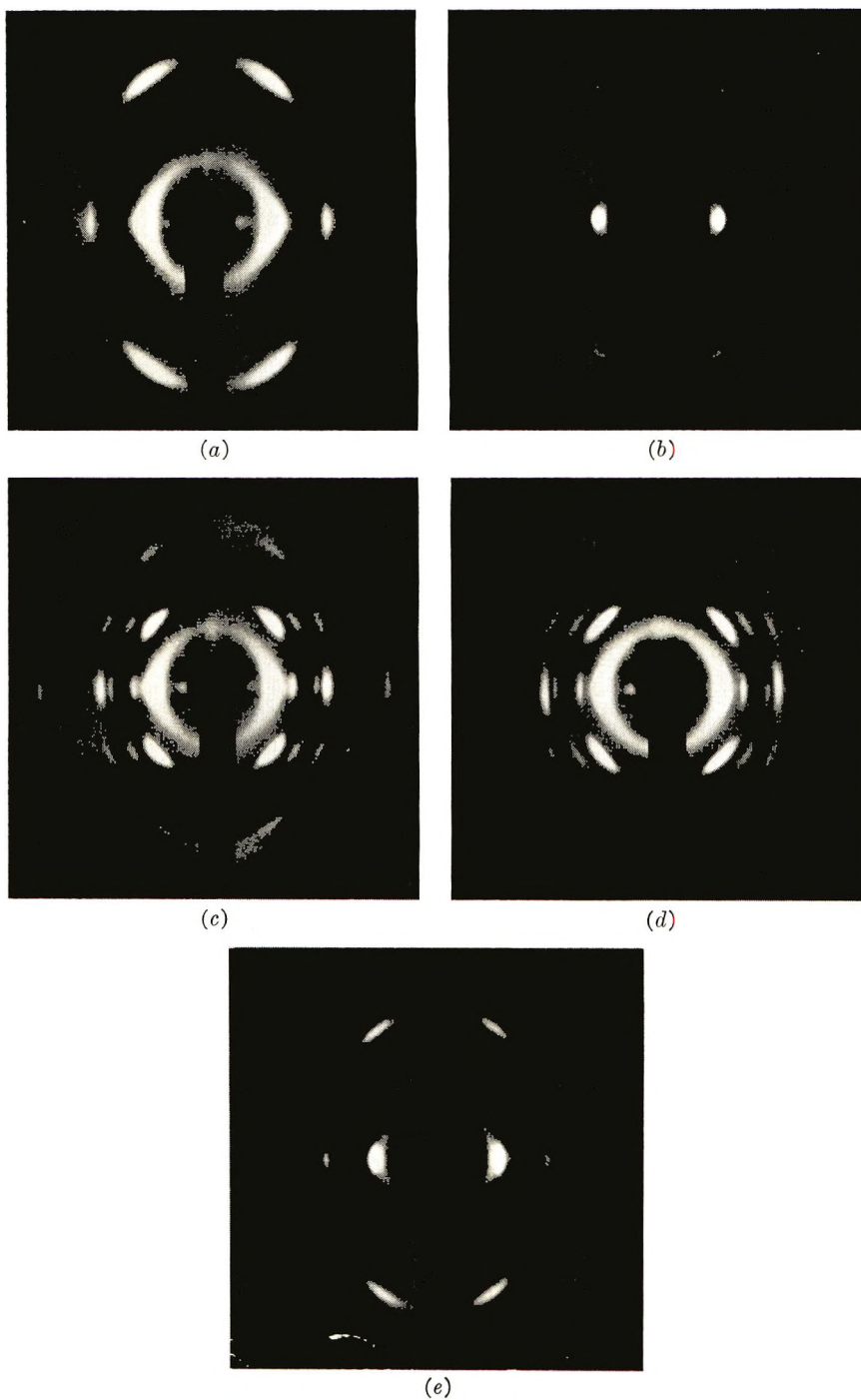


Fig. 1. Change in x-ray diffraction pattern of drawn poly(vinylidene fluoride) with draw temperature: (a) drawn at 50°C.; (b) drawn at 120°C.; (c) drawn at 140°C.; (d) drawn at 160°C.; (e) drawn at 120°C., then rolled at room temperature.

TABLE I
Comparison of Calculated and Observed Intensities

Index and multiplicity	Corrected observed intensity, KI_{obs}	Corrected calculated intensity, $I_{\text{calc}} \exp\{-2B \sin^2 \theta / \lambda^2\}$
2(110) + (200)	1710	1540
2(310) + (020)	720	836
2(220) + (400)	92	109
2(510) + 2(420) + 2(130)	444	481
2(330) + (600)	65	86
2(620) + (040)	24	10
2(710) + 2(530) + 2(240)	39	47
2(111) + (201)	605	665
2(311) + (021)	175	268
2(221) + (401)	99	150
2(511) + 2(421) + 2(131)	67	108
2(331) + (601)	96	76
(001)	553	554
(002)	174	172

TABLE II
Proposed Atomic Positions in Unit Cell of Phase I^a

	x	y	z
Fluorine 1	0.130	0.000	0.500
2	0.870	0.000	0.500
3	0.630	0.500	0.500
4	0.370	0.500	0.500
Carbon A 1	0.000	0.158	0.500
2	0.500	0.658	0.500
Carbon B 1	0.000	0.334	0.000
2	0.500	0.834	0.000

^a x , y , and z are the fractions of the unit cell in the a , b , and c directions, respectively.

180° oscillation photographs taken with the draw direction of the sample aligned perpendicular to the camera axis. These data are listed in Table I.

Phase I crystallizes in an orthorhombic unit cell having systematic absences corresponding to space group $Cm2m$ (no. 38),¹⁰ with lattice constants $a = 8.47$, $b = 4.90$, c (chain axis) = 2.56, and an x-ray determined density of 2.00 g./cc. There must be two polymer chains and two monomer units in this unit cell. The c axis spacing of 2.56 Å. indicates a planar zigzag conformation of the chain with the carbon-carbon-carbon bond angle opened to 112°20'. Since all reflections on photographs such as Figure 1a for a unit cell having these lattice constants are really superpositions of two or more independent reflections only the sum of the intensities of these reflections could be experimentally determined.

It should be noted that the reflections in Figure 1a can be indexed in an apparent hexagonal unit cell with $a = b = 4.90$ Å. and $c = 2.56$ Å. How-

ever, a review of the possible space groups¹⁰ indicated that this polymer chain could not crystallize in a hexagonal unit cell. Also, it was found from Weissenberg photographs of a rolled sample that reflections which should have equal intensity in a hexagonal unit cell were, in fact, different. However, the biaxial orientation was not sufficient to obtain good relative intensities.

By using the space group $Cm2m$ and the restrictions on atomic position imposed by the polymer chain, it was possible to determine that the four fluorine atoms must lie on the special positions $(xy^{1/2})(x + 1/2, y + 1/2, 1/2)$ $(\bar{x}y^{1/2})(\bar{x} + 1/2, y + 1/2, 1/2)$ and the four carbon atoms on the two sets of special positions $(0y^{1/2})(1/2, y + 1/2, 1/2)$ and $(0y0)(1/2, y + 1/2, 0)$. On taking the carbon-carbon bond as 1.541 Å,¹⁰ the carbon-fluorine bond as 1.344 Å,¹⁰ and the fluorine-carbon-fluorine bond angle as $109^\circ 28'$,¹¹ in conjunction with the above-mentioned data, it was possible to arrive at the atomic positions listed in Table II.

The intensity $I_{(hkl)}$ of individual x-ray reflections was calculated from the equation¹⁰

$$I_{(hkl)} = \left(\sum_r f_r A_r \right)^2 + \left(\sum_r f_r B_r \right)^2$$

where r designates the atom being considered, f_r is the scattering factor for the r th atom and

$$A_r = \cos 2\pi hx, \cos 2\pi ky, \cos 2\pi lz,$$

and

$$B_r = \cos 2\pi hx, \sin 2\pi ky, \cos 2\pi lz,$$

In Table I the corrected observed relative intensities of x-ray reflections are compared to the calculated values after temperature factor correction and normalizing. The value of the temperature factor constant B for $(00l)$ reflections was found to be 3.8, while for the remaining reflections a value of 7 was found. The proportionality constant K between calculated and observed reflections was found to be 0.235 for $(00l)$ reflections and 0.311 for the remaining reflections. It should be noted that for (hkl) reflections only approximate absorption corrections of observed intensities were made. The experimentally observed intensities of these reflections along with all other reflections having a nonzero l index will be most affected by the head-to-head monomer component along the chain.

The agreement between observed and calculated x-ray intensities is very good indicating that the proposed structure represented in Figure 2 is very probable. However, the experimental x-ray data is limited. Also the distance between fluorine atoms along the chain in the proposed planar conformation is only 2.56 Å. (2.70 Å. would be twice the van der Waals radius of fluorine). Therefore, supporting evidence for the planar zigzag conformation appears necessary.

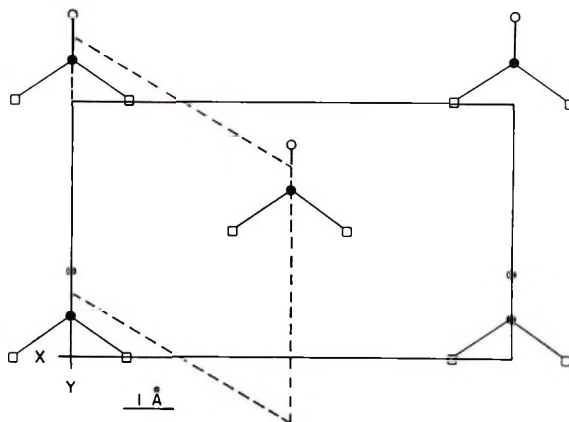


Fig. 2. Representation of the structure of poly(vinylidene fluoride) drawn at 50°C.; Projection onto (ab) plane: $X = ax$, $Y = by$, (\bullet) carbon, $Z = 1/2c$; (\circ) carbon, $Z = 0$; (\square) fluorine, $Z = 1/2c$.

Nuclear Magnetic Resonance

The second moment of poly(vinylidene fluoride) film, drawn at 50°C. (phase I), as a function of the angle between the magnetic field and the draw direction was obtained from the corresponding NMR spectra at -196°C . At this temperature the second moment does not vary with decreasing temperature. The experimental second moment $\langle \Delta H^2 \rangle_{\text{exp}}$ is defined for a given angle as

$$\langle \Delta H^2 \rangle_{\text{exp}} = \int_{-\infty}^{+\infty} f(H)(H - H_0)^2 dH / \int_{-\infty}^{+\infty} f(H) dH$$

where $f(H)$ is the NMR absorption as a function of the magnetic field and H_0 is the value of the magnetic field at the center of resonance. By using the atomic positions of the proposed structure and assuming the carbon-hydrogen bond length to be 1.094 Å. and the hydrogen-carbon-hydrogen bond angle to be $109^\circ 28'$, the second moment for a rigid lattice was also calculated theoretically from a modified⁶ van Vleck equation⁷ as applied to a uniaxially oriented system containing two nuclear species with nonzero spin.

$$\begin{aligned} \langle \Delta H^2 \rangle(\gamma)_{\text{calc}} &= \frac{3}{16} I(I+1)g^2\mu_0^2N^{-1} \\ &\quad \times \left(9 \cos^4 \gamma \sum_{j>k} A_{jk} - 6 \cos^2 \gamma \sum_{j>k} B_{jk} \times \sum_{j>k} C_{jk} \right) \\ &+ \frac{1}{24} I_F(I_F+1)g_F^2\mu_0^2N^{-1} \\ &\quad \times \left[9 \cos^4 \gamma \sum_{j,f} A_{jf} - 6 \cos^2 \gamma \sum_{j,f} B_{jf} + \sum_{j,f} C_{jf} \right] \end{aligned}$$

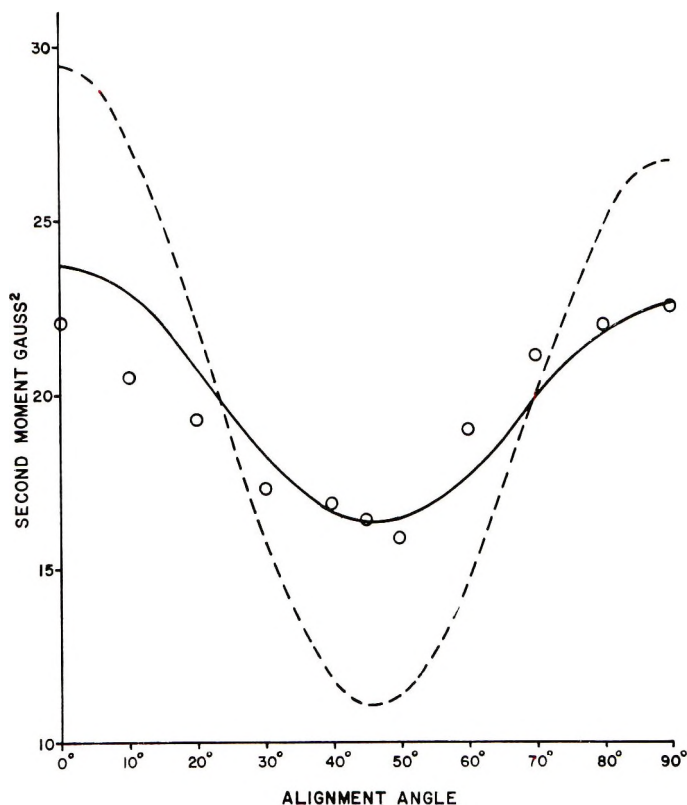


Fig. 3. Plot of the NMR second moment of poly(vinylidene fluoride) drawn at 50°C. against alignment angle: (---) calculated theoretical curve; (—) corrected theoretical curve; (O) experimental points.

In this equation γ is the alignment angle between the magnetic field and the draw direction, I , I_F are the nuclear spin numbers of the proton and the fluorine nucleus, respectively, g , g_F are the nuclear g factors, μ_0 is the nuclear magneton, and N is the number of protons over which the sums are taken. The quantities A , B , and C are defined as:

$$A_{jk} = (35 \cos^4 \theta'_{jk} - 30 \cos^2 \theta'_{jk} + 3)r_{jk}^{-6}$$

$$B_{jk} = (45 \cos^4 \theta'_{jk} - 42 \cos^2 \theta'_{jk} + 5)r_{jk}^{-6}$$

$$C_{jk} = (27 \cos^4 \theta'_{jk} - 30 \cos^2 \theta'_{jk} + 11)r_{jk}^{-6}$$

Here θ'_{jk} is the angle between the draw direction and the vector joining the nuclei j and k and r_{jk} is the internuclear distance.

As can be seen in Figure 3 both the theoretical curve and the experimental points have the same general shape with a minimum at 45°, indicating the probability of a planar zigzag conformation. However the agreement between the theoretical curve and the experimental points is not good. This was to be expected since the former was determined under the assump-

tion of ideal orientation of the polymer chains in the draw direction. The actual sample deviated from the theoretical model in that x-ray photographs show an appreciable more or less unoriented amorphous halo and imperfect crystallite orientation. In addition the presence of head-to-head linkages^{4,5} implies that parts of oriented chains may not have methylene hydrogen-to-hydrogen vectors perpendicular to the draw direction.

With a simple correction to the theoretical curve we can take these factors into account. Let us assume a mass fraction X of material that is isotropically distributed. The second moment of this isotropic fraction $\langle \Delta H^2 \rangle_{is}$ does of course not depend on the alignment angle. The total second moment $\langle \Delta H^2 \rangle_{tot}$ is given by

$$\langle \Delta H^2 \rangle_{tot} = (1 - X)\langle \Delta H^2 \rangle_{calc} + X\langle \Delta H^2 \rangle_{is}$$

A value for $\langle \Delta H^2 \rangle_{is}$ of 19.9 is obtained by averaging the experimental curve over the solid angle. Now X is so adjusted that $\langle \Delta H^2 \rangle_{tot}$ fits the experimental curve in the minimum at 45° . The value obtained for X of 0.60, being a measure of total disorientation, should not be confused with the amorphous fraction. As seen in Figure 3, the $\langle \Delta H^2 \rangle_{tot}$ curve thus obtained agrees quite well with the experimental points. The proposed crystal structure of poly(vinylidene fluoride) obtained from the x-ray data is therefore in agreement with the NMR measurements.

DISCUSSION

The origin of the pseudo-hexagonal character of the x-ray photographs of phase I of poly(vinylidene fluoride) can easily be seen from Figure 2. The dashed lines represent the base plane of the pseudo-hexagonal cell. It is apparent that there is not true hexagonal symmetry. This phenomenon apparently occurs in other vinyl polymers. Poly(vinyl fluoride), which has been reported to have a planar zigzag conformation and to crystallize in a hexagonal unit cell,¹² yields x-ray fiber patterns¹² with the same reflections as in Figure 1a, having only slightly different spacings. Apparently the true unit cell of poly(vinyl fluoride) is also orthorhombic, space group $Cm2m$.¹³ Another example is syndiotactic polyacrylonitrile, which has been reported to have a planar zigzag conformation¹⁴ and to crystallize in a hexagonal¹⁵ and an orthorhombic¹⁴ unit cell. The relationship between the lattice constants of the hexagonal and orthorhombic unit cells reported for acrylonitrile is the same as that between the pseudo-hexagonal and the true orthorhombic unit cells of poly(vinylidene fluoride). Therefore it is probable that the true unit cell of syndiotactic polyacrylonitrile is orthorhombic.

As has been seen, the chain conformation in drawn poly(vinylidene fluoride) film is markedly influenced by draw temperature. Apparently drawing at low temperature pulls out the polymer helix (phase II) into a planar zigzag conformation (phase I). This phenomenon may be influenced by the fact that the density of phase I is apparently greater than

that of phase II. The mixtures of the two phases obtained when drawing is carried out between 120 and 160°C. apparently explain the lattice constants previously reported for poly(vinylidene fluoride).¹⁶

The most unusual feature of the structure of phase I, as determined from the x-ray data and confirmed by NMR measurements, is the fluorine-fluorine spacing along the chain axis of 0.14 Å. less than twice the van der Waals radius of fluorine. Therefore, the fluorine atoms must be crowded along the chain axis and it is to be expected that atomic motion will be restricted along the *c* axis. This conclusion is supported by the fact that the (00*l*) x-ray reflections appear to have a temperature factor ($B = 3.8$) far less than that for reflections having nonzero *h* and *k* indices ($B = 7.0$).

Note Added in Proof. The authors wish to thank one of the referees for calling our attention to a recently published article by E. L. Galperin, Yu. V. Strogalin, and M. P. Mlenik, *Vysokomol. Soedin.*, **7**, No. 933 (1965) entitled "Crystalline Structure of Poly(vinylidene Fluoride)." These authors also report the existence of two crystalline forms of poly(vinylidene fluoride). They find the same space group ($Cm2m$) and lattice constants as we do for the form we have designated phase I. However, noting the crowding of the fluorine atoms along the chain axis assuming a planar zigzag conformation, they have tentatively proposed that the CF_2 groups are twisted out of this conformation, neighboring CF_2 groups twisting in opposite directions. They recognize that this would double the repeat distance along the chain axis and would mean that an intermediate layer line, which is absent, should appear. However they apparently ignore the fact that this chain conformation is not compatible with the space group $Cm2m$. Since the necessary twist is not negligible ($\sim 10^\circ$), we feel that our interpretation of the structure of phase I, a planar zigzag conformation with large torsional motions, is probably correct.

Galperin et al. have reported a monoclinic unit cell with a β angle of $87^\circ 17'$ for the form we have designated phase II. With the data we have at present we cannot differentiate between the fit of their lattice constants and those of the orthorhombic cell we have tentatively proposed. However, we agree with the almost planar *cis* chain conformation they propose for phase II, this being a special case of a 2_1 helix. We intend to discuss phase II in greater detail in a later publication.

The authors wish to express their appreciation for the financial support of this work by the Camille and Henry Dreyfus Foundation. They also wish to thank Dr. W. D. Silcox Jr., of Pennsalt Chemicals Corporation for providing them with the PVF samples used.

References

1. Pake, G. E., *J. Chem. Phys.*, **16**, 327 (1948).
2. Gutowsky, H. S., G. B. Kistiakowsky, G. E. Pake, and E. M. Purcell, Jr., *J. Chem. Phys.*, **17**, 972 (1949).
3. Behrsohn, R., and H. S. Gutowsky, *J. Chem. Phys.*, **23**, 651 (1954).
4. Naylor, R. E., and S. W. Lasoski, *J. Polymer Sci.*, **44**, 1 (1960).
5. Wilson, C. W., *J. Polymer Sci. A*, **1**, 1305 (1963).
6. Olf, H. G., and A. Peterlin, *J. Appl. Phys.*, **35**, 3109 (1964).
7. van Vleck, J. H., *Phys. Rev.*, **74**, 1168 (1948).
8. Buerger, M. J., *Crystal Structure Analysis*, Wiley, New York, 1960, p. 86.
9. Philips, D. C., *Acta Cryst.*, **9**, 819 (1956).
10. *International Tables for X-ray Crystallography*, Vols. I, II, III, Kynoch Press, Birmingham, England, 1962.
11. Stuart, H. A., *Die Physik der Hochpolymeren*, Vol. I, Springer-Verlag, Berlin, Germany, 1952, p. 171.

12. Golike, R. C., *J. Polymer Sci.*, **42**, 583 (1960).
13. Natta, G., I. W. Bassi, and G. Allegra, *Atti Accad. Nazl. Lincei, Rend. Classe Sci. Fis. Mat. Nat.*, **31**, 350, 1961.
14. Stefani, R., N. Chevreton, M. Garnier and C. Eyraud, *Compt. Rend.*, **251**, 2174 (1960).
15. Natta, G., F. Danusso, and P. Corradini, *Atti Accad. Nazl. Lincei, Rend. Classe Fis. Mat. Nat.*, **25**, 3 (1958).
16. Leshchenko, S. S., V. L. Karpov, and V. A. Kargin, *Vysokomol. Soedin.*, **1**, 1538 (1959).

Résumé

Dans cette étude la résonance nucléaire magnétique a larges bandes et la diffraction aux rayons-X ont été utilisées en conjonction afin d'étudier la structure cristalline du fluorure de polyvinylidène. Un film étiré de fluorure de polyvinylidène contient deux phases cristallines, dont les quantités relatives dépendent de la température d'étirement. Par étirement à 50°C, on obtient une phase unique désignée phase I, tandis que l'étirement à température entre 120 et 160°C fournit un mélange de phase I et de phase II. La fraction de phase II croît avec une température croissante d'étirement, mais cette phase ne peut jamais être obtenue sans la présence de phase I. Une cellule unitaire orthorhombique est proposée à titre explicatif pour la phase II. La structure de la phase I a été déterminée par des données aux rayons-X. La cellule unitaire est orthorhombique la groupe spatial $Cm2m$, ayant des constantes de réseaux $a = 8.47$, $b = 4.90$ et c (axe de la chaîne) = 2.56 Å. Il y a deux chaînes polymériques dans cette cellule unitaire. La conformation des chaînes polymériques est plane en zig-zag. Les détails de cette structure ont été confirmés expérimentalement en déterminant à -196°C le changement de second moment NMR avec l'angle entre le champ magnétique et la direction d'étirement de la phase I (étirée à 50°C) et en comparant ces résultats avec un calcul théorique de second moment, utilisant des positions atomiques obtenues au départ des structures proposées.

Zusammenfassung

In der vorliegenden Untersuchung wurden Breitlinien-NMR und Röntgenbeugung gemeinsam zur Untersuchung der Kristallstruktur von Polyvinylidenfluorid verwendet. Es zeigte sich, daß ein gereckter Polyvinylidenfluoridfilm zwei Kristallphasen enthält, deren relative Menge von der Reckungstemperatur abhängt. Reckung bei 50°C liefert eine einzelne Phase, als Phase I bezeichnet, während Reckung bei Temperaturen zwischen 120 und 160°C eine Mischung der Phase I und einer zweiten Phase (Phase II) liefert. Der Bruchteil an Phase II nimmt mit steigender Reckungstemperatur zu, jedoch wurde diese Phase niemals ohne einen Anteil an Phase I erhalten. Vorläufig wird für Phase II eine orthorhombische Elementarzelle vorgeschlagen. Die Struktur der Phase I wurde aus Röntgendaten bestimmt. Die Elementarzelle ist orthorhombisch, Raumgruppe $Cm2m$, mit den Gitterkonstanten $a = 8,47$, $b = 4,90$ und c (Kettenachse) = 2,56 Å. Die Elementarzelle enthält zwei Polymerketten. Die Polymerketten besitzen eine ebene Zickzackkonformation. Die Einzelheiten dieser Struktur wurden durch experimentelle Bestimmung der Abhängigkeit des zweiten NMR-Moments vom Winkel zwischen Magnetfeld und Reckungsrichtung von Phase I (gereckt bei 50°C) bei -196°C sowie durch Vergleiche dieser Ergebnisse mit einer theoretischen Berechnung der zweiten Momente mit den aus der vorgeschlagenen Struktur erhaltenen Atomlagen bestätigt.

Received July 26, 1965

Revised October 12, 1965

Prod. No. 4938A

Application of the Flory-Mandelkern Equation to Individual Unfractionated Polymer Samples

MAURYCY KALFUS and JAN MITUS, *Research and Development Department, Oświęcim Chemical Works, Oświęcim, Poland*

Synopsis

A method is developed for the application of the Flory-Mandelkern equation to the determination of the weight-average molecular weights of individual, broad, unfractionated polymer samples. The method includes appropriate averaging of the sedimentation constants and of the intrinsic viscosity of an unfractionated polymer sample in a θ solution from the velocity sedimentation data. By means of the method, individual samples of polystyrene, poly(isooctyl methacrylate) and of the copolymer of styrene with 20% isooctyl methacrylate prepared under the same emulsion polymerization conditions from commercial monomers have been investigated. Appropriate θ solvents have been found by the Elias method. Equations for the dependence of the sedimentation constants and of the intrinsic viscosities in the θ solvents on the molecular weights have been established for the polymers without fractionation. Osmometric and light-scattering measurements as well as Archibald experiments have shown that by the proposed method the molecular weight cut-off effect is eliminated in the above equations and in the polydispersity parameter \bar{M}_w/\bar{M}_n . Molecular weight distributions have been determined for the polymer samples.

INTRODUCTION

The most reliable molecular weight distributions (MWD) are calculable from velocity sedimentation runs carried out in θ conditions, and a method avoiding many of the usual complications has been developed for commercial polymers by standardization of the ultracentrifugation conditions and calibration of the dependence of apparent sedimentation coefficients on molecular weights.¹ The method is suitable for current determinations of MWD for a given polymer type.² However, when new polymers are being developed and changing the polymerization conditions may appreciably influence the hydrodynamic properties of the macromolecules (e.g., by changing the ratio of mers in a copolymer) it is necessary to establish for each sample the relation:

$$s_0 = K_s M^a \quad (1)$$

where s_0 is the sedimentation constant, M is the corresponding molecular weight, and a and K_s are constants for a given polymer-solvent system.

A method suitable for individual samples with broad MWD is presented. Its application to the determination of the MWD of poly(iso-

octyl methacrylate (PiOM) and of its copolymer with styrene (PiOMS) is described.

THEORY

The constants K_s and a in eq. (1) are usually determined from measurements on fractions³⁻⁹ or special polymer samples with narrow MWD¹⁰ covering the corresponding range of M . With averaged values of s_0 in θ conditions, eq. (1) has been derived from measurements on broad peroxide-initiated polystyrene samples with varying amounts of divinylbenzene in commercial styrene.² The averaging was carried out according to the equation:

$$\bar{s}_0 = \left(\sum_{i=1}^m s_{0i}^{1/a} w_i \right)^a \quad (2)$$

where \bar{s}_0 is proportional to the weight-average molecular weight \bar{M}_w of the sample, s_{0i} is the sedimentation constant, w_i is the weight fraction of the i th fraction of the polymer sample, and a is the constant in eq. (1), assumed to be 0.5 for the θ conditions.¹² The values of s_{0i} and w_i are calculable from the sedimentation diagrams.^{1-4,11}

The constants in eq. (1) may be calculated, however, from measurements on one fraction.¹¹ It should be possible, therefore, to determine these constants from measurements on a single unfractionated polymer sample also. The task is largely facilitated under θ conditions, where $a = 0.5$ may be assumed in eqs. (1) and (2) with sufficient accuracy.^{2,4,6,10,12} This method is not as precise and reliable as the above discussed methods since some scattering of \bar{s}_0 versus \bar{M}_w has been observed,² but due to its quickness and low cost it may be useful in MWD determinations by developing on new polymers.

Independently measured molecular weights are necessary to determine eq. (1). In the case of unfractionated samples, \bar{M}_w is necessary according to eq. (2). \bar{M}_w is usually calculated from light-scattering,¹³ sedimentation equilibrium, or Archibald experiments.¹⁴ With broad MWD, additional difficulties due to the molecular weight cut-off¹⁵ arise, however:^{2,16,17} the polymer solutions must be prepared in the same way both for \bar{s}_0 and \bar{M}_w determinations and therefore light-scattering is not applicable. Although the Archibald and sedimentation rate experiments may be carried out in the same ultracentrifugation run,^{3,17} in case of broad MWD the method is unreliable,^{17,18} and other purely ultracentrifugal methods fail.¹⁹⁻²¹

In some recent publications^{2,7,8} eq. (1) has been determined with M calculated from the Flory-Mandelkern equation,^{12,22,23} which may be represented in the following form:

$$M = \{N\eta_0/[\Phi^{1/3}P^{-1}(1-v\rho)]\}^{1.5} s_0^{1.5} [\eta]^{0.5} = K_F s_0^{1.5} [\eta]^{0.5} \quad (3)$$

where $N = 6.024 \times 10^{23}$, η_0 is the solvent viscosity, ρ is the solvent density, v is the partial specific volume of the solute, $[\eta]$ is the intrinsic

viscosity of the solute, and the Flory-Mandelkern universal constant $\Phi^{1/2}P^{-1} = 2.5 \times 10^6$ when s_0 is expressed in Svedberg units and $[\eta]$ in deciliters per gram. The above value of the Flory-Mandelkern constant has been found for fractions which of course have not been ideally monodisperse. Therefore the value of the constant slightly differs from the theoretical value.¹² The s_0 and $[\eta]$ values have been averaged according to the experimental conditions, but, in spite of this, the experimental values of the constant are fairly close to 2.5×10^6 for very different polymers,^{6,12,24} since only negligible differences arise from different averages of s_2 and s_0 and $[\eta]$ in sufficiently narrow fractions.

Equation (3) is very useful for the determination of the constants K_s and a in eq. (1), since in both equations M is a function of the same sedimentation constant s_0 . Errors in $[\eta]$ are of minor importance since its exponent in eq. (3) is only one-third the exponent of s_0 . As stated above, eq. (3) may be directly applied only to fractions, however. In case of samples with broad MWD, the s_0 and $[\eta]$ values must be averaged. No difficulties arise in averaging s_0 according to eq. (2) from the results of sedimentation velocity. Averaging of $[\eta]$ would involve fractionation, however. Thus eq. (3) seems inapplicable to the determination of eq. (1) for measurements on a single unfractionated polymer sample. This difficulty is easily overcome, however, in θ conditions, since then:

$$[\eta]_{\theta} = K_{\eta}M^{0.5} \quad (4)$$

By measurement of $[\eta]$ the averaging proceeds according to the summation:

$$[\eta] = \sum_{i=1}^m [\eta_i]w_i \quad (5)$$

where $[\eta_i]$ is the intrinsic viscosity and w_i the weight fraction of the i th polymer fraction. According to eq. (4) the averaging yielding $[\eta]$ proportional to \bar{M}_w is:

$$[\bar{\eta}]_{\theta} = \left(\sum_{i=1}^m [\eta_i]^2 w_i \right)^{0.5} \quad (6)$$

From eqs. (1) and (4) with $a = 0.5$ for a narrow fraction under θ conditions:

$$[\eta]_{\theta} = (K_{\eta}/K_s)s_0 \quad (7)$$

and therefore from eqs. (2) and (6) with $a = 0.5$:

$$[\bar{\eta}]_{\theta} = (K_{\eta}/K_s)\bar{s}_0 \quad (8)$$

and as well for a sample with broad MWD and $(s_0)_w$ calculated from eq. (2) with $a = 1$, i.e., from an equation corresponding to eq. (5), the following relation holds:

$$[\eta]_{\theta} = (K_{\eta}/K_s)(s_0)_w \quad (9)$$

According to eqs. (8) and (9), $[\eta]_{\theta}$ is calculable from the sedimentation velocity data:

$$[\bar{\eta}]_{\theta} = [\bar{s}_0/(s_0)_w] [\eta]_{\theta} \quad (10)$$

Equation (3), with $[\bar{\eta}]_{\theta}$ and \bar{s}_0 substituted for $[\eta]$ and s_0 , respectively, then yields M_w .

Under θ conditions with $a = 0.5$ the constant K_s may be calculated directly from eq. (1) and the \bar{M}_w and \bar{s}_0 values with satisfactory approximation to the degree of accuracy of the assumption of $a = 0.5$. Since \bar{M}_w is a function of \bar{s}_0 in eq. (3), the molecular cut-off effect¹⁵ is eliminated in the determination of K_s . Thus this method of application of the Flory-Mandelkern equation is very advantageous for individual samples with broad MWD. It is emphasized as well that changes in the composition or in the degree of branching in the copolymer influence the thermodynamic properties much less than the hydrodynamic properties. The changes of the partial specific volume are also minor. Thus the same θ solvent and the same v value may be used for similar polymers, and only the constants in eq. (1) must be determined in the above way for each kind of polymer.

EXPERIMENTAL

Polymer Samples

The samples of PiOM and PiOMS, as well as a sample of polystyrene,² were prepared under the same experimental conditions by peroxide-induced emulsion polymerization in a laboratory reactor at 70°C. All reagents were commercial products used as received, and the monomers were commercial products of the Oświęcim Chemical Works, Poland. Details on polymerization are subject of another publication.²⁵

The samples investigated were purified after coagulation only by repeated washing with methanol. The copolymer contained 20% of iso-octyl methacrylate and was practically free from homopolymers.²⁵

Solvents

The components of the mixed θ solvents used were so selected as to secure the maximum resolving power of the ultracentrifuge as of the mass spectrometer,¹ special attention being given to achieving the lowest viscosity of the θ solvents. The composition of the θ solvents was established by the titrimetric method of Elias.²⁶ A Zeiss photoelectric turbidimeter was used for the titration. Satisfactory linear graphs were obtained for the concentrations 2.2–0.066 and 8.9–0.084 g./l. of PiOM and PiOMS, respectively. The resulting θ solvents at 25°C. contained 359 ml. of *n*-heptane + 641 ml. of acetone and 994 ml. butanone + 6 ml. methanol for PiOM and PiOMS, respectively. The solvents and precipitants were of chemical pure grade.

Osmometry

The number-average molecular weights \bar{M}_n were determined by static osmotic pressure measurements in benzene and in the θ solvents at 25°C. Pinner-Stabin osmometers and Pecell 600 membranes were used.¹³ The results are given in Table I.

The second virial coefficient was practically zero in the θ solvents, thus confirming their pseudoideality, although the experimental points did not fall exactly on a straight line, which is normal with mixed solvents.

Viscometry

Intrinsic viscosities were measured in benzene and in θ solvents at 25°C. in Ubbelohde-type viscometers.²⁷ All measurements were carried out at four different concentrations below 10 g./l. and all graphs, including those for θ solvents were quite good. The results are given in Table I.

Viscosities of the θ solvents at 25°C. were measured with the same viscometers. The viscosities were calculated from the viscosity of water measured under the same conditions. The densities were accounted for. The η_0 values were 3.34×10^{-3} P. and 3.65×10^{-3} P. for the θ solvents for PiOM and PiOMS, respectively, in good agreement with the viscosities of the components of the mixtures.

Pycnometry

ρ and v were determined by measurements in a 50-ml. double-walled pycnometer with an inner thermometer with 0.2°C. gradations. The pycnometer was thermostatted, with temperatures established at 25.5 or 24.5°C. The 25.0°C. mark of the thermometer of the pycnometer could be observed by means of a magnifying glass and when it was reached the level of the liquid in the pycnometer capillary was brought to the mark. The averages of the ascending and descending measurements were used in the calculations. The resulting ρ values are 0.7394 and 0.8020 g./ml., and the v values obtained 0.900 and 0.761 ml./g., yielding fairly high $1-v\rho$ values (0.334 and 0.390 for PiOM and PiOMS, respectively).

The densities of the polymer films have been found to be 0.8038 and 0.8608 g./ml. for PiOM and PiOMS, respectively. These results, on comparison with the v values, show a considerable contraction of the polymers in the θ solvents i.e., considerable solvation of the polymers by the "good" solvent in the mixture.

Light Scattering

Although, as stated in the theoretical part, good agreement of results could not be expected, light-scattering measurements by the Zimm method¹³ were carried out for PiOM in *n*-heptane with the Peaker light-scattering apparatus.¹³ The measurements were carried out by Strzelecka et al.² and they yielded the refractive increment 0.109 ml./g., $\bar{M}_w = 8.47 \times 10^5$, and $\bar{M}_n = 2.13 \times 10^5$.

TABLE I
Molecular Weights from Osmometry, Light Scattering, Archibald Method, and the Flory-Mandelkern Equation for PiOM, PiOMS, and Polystyrene (PS) Obtained under the Same Polymerization Conditions

	PiOM		PiOMS		PS
	g./ml.	g./ml.	g./ml.	g./ml.	
Osmometry ($c \rightarrow 0$)					
$\bar{M}_n \times 10^{-5}$ in C_6H_6	2.5	1.67	0.83	2.5	0.83
$\bar{M}_n \times 10^{-5}$ in θ solvent		6.49		1.67	2.0
Light scattering ($c \rightarrow 0$)		5.86		4.69	5.23
$\bar{M}_w \times 10^{-5}$		8.47		—	21.7
$\bar{M}_n \times 10^{-5}$		3.13		—	3.3
Archibald experiments					
Relative deviation of points in the graphs, %					
$\bar{M}_w \times 10^{-5}$ (slopes)	5.06	6.79	12.03	—	2.68
$\bar{M}_w \times 10^{-5}$ (ordinates)	10.36	6.02	5.09	—	9.00
	8.75	5.75	6.00	—	7.51

Velocity sedimentation:									
$(s_0)_w, S, [\text{eq.}(2), a = 1]$	62.97	63.53	57.61	28.47	25.87	24.55	35.76		
$s_0, S, [\text{eq.}(2), a = 0.5]$	67.5	68.7	63.4	32.80	28.42	27.44	37.82		
Viscometry									
$[\eta]$ in C_6H_6 , dl./g.		3.95			2.89		5.9		
$[\eta]_0$, dl./g.		0.375			1.65		1.95		
$[\eta]_0$, dl./g. [eq.(10)]	0.403	0.406	0.413	1.90	1.81	1.845	2.07		
Flory-Mandelkern eq. (3)									
$\bar{M}_w \times 10^{-5}$	13.1	13.5	12.1	8.78	6.92	6.64	17.3		
$1/K_s$, [eq.(1), $a = 0.5$]	288	286	301	819	857	881	1208		
Deviation from $1/K_s$ for									
$c = 2.5 \text{ g./l., } \%$	0.0	0.7	4.5	0.0	4.6	7.6	—		
$10^{-5}/K_\eta$ [eq.(4)]	80.7	81.7	70.8	2.43	2.11	1.96	3.03		
Deviation from $10^{-5}/K_\eta$ for									
$c = 2.5 \text{ g./l., } \%$	0.0	1.2	12.4	0.0	13.2	19.3	—		
$\bar{M}_n \times 10^{-5}$ [eq.(19)] ^a	2.40	2.42	—	2.32	1.50	—	4.90		
				(0.65)	(0.60)				
\bar{M}_w/\bar{M}_n	5.5	5.6	—	3.8	4.6	—	3.5		

^a The \bar{M}_n values in parentheses are for $M < 5 \times 10^3$, for which the w_i values are too small to be measured in the case of the homopolymers PiOM and PS.

For the polystyrene sample in carbon tetrachloride the refractive increment was 0.166 ml./g., $\bar{M}_w = 2.17 \times 10^6$, and $\bar{M}_n = 3.3 \times 10^5$.

Due to special problems arising in light scattering of copolymers,²⁸ measurements were not carried out for PiOMS.

Ultracentrifugation

Ultracentrifugation was carried out as described in a previous publication¹ in the Spinco E ultracentrifuge at 25°C. and 9341 rpm in case of PiOM and PiOMS. The ultracentrifugation of the polystyrene sample is described elsewhere.² The Archibald experiments were carried out for 7–66 min. of sedimentation at the beginning of the same runs as the sedimentation velocity experiments.^{2,3,18} The duration of the Archibald experiment varied in the above range depending on the sample and the concentration of its solution. The standard sedimentation time,¹ at which the effect of diffusion could be neglected, was 200 and 300 min. for PiOM and PiOMS, respectively. A 30-mm. high single-sector cell was used to measure the sedimentation at the lowest polymer concentrations,¹ which for the above polymers and experimental conditions were 2.5, 1.67, and 0.83 g./l. The solvent baseline was photographed at the beginning of each run just after reaching a stable rotation velocity. Since the horizontal reference lines are not stable and exact enough²⁹ the baseline was fitted to the solution curves from the same run by the meniscus image and a point in the plateau region. The coordinates of the schlieren solution curve were measured with respect to the center of rotation, i.e. to the vertical reference line, and to the baseline by means of a special photomicrocomparator³⁰ and according to the Trautman tables.³¹

Calculations of \bar{M}_w from the Archibald experiments were made according to a version of the Trautman method from the slopes of his graphs.^{2,3,18,32} The methods of Abe and Prins³³ and Elias³⁴ were used in another version of the method,^{2,18} in which \bar{M}_w is calculated from the ordinate extrapolated in the Trautman graph to zero sedimentation time and from the surface under the sedimentation curve corresponding to the initial polymer concentration. Both \bar{M}_w values are given in Table I. The slopes and the extrapolated ordinates of the Trautman graphs were calculated by the least-squares method by use of the Polish ZAM-2 computer. The relative deviations of the experimental points in the graphs were calculated as the ratio of their standard deviations to the respective extrapolated ordinates. The surfaces under the sedimentation curves were calculated in the Trautman coordinates³¹ from photodiagrams made at the standard sedimentation time. Examples of the graphs are given in Figure 1.

The distributions of the sedimentation coefficients were calculated according to Trautman.³¹ The differential distribution curves in Figure 2 show that at the standard sedimentation times the diffusion effects may be neglected, also, since at different sedimentation times different distances from meniscus correspond to a given sedimentation coefficient, the

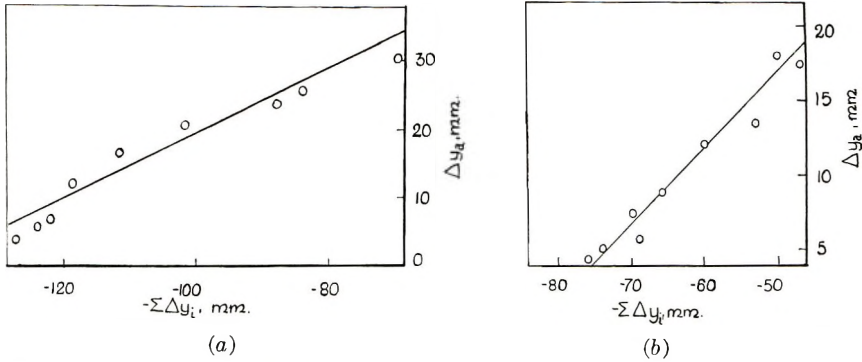


Fig. 1. Examples of the Trautman graphs ($\Delta Z = 2$): (a) PiOM, $c = 2.5$ g./l.; (b) PiOMS, $c = 0.83$ g./l.

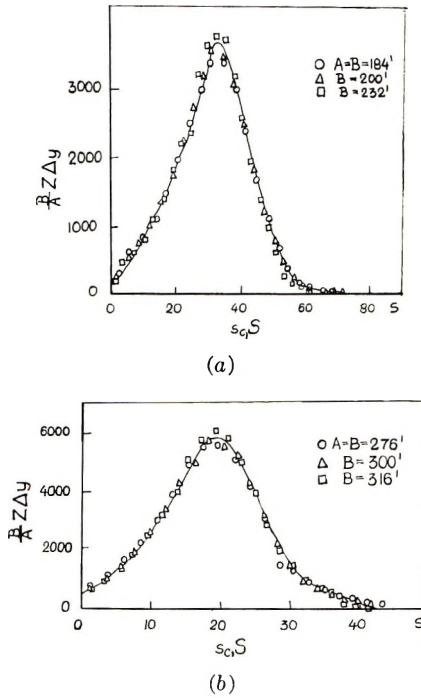


Fig. 2. Differential distribution curves of the sedimentation coefficients s_c for $c = 2.5$ g./l.: (a) PiOM, sedimentation times 184, 200, and 232 min.; (b) PiOMS, sedimentation times 276, 300, and 316 min.

curves show that the effects of concentration and pressure on their shape may be neglected as well. This is consistent with the low rotation velocity and θ solutions used.¹ However slight, the concentration dependence of the sedimentation coefficients must be accounted for by the determination of MWD even in θ solutions.^{1,2,6,35} From the integral distribution curves of the sedimentation coefficients in the ranges of the integral distribution

function $G(s)$ (0.15–0.85 and 0.25–0.90 for PiOM and PiOMS, respectively) at concentrations of 2.5 and 1.67 g./l. (the measurements at $c = 0.83$ g./l. were not reliable enough), the following dependencies were found for PiOM and PiOMS, respectively.

$$s_0 = s_c (1 + 0.425c) \quad (11)$$

and

$$1/s_0 = 1/s_c - 0.00629c \quad (12)$$

Equation (12) for the PiOMS solutions, where the concentration dependence is very slight, is consistent with the findings of Poddubnyĭ and Grechanovskii.³² Equations (11) and (12) were used for the calculations of the distributions of the sedimentation constants, which yielded the data necessary for the eqs. (1), (2), (3), and (10) and for the calculations of MWD.

All calculations were carried out with the ZAM-2 computer according to a program developed by B. Jermakowicz on the basis of an algorithm derived by one of the authors^{2,17} from the Trautman calculation method.³¹

RESULTS AND DISCUSSION

The differential distribution curves of the sedimentation coefficients s_c for $c = 2.5$ g./l. are presented in Figure 2. The curves for PiOM and PiOMS are similar and of Gaussian type, the curve for PiOM being much broader. Both curves are similar to the curve for the polystyrene sample.² The weight-average sedimentation coefficients $(s_c)_w$ calculated from eq. (2) with $a = 1$, are very different, however. They are 30.6, 18.4, and 27.6 S. for PiOM and PiOMS at $c = 2.5$ g./l. and for the polystyrene sample at $c = 2.0$ g./l., respectively. Not much more information on the polymers is obtainable from the curves. This shows the necessity of the MWD curves.

The data resulting from the procedures described in the theoretical and experimental parts are presented in Table I. The constants K_F in eq. (3) calculated from the experimental η_0 , ρ , and v values are 3.19×10^3 and 2.91×10^3 for PiOM and PiOMS, respectively.

The \bar{M}_w values determined by different methods are not consistent for a polymer sample; they agree only to the order of magnitude. As stated in the theoretical part, better agreement could not be expected for these samples with broad MWD due to the different molecular weight cut-off effects by different methods. The cut-off effect is considerable in static osmometry as well. Good agreement is observed in Table I only for the polystyrene sample, since values of $M < 10^5$ are cut off in eq. (19) discussed below; the corresponding w_i values were too low to be measured. The \bar{M}_n values from osmometry are much higher than those from ultracentrifugation for PiOM and PiOMS and than \bar{M}_n from light scattering for PiOM. Nevertheless, the data in Table I confirm the evidence^{2,3} that

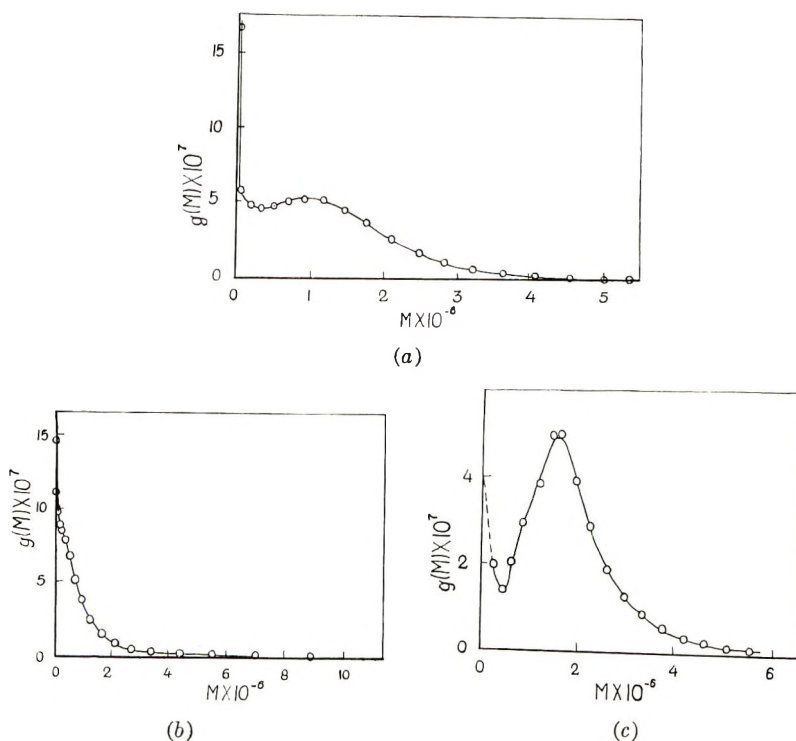


Fig. 3. Differential MWD curves: (a) PiOM; (b) PiOMS; (c) PS.

the problem of number-average molecular weights of commercial polymers is more complex than generally realized.¹⁷

The Trautman graphs in Figure 1 seem satisfactory, and the relative deviation of the experimental values given in Table I is not too great, except for the experiment with PiOM at $c = 0.83$ g./l. Except for this experiment, the differences in \bar{M}_w values calculated from the slopes and from the ratio of the extrapolated ordinates to the corresponding surface are also not too great, and, in agreement with theory,^{18,33,34} the first are higher than the second. They differ enough, however, to show a considerable fractionation of the polymer at the meniscus during the Archibald experiments. Much greater losses of the heaviest fractions take place at the meniscus during the time elapsing between the start of sedimentation and the start of photographic Photographing may be started only after the disappearance of the infinite concentration gradient image. If the period could be accounted for, the graphs would be curved upwards.^{18,34} Therefore the cut-off effect in the Archibald experiments is quite indefinite for broad polymer samples. The changes in the resulting \bar{M}_w values are not due to the second virial coefficient in the θ solutions.

Cut-off effects by preparation of the polymer samples and solutions for light-scattering measurements may explain the difference of the results in comparison with other data in Table I.

Since the concentrations are low enough and the accuracy of sedimentation measurements decreases with decreasing polymer concentration, the most reliable sedimentation velocity data correspond to 2.5 g./l. From these data the eqs. (13)–(16) result.

$$\text{For PiOM: } \bar{M}_w = 288 \bar{s}_0^2 \quad (13)$$

$$M_\eta = 8.07 \times 10^6 [\eta]_0^2 \quad (14)$$

$$\text{For PiOMS } \bar{M}_w = 819 \bar{s}_0^2 \quad (15)$$

$$M_\eta = 2.43 \times 10^5 [\eta]_0^2 \quad (16)$$

It is worth noting that \bar{s}_0^2 is equal to the expression in parenthesis in eq. (2), i.e., to the summation made directly from the experimental data.

The differential MWD curves in Figure 3 were calculated from eqs. (13) and (15), where \bar{M}_i and s_{0i} values were substituted for the respective averages. The third MWD curve was calculated with $1/K_s = 1208$ as stated in Table I for the polystyrene sample. This value differs very distinctly from the mean value $1/K_s = 814.9$ obtained for a series of polymer samples prepared from the same commercial styrene in other polymerization conditions,² thus confirming the necessity of the determination of eq. (1) for each polymer sample in changing polymerization conditions. Separate turbidimetric titration of the sample has yielded, however, the same composition of the θ solvent² as for other polystyrene samples, and the same K_F value in the Flory-Mandelkern equation, eq. (3), could be used. Comparison of the MWD curves in Figure 3 with the corresponding curves in Figure 2 shows that only from the MWD curves can sufficient information be obtained. Since¹¹

$$g(M) = g(s) a K_s (s_0/K_s)^{(a-1)/a} \quad (17)$$

where $g(M)$ and $g(s)$ are the differential distribution functions of the molecular weights and of sedimentation constants, respectively, the curves in Figure 3 have quite a different shape than the curves in Figure 2. Details of the MWD curves are seen which could not be predicted from the curves in Figure 2. The polydispersity of the samples cannot be as well estimated from the curves in Figure 2. Although methods for the expression of polydispersity are still being discussed,^{36,37} it is usually quite satisfactorily characterized by the ratio \bar{M}_w/\bar{M}_n . It may be, however, easily shown that¹¹

$$M_w = K_s^{-1/a} \bar{s}_0^{1/a} \quad (18)$$

$$\text{and} \quad M_n = K_s^{1/a} \sum_{i=1}^m s_{0i}^{-1/a} \nu_i \quad (19)$$

thus yielding

$$\bar{M}_w/\bar{M}_n = K_s^{-2/a} \bar{s}_0^{1/a} / \sum_{i=1}^m s_{0i}^{-1/a} \nu_i \quad (20)$$

i.e., the polydispersity parameter \bar{M}_w/\bar{M}_n is inversely proportional to the square of K_s . Thus the above discussed method of the determination of

K_s is necessary for the estimation of the polydispersity as well. The advantage of the method that the K_s value is independent of the cut-off effect is therefore emphasized. With the proposed method, ultracentrifugation conditions for similar polymer types can be standardized, and the results may therefore be easily compared.

Discussion of the differences between the MWD curves for PiOM, PiOMS, and polystyrene samples obtained under the same polymerization conditions is the subject of another publication.²⁵

CONCLUSION

It is found for three different polymers prepared from commercial monomers that all necessary data for the calculation of the dependence of the sedimentation constants and of the intrinsic viscosities on molecular weights are obtainable for an individual polymer sample from the sedimentation velocity and intrinsic viscosity in a θ solvent. The molecular weight cut-off effect is eliminated. The method is especially suitable for the determination of the molecular weight distribution or of the polydispersity parameter \bar{M}_w/\bar{M}_n .

References

1. Kalfus, M., *Ann. Soc. Chim. Polon.*, **39**, 309 (1965).
2. Kalfus, M., J. Graff, and M. Strzelecka, paper presented at the High Polymer Conference, in Magdeburg, Germany, February 24, 1965.
3. Kalfus, M., *Polimery*, **9**, 250 (1964).
4. Cantow, H. J., *Makromol. Chem.*, **30**, 169 (1959).
5. Schulz, G. V., and H. Horbach, *Makromol. Chem.*, **29**, 93 (1959).
6. Poddubnyi, I. Ya., V. A. Grechanovskii, M. I. Mosevitskii, and A. V. Podalinskiĭ, *Vysokomolekul. Soedin.*, **5**, 1042 (1963).
7. Pavlov, A. V., V. G. Al'doshin, and S. Ya. Frenkel, *Vysokomolekul. Soedin.*, **6**, 1600 (1964).
8. Pavlov, A. V., C. E. Bresler, and S. R. Rafikov, *Vysokomolekul. Soedin.*, **6**, 2068 (1964).
9. Kawahara, K., *Makromol. Chem.*, **73**, 1 (1964).
10. McCormick, H. W., *J. Polymer Sci.*, **36**, 341 (1959).
11. Baldwin, R. L., and K. E. van Holde, *Fortschr. Hochpolymer. Forsch.*, **1**, 451 (1960).
12. Flory, P. J., *Principles of Polymer Chemistry*, Cornell Univ. Press, Ithaca, N. Y., 1953.
13. Allen, P. W., *Techniques of Polymer Characterization*, Butterworths, London, 1959.
14. Fujita, H., *Mathematical Theory of Sedimentation Analysis*, Academic Press, New York-London, 1962.
15. Kotliar, A. M., *J. Polymer Sci. A*, **2**, 4303 (1964).
16. Kalfus, M., *Polimery*, **10**, 225 (1965).
17. Kalfus, M., *Polimery*, **10**, in press.
18. Kalfus, M., *Wiadomości Chem.*, **19**, 745 (1965).
19. Losting, L. I., *J. Am. Chem. Soc.*, **74**, 1548 (1952).
20. Gehatia, M., *Makromol. Chem.*, **37**, 85 (1960).
21. Yphantis, D. A., *Ann. N. Y. Acad. Sci.*, **88**, 586 (1952).
22. Mandelkern, L., and P. J. Flory, *J. Chem. Phys.*, **20**, 212 (1952).

23. Mandelkern, L., W. R. Krigbaum, M. A. Scheraga, and P. J. Flory, *J. Chem. Phys.*, **20**, 1392 (1952).
24. Kalfus, M., *Makromol. Chem.*, **83**, 287 (1965).
25. Mituś, J., Thesis for the degree of doctor of technical science, Silesian Polytechnic School, Gliwice, Poland, 1965.
26. Elias, H. G., *Makromol. Chem.*, **50**, 1 (1961).
27. Sachajdak, J., and M. Kalfus, *Przem. Chem.*, **41**, 454 (1962).
28. Lang, M., C. Strazielle, and H. Benoit, *J. Chim. Phys.*, **60**, 501 (1963).
29. Klainer, M., and G. Kegeles, *J. Phys. Colloid Chem.*, **59**, 952 (1955).
30. Kalfus, M. K., *Pribory Tekhn. Eksperim.*, **10**, 185 (1965).
31. Trautman, R., *J. Phys. Chem.*, **60**, 1211 (1956).
32. Trautman, R., and C. F. Crampton, *J. Am. Chem. Soc.*, **81**, 4036 (1959).
33. Abe, H., and W. Prins, *Makromol. Chem.*, **42**, 216 (1961).
34. Elias, H. G., *Dechema Monograph.*, **44**, 1 (1963).
35. Poddubnyĭ, I. Ya., and V. A. Grechanovskii, *Dokl. Akad. Nauk SSSR*, **153**, 1122 (1963).
36. Brestkin, Ya. V., and M. M. Chochieva, *Vysokomolekul. Soedin.*, **6**, 2097 (1964).
37. Geller, B. E., and I. M. Meskin, *Vysokomolekul. Soedin.*, **6**, 2100 (1964).

Résumé

On a développé une méthode d'application de l'équation de Flory-Mandelkern à la détermination des masses moléculaires moyennes en poids d'échantillons individuels, larges et non-fractionnés de polymères. La méthode comprend le calcul des moyennes appropriées des constantes de sédimentation et de viscosité intrinsèque d'un échantillon non-fractionné dans un solvant thêta, employant des résultats de mesures de vitesse de sédimentation. Grâce à cette méthode, on a étudié des échantillons éventuels individuels de polystyrène, de polyméthacrylate d'iso-octyle et de copolymère de styrène avec 20% de méthacrylate d'iso-octyle préparés dans les mêmes conditions de polymérisation en émulsion des monomères techniques. Les solvants thêta appropriés ont été déterminés par la méthode d'Elias. On a déterminé les équations de la dépendance des constantes de sédimentation et des viscosités intrinsèques dans les solvants thêta en fonction des masses moléculaires, sans fractionner les échantillons. Grâce à des mesures osmométriques et de diffusion de lumière de même qu'avec les expériences d'Archibald, on a constaté que la méthode proposée élimine l'effet "cut-off" des masses moléculaires dans les équations susnommées et dans le paramètre de la polydispersité M_w/M_n . Les distributions des masses moléculaires ont été établies pour les échantillons surnommés.

Zusammenfassung

Auf der Grundlage der Flory-Mandelkern-Gleichung wurde eine Methode zur Bestimmung des Gewichtsmittels des Molekulargewichts von breiten, individuellen und unfraktionierten Polymerproben entwickelt. Dabei werden die entsprechenden Mittelwerte der Sedimentationskonstanten und der Viskositätszahl einer gegebenen Probe in einem θ -Lösungsmittel aus Sedimentationsgeschwindigkeitsdaten ausgewertet. Die Methode wurde zur Untersuchung von individuellen Proben von Polystyrol, Poly(Iso-Octylmethacrylat) und des Kopolymeren aus Styrol und 20% iso-Octylmethacrylat angewendet. Geeignete θ -Lösungsmittel wurden nach der Methode von Elias ausgewählt. Die Beziehungen für die Abhängigkeit der Sedimentationskonstanten und der Viskositätszahlen vom Molekulargewicht wurden für die oben genannten, unfraktionierten Polymeren bestimmt. Osmotische und Lichtstreuungsmessungen sowie Messungen nach dem Archibald-Verfahren haben gezeigt, dass mit der vorgeschlagenen Methode der Molekulargewichts "cut off" Effekt in den angeführten Gleichungen und im Polydispersitätsparameter M_w/M_n eliminiert wird. Die Molekulargewichtsverteilung der Polymeren wurde bestimmt.

Received March 9, 1965

Prod. No. 4901A

NOTES

*X-ray Scattering from Mixtures of Nylon 6 and *m*-Cresol*

When a crystalline polymer absorbs a diluent having a strong affinity for the polymer, it is most likely that the crystalline state in the polymer will be altered markedly during the course of swelling. In the case of water employed as a diluent, several x-ray investigations have been reported for various polymers such as gelatin,¹ sodium pectate,² cellulose,³⁻⁵ and poly(vinyl alcohol).^{6,7} The aim of the present short communication is to provide further evidences to this problem by studying mixtures of nylon 6 and *m*-cresol by use of the x-ray scattering technique.

The measurement of x-ray scattering was made on the mixtures covering a whole range of composition, i.e., from the pure solvent to the pure polymer, at room temperature (20°C.). Nickel-filtered copper radiation was used as an incident beam and the intensity of scattering from the samples was measured by means of an ordinary x-ray diffractometer. A liquid-sample cell was required for measuring the scattering from 10 and 20% polymer solutions as well as from the pure solvent. The intensities of scattering observed for samples with different thicknesses and/or different compositions were normalized to the same basis by the use of x-ray absorption data for each sample.⁸ Figure 1 shows some examples of normalized scattering curves. The hatched area in Figures 1a and 1d represents the correction for incoherent scattering. By introducing several assumptions, the total scattering curve (A) (in Figs. 1b and c) is divided into two parts, one

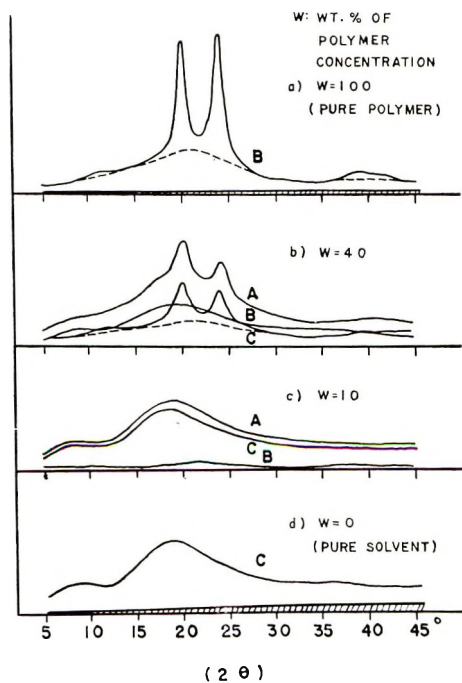


Fig. 1. X-ray scattering curves for mixtures of nylon 6 and *m*-cresol.

due to the contribution from the polymer (curve *B*) and the other due to the solvent (curve *C*). With respect to curve *B* (Figs. 1*a* and *b*), we further separated the intensity diffracted by the crystalline part from that scattered by the amorphous part. The latter is indicated by dotted lines in Figures 1*a* and *b*. The procedure for normalizing the scattered intensity for a binary mixture and the method of evaluating the crystallinity will be discussed elsewhere.

It was observed that the major crystalline portion disappears in the range of polymer concentration from 30 to 20%. This result agrees with the visual observation that the sample becomes transparent in the same concentration region. It was also observed that the positions of two principal diffraction peaks, which correspond to the spacings of 3.7 and 4.4Å., are kept unchanged with increase of the diluent concentration. That is to say, the dimension of the basal planes of the unit cell⁹ remains constant during the swelling process. Thus, it may be concluded that the diluent molecules do not penetrate into the crystallites.

On the other hand, the relative intensity of the peak at 3.7Å. to that at 4.4Å. decreases gradually with increase of the diluent concentration. This fact suggests that the diluent molecules would attack predominantly against the (002) plane of the hydrogen-bonded sheets.⁹ It may be due to the fact that *m*-cresol has strong polar interaction with the amide groups along the polymer chains, as can be expected from the large negative value of the Flory-Huggins interaction parameter for the present system.¹⁰

Finally, we should like to comment on the scattering from concentrated solutions of this polymer. It is interesting to see that the scattering curve for the polymer component in the 10% solution (curve *B* in Fig. 1*c*) is a broad, diffuse one which has a maximum corresponding to the Bragg spacing of 4.2Å. The feature of such a curve will be attributed to a poorly ordered state of the hexagonal packing between adjacent molecular chains which may exist even in the concentrated solution.

The author wishes to express his sincere gratitude to Dr. M. Tsuruta for his encouragement and to Professor H. Inagaki of Kyoto University for his advice and criticisms.

References

1. Katz, J. R., and J. C. Derksen, *Rec. Trav. Chim.*, **51**, 513 (1932).
2. Palmer, K. J., T. M. Shaw, and M. Ballantyne, *J. Polymer Sci.*, **2**, 318 (1947).
3. Kratky, O., and A. Sekora, *Kolloid Z.*, **108**, 169 (1944).
4. Hermans, P. H., and A. Weidinger, *J. Colloid Sci.*, **1**, 185 (1949).
5. Hermans, P. H., and A. Weidinger, *Makromol. Chem.*, **18**, 75 (1956).
6. Sakurada, I., Y. Nukushina, and Y. Sone, *Kobunshi Kagaku*, **12**, 506, 510, 514, 517 (1955).
7. Tadokoro, H., K. Kozai, S. Seki, and I. Nitta, *J. Polymer Sci.*, **26**, 379 (1957).
8. Hermans, P. H., and A. Weidinger, *J. Polymer Sci.*, **4**, 709 (1949); S. Krimm, and A. V. Tobolsky, *Textile Res. J.*, **21**, 805 (1961).
9. Holmes, D. R., C. W. Bunn, and D. J. Smith, *J. Polymer Sci.*, **17**, 159 (1955).
10. Schaeffgen, J. R., and P. J. Flory, *J. Am. Chem. Soc.*, **72**, 689 (1950).

M. HIRAMI

Nylon Department
Nippon Rayon Company
Uji, Kyoto, Japan

Received May 6, 1964

**Interaction between Alkaline Earth Metal Cations and
Polymethacrylic Acid in Dilute Solutions.
II. Potentiometric Titration**

It is known from published papers that undissociated poly(methacrylic acid) (PMA) molecules are highly coiled and that during the neutralization with monovalent hydroxides they are extended due to the repulsions of carboxylate groups. The conformational changes of polymer chains affect the solution properties.¹⁻⁸ Since the net charge

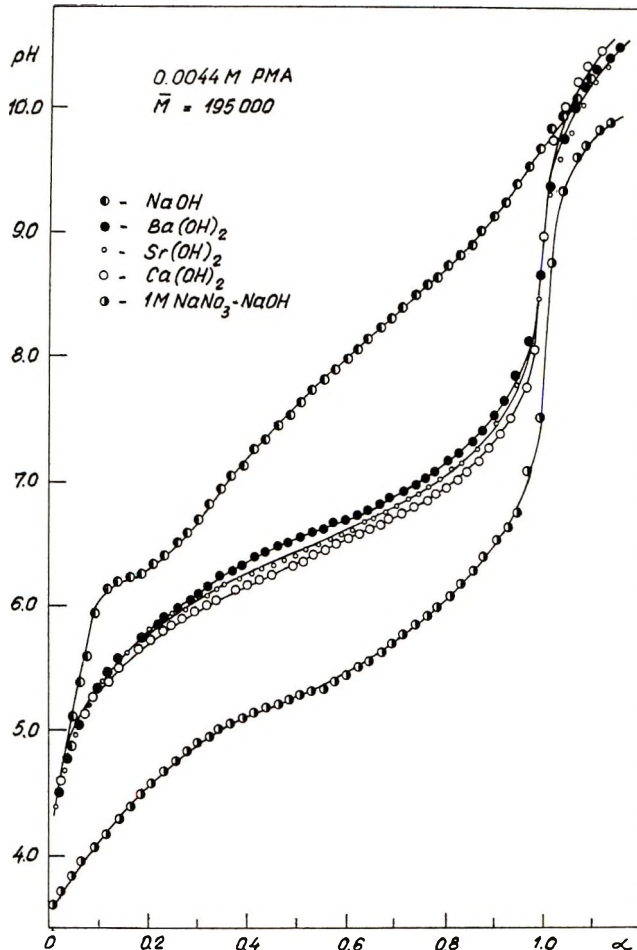


Fig. 1. Titrations of 0.0044M PMA-II with barium, strontium, and calcium hydroxides in the absence of salt and with sodium hydroxide both in the absence of salt and in 1M NaNO₃ solution.

of polyanions may be decreased by the shielding effect of counterions, properties of the polyacid solutions depend upon the ionic strength.^{5,9,10}

Previous authors' papers¹¹⁻¹³ have shown that the conductometric and viscometric behaviors of PMA are quite different when the poly(methacrylic acid) is neutralized with alkaline earth metal hydroxides than when it is neutralized with monovalent hydroxides. These differences were ascribed to the association of divalent counterions

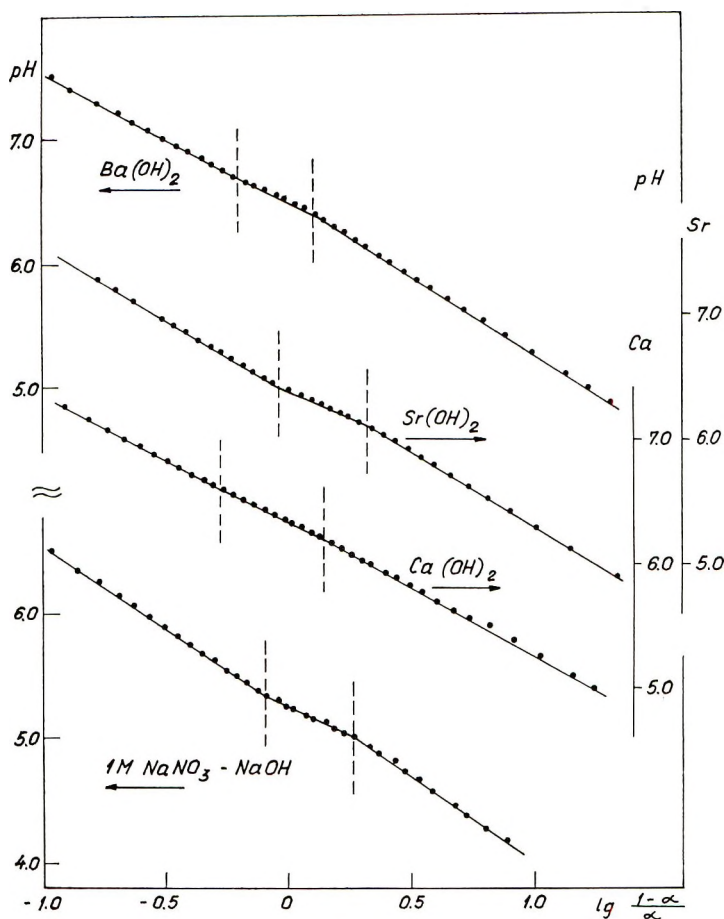


Fig. 2. Henderson-Hasselbalch plots for 0.0044M PMA-II neutralized with barium, strontium, and calcium hydroxides in the absence of salt and with sodium hydroxide in 1M NaNO₃. Note that the ordinate has been displaced for each curve.

with carboxylate groups. They are also connected with the diminution of the net charge of polyanions, which has an influence on the potentiometric properties of PMA solutions.

Experimental

The samples of PMA were the same as those used for the conductometric and viscometric measurements.¹³ Their average molecular weights were: PMA-I 33,000; PMA-II 195,000; PMA-III 826,000. The concentrations of PMA were determined by potentiometric titrations with standard Ba(OH)₂.¹⁴ Potentiometric titrations were performed using a Radiometer pH-meter 22 with glass and calomel electrodes in a nitrogen atmosphere in a titration vessel which had the temperature maintained at 25 ± 0.1°C. The neutralizations of PMA with alkaline earth metal hydroxides [Me(OH)₂], and for comparative purposes with sodium hydroxide in the absence of salt and in the presence of sodium nitrate, were carried out.

Results and Discussion

From Figure 1 we can see that titration curves of PMA with Me(OH)₂ have some characteristic features. They are in a region of lower pH values than those obtained

with NaOH in the absence of salt, and do not exhibit the marked inflection in the transition region which can be observed when NaOH is used.¹⁰ The experimental points obtained with $\text{Me}(\text{OH})_2$ in the region of α , below 0.2, lie on the same curve. Then we can see an appreciable shift in titration curves to lower pH values upon going from barium to strontium to calcium hydroxide. It is in line with the order of size of ionic radii of these cations. A similar shift was observed by Gregor and Frederick⁷ for poly(acrylic acid) and alkali metal hydroxides in the presence of corresponding chlorides.

From Figure 1 it is also seen that the increase of pH values at the end of neutralization of PMA with $\text{Me}(\text{OH})_2$ is large just as the one observed with NaOH in the presence of added salt. It has been used for the potentiometric determination of PMA.¹⁴

In Figure 2 the experimental results are expressed in terms of the modified Henderson-Hasselbach equation

$$\text{pH} = \text{p}K_a - n \log (1 - \alpha)/\alpha$$

A marked conformational transition region is observed when NaOH is used in the presence of 1M NaNO_3 . It is displaced to a still higher α value than that obtained with 0.1M NaOH.¹⁰ Similarly, both $\text{p}K_a$ and n values are diminished even more. This may be related to the increase of the screening effect of counterions and the diminution of interactions between ionizing groups.^{6,9,10} The curves obtained with $\text{Me}(\text{OH})_2$ in the absence of salt can be divided into three straight-line segments. The inflections are almost in the same region of α as that observed with NaOH in the presence of 1M NaNO_3 ; however, they are not so marked. This can also be seen from the average $\text{p}K_a$ and n values calculated for each segment of the curves by the method of least squares. Table I presents the results of the calculations.

TABLE I
Henderson-Hasselbach Parameters for Titration 0.0044M PMA-II with $\text{Me}(\text{OH})_2$,
with NaOH in the Absence of Added Salt*

$\text{Ba}(\text{OH})_2$		$\text{Sr}(\text{OH})_2$		$\text{Ca}(\text{OH})_2$		NaOH			
						No salt		1M NaNO_3	
$\text{p}K_a$	n	$\text{p}K_a$	n	$\text{p}K_a$	n	$\text{p}K_a$	n	$\text{p}K_a$	n
6.54	1.25	6.50	1.21	6.36	1.09			5.38	1.39
6.51	0.91	6.39	0.94	6.35	0.97	7.55	2.27	5.26	0.90
6.47	1.09	6.36	1.18	6.31	1.06			5.20	1.36

* They are calculated in the region of $\alpha = 0.3-0.7$ and in 1M NaNO_3 solution.

The low n values obtained with $\text{Me}(\text{OH})_2$ show that interactions between carboxylate groups, which appeared during the neutralization are also significantly reduced, but in this case we can not tell about the screening effect of counterions because of the low concentration. The diminution of the charge which exerts the repulsive forces on the polymer chains may be ascribed to the divalent counterions associated with carboxylate groups.

It is worth noting that the lowest n values obtained with $\text{Ca}(\text{OH})_2$ and the highest n values obtained with $\text{Sr}(\text{OH})_2$ are in accordance with the lowest and the highest fractional charge of polyanions, respectively.¹³

The lack of a marked conformational transition region on potentiometric titration curves obtained with $\text{Me}(\text{OH})_2$ and low n values shows that the size of PMA molecules during the neutralization is changed very slightly. This points out that potentiometric titration of PMA with $\text{Me}(\text{OH})_2$ leads to the qualitative conclusions that are in accordance with the results of conductometric and viscometric measurements of the same system.¹³

It has been proved on three different samples that potentiometric titration of PMA with $\text{Ba}(\text{OH})_2$ is independent of molecular weight.

The author wishes to thank Prof. Dr. Alina Ulińska for helpful discussion.

References

1. Katchalsky, A., and H. Eisenberg, *J. Polymer Sci.*, **6**, 145 (1951).
2. Oth, A., and P. Doty, *J. Phys. Chem.*, **56**, 43 (1952).
3. Gregor, H. P., D. H. Gold, and M. Frederick, *J. Polymer Sci.*, **23**, 467 (1957).
4. Katchalsky, A., *J. Polymer Sci.*, **7**, 393 (1951).
5. Arnold, R., and J. Th. G. Overbeek, *Rec. Trav. Chim.*, **69**, 192 (1950).
6. Arnold, R., *J. Colloid Sci.*, **12**, 549 (1957).
7. Gregor, H. P., and M. Frederick, *J. Polymer Sci.*, **23**, 451 (1957).
8. Kodem, O., and A. Katchalsky, *J. Polymer Sci.*, **15**, 321 (1955).
9. Katchalsky, A., and P. Spitnik, *J. Polymer Sci.*, **2**, 432 (1947).
10. Leyte, J. C., and M. Mandel, *J. Polymer Sci. A*, **2**, 1879 (1964).
11. Wojtczak, Z., *Chem. Anal. (Warsaw)*, **6**, 587 (1961).
12. Wojtczak, Z., *J. Polymer Sci. B*, **2**, 661 (1964).
13. Wojtczak, Z., *J. Polymer Sci. A*, **3**, 3613 (1965).
14. Wojtczak, Z., *Chem. Anal. (Warsaw)*, **10**, 737 (1965).

ZBIGNIEW WOJTCZAK

Department of General Chemistry
Copernicus University
Toruń, Poland

Received August 27, 1965

Revised November 3, 1965

**The Polymerization of Tetrahydrofuran with
Niobium Pentachloride and Tantalum
Pentachloride**

A variety of catalysts for the polymerization of tetrahydrofuran have been reported in the literature: (1) Lewis acid-cocatalyst systems,^{1,2} (2) triethylaluminum-cocatalyst systems,³⁻⁵ (3) triethylaluminum-water (1:1)-cocatalyst systems,³ (4) ferric chloride-triphenylphosphite,⁶ (5) phosphorous pentafluoride,^{7,8} (6) antimony pentachloride,⁷ and others. However, little attention has been paid to the high catalytic activity of heavy transition metal halides. We recently pointed out that anhydrous tungsten hexachloride⁹ without any cocatalysts has a high catalytic activity for the polymerization of tetrahydrofuran. As a part of the investigation on the catalytic activity of transition metal halides, anhydrous niobium pentachloride and anhydrous tantalum pentachloride will now be reported as new catalysts of high activity.

Tetrahydrofuran monomer was dried over sodium and distilled just before use. Anhydrous niobium pentachloride and anhydrous tantalum pentachloride were obtained commercially. The division and storage of these halides were carried out under a nitrogen atmosphere. The polymerization reaction was carried out in a sealed tube which was occasionally shaken to disperse the catalyst. The crude polymer was dissolved in tetrahydrofuran-water (20:1) and a white polymer was recovered by pouring the solution into a large amount of water. The isolated polymer was dried *in vacuo* at room temperature. Although the polymerization mixtures were colored (Nb, red-brown; Ta, pink), the polymers were always pure white and possessed the infrared spectrum of polytetrahydrofuran.

TABLE I
The Polymerization of Tetrahydrofuran Catalyzed by Heavy
Transition Metal Halides^a

Catalyst	Conc. of catalyst, mole %	Reaction time, hr.	Yield, %	Reduced viscosity, ^b dl./g.
NbCl ₅	0.25	24	30.8	0.75
	0.5	24	64.2	0.45
	1.0	24	62.0	0.50
	2.0	24	77.7	0.25
	2.0	2	64.5	0.40
	4.0	24	66.5	0.25
	0.5	2	29.3	0.32
	0.5	8	34.9	0.41
	0.5	72	53.0	0.57
	TaCl ₅	0.25	2	9.6
0.25		8	25.8	0.88
0.25		16 ^c	51.5	1.05
WCl ₆	0.5	4	64.0	1.30
	0.5	8	81.1	1.15

^a Reaction temperature, 0°C.; tetrahydrofuran, 10 ml.

^b The reduced viscosity was measured on a solution of 0.2 g. polymer in 100 ml. of benzene at 30°C.

^c Longer reaction periods gave no higher yields or viscosities.

The yield and the reduced viscosity of the polymer are summarized in Table I. For purposes of comparison, several typical data on the polymerization catalyzed by tungsten

hexachloride, reported in a preceding paper,⁹ are also included in Table I. The data indicate (1) the niobium pentachloride level of 3.5 mole-% or the tantalum pentachloride level of 0.25 mole-%, based on tetrahydrofuran, is sufficient to effect the polymerization; (2) polymerization at 0°C. was much more satisfactory than at 30°C.; (3) the catalysts gave roughly equal rates; (4) viscosities were obtained in the order W > Ta > Nb.

References

1. Meerwein, H., D. Delfs, and H. H. Morschel, *Angew. Chem.*, **72**, 927 (1960).
2. Saegusa, T., H. Imai, and J. Furukawa, *Makromol. Chem.*, **54**, 218 (1962).
3. *Ibid.*, **65**, 60 (1963).
4. Weissermel, K., and E. Nölken, *Makromol. Chem.*, **68**, 140 (1963).
5. Yamashita, I., M. Serizawa, and T. Miyakawa, *Bull. Chem. Soc. Japan*, **36**, 1368 (1963).
6. Yamashita, I., and M. Serizawa, *Bull. Chem. Soc. Japan*, **37**, 1721 (1964).
7. Muetterties, E. L., U.S. Pat. 2,856,370 (1958). In this patent Muetterties compared two polymers prepared with phosphorous pentafluoride and with antimony pentachloride.
8. Sims, D., *J. Chem. Soc.*, **1964**, 864.
9. Takegami, Y., T. Ueno, and R. Hirai, *Bull. Chem. Soc. Japan*, **38**, 1222 (1965).

YOSHINOBU TAKEGAMI
TORU UENO
RYUICHI HIRAI

Faculty of Engineering
Kyoto University
Kyoto, Japan

Received September 20, 1965
Revised October 22, 1965

Iodine Complex of Grafted Latex

The addition of bactericides and fungicides to latexes is generally effective during the storage of the latex. Upon exposure of these latexes in the form of protective coatings to weathering tests, the additives often lose their effectiveness. This may be caused by leaching action. A solution to this problem is to have the bactericide or fungicide united chemically with the latex polymer. One method of accomplishing this is to graft a monomer onto the latex polymer, thereby forming a graft copolymer which will complex with the bactericide, e.g., iodine. A similar approach has been taken in preparing metal coatings¹ where a metal surface was complexed with a grafted coating. The fungicidal properties of the iodine complex of poly(4-vinyl-3-morpholinone) are known.² We set out to prepare an effective fungicidal latex by incorporating the grafting technique.

The graft copolymer was formed by irradiating a styrene-butadiene latex to a dose of 0.5 Mrad. The radiation source was 3450 c. of Co⁶⁰. The dose rate was approximately 0.25 Mrad/hr. A 50% solution of *N*-vinyl morpholinone was added to the latex, stirred thoroughly, and allowed to stand overnight at room temperature. Since the technique involved pre-irradiation, and no elevated temperatures, we can assume that no homopolymerization occurred. The amount of monomer added was equal to 5 wt.-% of the latex solids. This sample was designated sample A. Two samples were prepared for comparison—one with monomer but no irradiation (Sample B) and one which was irradiated but no monomer was added (Sample C).

A 10% solution of iodine in methanol was prepared. Sufficient amount of this solution was added to samples A, B, and C so that the iodine equalled 2 wt.-% of the latex solids. Results of the iodine addition are shown in Table I. Sample A turned brown at first, but after a few minutes the color disappeared and there was no coagulation. This was evidence that the iodine was complexed by the polyvinylmorpholinone.

TABLE I
Effect of Iodine Addition to Latexes

Sample	Rad. dose, Mrad	N-VM, %	Treatment	Results
A	0.5	5	2% I ₂	White; no coagulation
B	0	5	2% I ₂	Brown; coagulation
C	3.5	0	2% I ₂	Brown; coagulation

Samples with iodine added were designated A-1, B-1, and C-1. However, since B-1 and C-1 coagulated, they could not be used in further comparisons.

A portion of Samples A-1 (with iodine complex) and B were inoculated with a pseudomonos-infected latex. After three inoculations, Sample B became infected permanently. The base latex contained a standard bactericidal compound, which

TABLE II
Exposure of Clear Coatings

Sample	Rad. dose, Mrad.	N-VM, %	I ₂ , %	Results
A-1	0.5	5	2	No mildew
A	0.5	5	0	Moderate mildew
B	0	5	0	Moderate mildew
C	0.5	0	0	Moderate mildew

protected it against the first two inoculations. After the third inoculation, it was no longer effective. Sample A-1 withstood more than 15 inoculations, killing the bacteria each time.

Samples A-1, A, B, and C were applied to pine panels as a clear coating. These panels were put on outdoor exposure racks for five months. Results are shown in Table II.

A portion of Samples A-1, A, B, and C were pigmented with a standard TiO₂ pigment dispersion which contained a bactericidal-fungicidal compound. These were then applied to pine panels and put on exposure for eight months. Results are shown in Table III.

TABLE III
Exposure of Pigmented Coatings

Sample	Rad. dose, Mrad.	N-VM, %	I ₂ , %	Results
A-1	0.5	5	2	No mildew
A	0.5	5	0	Moderately light mildew
B	0	5	0	Moderately light mildew
C	0.5	0	0	Moderately light mildew

Thus, an effective bactericidal-fungicidal latex may be prepared by this technique.

References

1. J. B. Gardner, and B. G. Harper, *J. Appl. Poly. Sci.* **9**, 715-727 (1965).
2. French Pat. 1,354,115.

JOHN B. GARDNER
BILLY G. HARPER

Basic Research Laboratory
Texas Division
The Dow Chemical Company
Freeport, Texas

Received May 19, 1965
Revised November 17, 1965